

Copy No. _____

SNA-8-D-027(I)
Revision 3



NATIONAL AERONAUTICS AND SPACE ADMINISTRATION

CSM/LM SPACECRAFT OPERATIONAL DATA BOOK

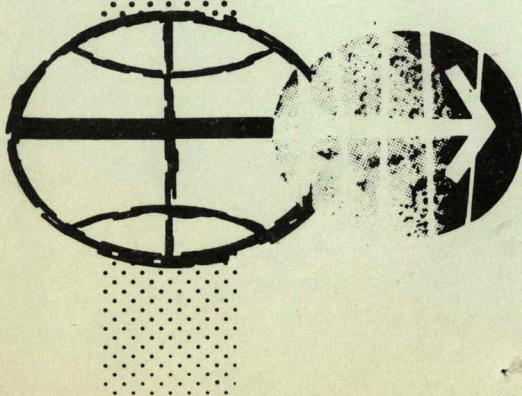
VOLUME I
CSM DATA BOOK

Part I
Constraints and Performance

SD 68-447-1B

Revision 3

15 April 1970



MANNED SPACECRAFT CENTER
HOUSTON, TEXAS

CSM/LM SPACECRAFT OPERATIONAL DATA BOOK

VOLUME I

CSM DATA BOOK

Part 1

Constraints and Performance

SD 68-447 - 1B

Prepared By

North American Rockwell Corporation

Space Division

For

Systems Engineering Division

Apollo Spacecraft Program Office

Manned Spacecraft Center

Contractor
Concurrence

M.M. Vucelic
M.M. VUCELIC, Manager
Mission Requirements

Concurrence

A.A. Sjoberg
for C.C. KRAET, JR., Director
Flight Operations

Concurrence

Owen E. Maynard
OWEN E. MAYNARD, Chief
Systems Engineering Division

Concurrence

M.A. Faget
M.A. FAGET, Director
Engineering and Development

Concurrence

D.K. Slayton
D.K. SLAYTON, Director
Flight Crew Operations

Approved by

George M. Low 5-7-68
GEORGE M. LOW, Manager
Apollo Spacecraft Program

SNA-8-D-027(I)
Revision 3

CSM/LM SPACECRAFT
OPERATIONAL DATA BOOK

Volume I
CSM Data Book

MANNED SPACECRAFT CENTER, HOUSTON, TEXAS

PREFACE

This document is the third revision of the CSM Data Book, Part 1. It incorporates amendments through Number 38. Amendments released after publication of this revision will continue in sequence from Number 38. This data book provides the mission planner with ready visibility of mission constraints and limitations and spacecraft performance capabilities and consumable requirements. All sections of the document are continually undergoing review with the intent to update information where required; therefore, it is imperative that amendments be inserted in sequential order. A complete description of the contents and amendment procedures is provided in Section 1.0, Introduction.

CONTENTS

Section		Page
1.0	INTRODUCTION	1-1
	1.1 PURPOSE	1-1
	1.2 CONTENT	1-1
	1.3 AMENDMENTS	1-2
	1.4 SELECTED ABBREVIATIONS AND ACRONYMS	1-3
2.0	SPACE VEHICLE CONFIGURATION	2-1
3.0	SPACECRAFT CONSTRAINTS AND OPERATIONAL LIMITATIONS	3.1-1
	3.1 ELECTRICAL POWER SUBSYSTEM	3.1-1
	3.2 ENVIRONMENTAL CONTROL SUBSYSTEM	3.2-1
	3.3 SERVICE MODULE REACTION CONTROL SUBSYSTEM	3.3-1
	3.4 COMMAND MODULE REACTION CONTROL SUBSYSTEM	3.4-1
	3.5 SERVICE PROPULSION SUBSYSTEM	3.5-1
	3.6 GUIDANCE AND CONTROL SUBSYSTEM	3.6-1
	3.7 COMMUNICATIONS SUBSYSTEM	3.7-1
	3.8 STRUCTURES	3.8-1
	3.9 LAUNCH ESCAPE SUBSYSTEM AND EARTH LANDING SUBSYSTEM	3.9-1
	3.10 CREW AND CREW SYSTEMS	3.10-1
	3.11 THERMAL SUBSYSTEMS	3.11-1
4.0	SUBSYSTEM PERFORMANCE AND OPERATIONAL DATA	4.1-1
	4.1 ELECTRICAL POWER SUBSYSTEM	4.1-1
	4.2 ENVIRONMENTAL CONTROL SUBSYSTEM	4.2-1
	4.3 SERVICE MODULE REACTION CONTROL SUBSYSTEM	4.3-1
	4.4 COMMAND MODULE REACTION CONTROL SUBSYSTEM	4.4-1
	4.5 SERVICE PROPULSION SUBSYSTEM	4.5-1
	4.6 GUIDANCE AND CONTROL SUBSYSTEM	4.6-1
	4.7 COMMUNICATIONS SUBSYSTEM	4.7-1
	4.8 STRUCTURES	4.8-1
	4.9 LAUNCH ESCAPE SUBSYSTEM AND EARTH LANDING SUBSYSTEM	4.9-1
	4.10 CREW AND CREW SYSTEMS	4.10-1

Section		Page
5.0	AERODYNAMICS	5-1
6.0	SPACECRAFT BENDING MODES	6-1
7.0	PROPELLANT SLOSH	7-1
APPENDIXES*		
101.	CSM 101 (Effective Through 11 October 1968)	101-1
103.	CSM 103 (Effective Through 21 December 1968)	103-1
104.	CSM 104 (Effective Through 3 March 1969)	104-1
106.	CSM 106 (Effective Through 18 May 1969)	106-1
107.	CSM 107 (Effective Through 16 July 1969)	107-1
108.	CSM 108 (Effective Through 14 November 1969)	108-1
109.	CSM 109 (Effective Through 11 April 1970)	109-1
110.	CSM 110 (Effective Through 31 January 1971)	110-1
112.	CSM 112 (Effective Through 26 July 1971)	112-1
113.	CSM 113	113-1
114.	CSM 114	114-1

*Appendixes for CSM's 101 through 112 are deleted and have not been included in this printing. The deleted appendixes are listed because they may have been retained by some users.

1.0 INTRODUCTION

-Missions

Individual appendix for each spacecraft.
Particular spacecraft, while the main text

1.0 INTRODUCTION

1.1 PURPOSE

This document presents operational information on the capabilities and limitations of the spacecraft. The information is intended for use in nominal mission planning and for providing specialized data related to premission studies. The information should assist in the execution of two basic functions:

1. The initial design of trajectories and mission plans that are within the capabilities of the combined crew/spacecraft.
2. The real-time planning of missions with maximum planning flexibility.

1.2 CONTENT

The complete CSM/LM Spacecraft Operational Data Book for the manned missions will consist of seven separate volumes. These are defined as follows:

Volume I - CSM Data Book

Part I - Constraints and Performance

Part II - Launch Mission Rule Redlines

Volume II - LM Data Book

Part I - Constraints and Performance

Part II - Launch Mission Rule Redlines

Volume III - Mass Properties Data Book

Volume IV - EMU Data Book

Volume V - ALSEP Data Book

Volume VI - CSM Experiments Data Book for J-Missions

Volume VII - LCRU/GCTA Data Book

Volume I, Part I, is divided into seven sections plus an individual appendix for each spacecraft. Each appendix will contain unique data applicable to the particular spacecraft, while the main text

of Volume I, Part I, will contain data of a more universal nature that can be used for mission planning. A brief discussion of the scope of the sections of Volume I, Part I, follows:

Section 1.0, Introduction. The Introduction describes the purpose and scope of the overall data book and summarizes the content of the remaining sections.

Section 2.0, Space Vehicle Configuration. This section contains pictorial representations of the space vehicle, showing axes, station lines, separation planes, etc. These data are intended as reference material for use throughout the book.

Section 3.0, Spacecraft Constraints and Operational Limitations. The restrictions, limitations, and special recommendations on the use of the spacecraft and its subsystems are contained in this section. The section is arranged by subsystem, for convenience. It should be used by mission planners as the single source for spacecraft constraints.

Section 4.0, Subsystem Performance and Operational Data. This section contains the supporting discussion for the constraints and limitations presented in Section 3.0. It also contains descriptions of the fundamental performance of subsystems and subsystem components. Typically, fundamental data are used for system analyses and for the formulation of models for computer studies. Consequently, data are defined at a basic level, and the user is responsible for properly utilizing the data for evaluation purposes.

Section 5.0, Aerodynamics. Command module reentry aerodynamics characteristics are presented in this section. Also included are coefficients for the launch escape and parachute subsystems.

Section 6.0, Spacecraft Bending Modes. This section presents three-dimensional vibration modes for the CSM/LM configuration. Data are presented for various vehicle weights corresponding to propellant loading.

Section 7.0, Propellant Slosh. The data presented in this section represent sloshing models of the SPS storage and sump tanks and are applicable for defining acceleration conditions of the SPS engine thrusting. These data consist of slosh mass, frequency, and point of attachment.

Appendixes. An appendix is included for each spacecraft. Each appendix contains data unique to the particular spacecraft and deviations from the baseline data contained in the body of the Data Book. The format and paragraph numbers in the appendixes conform to those in the body of the Data Book.

1.3 AMENDMENTS

Amendments to this document will be made by page additions or replacements. Data changed by an amendment will be denoted by an amendment date and number in the upper right-hand

corner of the page and a vertical bar in the page margin to locate the change. Where the complete page constitutes a new addition to the Data Book, no change bar will be placed in the margin.

A revision page showing the accumulative changes that have been made will be issued with each amendment. This revision page should be placed just behind the title page and will provide an up-to-date listing of all amendments.

1.4 SELECTED ABBREVIATIONS AND ACRONYMS

AGC	Apollo guidance computer
ALSEP	Apollo lunar scientific experiments package
AOH	Apollo Operations Handbook
APS	Ascent propulsion subsystem
ASD	Acceleration spectral density
BMAG	Body-mounted attitude gyro
CDU	Coupling display unit
CGSS	Cryogenic gas storage subsystem
CM	Command module
CMC	Command module computer
CMP	Command module pilot
COAS	Crewman optical alignment sight
CSM	Command and service modules (mated)
DB	Deadband
Delta P (ΔP)	Pressure differential
Delta V (ΔV)	Velocity change
DPS	Descent propulsion subsystem
DSE	Data storage equipment
DSKY	Computer display keyboard
DVM	Digital voltmeter
ECS	Environmental control subsystem
EDS	Emergency detection subsystem
ELS	Earth landing subsystem
ELSC	Earth landing sequence controller
EMS	Entry monitor subsystem
EMU	Erasable memory unit
EMU	Extravehicular mobility unit
EPS	Electrical power subsystem
EV	Extravehicular
EVA	Extravehicular activity
EVT	Extravehicular transfer

FC	Fuel cell
FCSM	Flight combustion stability monitor
FDAI	Flight director attitude indicator
GA	Gyro assembly
GCTA	Ground command television assembly
GDC	Gyro display coupler
G&N	Guidance and navigation
GN&C	Guidance, navigation, and control
HBR	High bit rate
HGA	High-gain antenna
ICD	Interface Control Documents
IMU	Inertial measurement unit
IVT	Intravehicular transfer
KOH	Potassium hydroxide
LBR	Low bit rate
LCRU	Lunar communication relay unit
LDEC	Lunar docking event controller
LES	Launch escape subsystem
LESM	Launch escape subsystem motor
LLOS	Landmark line of sight
LM	Lunar module
LOI	Lunar orbit injection
LOR	Lunar orbital rendezvous
LSSC	LM-SLA separation controller
MEEL	Master electrical equipment list
MESC	Master events sequence controller
MMH	Monomethylhydrazine
MPAD	Mission Planning and Analysis Division
MSC	Manned Spacecraft Center
MSFN	Manned Space Flight Network
nm	Nautical mile
OPS	Oxygen purge subsystem
PCM	Pulse code modulation
PCM	Pitch control motor
PCVB	Pyrotechnic continuity verification box
PGA	Pressure garment assembly
PGNCS	Primary guidance and navigation control subsystem

PIPA	Pulse integrating pendulous accelerometer
PLSS	Portable life support subsystem
PLV	Postlanding ventilation
PQGS	Propellant quantity gauging subsystem
PRN	Pseudo-random noise
PTC	Passive thermal control
PUGS	Propellant utilization and gauging subsystem
PVT	Pressure, volume, and temperature
RCS	Reaction control subsystem
rph	Revolutions per hour
RR	Rendezvous radar
RTG	Range to go
SBPA	S-band power amplifier
SCS	Stabilization and control subsystem
SCT	Scanning telescope
SECS	Sequential events control subsystem
SIM	Scientific instrument module
SLA	Spacecraft-LM adapter
SLOS	Star line of sight
SM	Service module
SMJC	Service module jettison controller
SPS	Service propulsion subsystem
SXT	Sextant
TBD	To be determined
TCC	Temperature control circuit
TCS	Thermal control subsystem
TD	Time delay
TEI	Transearth injection
TJM	Tower jettison motor
USB	Unified S-band
VW	Secondary fuel tank helium isolation valve
WSTF	White Sands Test Facility

Amendment 88
2/16/72

2.0 SPACE VEHICLE CONFIGURATION

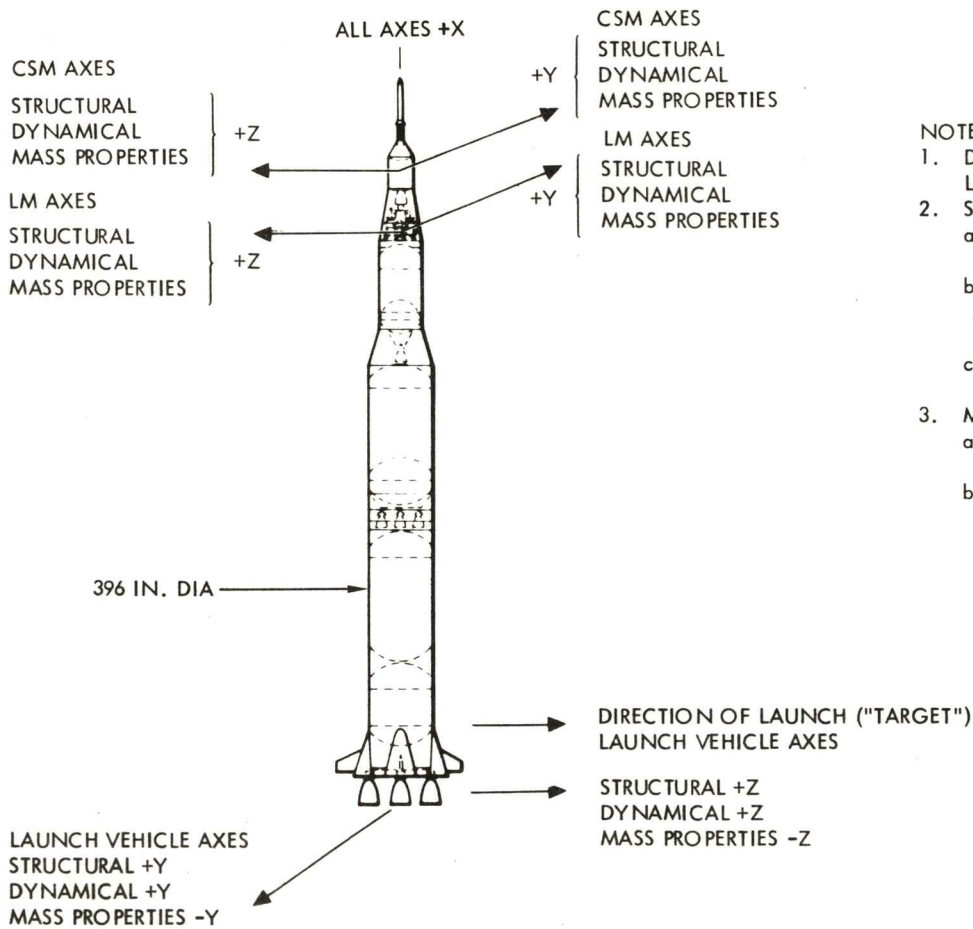
2.0 SPACE VEHICLE CONFIGURATION

S-D-027(I), REV 3

2.0 SPACE VEHICLE CONFIGURATION

The vehicle coordinate axes conventions and notation system are summarized in Figure 2-1. All dimensions in this section were obtained from the latest available coordinate standards, specifications, and Interface Control Documents (ICD).

The outboard profile and reference dimensions of the Saturn V Apollo space vehicle are presented in Figures 2-2 and 2-3. The Saturn V configuration will be used for all manned missions except the first.



NOTES:

1. DYNAMICAL AXES ORIGIN. THE DYNAMICAL AXES ORIGINS ARE LOCATED AT THE CENTER OF MASS FOR EACH CONFIGURATION.
2. STRUCTURAL AXES ORIGIN.
 - a. THE LAUNCH VEHICLE STRUCTURAL AXIS ORIGIN IS 100 INCHES BELOW THE S-IC GIMBAL REFERENCE PLANE.
 - b. THE CSM STRUCTURAL AXIS ORIGIN IS 1000 INCHES BELOW THE MOLD LINE OF THE HEAT SHIELD MAIN STRUCTURE ABLATION INTERFACE.
 - c. THE LM STRUCTURAL AXIS ORIGIN IS 200 INCHES BELOW LM ASCENT STAGE BASE.
3. MASS PROPERTIES AXES ORIGIN.
 - a. THE SPACECRAFT MASS PROPERTIES AXIS ORIGIN IS COINCIDENT WITH THE CSM STRUCTURAL AXIS ORIGIN.
 - b. THE LAUNCH VEHICLE MASS PROPERTIES AXIS ORIGIN IS COINCIDENT WITH ITS STRUCTURAL AXIS ORIGIN.

* POSITIVE ROTATIONS ARE DEFINED USING AXES FOR VEHICLE BEING CONSIDERED
 $\theta_{CSM} = -\theta_{LV}$, $\psi_{CSM} = -\psi_{LV}$

AXIS	AXIS SYMBOL	MOMENT SYMBOL	POSITIVE * ROTATION	LAUNCH VEHICLE ANGLE	CSM ANGLE	LM ANGLE	ANGLE SYMBOL	LINEAR VELOCITY	ANGULAR VELOCITY
LONGITUDINAL	X	L	+Y TO +Z	ROLL	ROLL	ROLL	ϕ	u	p
TRANSVERSE (PITCH)	Y	M	+Z TO +X	PITCH	PITCH	PITCH	θ	v	q
TRANSVERSE (YAW)	Z	N	+X TO +Y	YAW	YAW	YAW	ψ	w	r

Figure 2-1. Vehicle Coordinate Axes and Notation System

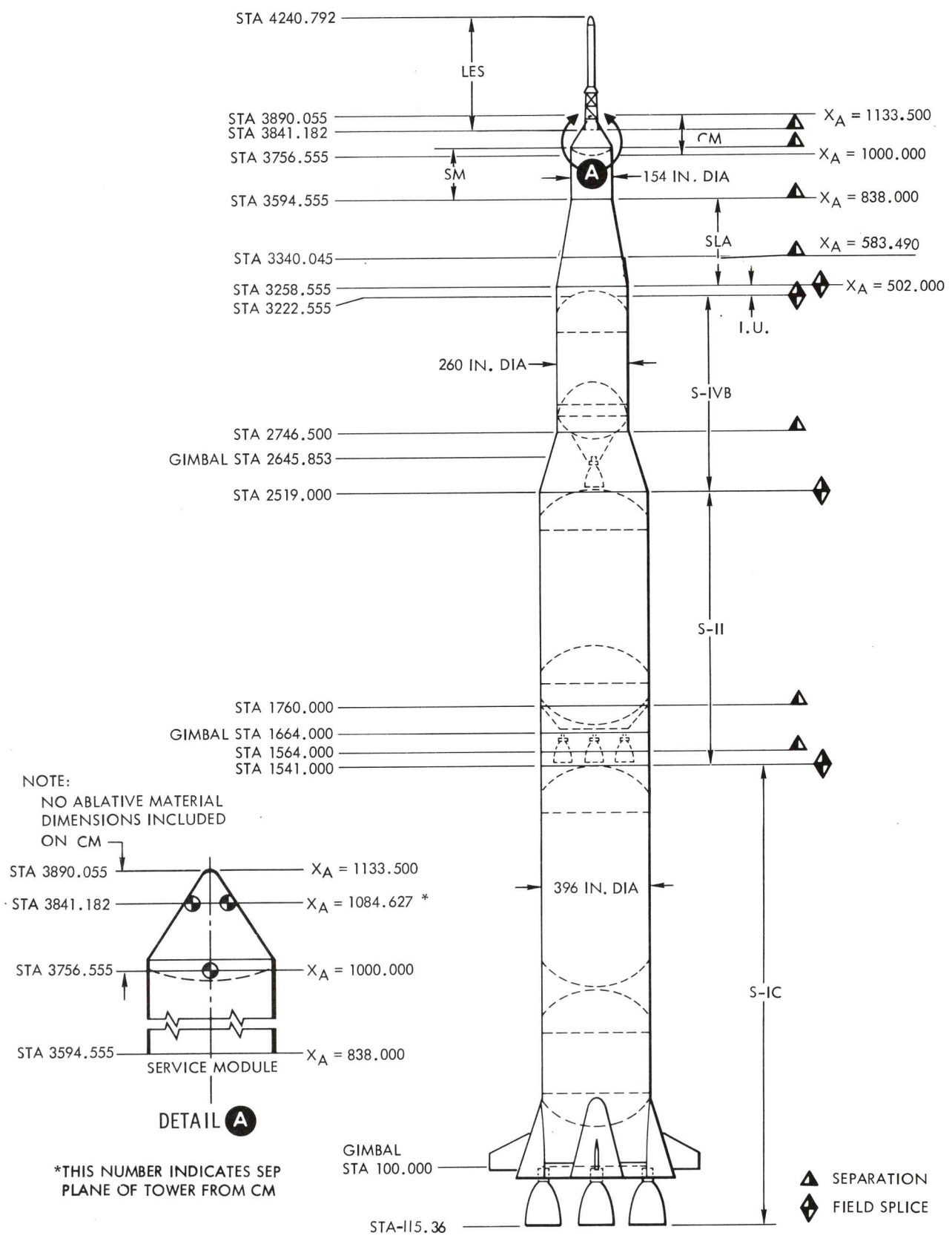


Figure 2-2. Saturn V/Apollo Configuration

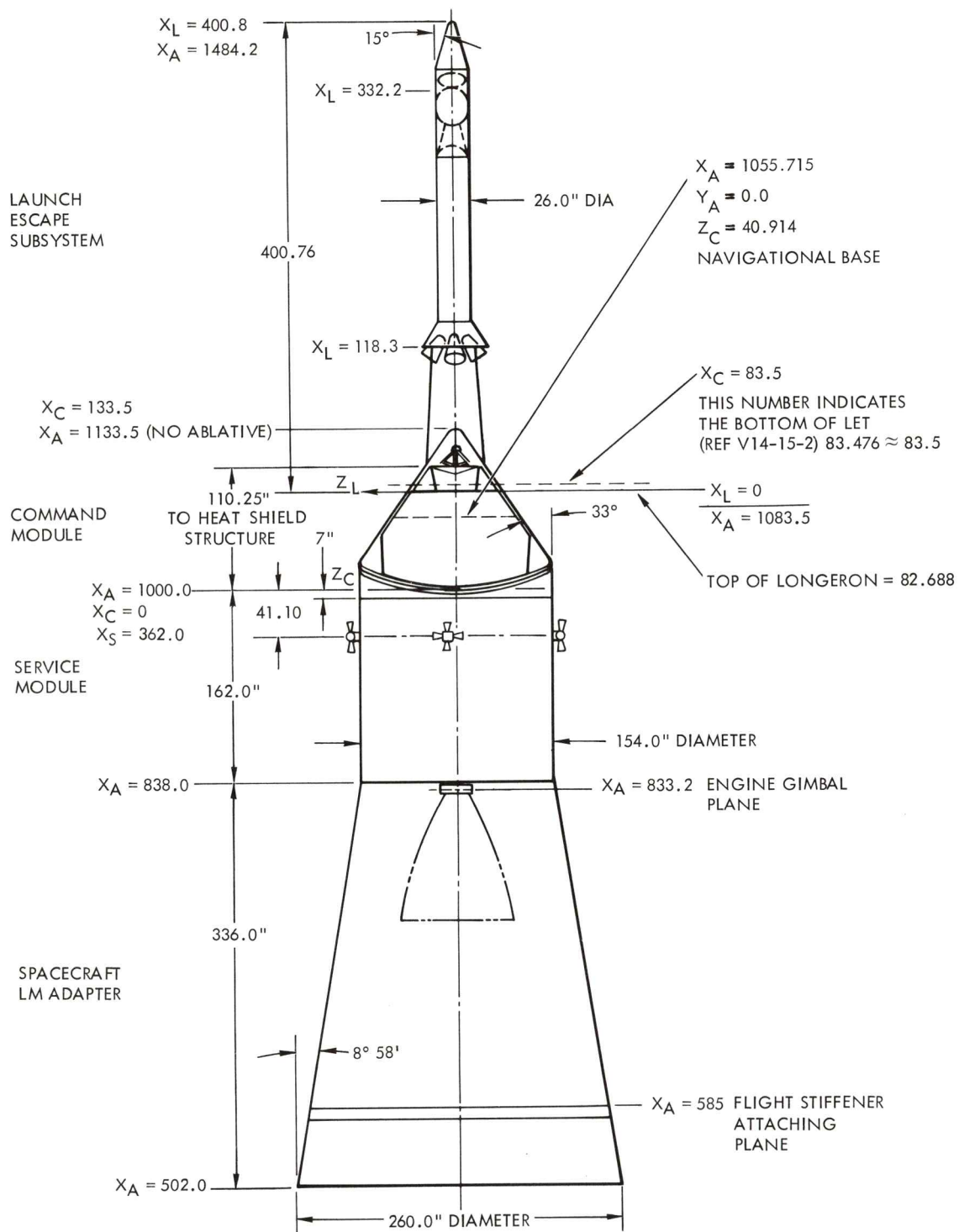


Figure 2-3. Apollo Spacecraft Reference Dimensions

2-5

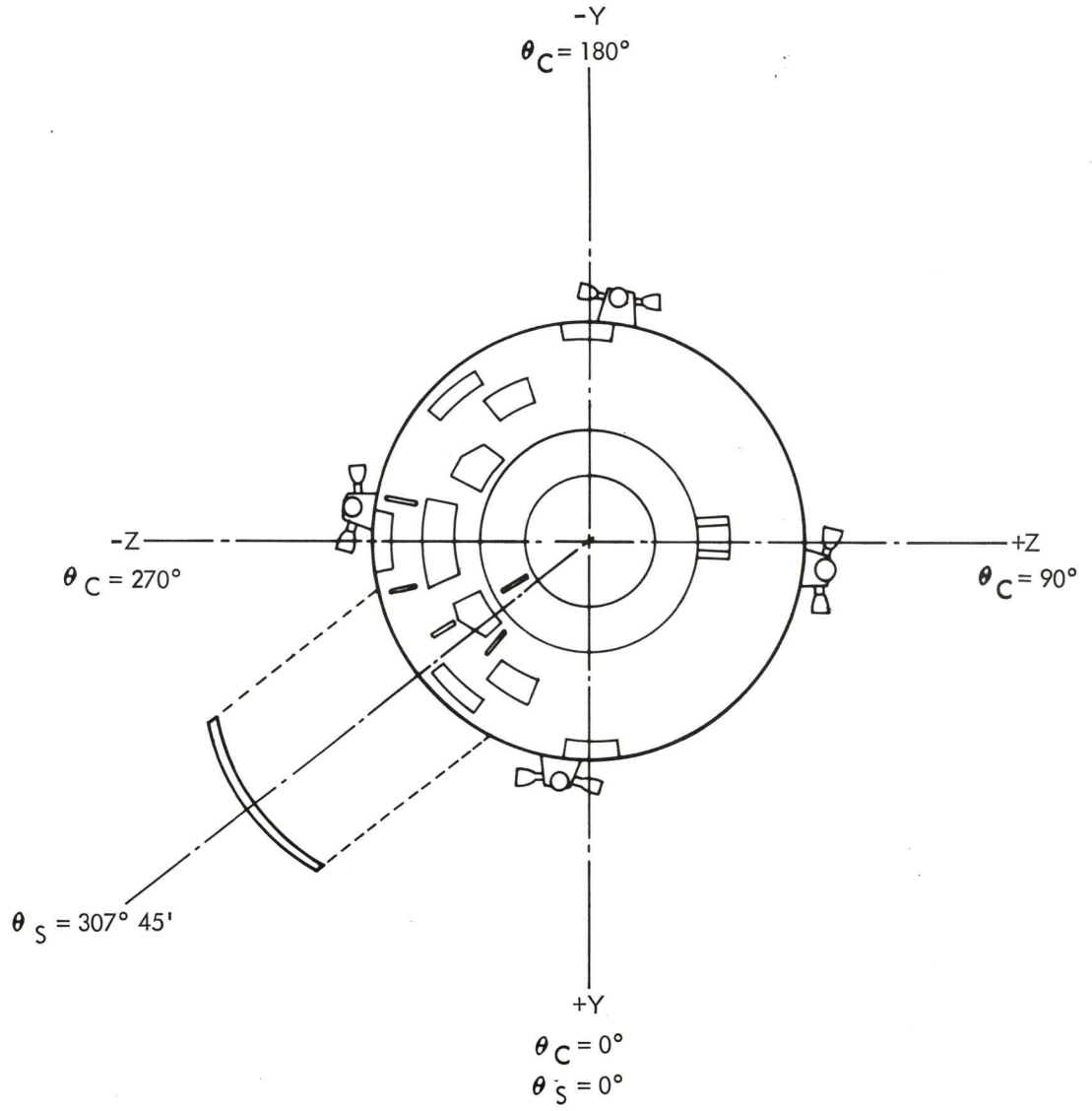
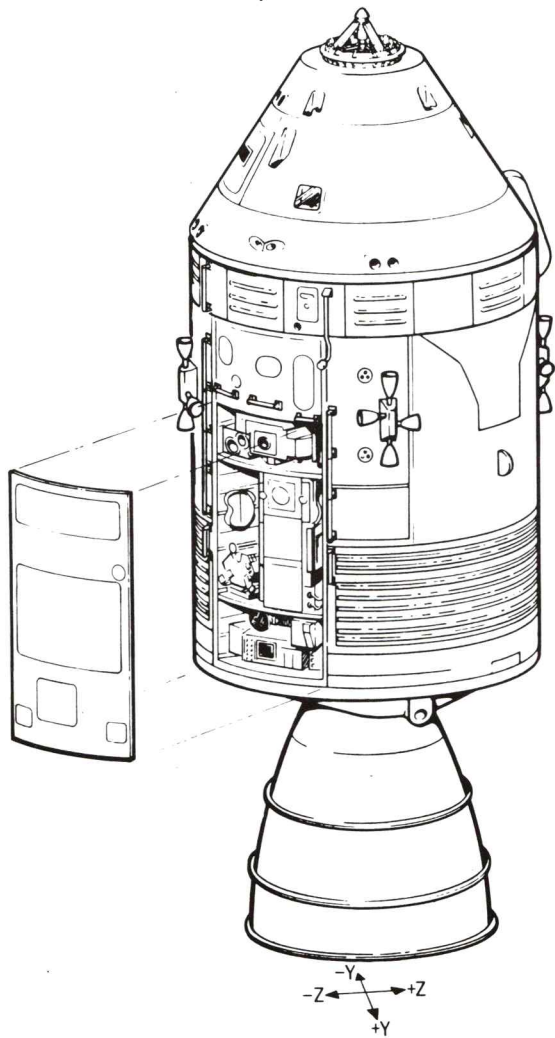


Figure 2-4. SIM Door Jettison

LIMITATIONS

ould be used for mission
f exceeded, may result
itation is that limit a
spacecraft operation.

d limitations are
are presented

3.0 SPACECRAFT CONSTRAINTS AND OPERATIONAL LIMITATIONS

3.0 SPACECRAFT CONSTRAINTS AND OPERATIONAL LIMITATIONS

This section contains the spacecraft constraints and limitations that should be used for mission planning. A spacecraft constraint is a spacecraft imposed limitation which, if exceeded, may result in degradation of system performance or a system failure. An operational limitation is that limit a mission planner should not exceed in order to avoid interference with nominal spacecraft operation.

For the convenience of mission planning and flight control, the constraints and limitations are discussed in this section under the individual subsystem headings. Supporting data are presented under similar headings in Section 4.0.

3.1 ELECTRICAL POWER SUBSYSTEM (EPS)

3.1.1 BUS VOLTAGE

Main bus voltage must not exceed 31 volts dc or fall below 26.5 volts dc. (A complete discussion can be found in paragraphs 4.1.1.1 and 4.1.1.5).

3.1.2 MINIMUM LOAD VOLTAGE REQUIREMENTS

Table 3.1-1 lists the minimum voltage requirements as defined at the load interface and the command module main dc bus for certain critical spacecraft equipment. The voltage drops between bus and load are estimated values. Off-limits testing for low voltage has not been conducted on most spacecraft electrical equipment, and minimum voltages can only be estimated. In any case, minimum voltage requirements are rather qualitative, since they may define the level at which the equipment no longer meets specification minimum control rates, regulation, pulse width, etc., but not actually inhibit equipment operation.

3.1.3 FUEL-CELL TEMPERATURE

Fuel-cell stack temperature must not exceed 500 F or fall below 360 F. Fuel-cell radiator outlet temperature must be maintained above -30 F. Condenser exit temperature should not exceed 225 F. (A complete discussion can be found in paragraph 4.1.2.2).

3.1.3.1 Fuel-Cell Lifetime with Reactant Valves Closed

Fuel-cell pumps may not restart following wet (in-flight) shutdown due to insulation resistance degradation. In-line heater operation without operating pumps will result in loss of heater due to lack of cooling. (A complete discussion can be found in paragraph 4.1.2.5.6.)

3.1.4 INVERTER TEMPERATURE AND UPPER VOLTAGE LIMITS

3.1.4.1 Temperature

Inverter temperature must not exceed 248 F. (A complete discussion of inverter operation without cooling can be found in paragraph 4.1.5.2).

3.1.4.2 DC Voltage Input

The inverter can take a maximum of 33 Vdc and for a sustained period of time.

3.1.5 ELECTRICAL EQUIPMENT

Temperature limitations can be found in Table 3.11-1.

3.1.5.1 CSM Power to LM

The maximum steady-state current carrying capability of the power transfer umbilical assuming equal load sharing through the associated CM circuit breakers, a circuit breaker temperature of approximately 100 F, and the use of either one of both umbilicals, is:

Vacuum - 10.8 amps
5 psia - 15.0 amps

The rationale for this limit is that the circuit breaker rating for continuous operation with no trip will be violated and the circuit breaker will eventually open.

3.1.6 CRYOGENIC EQUIPMENT

Temperature limitations can be found in Table 3.11-1.

3.1.6.1 Cryogenic Hydrogen Tank Pressure-Temperature Limit Relationships

Pressure-temperature limit relationships for the cryogenic hydrogen tanks are presented in the appropriate spacecraft appendixes.

3.1.6.2 Oxygen Tank Temperature Limits

The oxygen tank heater and bulk temperatures as read out by the temperature sensor should not exceed the following values.

Heater	350 F
Bulk Fluid	80 F

The rationale for these limits are:

- 1) The limit of 350°F assures that the hottest location on the heater does not result in exceeding temperature limits on any material in the tank.
- 2) The O₂ tank wall fracture mechanic limits of 200 F will not be approached.

3.1.7 TRANSEARTH COAST - SIM ELECTRICAL POWER SHUTDOWN

Before and during EVA while in transearth coast, electrical power to the SIM must be shut down for crew safety purposes.

Table 3.1-1. Minimum Voltage

System	Item	Estimated Minimum Volts at Load	Estimated Minimum Volts at Bus	Data Source	Estimated Maximum Volts at Load	Data Source	Remarks
SPS	Gimbal motors	14.0	14.0 ①	Test and analysis	30.0	Specification	No control instability-limited by motor stall.
	Engine prevalves	18.0	19.5	Test			
	Engine pilot valves	20.0	24.5	Test			
	Helium valves	8.3	10.0	Test			
	Control relays	18.0	21.0	Test and specification			
RCS	Engines						
	SM Auto	17.0	22.0	Test			
	SM Direct	16.0	21.0	Test			
	CM Auto	16.0	21.0	Test			
	CM Direct	14.0	17.0	Test			
	Propellant isolation valves	17.8	21.0	Test			
	CM RCS controller	19.0	22.0	Test and analysis			
	Quad heaters	23.0	27.0	Analysis			
G&N	DC	25.8	26.5	Test and Specification	30.8	Test and Specification	Limited by the IMU Electronics
③SECS	MESC, SMJC, PCVB, LDEC, LSSC, ELSC	20.0	22.0 ②	Test			

Notes:

- ① Service module bus
 - ② Battery buses
 - ③ SECS Sequential event control subsystem
- MESC Master event sequence controller
 SMJC Service module jettison controller
 PCVB Pyro continuity verification box
 LDEC LM docking event controller
 LSSC LM/SLA separation controller
 ELSC Earth landing sequence controller

3.1-3

SNA-8-D-027(I), Rev 3

3.2 ENVIRONMENTAL CONTROL SUBSYSTEM (ECS)

3.2.1 SUBSYSTEM TEMPERATURES

3.2.1.1 Radiator Outlet Temperature

ECS radiator outlet temperature should be maintained above -20 F and below 85 F. Orienting the spacecraft -X axis toward the sun for a period in excess of 3 hours while sustaining a low ECS heat load (approximately 4400 Btu/hr) could produce temperatures less than -20 F. (See Table 3.11-2 for this and other ECS temperature limitations.)

3.2.2 RADIATOR STABILIZATION TIME

Minimum time required to evaluate glycol radiator flow after opening glycol-to-radiator valve is 2.5 minutes. This limit is based on the time required for stabilization of radiator inlet and outlet temperature sensors.

3.2.3 PRESSURIZATION

3.2.3.1 Tank/Bottles Recharge

Recharge of surge tank and oxygen bottles to 865 psia requires 63.5 minutes after the cabin is pressurized to 5.0 psia and is required before another cabin repressurization may be performed.

3.2.3.2 Cabin Rapid Repressurization

Rapid repressurization of command module requires 60 seconds from zero psia to 3.0 psia and 25 minutes from zero to 4.8 psia. This requirement is based on using a repressurization source consisting of the surge tank and three 1-pound bottles at a pressure of 865 psia.

3.2.4 LEAKAGE

3.2.4.1 Total Oxygen

Total oxygen leakage rate must not exceed 4.0 pounds per hour. (For further details, see paragraph 4.2.1.2.)

3.2.4.2 Cabin Leakage

Cabin leakage must not exceed 0.2 pound per hour at a 5-psi cabin-to-ambient pressure differential (see paragraph 4.2.1.6).

3.2.5 LUNAR MODULE PRESSURIZATION*

See Volume II, Part 1, paragraph 3.9, LM Structures Constraint S-II.

3.2.6 SUBSYSTEM COMPONENT PRESSURES

3.2.6.1 CO₂ Control

The CO₂ specification maximum partial pressure requirement on the LiOH canisters is 7.6 mmHg. According to test data, approximately 37 hours elapse before CO₂ partial pressure exceeds the 7.6-mmHg value (see paragraph 4.2.2.5).

3.2.7 SUIT COMPRESSOR OPERATION

When only one oxygen hose assembly is in use and the other hose nozzles are blocked by barriers in the oxygen hose couplings and the suit flow relief valve is in the OFF position, only one of the two suit compressors should be operated to preclude possible compressor damage from flows less than 10 cfm. Neither of the suit compressors should be operated when all of the hose nozzles are blocked by barriers in the oxygen hose couplings and the suit flow relief valve is in the OFF position.

3.2.8 GLYCOL EVAPORATOR

The glycol evaporator has a maximum heat transfer rate of 7620 Btu per hour under the conditions given in paragraph 4.2.3.4. Evaporator activation is required during EVA to facilitate suit circuit water removal and to preclude helmet fogging, especially during lunar orbit EVA.

3.2.9 URINE SYSTEM OPERATION*

Rinsing of the urine receptacle assembly (URA) after use should be limited to approximately 10 seconds. After the URA appears to be empty, the cover should be replaced and the vent valve should be left open for two to five minutes to clear the system of liquid to prevent freezeup.

3.2.10 EFFECT OF LOSS OF PRIMARY COOLANT LOOP ON CSM EVA

The CSM EVA should not be continued if the primary glycol loop is lost before CMP egress since the minimum qualification temperature limit for the 603 panel components will be exceeded in approximately 13 minutes. If loss of primary glycol flow occurs after CMP egress, the EVA may be continued to achieve mandatory objectives with the following predicted result:

Time After Failure	Event	Result
13 minutes	603 panel outlet (umbilical inlet temperature decreases to 0 F	0 F qualification temperature limit No failure expected

For further details, see paragraph 4.2.3.11 and Figure 4.2-34.1.

*NASA Data Source

3.2.10 EFFECT OF LOSS OF PRIMARY COOLANT LOOP ON CSM EVA

The CSM EVA should not be continued if the primary glycol loop is lost before CMP egress since the minimum qualification temperature limit for the 603 panel components will be exceeded in approximately 13 minutes. If loss of primary glycol flow occurs after CMP egress, the EVA may be continued to achieve mandatory objectives with the following predicted result:

<u>TIME AFTER FAILURE</u>	<u>EVENT</u>	<u>RESULT</u>
13 minutes	603 panel outlet (umbilical inlet temp) decreases to 0 F.	0 F qual temp limit, no failure expected.

For further details, see paragraph 4.2.3.11 and Figure 4.2-34.1.

3.3 SERVICE MODULE REACTION CONTROL SUBSYSTEM

3.3.1 PLUME IMPINGEMENT RESTRICTIONS

3.3.1.1 RCS Usage During EVA

During extravehicular activities, vehicle attitude is to be maintained by the service module RCS in either wide or narrow dead-band attitude hold utilizing either CMC/AUTO or SCS mode. Jets which fire into the EVA path are to be disabled to avoid plume impingement on the EVA crewman.

3.3.1.2 CSM RCS -X Jet Firing Restrictions

The CSM (SM) -X (forward firing engine) RCS jets cannot be fired continuously for over seven seconds when in the docked configuration. Failure to comply with this constraint will cause damage to the lunar module ascent stage thermal insulation.

3.3.1.2.1 Lunar Module S-Band Steerable Antenna*

Plume torque from the CSM RCS may cause the LM S-band steerable antenna to lose lock, providing the CSM RCS firings are of sufficient duration. Table 3.3-1 tabulates, for various antenna positions, the duration of RCS pulse firings which could cause loss of lock.

3.3.1.2.2 Lunar Module Rendezvous Radar Antenna

In the docked configuration, the service module RCS jet B3 (-X) must be deactivated while the lunar module rendezvous radar is operated. Plume impingement on the antenna while the rendezvous radar is operating can cause corona arcing, resulting in antenna damage.

3.3.1.3 Lunar Module RCS -X Jet Firing Restriction

With an initial command module ablator surface temperature of 200 F or less, the lunar module -X (up-firing engine) RCS jets are limited to 15 seconds firing duration while in the docked configuration. Failure to comply with this constraint will result in damage to the thermal coating.

3.3.1.4 Maximum SM RCS Engine Burn Duration

Continuous engine burn duration for the +X (aft-firing) engines should not exceed 750 seconds on any one engine. Violation of this constraint causes damage to service module insulation and results in service module SPS and RCS tank temperature increases.

*NASA Data Source

3.3.1.5 Lunar Orbit - SIM Experiments

After SIM door jettison, SM RCS jets A2, A4, B1, and B4 must be inhibited during experiment data collection phases. In addition, jets C1 and C3 will be inhibited during mass spectrometer operation. RCS control requirements for ullages, SPS burns, rendezvous, and docking will be satisfied and these operations should be performed to minimize the total accumulated interval of RCS plume impingement into the SIM bay.

3.3.1.6 Transearth Coast - SIM Experiments

During experiment data acquisition, SM RCS jets A2, A4, B1 and B4 must be inhibited to prevent experiment contamination, unless quad propellant imbalance requires their activation. In addition, jets C1 and C3 will be inhibited during mass spectrometer operation.

Operations with extended booms will require deactivation of the control system before boom extension. (Boom-mounted experiments are operated during PTC in transearth coast.)

3.3.1.7 EVA - SIM Experiments

SM RCS quads A & B must be inhibited during EVA for crew safety purposes.

3.3.1.8 SM RCS Jet Firing Restrictions--SIM Experiments

Refer to paragraphs 2.8 and 2.10 of Volume VI, CSM Experiments Data Book for J-Missions.

3.3.2 ENGINE FIRING DATA

3.3.2.1 Minimum Engine Inlet Pressure

The minimum engine inlet pressure is 75 psia.

3.3.2.2 Firing Time Limitations

Critical engine on-off time sequence limitations (thermal effects not included) are as follows:

Automatic coil	Maximum pulsing frequency of 60 cycles per second.
Direct coil	Minimum of 100 ms off-time between pulses.
	Maximum pulsing frequency of 8 cycles per second.

Qualification limits are as follows:

Single firing	500 seconds (supplemental tests have shown that, within the propellant capabilities onboard, there is no limit to the single firing duration.)
Accumulative firing pulse mode plus steady state	1000 seconds
Number of firing cycles	10,000

3.3.3 VOLTAGE LIMITATIONS

Engine propellant valves	Operating range of 21 to 32 vdc at valves
Helium isolation valves	18 vdc minimum, 33 vdc maximum
Propellant isolation valves	18 vdc minimum, 33 vdc maximum

3.3.4 PROPELLANT ISOLATION VALVE USE LIMITATIONS

The propellant isolation valves are not for propellant management (see paragraph 4.3.6.3).

3.3.5 MINIMUM HELIUM PRESSURE

The minimum helium pressure required to use all deliverable propellants in normal firing modes is 2080 psia at 70 F. This value is based upon the following assumptions: maximum regulator pressures and tank volumes, and system condition at propellant depletion of the following:

Helium bottle	300 psia at 20 F
Propellant tanks	187 psia at 40 F
Ullage saturation	100 percent

3.3.6 SERVICE MODULE RCS HELIUM BOTTLE PRESSURE-TEMPERATURE LIMITATIONS

For service module RCS helium bottle pressure-temperature limitations, see paragraph 3.3.6 in the appropriate spacecraft appendixes.

3.3.7 TEMPERATURE LIMITS

Detailed temperature limits are presented in Table 3.11-3.

3.3.8 PRESSURE-TEMPERATURE LIMIT RELATIONSHIP FOR SERVICE MODULE RCS PROPELLANT TANKS

For pressure-temperature limit relationship for service module RCS propellant tanks, see paragraph 3.3.8 in the appropriate spacecraft appendixes.

Table 3.3-1. Time of GSM RCS Plume Impingement on S-Band Antenna Until Loss of Earth Track (Seconds) (NASA Data Source) (See Paragraph 3.3.1.2.1)

Yaw Angle	Pitch Angle																						
	-75	-60	-45	-30	-15	0	15	30	45	60	75	90	105	120	135	150	165	180	195	210	225	240	255
87	0.192	0.178	0.175	0.188	0.240	0.867	*	0.449	0.216	0.175	0.163	0.162	0.170	0.187	0.217	0.280	0.494	*	*	*	*	0.400	0.280
80	0.199	0.186	0.183	0.211	0.312	*	*	0.321	0.217	0.178	0.172	0.172	0.181	0.199	0.237	0.282	0.443	*	*	*	*	0.600	0.296
75	0.208	0.197	0.194	0.237	0.471	*	*	0.275	0.218	0.181	0.181	0.182	0.192	0.211	0.259	0.296	0.420	*	*	*	*	1.471	0.336
70	0.220	0.214	0.211	0.282	*	*	0.675	0.254	0.219	0.188	0.194	0.198	0.208	0.233	0.282	0.312	0.420	0.980	*	*	*	*	0.400
65	0.245	0.231	0.241	0.368	*	*	0.400	0.240	0.220	0.203	0.211	0.224	0.243	0.262	0.471	0.333	0.418	0.816	*	*	*	*	0.627
60	0.296	0.282	0.318	*	*	*	0.331	0.233	0.221	0.237	0.270	0.285	0.321	0.368	0.347	0.400	0.471	0.980	*	*	*	*	*
55	0.420	0.400	0.504	*	*	*	0.296	0.237	0.249	0.303	0.400	0.431	0.786	0.786	0.400	0.546	0.546	0.980	*	*	*	*	*
50	*	*	*	*	*	0.546	0.282	0.249	0.296	0.420	0.980	1.315	*	*	0.504	0.980	0.786	0.980	*	*	*	*	*
45	*	*	*	*	*	0.365	0.282	0.281	0.383	0.497	*	*	*	*	0.600	*	*	1.572	*	*	*	*	*
40	*	*	*	*	0.600	0.303	0.288	0.321	0.675	0.504	1.471	1.471	*	*	0.867	*	*	*	1.471	*	*	*	*
35	*	*	*	*	0.342	0.296	0.303	0.400	*	0.471	0.546	0.487	0.786	*	1.471	*	*	*	*	*	*	*	*
30	*	*	*	0.443	0.312	0.288	0.342	0.675	*	0.420	0.368	0.331	0.400	0.675	*	*	*	*	*	*	*	*	*
25	*	1.154	0.420	0.340	0.291	0.299	0.395	*	*	0.377	0.303	0.282	0.301	0.378	0.980	*	*	*	*	*	*	1.074	4.159
20	0.504	0.368	0.331	0.296	0.275	0.342	0.504	*	0.867	0.321	0.264	0.249	0.254	0.312	0.675	*	*	*	*	*	2.401	0.546	0.786
15	0.336	0.312	0.275	0.270	0.282	0.420	1.471	*	0.504	0.264	0.237	0.230	0.230	0.275	0.443	*	*	*	*	*	1.471	0.471	0.546
10	0.282	0.259	0.249	0.259	0.288	0.546	*	*	0.383	0.249	0.220	0.214	0.217	0.249	0.354	0.786	*	*	*	*	0.980	0.443	0.410
5	0.252	0.237	0.237	0.249	0.303	0.980	*	0.980	0.321	0.233	0.208	0.203	0.208	0.237	0.313	0.546	*	*	*	*	0.980	0.420	0.354
0	0.249	0.236	0.235	0.256	0.328	1.698	*	0.468	0.289	0.226	0.204	0.201	0.208	0.232	0.287	0.457	*	*	*	*	0.278	0.443	0.328
-5	0.252	0.237	0.249	0.275	0.443	1.860	*	0.383	0.282	0.230	0.208	0.203	0.211	0.237	0.282	0.400	1.471	*	*	*	*	0.471	0.342
-10	0.254	0.245	0.296	0.331	0.786	1.386	*	0.342	0.275	0.233	0.217	0.214	0.220	0.245	0.282	0.383	0.786	*	*	*	*	0.546	0.391
-15	0.270	0.259	0.354	0.420	*	1.315	0.980	0.321	0.270	0.245	0.226	0.226	0.233	0.259	0.285	0.383	0.675	*	*	*	*	0.786	0.471
-20	0.296	0.282	0.420	0.600	*	1.254	0.600	0.312	0.275	0.259	0.245	0.249	0.254	0.275	0.303	0.383	0.675	*	*	*	*	0.600	0.500
-25	0.345	0.332	0.675	0.954	*	1.200	0.471	0.326	0.296	0.280	0.280	0.282	0.285	0.293	0.331	0.389	0.594	*	*	*	*	*	0.532
-30	0.443	0.471	0.627	*	*	0.675	0.400	0.331	0.331	0.331	0.383	0.368	0.342	0.354	0.368	0.400	0.600	*	*	*	*	*	*
-35	0.980	*	0.600	*	*	0.600	0.400	0.368	0.420	0.504	0.786	0.675	0.546	0.504	0.457	0.504	0.600	*	*	*	*	*	*
-40	*	*	0.600	*	1.471	0.546	0.420	0.443	0.980	*	*	*	*	*	0.786	0.675	0.675	*	*	*	*	*	*
-45	*	*	0.600	1.471	0.620	0.504	0.484	0.832	*	*	*	*	*	*	*	*	*	*	*	*	*	*	*
-50	*	*	0.546	0.675	0.471	0.546	0.600	*	*	*	*	*	*	*	*	*	*	*	*	*	*	*	*
-55	*	*	0.546	0.546	0.420	0.786	*	*	*	*	*	*	*	*	*	*	*	*	*	*	*	*	*
-60	0.980	0.980	0.524	0.443	0.420	0.980	*	*	*	*	*	*	*	*	*	*	*	*	*	*	*	2.941	1.154
-65	0.600	0.497	0.504	0.412	0.449	1.154	*	*	*	*	0.800	0.980	*	*	*	*	*	*	*	*	*	0.980	0.675
-70	0.420	0.443	0.471	0.420	0.471	*	*	*	0.600	0.400	0.504	0.600	*	*	*	*	*	*	*	*	*	0.786	0.546
-75	0.383	0.383	0.443	0.443	0.675	*	*	*	1.471	0.368	0.303	0.368	0.400	*	*	*	*	*	*	*	*	0.675	0.471
-80	0.354	0.368	0.420	0.504	*	*	*	*	0.443	0.289	0.254	0.288	0.321	0.600	*	*	*	*	*	*	*	0.600	0.420
-87	0.341	0.343	0.391	0.666	*	*	*	0.501	0.281	0.235	0.225	0.237	0.275	0.372	1.154	*	*	*	*	*	*	0.600	0.420

*No loss of track, motor torque exceeds plume induced torque.

3.3-4

SNA-8-D-027(I), Rev 3

3.4 COMMAND MODULE REACTION CONTROL SUBSYSTEM

3.4.1 ENGINE FIRING DATA

3.4.1.1 Minimum Engine Inlet Pressure

No minimum limit has been determined; however, performance degradation occurs at low inlet pressure.

3.4.1.2 Minimum Injector Temperature

The minimum injector temperature for reliable engine operation is 28 F. If the indicated temperature is below 28 F, the command module RCS injectors require 20 minutes of heating within one hour of CM/SM separation to prevent propellant freezing at the injector. See paragraph 4.4.4 for discussion.

3.4.1.3 Firing Time Limitations

Critical engine on-off time sequence limitations are as follows:

Automatic coil	None; maximum pulsing frequency - 30 cycles per second.
Direct coil	None was found during testing based on normal usage of the hand controller.

Qualification Limit	*De-Orbit Burn	Normal Entry
Single firing	200 seconds at the performance shown in Figure 4.4-4; 50 seconds at unspecified performance.	30 seconds; 70 seconds at unspecified performance.
Accumulative firing (pulse mode plus steady state)	200 seconds at the performance shown in Figure 4.4-4; 15 seconds of unspecified pulse mode performance and 50 seconds of steady-state unspecified performance.	130 seconds of pulse mode; 70 seconds steady state at unspecified performance.
Number of firing cycles	106	3000

*Numbers for de-orbit burn are based on command module RCS duty cycle contained in Rocketdyne Report R-7444-1, Final Report, Second Supplemental Qualification Test Program for the Apollo Command Module Rocket Engines (6 August 1968) - pitch engines only.

3.4.1.3.1 LM Impingement

In a contingency situation with a normally docked LM and CM (SM jettisoned) and when the CM RCS is required to control attitude, the maximum allowable continuous firing of the CM RCS is 11.5 seconds. Exceeding this limit will cause damage to the LM thermal shield aluminum frames. Damage to the forward LM S-band omni antenna will occur after 14 seconds and damage to the ascent stage thermal blankets will result after 18 seconds.

3.4.2 VOLTAGE AND CURRENT LIMITATIONS

Engine propellant valves	Operating range 21 to 32 Vdc at valves
Propellant isolation valves	18 Vdc minimum, 33 Vdc maximum
Squib valves (controlled by current rather than by voltage):	
Helium isolation	5 amperes minimum as installed in CM, no maximum requirement
Helium interconnect	5 amperes minimum as installed in CM, no maximum requirement
Helium bypass	5 amperes minimum as installed in CM, no maximum requirement
Propellant interconnect	5 amperes minimum as installed in CM, no maximum requirement
Propellant overboard	5 amperes minimum as installed in CM, no maximum requirement

3.4.3 MINIMUM HELIUM SOURCE PRESSURE

Minimum helium source pressure required to use all deliverable propellants in normal firing modes: 3600 psia at 70 F.

Assumptions-Maximum regulator pressures and tank volumes, and system conditions at propellant depletion of the following:

Helium bottle	400 psia at -25 F
Propellant tanks	301 psia at 40 F
Ullage saturation	0 percent

3.4.4 COMMAND MODULE RCS PRESSURE-TEMPERATURE LIMITATIONS

For command module RCS pressure-temperature limitations, see paragraph 3.4.4 in the appropriate spacecraft appendixes.

3.4.5 TEMPERATURE LIMITS

Detailed temperature limit and rationale are presented in Table 3.11-4.

3.5 SERVICE PROPULSION SUBSYSTEM (SPS)

3.5.1 SPS BURN LIMITATIONS BETWEEN LUNAR MODULE DESCENT PROPULSION SUBSYSTEM FIRINGS

The use of the SPS after a prolonged -g environment is permissible only if the following operational rules are adhered to.

1. For normal SPS operations, ullage maneuvers are required if total propellant remaining is less than 22,300 pounds. If the individual PUGS readout for both the oxidizer and the fuel is greater than 56.4 percent, a minimum ullage in the sump tanks exists and no ullage maneuver is required. However, an ullage maneuver is normally required after a docked DPS burn regardless of gauge readings.
2. The number of LM firings is not restricted by the SPS nor is the number of SPS firings before and after docked lunar module burns. However, the first SPS firing following a lunar module docked burn should be of a minimum continuous duration of 40 seconds if the docked burn results in CSM -X acceleration in excess of 0.1 g. If the engine is shut down prematurely, the following apply:
 - a. A total accumulation of 4 seconds of burn time is permitted as long as the subsequent burn when combined with previous burns totals 40 seconds duration. All of these burns should be preceded by a four-jet ullage.
 - b. If the SPS burn following the docked DPS burn is terminated between 4 and 40 seconds, then a no-ullage restart is recommended as soon as possible until 40 seconds of accumulated burn time is achieved. This restart is to assure a low probability of helium bubbles being present next to the engine ball valves at time of ignition.
3. If the docked lunar module burn results in CSM -X acceleration less than 0.1 g, the subsequent SPS burn requires an ullage settling of the SPS in accordance with paragraph 4.5.3.1 but no other special procedure.

3.5.2 ULLAGE REQUIREMENTS

1. If the SPS must be reignited after a premature shutdown (except when both sump tanks are filled with propellants), a full direct service module RCS ullage is mandatory unless reignition is accomplished sooner than four seconds after a premature shutdown.
2. If RCS ullage is not available, a critical burn may be initiated without ullage.

7/9/71

3.5.3 SPS ENGINE FLANGE TEMPERATURE CONSTRAINT

The engine flange temperature limit during an SPS burn is 480 F. Ground tests indicate that above this value flange burn-through may be expected at any time, possibly resulting in chamber separation. If the flange temperature exceeds 480 F during a noncritical SPS burn, except during an LOI burn, the burn will be terminated and further noncritical SPS burns will be inhibited. The SPS may be used for subsequent critical burns if the flange temperature, as indicated by telemetry, has decreased to 145 F or less. Critical SPS burns and LOI burns will be continued if the engine flange temperature exceeds 480 F. (See Table 3.11-5.)

3.5.4 SPS HELIUM AND GN₂ PRESSURE-TEMPERATURE LIMITATIONS

The SPS helium and GN₂ bottle pressure-temperature limitations are given in paragraph 3.5.4 of the appropriate spacecraft appendixes. The GN₂ bottle pressurization lower limits are 450 and 400 psia for noncritical and critical burns, respectively. (A discussion of GN₂ bottle pressurization lower limits may be found in paragraph 4.5.5.1.)

3.5.5 PROPELLANT PRESSURIZATION LIMITS

The propellant tank inlet lower pressure limits are 115 and 160 psi for critical and noncritical burns, respectively. The limit on ΔP between the fuel and oxidizer tank pressures is 20 psi. (A discussion of these propellant pressurization limits can be found in paragraph 4.5.5.3.)

3.5.6 FUEL AND OXIDIZER FEEDLINE TEMPERATURE LIMIT

The fuel and oxidizer feedline temperature constraints (SP0048T and SP0049T) are as follows: Noncritical SPS burns shall be inhibited if the fuel or oxidizer feedline temperature is less than 40 F. Critical SPS burns shall be inhibited if the fuel or oxidizer feedline temperature is less than 25 F.

3.5.7 SPS ACTUATOR CLUTCH TEMPERATURE LIMIT

The established maximum operational temperature limit of the clutch at the end of an SPS firing is 500 F. (A discussion of SPS motor and clutch temperature characteristics can be found in paragraph 4.5.4.3.)

3.5.8 SPS ENGINE THRUST CHAMBER PRESSURE LIMIT

The SPS engine thrust chamber lower pressure limit for noncritical burns is 70 psia. (A discussion of this limit can be found in paragraph 4.5.5.3.)

1/21/71

3.5.9 MINIMUM BURN TIME FOR THE SPS ENGINE

The following constraints on the SPS engine minimum burn time have been established. (A discussion of them may be found in paragraph 4.5.1.2.)

For Noncritical Burns

1. No burn less than 0.50 second (time from engine start signal to engine shutdown signal, or G&C thrust-on signal duration of 0.35 second).
2. No two consecutive engine burns with accumulative burn time less than 1.5 seconds if the propellant valve temperature is colder than 40 F.
3. No three consecutive engine burns within a two-hour period with accumulative burn times less than 4.0 seconds if the propellant valve temperature is colder than 40 F.
4. No engine restart in less than 60 seconds after a previous shutdown.

For Critical Burns

5. For critical engine burns there is no minimum burn time or minimum coast period constraint.

A critical burn is any engine burn used to save the crew, vehicle, or mission from loss or failure.

3.5.10 PRESSURE-TEMPERATURE LIMIT RELATIONSHIP FOR SPS PROPELLANT TANKS

For SPS pressure-temperature limitations, see paragraph 3.5.10 in the appropriate spacecraft appendixes.

3.5.11 SPS ENGINE VALVE TEMPERATURE

See Table 3.11-5.

3.5.12 MAXIMUM SPS BURN TIMES

See communications constraint (paragraph 3.7.4.2) for high-gain antenna imposed limit.

3.6 GUIDANCE AND CONTROL SUBSYSTEM

3.6.1 IMU WARMUP AND POWER DOWN

The CMC must be in operation at any time IMU operate power is applied to ensure control and protection of the IMU, including proper moding, caution and warning functions, and synchronization pulses.

When the GNCS is powered up from standby it is ready for start of orbital IMU alignment within 100 seconds after application of IMU operate power. It is required to have the system in operate for 15 minutes before using the accelerometers. The 100 seconds allows the gyro wheels to reach proper operating speed and the 15 minutes allows the PIPA's to reach proper operating temperature.

In the event of a bus failure and subsequent IMU operate power dropout or removal of IMU operate power, a 5 minute delay must occur before reapplying operate power to the IMU.

If power is applied before the gyros spin down, the gyro wheel motors will be magnetized, causing the gyros to run at a lower temperature with the attendant performance shifts. Also the turn-on caging with the wheels running will put a higher than normal stress on the gyro wheel bearings, which may result in degraded performance and reliability.

3.6.2 IMU GIMBAL LOCK

The IMU should not be operated close to gimbal lock condition (i.e., middle gimbal angle of 90°). The GNCS provides a gimbal lock caution light when the middle gimbal reaches $\pm 70^\circ$ and automatically loses inertial reference (by switching to coarse align mode) when the middle gimbal angle exceeds $\pm 85^\circ$. Automatic attitude maneuvers should be monitored to avoid IMU gimbal lock condition, as there is no provision for automatic gimbal lock avoidance.

3.6.3 IMU ORIENTATION

IMU orientation determination sightings must be performed with the following spacecraft attitude constraints.

- 1) The spacecraft orientation should be such as to place the spacecraft between the sun and the scanning telescope aperture.
- 2) In the docked configuration the spacecraft orientation in addition to shadowing the sun should minimize reflected light from LM.

In earth and lunar orbit, sightings must be constrained to the shadow side of the body.

3.6.4 SCS GIMBAL LOCK

The FDAI ball has the plus and minus yaw poles marked in red, indicating the gimbal-lock area. The two red areas are for yaw angles of ± 75 degrees or greater. These markings provide the astronaut with a visual indication when the gimbal-lock region is being approached.

3.6.5 LINE-OF-SIGHT ANGLE TO LANDMARK

For earth landmarks the line-of-sight to the landmark must make an angle of less than 55 degrees with local vertical at the landmark. (Lack of contrast and foreshortening may otherwise cause landmark mis-identification). For lunar landmarks this constraint may be increased to 65 degrees.

3.6.6 OPTICS LINE-OF-SIGHT RATES

During landmark tracking in earth or lunar orbit, the maximum drive rates of the optics must not be exceeded. Drive rate limits and instructions for preventing the required drive rates from exceeding these limits are contained in paragraph 4.6.3.2, "Optical Blind Zone."

3.6.7 BODY MOUNTED ATTITUDE GYRO WARMUP TIME

The body mounted attitude gyros (BMAG's) require 40 minutes warmup time prior to use. Rate and attitude error accuracy are impaired if BMAG's are operated at other than nominal operating temperature.

3.6.8 OPTICS MINIMUM ALLOWABLE ANGLES

To prevent sun interference with use of the optics, the minimum angle from the sextant landmark line of sight to the vehicle sunline is a function of star magnitude, but must be no less than 10 degrees. The minimum angle from the telescope line of sight to the sun is 60 degrees.

The minimum allowable angle between the sextant star line of sight and the edge of the moon is 5.0 degrees. Reflected light from the lunar surface may obscure the star at angles of less than 5.0 degrees.

3.6.9 OPTICS WARMUP

Optics must be allowed to warm up for 30 minutes in the expected tracking attitude prior to use.

3.6.10 AUTOMATIC POSITIONING OF OPTICS

The IMU must be aligned before automatic positioning of optics can be used for star acquisition for navigation purposes.

3.6.11 OPTICS COVERAGE

The effective optics coverage is shown in Figure 4.6-2. Star/landmark, star/horizon, and any operations requiring use of the optics should be

planned to conform to the limitations imposed by Figure 4.6-2. The limitations of the scanning telescope may also apply to the sextant when the sextant and the telescope are used together.

3.6.12 SEXTANT CALIBRATION

The sextant must be calibrated prior to each batch of cislunar navigation optic sightings. If the sun is within a 15-degree half-cone angle from the LLOS, calibrations must be checked every 30 minutes during navigation optic sightings. Successful calibrations will occur when successive marks agree to within 0.003 degree.

3.6.13 HORIZON LIGHTING

During horizon sightings, the sun elevation at the substellar point must be greater than 10 degrees.

3.6.14 STAR BRIGHTNESS MAGNITUDE

Star brightness magnitudes must be equal to, or brighter than, +1.6 for star/earth landmark observations and +2.3 for star/lunar landmark observations; magnitude +3.5 is adequate for star/lunar horizon observations, and (assuming an upper threshold locator is used) stars of magnitude +3.0 or brighter may be used for star/earth horizon sightings.

3.6.15 IMU HEATERS MAXIMUM VOLTAGE

The maximum voltage at which the IMU heaters are capable of operating for periods up to 10 hours with normal coolant-flow is 32 Vdc. For the no-coolant-flow case, refer to Table 4.2-1.

Operation of the IMU heaters at 35 Vdc for a sustained period of time may cause the loss of the R63 resistor in the IRIG and PIPA module of the G&N signal conditioner. (One test case at 35 Vdc for 10 hours has been performed at Delco, Milwaukee during which R63 resistor did not fail.) The loss of this resistor would mean the loss of measurements CG2117V, CG2147V and CG2177V (IGA, MGA, OGA servo errors).

3.6.16 CMC MAXIMUM VOLTAGE

The maximum voltage at which the CMC is capable of operating with normal coolant-flow is 34 Vdc. For the no-coolant-flow case refer to Table 4.2-1.

3.7 COMMUNICATIONS SUBSYSTEM

3.7.1 USB EQUIPMENT

3.7.1.1 Warmup Time

The USB power amplifier must warm up approximately 90 seconds before normal RF amplification values are reached.

3.7.2 RENDEZVOUS RADAR

3.7.2.1 Transponder (X-Band) Warmup Time

The rendezvous radar transponder (X-band) requires approximately 24 minutes to reach operational stability.

3.7.2.2 Antenna Coverage Patterns

The maximum range for operation of the rendezvous radar is determined by the coverage pattern of the RR transponder in the CSM. The coverage pattern varies with CSM attitude. Paragraph 4.7.2 and corresponding figures show this coverage.

3.7.3 FLIGHT QUALIFICATION RECORDER

Intentionally left blank.

3.7.4 HIGH-GAIN ANTENNA

3.7.4.1 Maximum Slew Rate

The high-gain antenna maximum slewing rate is 5 degrees per second in any axis. (Reference Specification MC481-0008, Antenna Equipment, High Gain, states the tracking requirement of 5 deg/sec for vehicle rates.)

3.7.4.2 Limit on SPS Burn Duration

SPS burns of more than 450 seconds may result in permanent damage to the high-gain antenna. They may occur during SPS abort situations. Damage to the high-gain antenna under these circumstances is acceptable because communications by means of the omnidirectional antennas will be adequate.

3.7.5 VHF

3.7.5.1 Maximum Telemetry Range Between LM and CSM

The maximum range of VHF telemetry transmission between the LM and the CSM is 320 nautical miles. (Refer to LEM Performance and Interface Specification, Block II, SID 62-1244A.)

3.7.5.2 Maximum Voice Range Between LM and CSM

The maximum specified range of VHF voice transmission between the LM and CSM is 550 nautical miles. (Refer to LEM Performance and Interface Specification, SID 62-1244A.)

3.7.5.3 Maximum Range and Accuracy of VHF Ranging System Between CSM and LM

The maximum range of the VHF ranging system between the CSM and the LM is 200 nautical miles with an accuracy of ± 450 feet between 500 feet and 200 nautical miles. This range includes bias error (± 270 feet) and random error (± 180 feet). The bias error is a measurable quantity for each spacecraft and can be found in the appropriate appendixes.

3.7.5.4 Voice Constraint During Ranging Acquisition

VHF voice communications between the CSM and LM must be suspended during the acquisition phase of VHF ranging (approximately 12 to 14 seconds).

3.7.5.5 LM VHF PCM Data Constraint

LM PCM data cannot be transmitted to the CSM during VHF ranging operation.

3.7.5.6 Ranging Display Resolution

The display resolution of the entry monitor system is 0.01 nautical mile. The decimal point is blanked out in the VHF ranging mode.

3.7.5.7 Loss of "Data Good" Signal

Loss of the VHF ranging "data good" signal will be presented to the crewman as blanking of the EMS display with the exception of the last two digits on the right-hand side, which will show zeros.

3.7.5.8 Temperature Limitations

See Table 3.11-7.

3.8 STRUCTURES

The information presented in this subsection applies only to the Saturn V launches. Structural data pertinent to Saturn IB launches can be found in the individual spacecraft appendixes, where applicable.

3.8.1 BOOST PHASE

The boost profile must be limited to the maximum structural loads, maximum vibration, maximum acoustic levels, and aerodynamic heating for which the CSM was designed.

3.8.1.1 Maximum Dynamic Pressure and Maximum q_a

Structural loads in the maximum q_a region are calculated from a launch day simulation using measured winds aloft. These structural loads are compared with allowable load envelopes prepared by the contractor for that particular spacecraft.

3.8.1.2 Maximum Acceleration

Structural loads due to the end-of-boost maximum acceleration condition, as prescribed in the Mission Operational Trajectory, are evaluated before flight to assure that adequate factors of safety will be maintained.

3.8.1.3 Vibrations and Acoustics

Vehicle vibrations occur as low-frequency, sinusoidal oscillations resulting from booster engine excitations, and as broad-band, random vibration resulting from acoustic or aerodynamic noise impinging on the vehicle outer shell. The maximum sinusoidal vibration for a high performance booster occurs between 4 and 35 Hz, with a maximum amplitude of 0.25g peak. Vibrations for individual structures are as follows:

1. LES Vibrations

The maximum vibration occurring as broad-band, random vibrations resulting from engine or aerodynamic noise for high "Q" abort is: Acceleration spectral density (ASD) increasing at the rate of 6 dB/octave from 20 Hz to 400 Hz, and constant at 0.8 g^2/Hz , from 400 Hz to 2000 Hz.

2. CM Vibrations

The maximum vibration occurring as broad-band, random vibrations resulting from engine or aerodynamic noise for high "Q" abort is: ASD increasing at the rate of 9 dB/octave from 20 Hz to 100 Hz, and constant at 1.6 g^2/Hz from 100 Hz to 2000 Hz.

3. SM Vibrations

The maximum vibration occurring as broad-band, random vibrations resulting from engine or aerodynamic noise for the transonic (Mach 1) flight period is: ASD increasing at the rate of 9 dB/octave from 20 Hz to 200 Hz, constant at 35 g^2/Hz from 200 Hz to 400 Hz, and ASD decreasing at the rate of 6 dB/octave to 2000 Hz.

4. SLA Vibrations

The maximum vibration occurring as broad-band, random vibrations resulting from engine noise for lift-off is: ASD increasing at the rate of 6 dB/octave from 20 Hz to 100 Hz, constant at 2.25 g^2/Hz from 100 Hz to 350 Hz, and ASD decreasing at the rate of 6 dB/octave to 2000 Hz.

The CSM/SLA structures are adequate to withstand the random vibrations generated during an off-nominal boost in which the maximum aerodynamic pressure reaches 790 psf for an S-IC booster.

3.8.1.4 Aerodynamic Heating

The aerodynamic heating environment is evaluated prior to flight by comparing the mission operational trajectory velocity/altitude history with that of previously analyzed maximum aerodynamic heating design trajectories. If the mission operational trajectory parameters indicate more severe heating than the maximum design trajectory, a detailed thermal analysis is performed for the prediction of structural temperatures during the boost phase.

3.8.1.5 Cabin Overpressure

The CM inner structure is designed for an internal pressure of 8.3 psi above the external pressure and has an analytical factor of safety of 2.5. The maximum possible internal pressure differential of 16 psi (1.5 psid above ambient on the pad) has an analytical factor of safety of 1.3 associated with it. These data are based upon extrapolation of CM 004 test data (reference SD 68-293), analysis, and data from CM 012. The demonstrated capability for the CM internal pressure is 12.9 psi.

The critical area for internal pressure is the aft bulkhead. In the event that the cabin pressure relief valve fails to vent resulting in a 16 psid cabin pressure, the CM should not abort but go to orbit.

3.8.2 SPACE FLIGHT ENVIRONMENT

3.8.2.1 Unified Crew Hatch

The total allowable hatch open time has been reviewed for the nominal sun look angles during EVA. Analysis of temperatures induced by this orientation indicates that the hatch can remain open for 2.5 hours at which time elements of the hatch structure become heated to temperatures more severe than those encountered during the certification test of the unified crew hatch. See paragraph 3.10.5 of appropriate appendix.

3.8.2.1.1 CSM Attitude Constraint for Open Hatch Operation

Figure 3.8-2 defines the envelope of solar vectors necessary for prevention of CM cabin solar shafting during open hatch operations. (See paragraph 3.8.2.1.)

3.8.2.2 Service Module Plume Impingement

In order to prevent excessive SPS tank temperatures and local structure burn through, the maximum continuous burn time of the service module RCS engines is limited to 750 seconds.

3.8.2.3 Docking Velocity and Alignment

The LM/CSM docking must be accomplished within the following constraints:

- | | |
|--|--|
| 1. Axial (closing) velocity
Maximum = 1.0 ft/sec

Minimum = 0.1 ft/sec | Structural damage to both LM and CSM may result.

Required for latches to close. |
| 2. Radial (transverse) velocity

≤ 0.5 ft/sec | Structural damage to both LM and CSM may result. |
| 3. Angular velocity (about any axis)

≤ 1 deg/sec | Structural damage to both LM and CSM may result. |
| 4. Radial alignment of X axes

≤ 1.0 ft | To assure probe hits within drogue. |
| 5. Angular alignment of X axes

≤ 10 deg | Based on probe/drogue interference and CM structural strength during latch up. |
| 6. Roll attitude at probe retract is 60 ± 10 degrees between the CSM -Z axis and the LM +Z axis (refer to Figure 4.8-2). | To allow CM-LM umbilical connection and to prevent thruster impingement on RR antenna. |

3.8.2.4 Docking Probe Extension

If the docking probe does not extend the full 9.8 inches, the maximum axial closing velocity may be reduced below the 1.0-foot-per-second limit given in paragraph 3.8.2.3. (Note: All other contact criteria should be nominal, i.e., near zero.) Permissible axial velocities are shown in Figure 4.8-3.

3.8.2.5 Docking Latches

For docked DPS or SPS burns, at least nine latches are required.

3.8.2.6 Docking Probe Temperature

Probe temperature must not be lower than 0 F in earth orbit with a loaded (no restart) S-IVB vehicle or lower than -20 F during all other dockings. Structural damage to both lunar module and command module may result because of degradation in shock absorber capabilities. Additional information on temperature limitations is given in Table 3.11-9.

3.8.2.7 Docking Pre-Loaded Probe RCS Activity

For CM-to-tunnel ΔP of 0 to 3.5 psid, there should be no-jet control (roll command) about the docking tunnel centerline of either the LM or the CSM.

For CM-to-tunnel $\Delta P \geq 3.5$ psid, there should be no more than two-jet control (roll command) about the docking tunnel centerline of either the LM or the CSM.

For tunnel vented (CM-to-tunnel $\Delta P > 4.0$ psid for a minimum of 10 minutes), there should be no more than four-jet (roll command) control about the docking tunnel centerline of either the LM or the CSM.

3.8.2.8 LM/CSM Docked Maneuvers

The LM and CSM must be hard docked during any and all docked attitude or ΔV maneuvers, or the docking tunnel area structure may be damaged.

3.8.2.9 Passive Thermal Control

3.8.2.9.1 Service Module RCS Heaters Active

CSM passive thermal control (PTC) is an X-axis rotation mode (0.1 degree per second or greater) required for a minimum of approximately 80 percent of translunar and transearth coast time. PTC is executed when the angle between the sun vector and the normal to the CSM X-axis is no greater than ± 20 degrees. Excursions to ± 30 degrees are permitted should they be required to satisfy other constraints. However, these excursions are considered to fall outside the normal PTC activity and are subject to the same criteria as fixed attitude hold times that are limited to approximately 20 percent (cumulative) of translunar and transearth coast time.

Spacecraft design is based on attitude hold in an arbitrary attitude for a maximum of three hours. Hold periods in excess of this time may be allowable, depending on particular spacecraft attitudes and temperatures. Attitude hold periods nominally require subsequent PTC periods of five to seven times the duration of the attitude hold.

3.8.2.9.2 Service Module RCS Heaters Inactive

Deactivation of the service module RCS quad heaters during the PTC roll of the translunar phase is an emergency means of conserving cryogenics during flight. For this mode of operation, the following additional constraints are required:

1. The angle between the solar vector and a perpendicular to the CSM X-axis shall not exceed ± 20 degrees with heaters off.
2. The roll rate shall be 0.2 degree per second or greater with heaters off.
3. Any deviation from additional constraints 1 and 2 will require immediate service module RCS heater activation.

During this mode, PTC roll with service module RCS heaters inactive, the four package temperatures will fall below their lower caution and warning limits. Accordingly, the master alarm signal will be activated at least once and possibly three times for each quad after the mode initiation. The four service module RCS caution and warning lights will be activated in conjunction with the master alarms and will remain continuously "on" following the last master alarm.

3.8.2.10 Boom Retraction Restrictions

SIM instrument booms must be retracted and the instruments turned off prior to the establishment of coupled RCS jet attitude control, any SPS maneuver, or EVA. If, however, a boom cannot be retracted and is not within the proximity switch indication (extension ≤ 12 inches) it must be jettisoned prior to the establishment of coupled RCS control or SPS thrusting unless a real-time decision is made not to jettison the boom based upon the data presented in paragraphs 3.1.2.7, 3.1.2.8, 3.6.2.7, or 3.6.2.8 of Volume VI of this data book. Volume VI sections 3.1 and 3.6 also contain additional instrument boom data.

3.8.3 ENTRY PHASE

3.8.3.1 Deceleration Loads

Deceleration loads during entry shall not exceed 20 g's on the command module structure and 18 g's on the crew and the couches. Also see appropriate spacecraft appendices.

3.8.3.2 Aerodynamic Heating

The maximum design entry range is limited to 3500 nautical miles with a maximum inclination of 40 degrees and a maximum entry inertial velocity of 36,333 feet per second, all referenced to an entry altitude of 400,000 feet.

1/14/72

3.8.3.3 Uprighting Limitations

There is an envelope of command module impact center-of-gravity locations outside of which the uprighting subsystem will fail to upright the vehicle from a Stable II attitude. These center-of-gravity limits are shown in Figure 3.8-1. For the two-bag capability, it is assumed that any one bag has failed to inflate. Crew movement is based on two crewmen (140 and 145 pounds) leaving their couches after water impact and positioning themselves in the lower equipment bay area to effect uprighting.

That the command module will impact the water with its center of gravity within two-bag limit (two-crewman movement) line must be verified prior to each mission. See Figure 3.8-1 for the center-of-gravity limitations.

3.8.3.4 Cabin Underpressure

The CM inner structure has the capability to withstand an external pressure of 10 psi above the internal pressure with a factor of safety of 1.0, based on CM 004 test data (reference SD 68-293). Excessive external pressure was not a design condition.

Test data from water drop test 104 indicates the CM can withstand water impact with cabin pressure 1 psi below ambient.

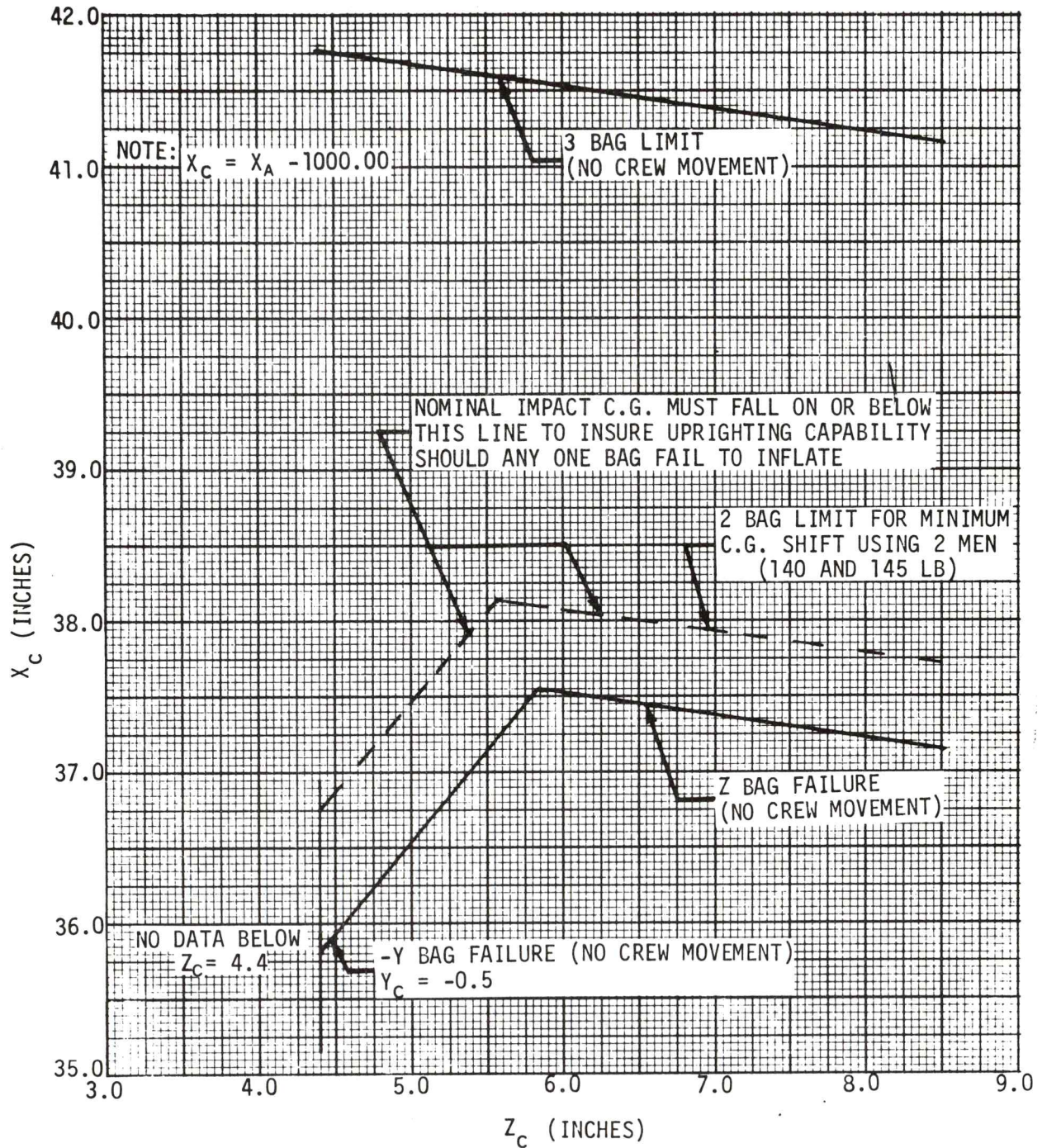


Figure 3.8-1. Block II Command Module Uprighting Capability (Flooded Toroidal Area)

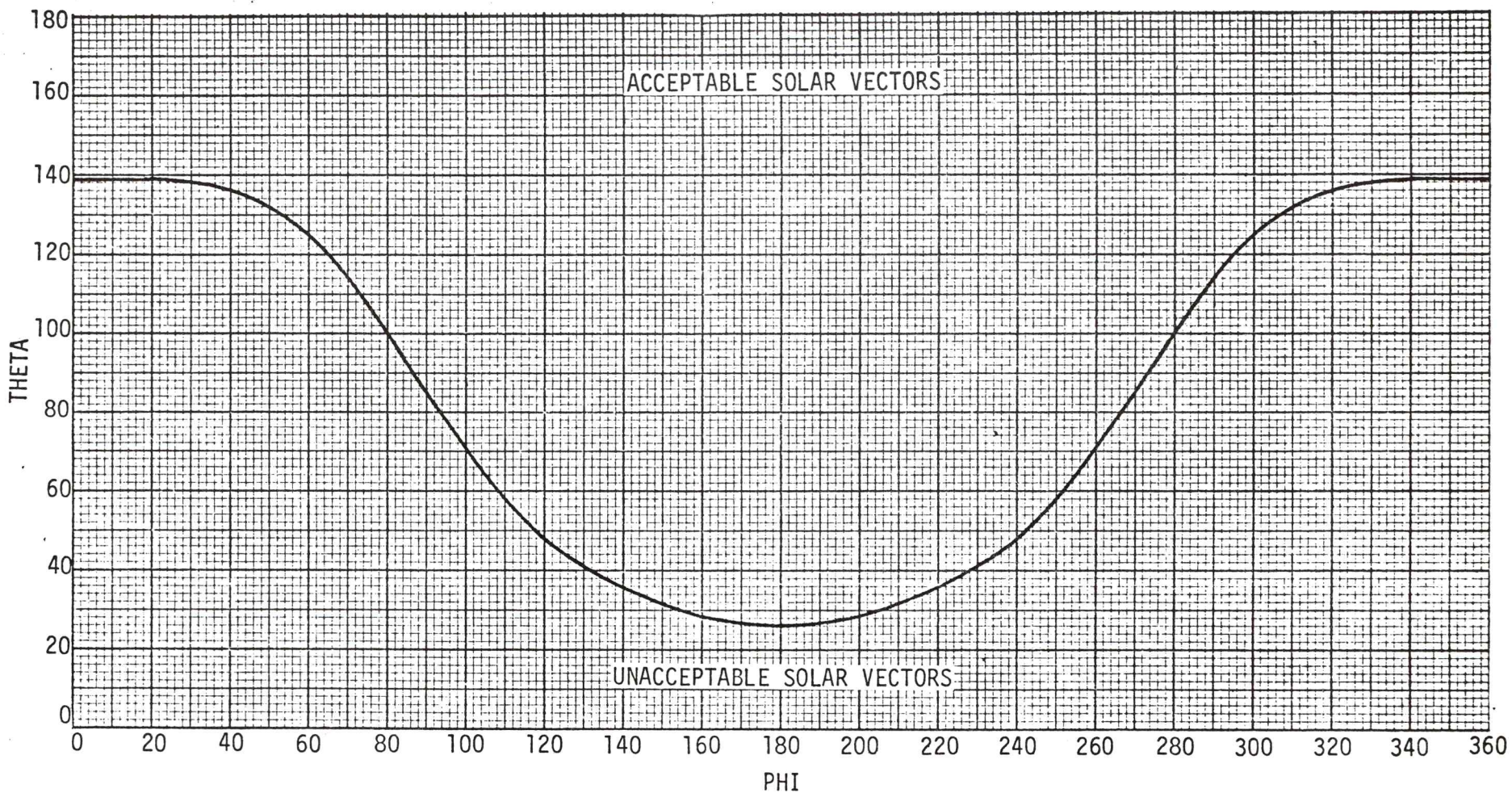


Figure 3.8-2. Envelope of Acceptable Solar Vectors in THETA-PHI Coordinates with Regard to Solar Shafting Through Open CM Side Hatch

3.9 LAUNCH ESCAPE SUBSYSTEM (LES) AND EARTH LANDING SUBSYSTEM (ELS)

3.9.1 LAUNCH ESCAPE SUBSYSTEM

3.9.1.1 Operational Temperature Limits - Solid Propellant Motors

The launch escape subsystem motors have been qualified to operate within the temperatures listed in Table 3.11-6.

3.10 CREW AND CREW SYSTEMS

3.10.1 EXTRAVEHICULAR ACTIVITIES (EVA)

3.10.1.1 Access

The portable life support system (PLSS) and oxygen purge system (OPS), the extravehicular (EV) gloves, and the EV visor assembly are stored in the lunar module (LM). Therefore, EVA's are limited until these items are accessible after docking. EVA's will be attempted only if the tunnel is not negotiable or if docking is not feasible following separated spacecraft maneuvers. EVA without the PLSS and the EV visor assembly is limited to the times when prolonged exposure to sunlight can be avoided and to the distance that the oxygen hose will extend from the command module side hatch. The oxygen hoses of the left and center crewmen are 72 inches long; the hose of the right crewman is 119 inches long. EVA can also be accomplished utilizing the EVA umbilical and OPS.

3.10.1.2 EVA Time Limitation

3.10.1.2.1 PLSS Usage

See SODB Volume IV for PLSS usage.

3.10.1.2.2 OPS Usage

See SODB Volume IV for OPS usage.

3.10.1.2.3 PLSS/OPS Usage

The OPS, when mounted on the PLSS, is a backup unit used only in case of PLSS subsystem failure. The OPS is the prime unit for EVT from the lunar module to the command module and may be used for intravehicular transfer (IVT) in depressurized vehicles.

3.10.1.2.4 Crew Systems Time Limits

The EVA umbilical hose must be maintained at a temperature such that the oxygen temperature at the suit inlet is in the range of 0 to 75°F. See Paragraph 4.10.3.3.

Figure 3.10-1 provides a curve giving umbilical outlet oxygen flow temperatures as a function of EVA elapsed time. The worst hot-case and worst cold-case conditions were generated based upon the related assumptions given on the figure. The figure shows for example, that if the EVA conditions are biased cold, the oxygen umbilical outlet will reach its lower limit of zero (0) degrees after 1.4 hours of elapsed time. Upper and lower umbilical design limits are also shown.

2/16/72

Figure 3.10-2 provides a curve giving oxygen flow suit inlet temperatures as a function of time for the IVA crewman during transearth EVA. "Full sun" based upon a theta (θ) of 140°F to 155°F as shown on Figure 3.10-3 is defined as that condition where the solar vector is perpendicular to the longitudinal axis of the umbilical. The full-sun condition may be problematical and dependent upon the precise tether position taken by the IVA crewman as he stands in the open hatch. For other than full-sun conditions the crewman may be required to move the umbilical so that it does lie perpendicular to the sun. Upper and lower umbilical design limits are also shown.

3.10.1.2.5 CMP PGA Oxygen Pressure with Severed Umbilical

See paragraph 4.10.3.4.

3.10.2 CSM MOTION CHANGES

3.10.2.1 Acceleration

Crew acceleration limits are presented in paragraph 4.10.1.1.

3.10.2.2 Impact

Impact limits of the crew are presented in paragraph 4.10.1.2.1.

3.10.3 CREW TASK REQUIREMENTS

3.10.3.1 Pad Emergency Egress

The command module hatch can be unlocked and opened by a crewman in not more than 3 seconds. The crew can egress (unaided) from the command module within 90 seconds when the boost protective cover (BPC) is installed.

3.10.3.2 Pressure Garment Assembly (PGA) Donning

Each crewman is allowed 20 minutes for PGA donning-60 minutes total for three crewmen (see paragraph 4.10.3.1).

3.10.3.3 CM Oxygen Depletion at Splashdown

If PGA's are worn during entry and the command module oxygen supply is exhausted at splashdown, helmets must be removed within one minute or asphyxiation may result.

3.10.3.4 Carbon Dioxide Buildup

CO₂ can be produced at a specification rate of 0.45 lbs/hr. This would result in a buildup rate of 9.43 mm Hg per hour in a nonventilated cabin. Considering the specification maximum of 16 mm Hg and an initial 3 mm Hg, the total nonventilated time must not exceed 1 hour and 22 minutes. Egress should be completed by this time. The following conditions result in a nonventilated cabin:

1. Stable I orientation and PLV valves cannot be opened.
2. Stable II.

3.10.3.5 Flotation Bag Usage

If the command module assumes the Stable I, apex up, orientation upon splashdown, the crew must wait 10 minutes after landing before inflating the postlanding flotation bags. This allows the ablator to cool sufficiently to avoid destruction of the bags by heat.

If the command module assumes the Stable II, apex-in-the-water, orientation upon splashdown, the forward heat shield will cool immediately. The crew may inflate the postlanding flotation bags without delay to upright the spacecraft. (Text continued on next page.)

3.10.3.6 Side Hatch Opening

The command module cabin pressure must be vented to the surrounding atmosphere and must not exceed 0.1 psi ΔP at initiation of side hatch opening (see paragraph 4.10.3.2).

3.10.3.7 Skin Burn Hazard from Unfiltered Ultraviolet Radiation*

Exposure to direct solar ultraviolet within the command module may result in painful burn somewhere in the range from 40 seconds to two minutes. Moist skin is most susceptible to ultraviolet burns. Also, the thinner the epidermis, the sooner the burn. The lips are second to the eyes in burn susceptibility. Untanned skin surfaces and skin irritated by abrasion also would be particularly sensitive. Table 3.10-1 summarizes the effects of exposure to ultraviolet radiation.

3.10.4 SM/SIM THERMAL DATA DURING EVA (PREDICTED)

(See Paragraph 3.11.4)

3.10.5 CSM ATTITUDE FOR EVA

3.10.5.1 Sun Look-Angle Envelope

Solar illumination of the CSM during EVA is constrained by the SIM, EVA crewmen, CM hatch, TV and film cameras, the high-gain antenna scan limit, ECS umbilical, and the crewman foot restraint. The approved operating area which satisfies these requirements is shown in Figure 3.10-3. *The actual constraint area is larger but will not be determined for the remaining missions because of the extensive analysis involved. Present mission planning indicates that because of the operational characteristics of the missions, definition of this actual constraint area is not required.

3.10.5.2 Nominal Sun Look-Angle for EVA

A solar look-angle which optimizes communications availability and satisfies all thermal and illuminations constraints is defined as $\theta_s = 145^\circ$, $\phi_s = 315^\circ$.

3.10.5.3 Communications Look-Angles for EVA

With the nominal solar look-angle orientation, the high-gain antenna will be in the automatic reacquisition region or the automatic tracking region of coverage. Figure 3.10-4 presents loci of earth positions for 0-30° earth-sun separation angles in 5° increments.

*NASA Data Source

Table 3.10-1 Times of Exposure to Various Ultraviolet Sources for Production of Skin Burns**

Skin Effect	Time Interval of Exposure* (min.)			
	Noon Sun	Solar Flux	Earth Albedo	Lunar Albedo
Erythema Threshold	15-60	0.13-0.40	38-97	58
Vivid Reddening, Later Tan	38-150	0.33-1.0	95-240	55-165
Painful Burn	75-300	0.65-2.0	190-480	110-330
Blistering	150-600	1.3 -4.0	380-960	215-650

* Exposure to noon sun is for a bright summer day on earth at 30° latitude. Other values apply to exposures in space. Values are for cumulative exposure within a 24-hour period.

Summer noonday sun is given to serve as an experience reference. If the exposed astronaut is aware of a particular exposure-to-burn relationship at the Houston latitude, his response to spacecraft flux levels may be identified with better accuracy. The minimum exposure times should be used as limits unless previously reviewed and approved by the MSC Medical Operations Division.

** NASA Data Source

CONDITIONS	HOT CASE	NOMINAL CASE	COLD CASE
Sun Look-Angle (θ_S)	140°	145°	155°
S/M Temperature ($T_{S/M}$)	100F	30F	-25F
EVA Distance from S/M (Z)	18 in	18 in	18 in

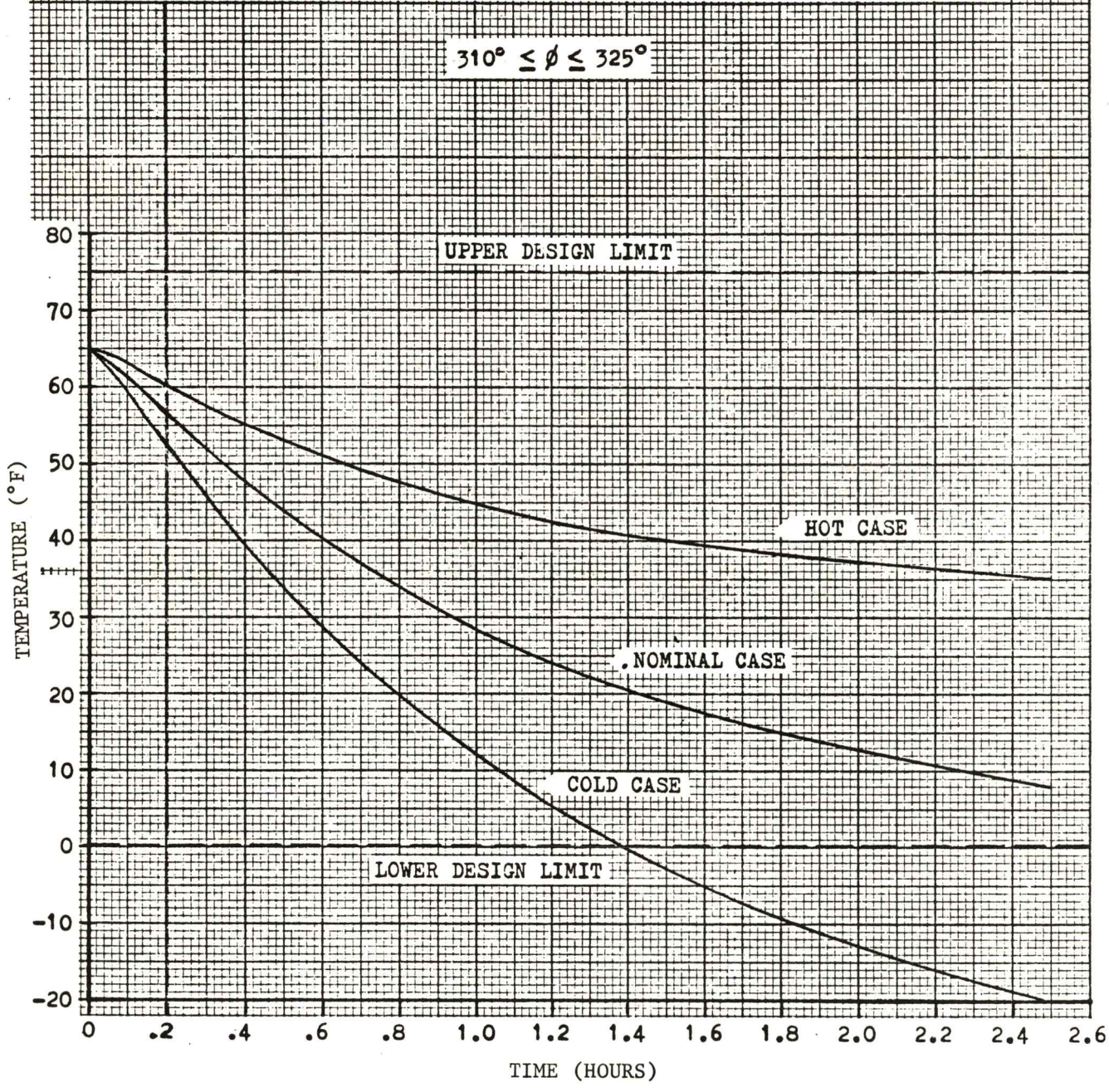


Figure 3.10-1. EVA Oxygen Umbilical Temperature vs. Time
(See paragraph 3.10.1.2.4)

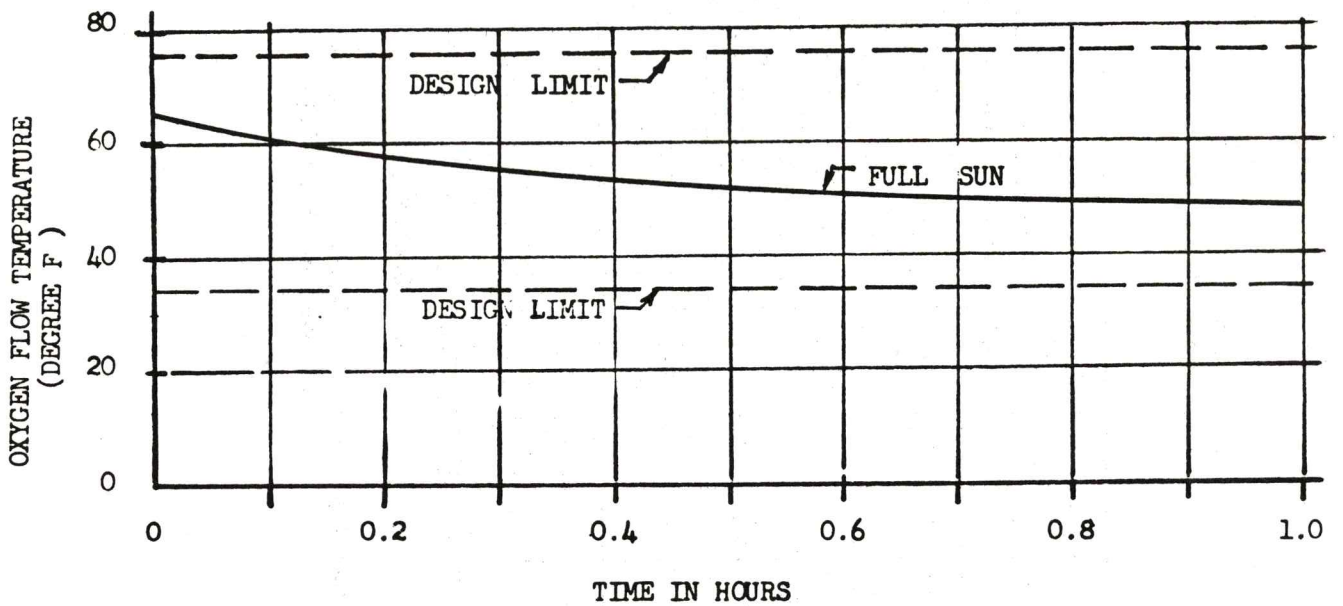


Figure 3.10-2. IVA Oxygen Suit Inlet Temperature vs. Time
(See paragraph 3.10.1.2.4)

*Note: Area defined does not represent an area of constraint, but defines the approved operating area.

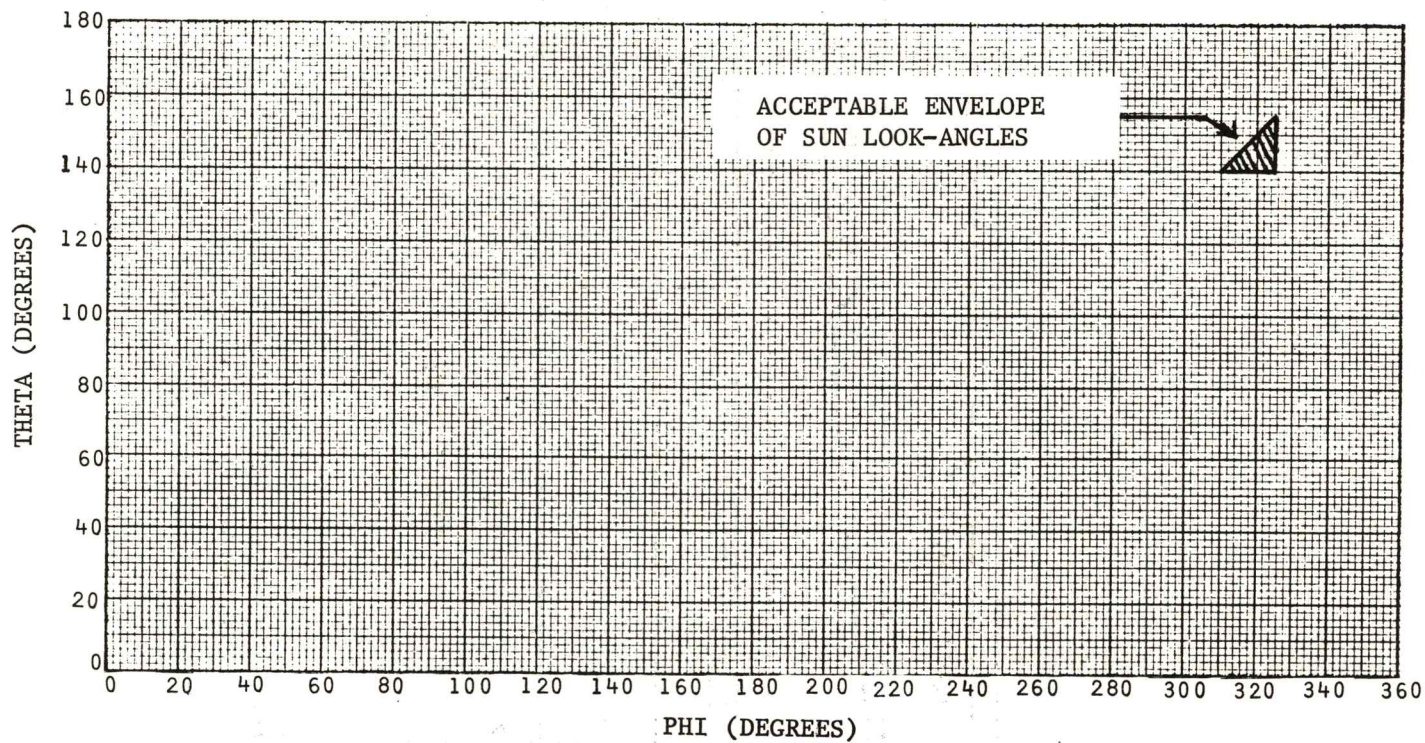


Figure 3.10-3. Envelope of Acceptable Sun Look-Angles for J-Missions EVA
(See Paragraph 3.10.5.1)

*NASA Data Source

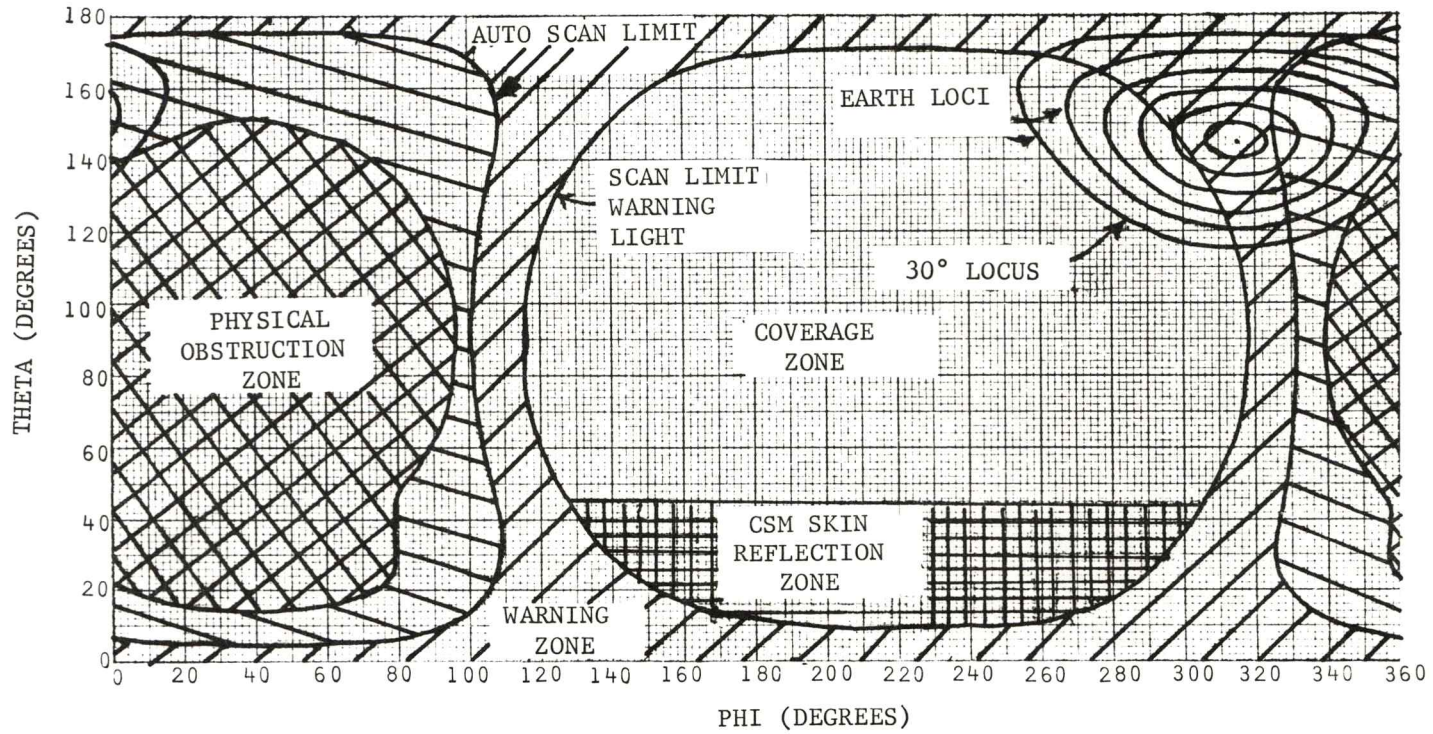


Figure 3.10-4. HGA Coverage--Loci of Earth Positions for 0-30° Earth-Sun Separation
Angles-Sun $\theta=145^\circ$, $\phi=315^\circ$ (See Paragraph 3.10.5.3)

3.11 THERMAL SUBSYSTEMS

3.11.1 TEMPERATURE LIMITS

Tables 3.11-1 through 3.11-10 present thermal data for each subsystem that is thermally critical. Additional supporting data to these thermal limits may be found in Section 4.0 and appropriate spacecraft appendixes.

3.11.2 COMMAND MODULE REENTRY THERMAL LIMITS*

Definition of the Apollo Block II thermal entry limits is based upon the ablation performance of the Avcoat 5026 heat shield at body point H-1. Body location H-1 becomes a critical thermal constraint due to the combination of local ablator thickness and local heating rate. The flight parameters which have the greatest effect on bondline temperature are shown in Table 3.11-11.

The thermal limits are presented as entry corridor maps and are grouped into sets of lift-to-drag ratios and orbit inclinations. Thermal limit line maps for the "guided" and "backup" (constant g) entry modes are presented in Figures 3.11-1 through 3.11-7.

3.11.2.1 Instructions for Use of Entry Thermal Limit Lines

3.11.2.1.1 Guided Entries

Select limit line chart number from Table 3.11-12 on basis of predicted vehicle L/D and orbit inclination at 400,000-foot entry interface. Locate the predicted γ_i and V_i on the selected chart. These entry conditions are thermally acceptable if the identified point is to the left of the range line which is labeled with the approximate predicted entry range from the entry interface location to the landing target. Linear interpolation between lines is permissible. Such conditions will result in bondline temperatures on the TPS below 600 F.

Note: The effects of changing entry range after initiation of entry cannot be predicted directly from these charts. Significant range changes are permissible only if all ranges are shown to be safe for the predicted γ_i and V_i .

3.11.2.1.2 Backup Mode Entries

Select limit line chart number from Table 3.11-12 on basis of predicted vehicle L/D and orbit inclination at 400,000-foot entry interface. Locate the predicted γ_i and V_i on the selected chart. These entry conditions are thermally acceptable for constant g entries if these conditions are to the left of the selected constant g level line.

*NASA Data Source

Note: Changes in g level toward higher g levels are permissible after initiation of entry. Changes to g level below those indicated as safe are not thermally acceptable during entry.

*3.11.3 CM THERMAL PERFORMANCE FOR RETURN ENHANCEMENT BATTERY OPERATION

A thermal simulation was conducted to determine the thermal response of the CM assuming an emergency return from lunar orbit without the LM and in the absence of CSM fuel-cell power. The electrical power profile is shown on Figure 4.1-51.3. With a 3-RPH PTC attitude, the enhancement mode timeline will maintain the CM water and RCS propellant tanks above their lower limits. The uncooled operation of the CM electronic equipment results in acceptable temperatures for all equipment except the SBPA. It should be noted that the SBPA constraint for noncooled operation is 1.3 hours.

The minimum cabin gas temperature predicted for the enhancement mode is 55 F. The cabin relative humidity is indicated to be 100 percent. Condensation on the structure was not included in the analysis; however, including this effect is not expected to result in significantly lower relative humidity conditions.

The predicted temperature responses are in the figures listed here.

CM Lifeboat Temperature Predictions

<u>Equipment</u>	<u>Figure</u>
Cabin Heat Exchanger	3.11-8
Helium Tanks	3.11-9
Waste Water Tank	3.11-10
Potable Water Tank	3.11-11
RCS Oxidizer Tank A	3.11-12
RCS Oxidizer Tank B	3.11-13
RCS Fuel Tank A	3.11-14
RCS Fuel Tank B	3.11-15
Inverters	3.11-16
Radiator Outlet	3.11-17
Suit Inlet	3.11-18

*NASA Data Source

3.11.4 SM/SIM THERMAL DATA DURING EVA (PREDICTED)

3.11.4.1 SM Temperature Map (Predicted)

(See Appropriate Spacecraft Appendix)

3.11.4.2 SIM Temperature Map (Predicted)

(See Appropriate Spacecraft Appendix)

Table 3.11-1. Electrical Power Subsystem (EPS) Temperature Limitations

Component	Temperature Limits (°F)		Low Limit Reason	High Limit Reason	Measurement	
	Low	High			Number	Location
Fuel cells						
Condenser exhaust	110 (Average)	225	An average of three temperatures \leq 110 F could result in a frozen water line. Since this temperature is below the measured limit, it would have to be verified by heat balance calculations.	Excessive water buildup in fuel cell above 225 F.	SC2081T SC2082T SC2083T	
Radiator outlet	-30	N/A	Flow of water and glycol becomes sluggish. Note: 2TV-1 never went below +30 F.	Condenser exhaust temperature is the only critical parameter.	SC2087T SC2088T SC2089T	
Stack skin	360	500	Borderline case for chemical reactions. KOH starts to solidify.	Short life of Teflon seals in fuel cells. Red line = 475 F. Maximum power = 440 F.	SC2084T SC2085T SC2086T	
Inverters						
(See paragraph 4.1.5.2)	N/A	248		Design maximum temperature. C&W set at 190 F.		
Cryogenics						
Signal conditioners	-65	170	Output drifts upward as temperature decreases below -20 F. Limit is lowest temperature from which unit will recover.	Qualification testing at 140 F. Satisfactory runs have been made at 170 F. Capacitors fail inside spacecraft.	None	N/A
<p>*Stack temperatures are in the middle of each stack, and a delta temperature of 40 F can occur between the middle and the ends of the stack. (See paragraph 4.1.5.2 for further discussion.)</p>						

3.11-3

SNA-8-D-027(1), Rev 3

Table 3.11-2. Environmental Control Subsystem (ECS)
Temperature Limitations

Component	Temperature Limits		Low Limit Reason	High Limit Reason	Measurement	
	Low	High			Number	Location
Radiator outlet	-20	90/75*	Irreversible damage to radiators will not occur above -35 F; however, corrective action is recommended at -20 F.	See primary evaporator outlet rationale below.	CF0020T	LH equipment bay
Suit circuit temperature	—	—	Determined by crew comfort.	Determined by crew comfort.	CF0008T	Inside suit circuit
Cabin air	58*	83*	2TV-1 data RH 55 percent	2TV-1 data RH 100 percent.	CF0002T	Upstream of cabin heat exchanger
Waste water tank	32	N/A	Line freeze up	No upper limit identified.	CR0004T**	Aft equipment bay
Potable water tank	32	N/A	Line freeze up	No upper limit identified.	CR0003T**	Aft equipment bay
Primary evaporator outlet	34	90/75	To prevent freezing of water supply. Instrumentation accuracy included in this number.	● It is permissible to exceed G&N ICD limit of 55 F when required for tracking, experiments, or emergency conditions. Peak temperature not to exceed 90 F. Average temperature for a 2 hour period not to exceed 75 F. Maximum steady-state coolant to IMU is 75 F with 75 F (or lower) structure temperature and when coolant flow and bus voltages are near nominal. Limits verified by ground test and analytic thermal model. Note: Telemetry readout limit for CF0018T is 76 F. For higher temperatures, reference radiator outlet (CF0020T) temperature above.	CF0018T	Glycol temperature at evaporator outlet
Evaporator Outlet during EVA	34	50.5	To prevent freezing of water supply. Instrumentation accuracy included in this number.	Facilitate suit circuit H ₂ O removal and preclude helmet fogging.	CF0018T	Glycol temperature at evaporator outlet
Urine dump nozzle	32	N/A	Freezing of H ₂ O. Urine dump testing.		CF0460T	On dump line upstream of nozzle
Steam duct	32	N/A	Freezing of H ₂ O		CF0034P	Steam duct upstream of evap back pres valve
					CF0018T	Gly evap outlet temp

*These limits do not apply to crew comfort.

**Water tanks will not freeze if helium tanks 1 and 2 are maintained above 34°F.

● NASA Data Source

3.11-4

SNA-8-D-027(I) REV 3

Amendment 86
1/21/72

Table 3.11-3. Service Module Reaction Control Subsystem (SM RCS)
Temperature Limitations

Component	Temperature Limits (°F)		Low Limit Reason	High Limit Reason	Measurement	
	Low	High			Number	Location
Helium bottle	20	†	To ensure -65 F after a long burn.		SR5013T through SR5016T	Bottle skin
Primary oxidizer						
Bulk tank	30	110	Bladder hardens.	Operational limit. Fracture mechanics.*	None	N/A
Quad A	30	*			None	N/A
Quad B						
Quad C						
Quad D						
Primary fuel						
Bulk tank	30	110	Bladder hardens.	Operational limit. Fracture mechanics.*	None	N/A
Quad A	30	*			SR5073T	Tank
Quad B						
Quad C						
Quad D						
Secondary oxidizer tank	30	*	Bladder hardens.	Fracture mechanics.*	None	N/A
Secondary oxidizer bulk	30	110	Bladder hardens.	Operational limit.	None	N/A
Secondary fuel tank	30	*	Bladder hardens.	Fracture mechanics.*	None	N/A
Secondary fuel bulk	30	110	Bladder hardens.	Operational limit.	None	N/A
Propellant lines	20	175	Oxidizer freezing temperature.	Engine limit (small quantities) below two-phase condition.	SR5069T through SR5072T	Oxidizer feed line at filter
Propellant component isolation valve	30	105	Operational limit.	Operational limit.	None	N/A
Pressure panel	20	150	Oxidizer freezing at check valves.	Operational limit. Qualification limit: 105 F Supplemental testing to 150 F	None	N/A
Engine valves	35	N/A	Operational limit.	N/A	None	N/A
Nozzle nut	30		Operational limit.		None	N/A

*See corresponding table in spacecraft appendixes (all RCS fracture mechanics limits - NASA Data Source).

†See Section 3.3 in spacecraft appendixes.

Table 3.11-4. Command Module Reaction Control Subsystem (CM RCS)
Temperature Limitations

Component	Temperature Limits (°F)		Low Limit Reason	High Limit Reason	Measurement	
	Low	High			Number	Location
Engine package (See paragraph 4. 3. 5. 4)	55	N/A	To hold a 30 F nozzle nut temperature.	N/A	SR5065T through SR5068T	Engine mount.
Helium bottle	20	†	To ensure -65 F after long burn (neglecting transients due to engine firing).		CR0003T CR0004T	Bottle skin
Propellant oxidizer tanks						
Bulk tank	30	110	} Bladder hardens.	} Qualification limit - bladder softens. } Fracture mechanics.*	None	N/A
Tank A	30	*				
Tank B	30	*				
Propellant fuel tanks						
Bulk tank	30	110	} Bladder hardens.	} Qualification limit - bladder softens. } Fracture mechanics.*	None	N/A
Tank A	30	*				
Tank B	30	*				
Propellant lines	20	200	Oxidizer freezing temperature.	Engine limits (small quantities) below two phase.	None	N/A
Helium panel	20	150	Oxidizer freezing at check valves.	Component operating limits.	None	N/A
Propellant panel	30	105	Component operating limits.	Component operating limits.	None	N/A
Engine valves	20**	225	Operating limit.	Operating limit.	None	N/A
Engine injector (See paragraph 4. 4. 4.)	28**	N/A	To ensure that engine valve is above minimum limit at activation.	N/A	CR2100T CR2103T CR2110T CR2114T CR2116T CR2119T	Engine injector

*See corresponding table in spacecraft appendixes (all RCS fracture mechanics limits - NASA Data Source).

**No limit during nonoperating portion of mission; limits apply just before system activation.

†See Section 3. 4 in spacecraft appendixes.

Table 3.11-5. Service Propulsion Subsystem (SPS) Temperature Limitations

Component	Temperature Limits (°F)		Low Limit Reason	High Limit Reason	Measurement	
	Low	High			Number	Location
Oxidizer sump tank bulk (see paragraph 4.5.4.1.)	30/40**	110	Limit of 30 F is dictated by minimum propellant temperature during qualification tests. Limit of 40 F is dictated by potential injector damage during shutdown transients.	Maximum propellant temperature during qualification tests.	None	N/A
Oxidizer sump tank skin	N/A	*	N/A	Fracture mechanics.*	SP0055T	On upper tank dome at X _S = 341
Oxidizer storage tank bulk (see paragraph 4.5.4.1.)	30/40**	110	Limit of 30 F is dictated by minimum propellant temperature during qualification tests. Limit of 40 F is dictated by potential injector damage during shutdown transients.	Maximum propellant temperature during qualification tests.	None	N/A
Oxidizer storage tank skin	N/A	*	N/A	Fracture mechanics.*	SP0058T	On upper tank dome at X _S = 343
Fuel sump tank bulk (see paragraph 4.5.4.1.)	30/40**	110	Limit of 30 F is dictated by minimum propellant temperature during qualification tests. Limit of 40 F is dictated by potential injector damage during shutdown transients.	Maximum propellant temperature during qualification tests.	None	N/A On tank at X _S = 280
Fuel sump tank skin	N/A	*	N/A	Fracture mechanics.*	SP0056T	On upper tank dome at X _S = 341
Fuel storage tank bulk (see paragraph 4.5.4.1.)	30/40**	110	Limit of 30 F is dictated by minimum propellant temperature during qualification tests. Limit of 40 F is dictated by potential injector damage during shutdown transients.	Maximum propellant temperature during qualification tests.	None	N/A
Fuel storage tank skin	N/A	*	N/A	Fracture mechanics.*	SP0059T	On upper tank dome at X _S = 343
Helium pressurization panel	0	150	The limit prior to a SPS firing is -5 F. For a continuous firing, the temperature will drop to -65 F in 450 seconds.	Maximum temperature during qualification tests. Solenoid valve is least tolerance component.	None	N/A
*See corresponding table in spacecraft appendixes. **Noncritical burns: 40 F; critical burns: 30 F.						

3.11-7

SNA-8-D-027(I), Rev 3

Amendment 74
7/21/71

Table 3.11-5. Service Propulsion Subsystem (SPS) Temperature Limitations (Cont)

Component	Temperature Limits (°F)		Low Limit Reason	High Limit Reason	Measurement	
	Low	High			Number	Location
Helium tank	40	†	Temperature necessary to maintain the helium above the -65 F dew-point temperature during a 450-second SPS firing.		SP0017T	Top skin of lower tank
PUGS control box	16	150	Calibration limit.	Qualification test limit for forward bulkhead temperature.	None	N/A
Gimbal actuator (See paragraph 4.5.4.3.)	30/0*	140	Qualification limit for gimbal operation.	Qualification limit prior to SPS engine firing.	None	N/A
Propellant feed lines (See paragraph 4.5.4.1.)	25/40	110	Qualification test and performance limit. Noncritical burns: 40 F. Critical burns: 25 F.	Qualification limit prior to engine firing. Because of soakback, this temperature may reach 140 F following a SPS engine firing.	SP0049T **SP0054T SP0048T **SP0057T	Oxidizer line Oxidizer line Fuel line Fuel line
PU valve	20/40	110	White Sands Testing Facility test lower limit. Noncritical burns: 40 F. Critical burns: 20 F.	Qualification limit prior to engine firing. May reach 140 F following engine firing.	-	-
Propellant valve	40	160	May go below this value after engine shutdown due to evaporative cooling. Before firing, use heaters to reach 50 F. Propellant temperature limit is 40 F.	Operating limitation for valve seats.	SP0045T	On propellant valve
SPS injector (See paragraph 3.5.3.)	N/A	480	N/A	Operation limitation to prevent damage to engine.	**SP0062T	

*For motor idling: 0 F; prior to ignition: 30 F. Warmup from 0 to 30 F (idle) takes approximately 5 minutes.

†See Section 3.5 in spacecraft appendixes.

**Deleted on CSM 112 only.

3.11-8

SNA-8-D-027(I), Rev 3

Amendment 74
7/21/71

Table 3.11-6. Launch Escape Subsystem (LES) Temperature Limitations

COMPONENT	TEMPERATURE LIMITS (°F)		LOW LIMIT REASON	HIGH LIMIT REASON	MEASUREMENT	
	LOW	HIGH			NUMBER	LOCATION
Launch Escape Motor	20	120	Qual. Limit. Motor performance below this limit is unknown.	Qual. Limit. Motor performance above this limit is unknown.		
Pitch Control Motor	20	140				
Tower Jettison Motor	20	140				

3.11-9

SNA-8-D-027 (I) REV 3

Amendment 40
6/17/70

Table 3.11-7. Communications Subsystem Temperature Limitations

SIM Scientific Data and Power Distribution Equipment	Temperature Limits (°F)		Low Limit Remarks	High Limit Remarks	Measurement	
	Low	High			Number	Location
Data Processor: Master	-30	160	Qualification limit (unit) Internal temperature measurement monitor lower range to -20F. Lower temperature limit reached on CSM 112 was 50 F.	Qualification limit (unit) Internal temperature measurement monitor upper range to +155 F. Upper temperature limit reached on CSM 112 was 126 F.	ST0562T (Available on HBR 51.2KBS)	SIM X _S =262.5
Slave	-30	160	Qualification limit (unit) (Same range as Master) Lower temperature limit reached on CSM 112 was 40 F.	Qualification limit (unit) (Same range as Master) Upper temperature limit reached on CSM 112 was 98 F.	ST0563T (Available on HBR 51.2KBS)	SIM X _S =262.5
Scientific Data System: Buffer Amplifier	-65	160	Qualification limit (unit) Lower temperature limit (determined from analysis of CSM 112 data) reached on CSM 112 was 12 F.	Qualification limit (unit) Upper temperature limit (determined from analysis of CSM 112 data) reached on CSM 112 was 128 F.	None	SIM X _S =262.5
Multiple Operations Module	-30	250	Qualification limit (unit) External temperature measurement monitor lower range to -100 F. Lower temperature limit reached on CSM 112 was 1 F.	Qualification limit (unit) External temperature measurement monitor upper range to 200 F. Upper temperature limit reached on CSM 112 was 153 F.	SL1215T (Available on HBR 51.2KBS)	SIM X _S =262.5

3.11-10

SNA-8-D-027(I) REV 3

Amendment 91
3/17/72

Table 3.11-7. Communications Subsystem Temperature Limitations (Continued)

Component	Temperature Limits (°F)		Low Limit Reason	High Limit Reason	Measurement	
	Low	High			Number	Location
S-Band high-gain Stripline	0	200	Qualification limit	Qualification limit	None	N/A
Operating	-70	90	Qualification limit (cracking of plastic material).	Qualification limit.	None	N/A
Nonoperating	0	105	Specification for long-time storage.	Specification (unit operated after being subjected to the 105 F temperature).		

3.11-10.1

SNA-8-D-027 (1) REV 3

Table 3.11-8. Structures Subsystem Temperature Limitations

Component	Temperature Limits (°F)		Low Limit Reason	High Limit Reason	Measurement	
	Low	High			Number	Location
Heat shield	-150	200*/ 150	Hairline cracking and delamination in the ablator may occur below this temperature. No data available below -150 F.	As the temperature surpasses 200 F, the low limit is raised because of volatile loss and material shrinkage caused by the over-temperature. The heat shield temperatures must be no higher than 150 F just before reentry (limited by 600 F bondline temperature for a 3500-nm design trajectory).	CA1820T CA1821T CA1822T CA1823T	CM ablator
Unified crew hatch (while open)						
Ablator	-95		Hatch closure has not been demonstrated below this temperature.			
Aluminum plate		160	Hatch closure has not been demonstrated above these limits.			
Surrounding ablator		155				
*Lunar orbit only.						

3.11-11

Table 3.11-9. Docking Subsystem Temperature Limitations

Component	Temperature Limits (°F)		Low Limit Reason	High Limit Reason	Measurement	
	Low	High			Number	Location
Docking probe	0/-20	200/250	Load-carrying capacity for transposition and docking with a loaded (no-restart) S-IVB. All other dockings at -20 F. See paragraph 3.8.2.6.	Specification limit for transposition loads. Lunar orbit docking permissible at 250 F due to reduced loads.	CS0220T	On main barrel
Docking drogue	-150	200/300	Demonstration limit.	200 F specification limit for transposition and docking loads. 300 F acceptable by analysis for lunar stay and lunar orbit docking.		
Attenuator	-80	+250	Qualification test.	Qualification test.	-	-

3.11-12

SNA-8-D-027(I), Rev 3

Amendment 74
7/21/71

Table 3.11-10. Non-Coldplated Equipment Temperature Limitations

Component	Temperature Limits (°F)		Low Limit Reason	High Limit Reason	Measurement	
	Low	High			Number	Location
Ordeal						
Operating	0	160	Qualification limit.	Qualification limit.	None	N/A
Nonoperating	-65	160	Qualification limit.	Qualification limit.	None	N/A

Table 3.11-11. Entry Condition Parameters at the
400,000-Foot Entry Interface

Parameters	Symbol or Abbreviation	Variable Range or Constant Value
Parameters Influencing Primary Temperature		
1. Entry velocity	V_i	35,500 to 38,500 ft/sec
2. Flight path angle	γ_i	-5.25 to -8.5 degrees
3. Guided entry mode range	R	1500 to 3500 nm
4. Backup entry mode g level		Constant 3, 4, and 5 g
5. Lift-to-drag ratio	L/D	0.25 to 0.40
Parameters Influencing Secondary Temperature		
1. Command module weight	CM weight	13,000 lb
2. Initial ablator temperature		100 F
3. Atmospheric model		Thin atmosphere (60 degree N latitude deviation)
Other Parameters		
1. Orbit inclination	i	0 to 90 degrees
2. Aft heat shield local transition Reynolds number		80,000

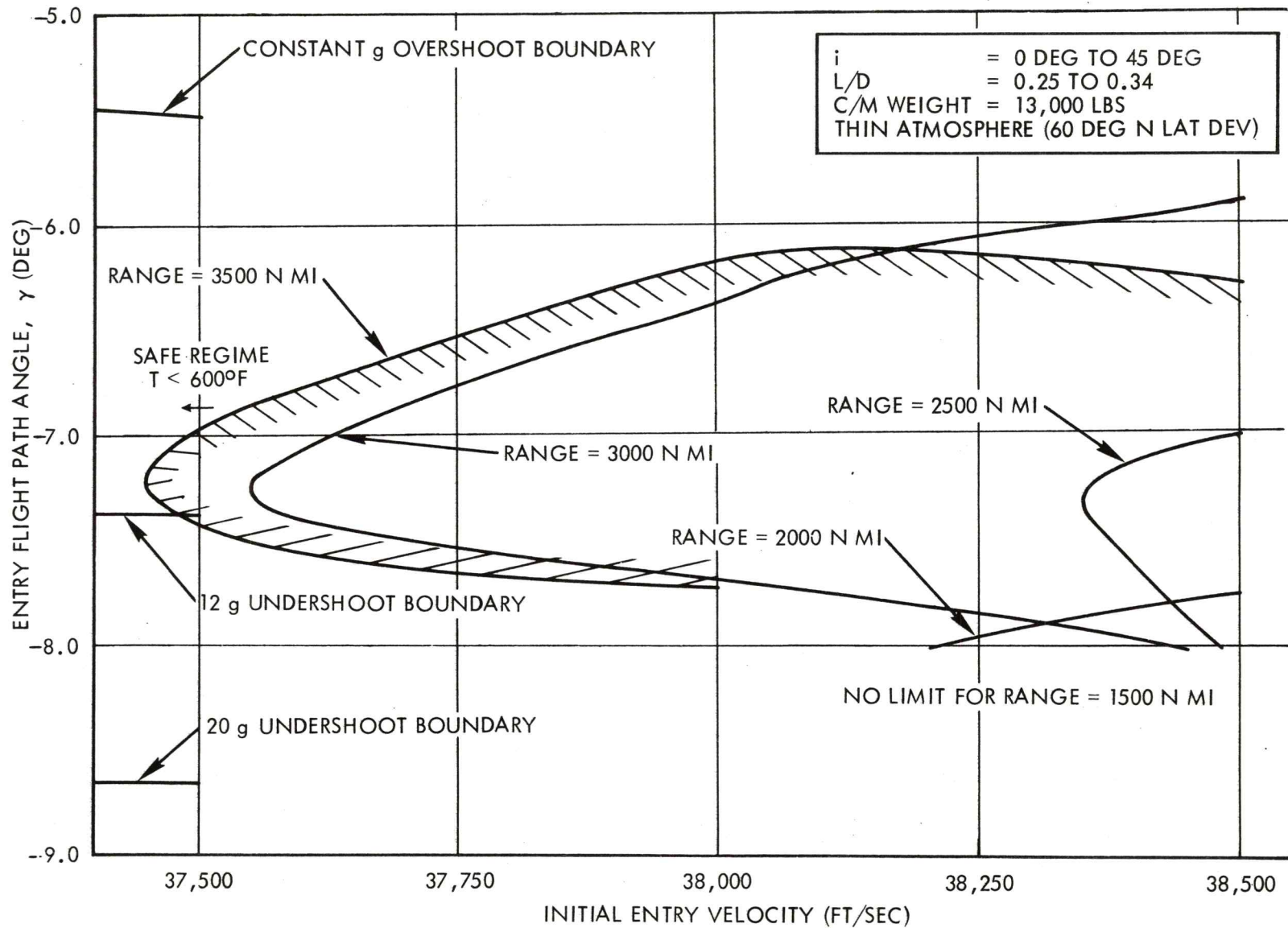
Table 3.11-12. Summary of Thermal Limit Line Study*

L/D Ratio	Guided Entry Mode, Orbit Inclination		Backup Entry Mode Orbit Inclination	
	$0^\circ \leq 45^\circ$	$> 45^\circ \leq 90^\circ$	$0^\circ \leq 45^\circ$	$> 45^\circ \leq 90^\circ$
$0.25 \leq L/D \leq 0.34$	Figure 3.11-1	Figure 3.11-3	Figure 3.11-5	Figure 3.11-6
$0.34 \leq L/D \leq 0.40$	Figure 3.11-2	Figure 3.11-4	Figure 3.11-5	Figure 3.11-7

*To be used in conjunction with Figures 3.11-1 through 3.11-7.

Note: All over- and under-shoot g boundaries shown in Figures 3.11-1 through 3.11-7 are defined for the following:

1. Guided entry mode
2. $i = 45$ degrees
3. $L/D = 0.25$
4. Thin atmosphere
5. CM weight = 13,000 pounds



(NASA DATA SOURCE)

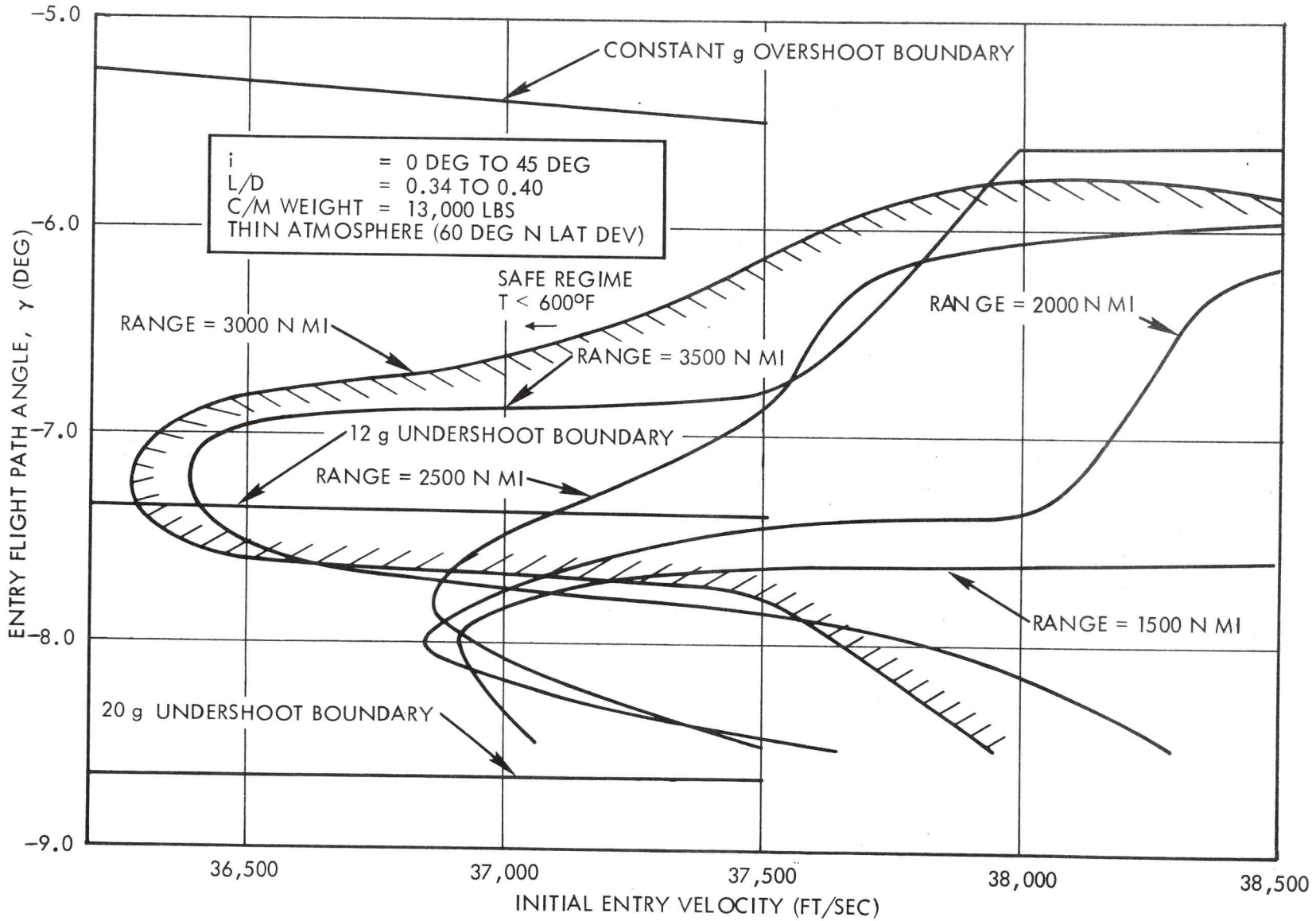
Figure 3.11-1. Apollo Block II Thermal Entry Corridor (Guided Entry Mode)

3.11-16

SNA-8-D-027(I), Rev 3

3.11-17

SNA-8-D-027(I), Rev 3



(NASA DATA SOURCE)

Figure 3.11-2. Apollo Block II Thermal Entry Corridor (Guided Entry Mode)

3.11-18

SNA-8-D-027(I), Rev 3

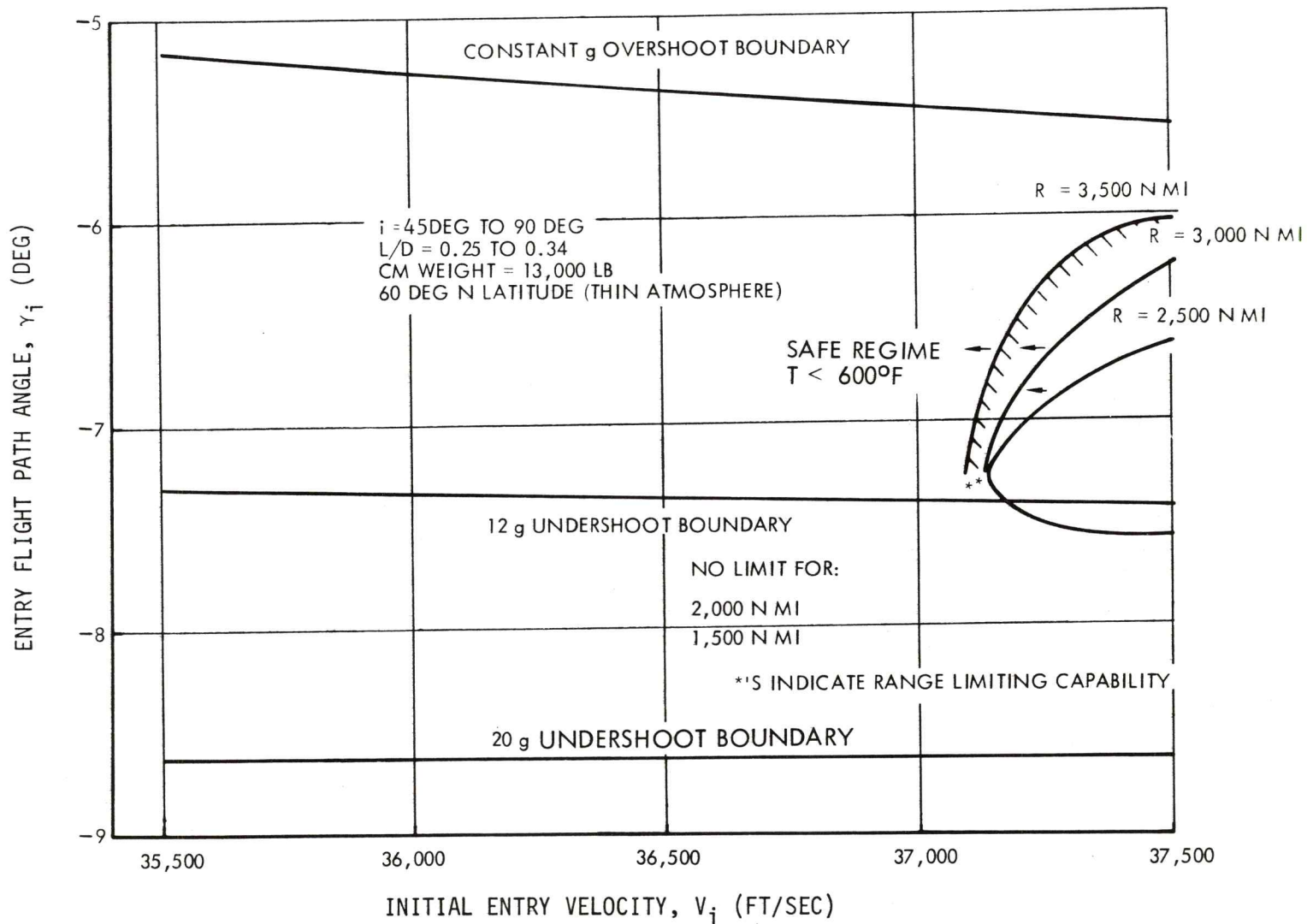


Figure 3.11-3. Apollo Block II Thermal Entry Corridor (Guided Entry Mode)

(NASA DATA SOURCE)

3.11-19

SNA-8-D-D-027(I), Rev 3

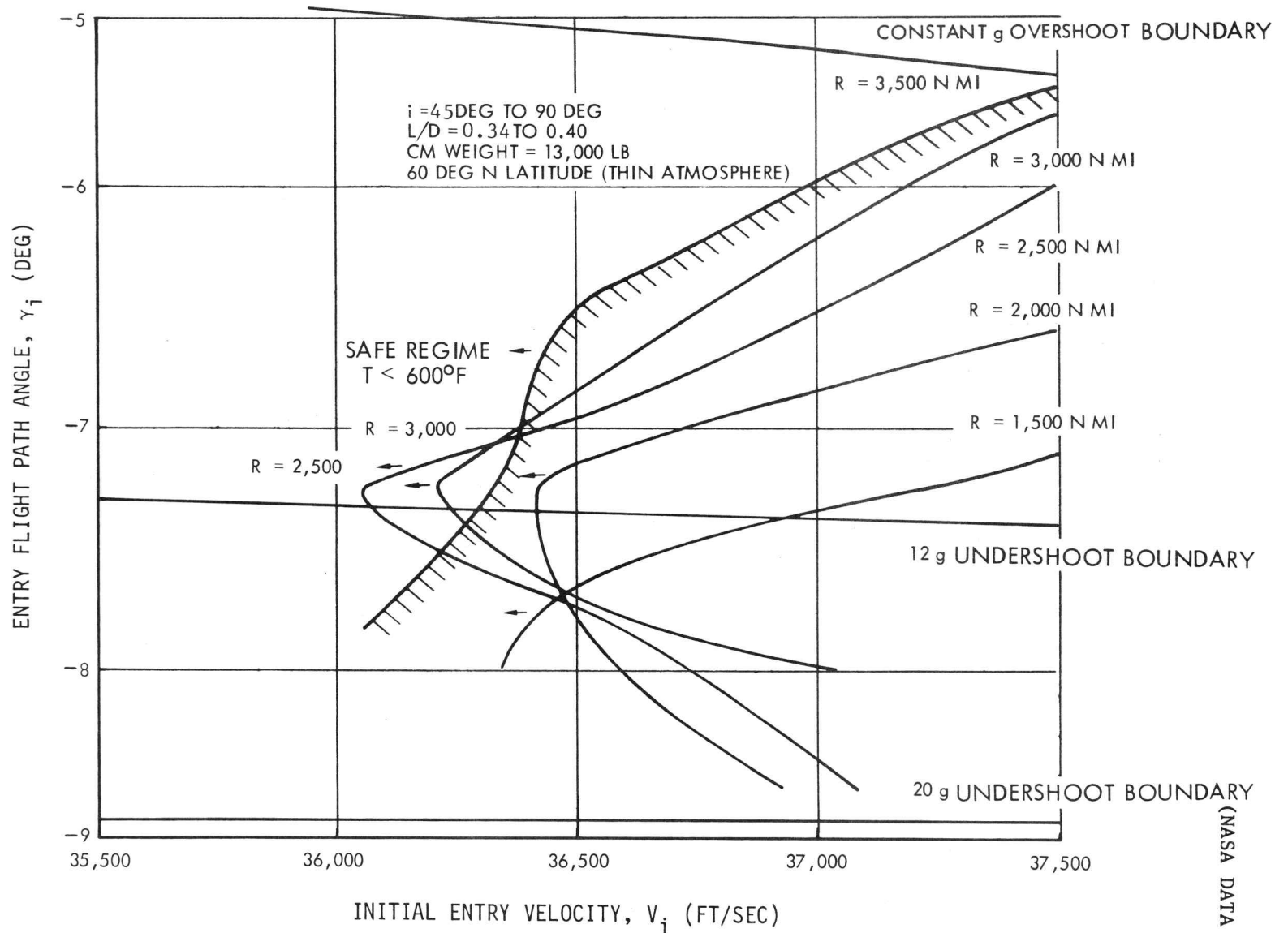


Figure 3.11-4. Apollo Block II Thermal Entry Corridor
(Guided Entry Mode)

(NASA DATA SOURCE)

3.11-20

SNA-8-D-027(I), Rev 3

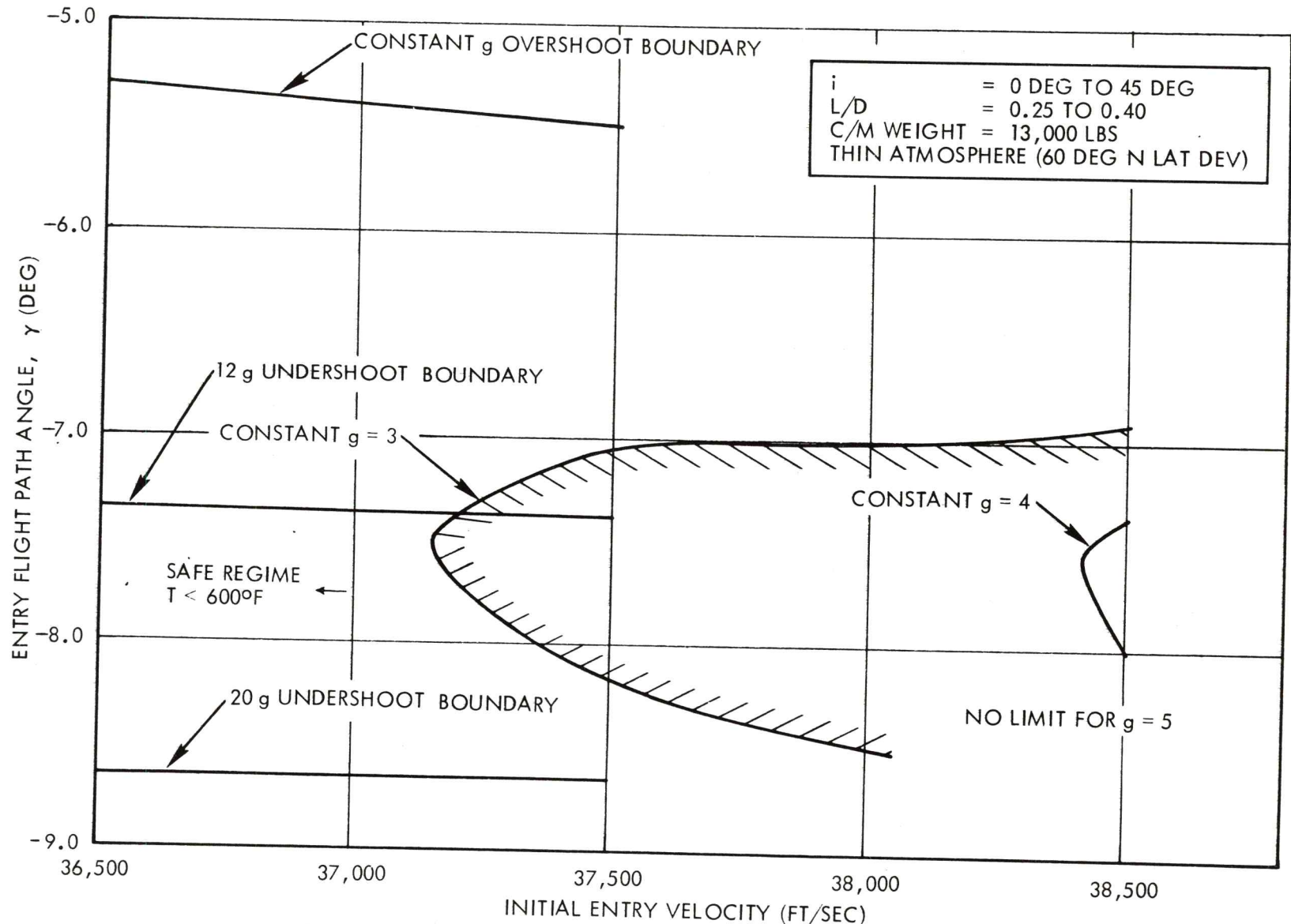


Figure 3.11-5. Apollo Block II Thermal Entry Corridor (Backup Entry Mode)

(NASA DATA SOURCE)

3.11-21

SNA-8-D-D-027(I), Rev 3

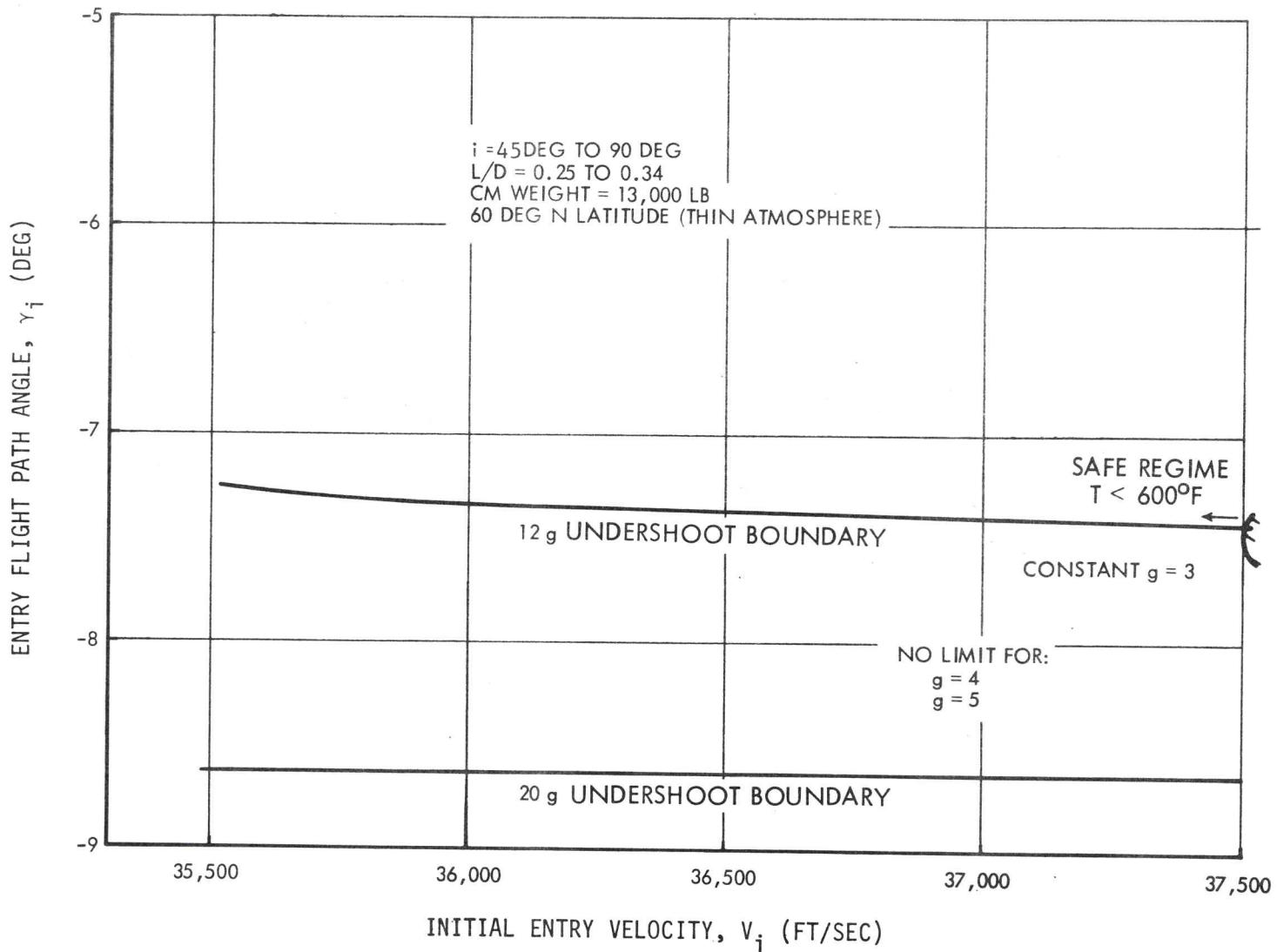
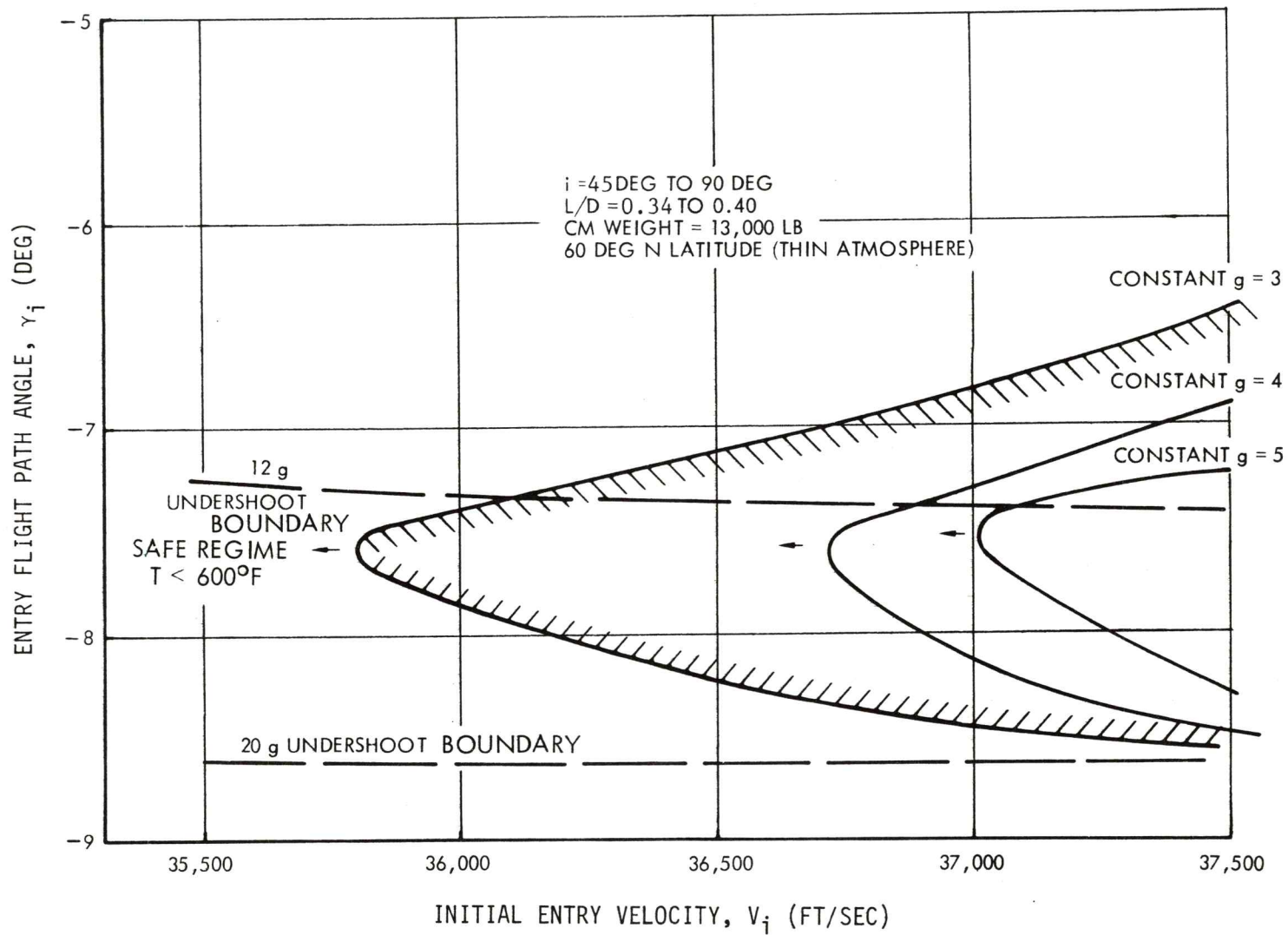


Figure 3.11-6. Apollo Block II Thermal Entry Corridor (Back-up Entry Mode)

(NASA DATA SOURCE)

3.11-22

SNA-8-D-027(I), Rev 3



(NASA DATA SOURCE)

Figure 3.11-7. Apollo Block II Thermal Entry Corridor (Back-up Entry Mode)

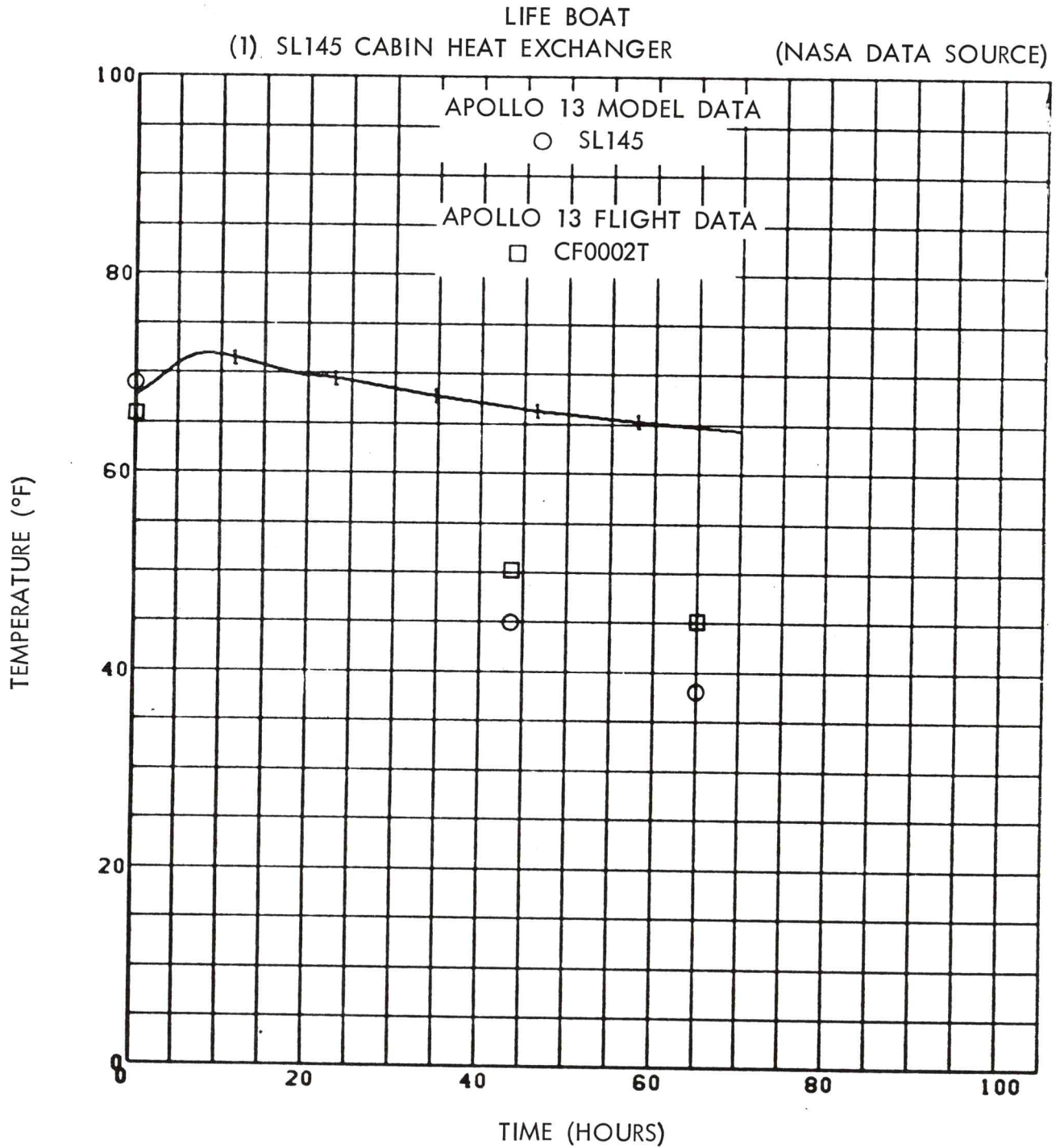


Figure 3.11-8. Cabin Heat Exchanger Predicted Temperature Response
(See Paragraph 3.11.3)

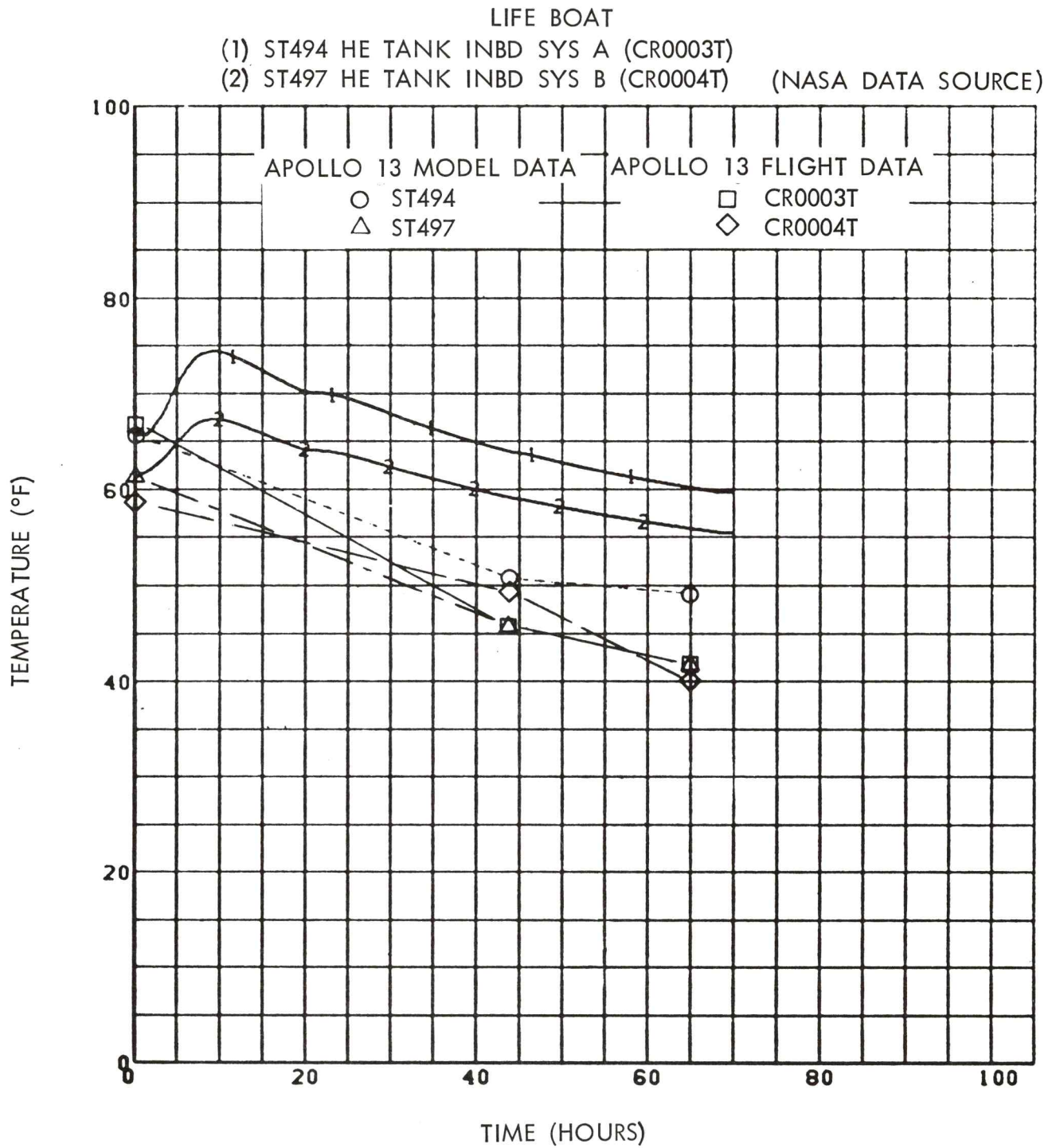


Figure 3.11-9. Helium Tanks Predicted Temperature Response
(See Paragraph 3.11.3)

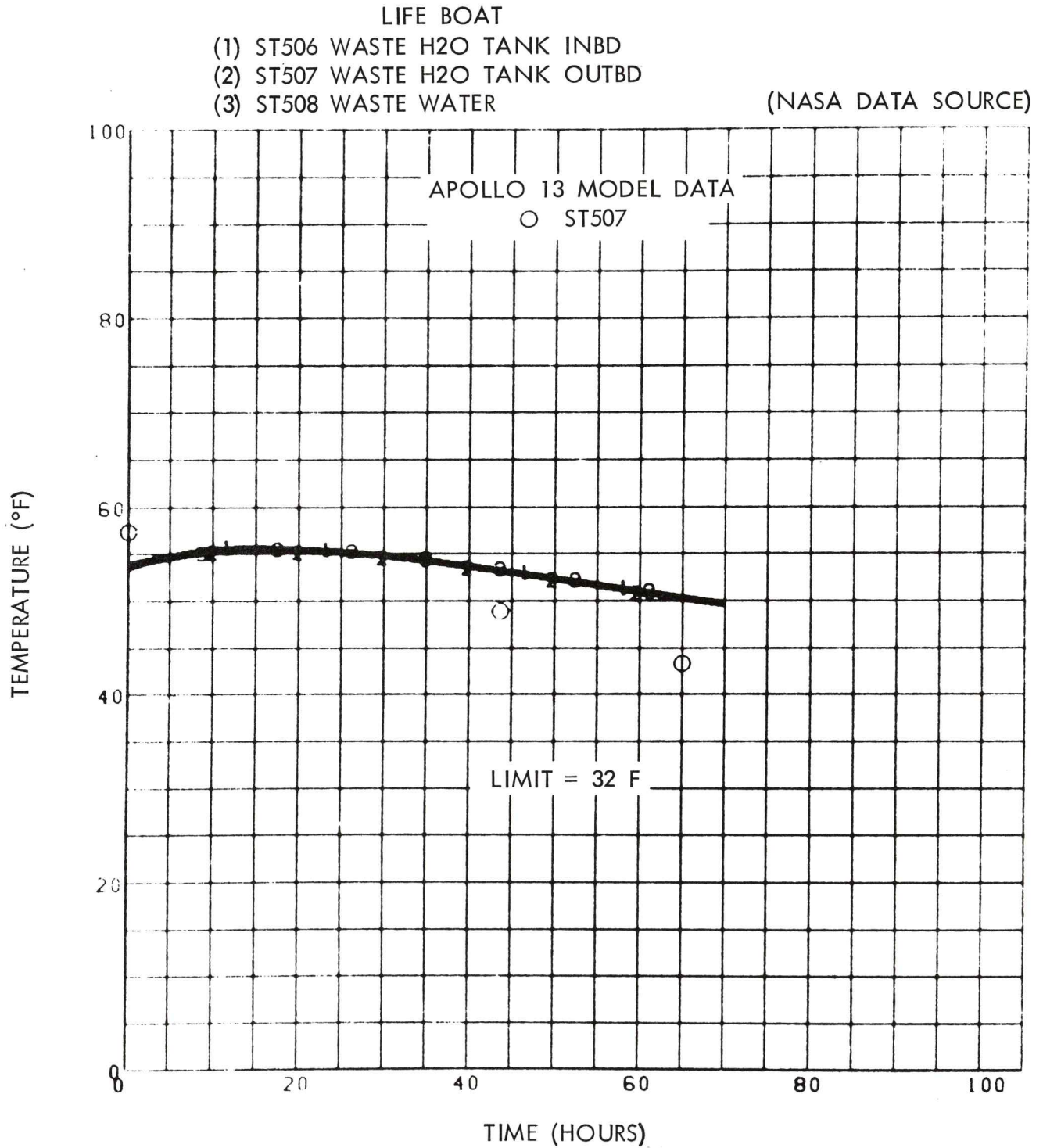


Figure 3.11-10. Waste Water Tank Predicted Temperature Response
(See Paragraph 3.11.3)

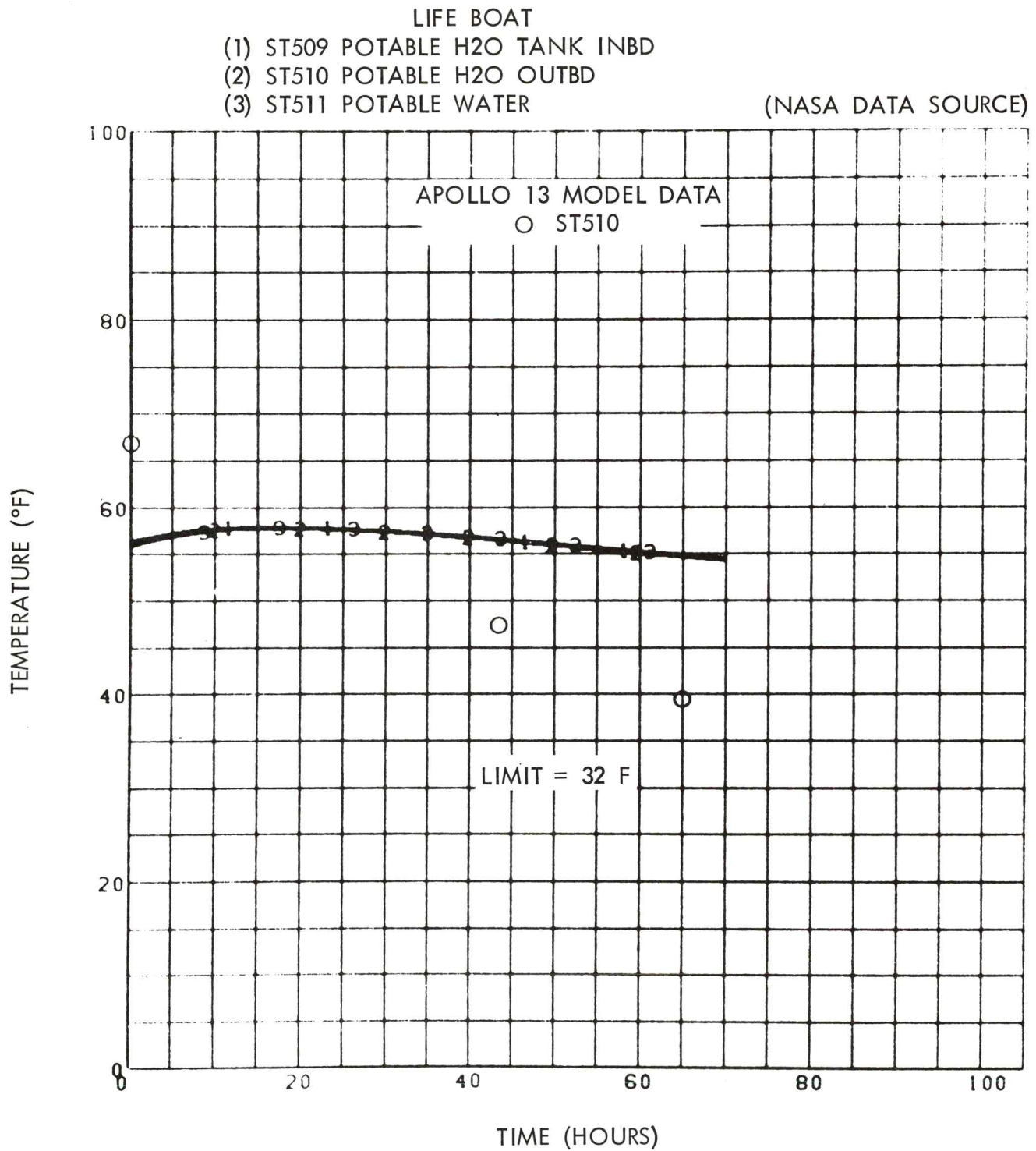


Figure 3.11-11. Potable Water Tank Predicted Temperature Response
(See Paragraph 3.11.3)

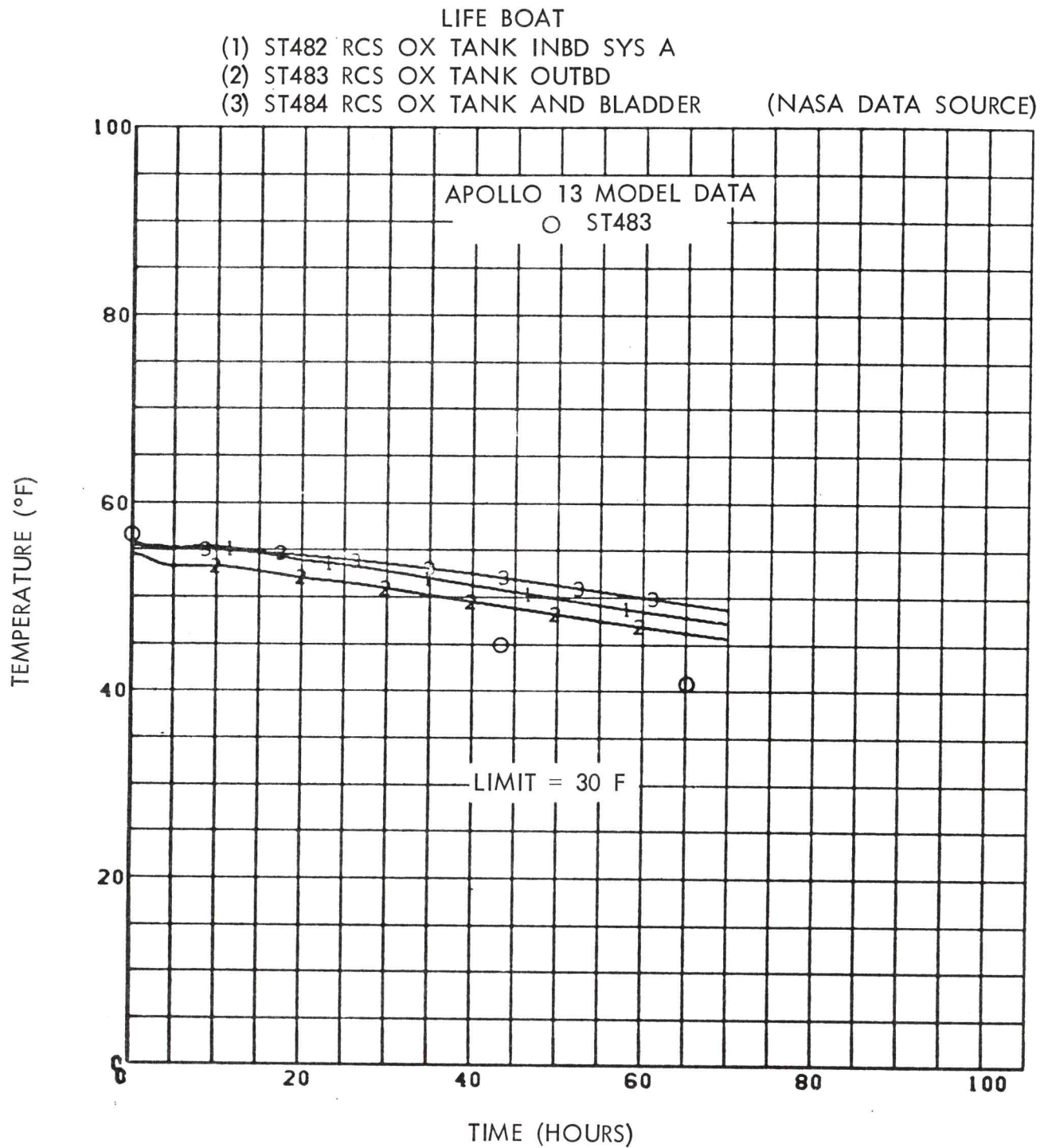


Figure 3.11-12. RCS Oxidizer Tank A Predicted Temperature Response
(See Paragraph 3.11.3)

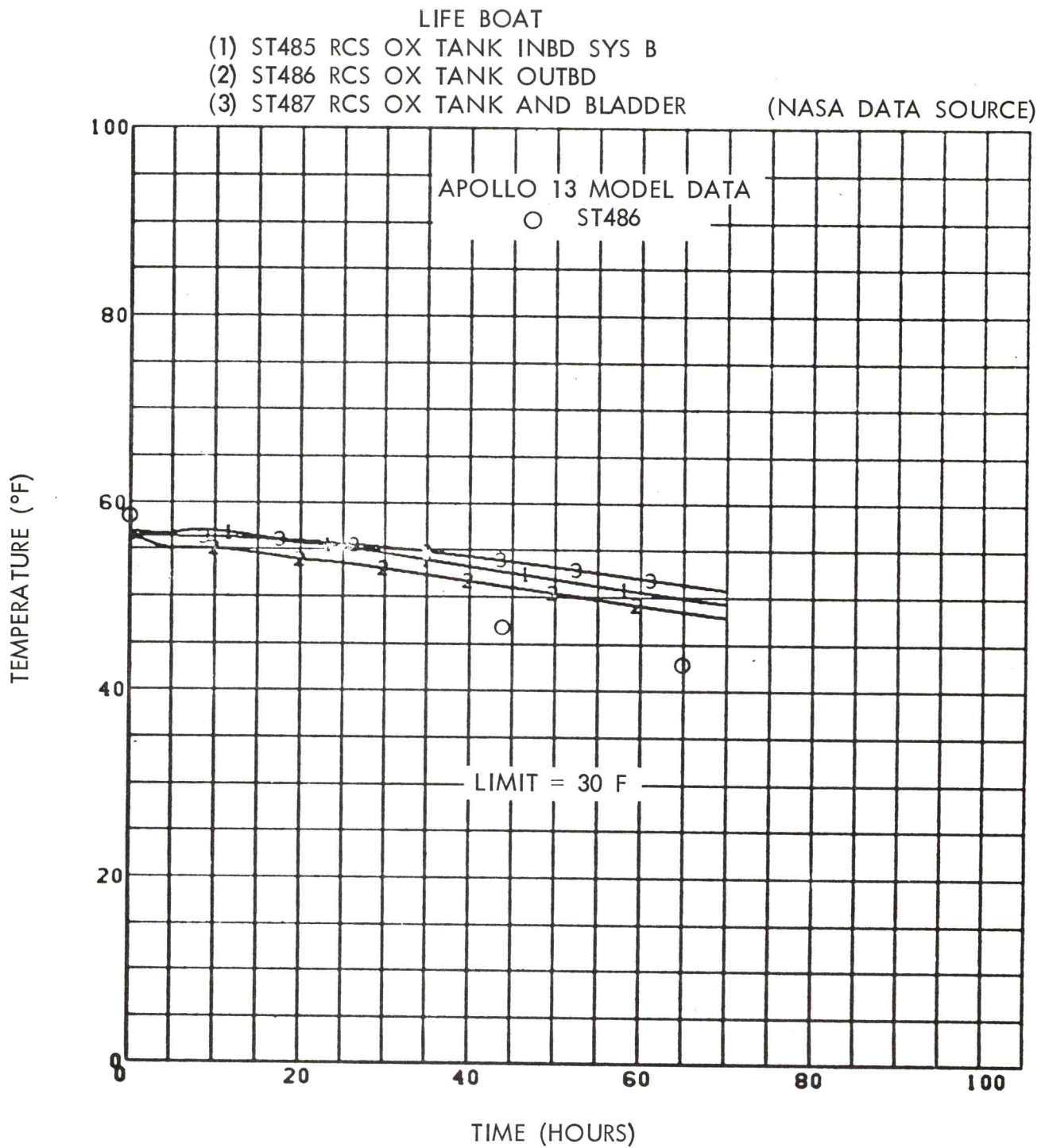


Figure 3.11-13. RCS Oxidizer Tank B Predicted Temperature Response
(See Paragraph 3.11.3)

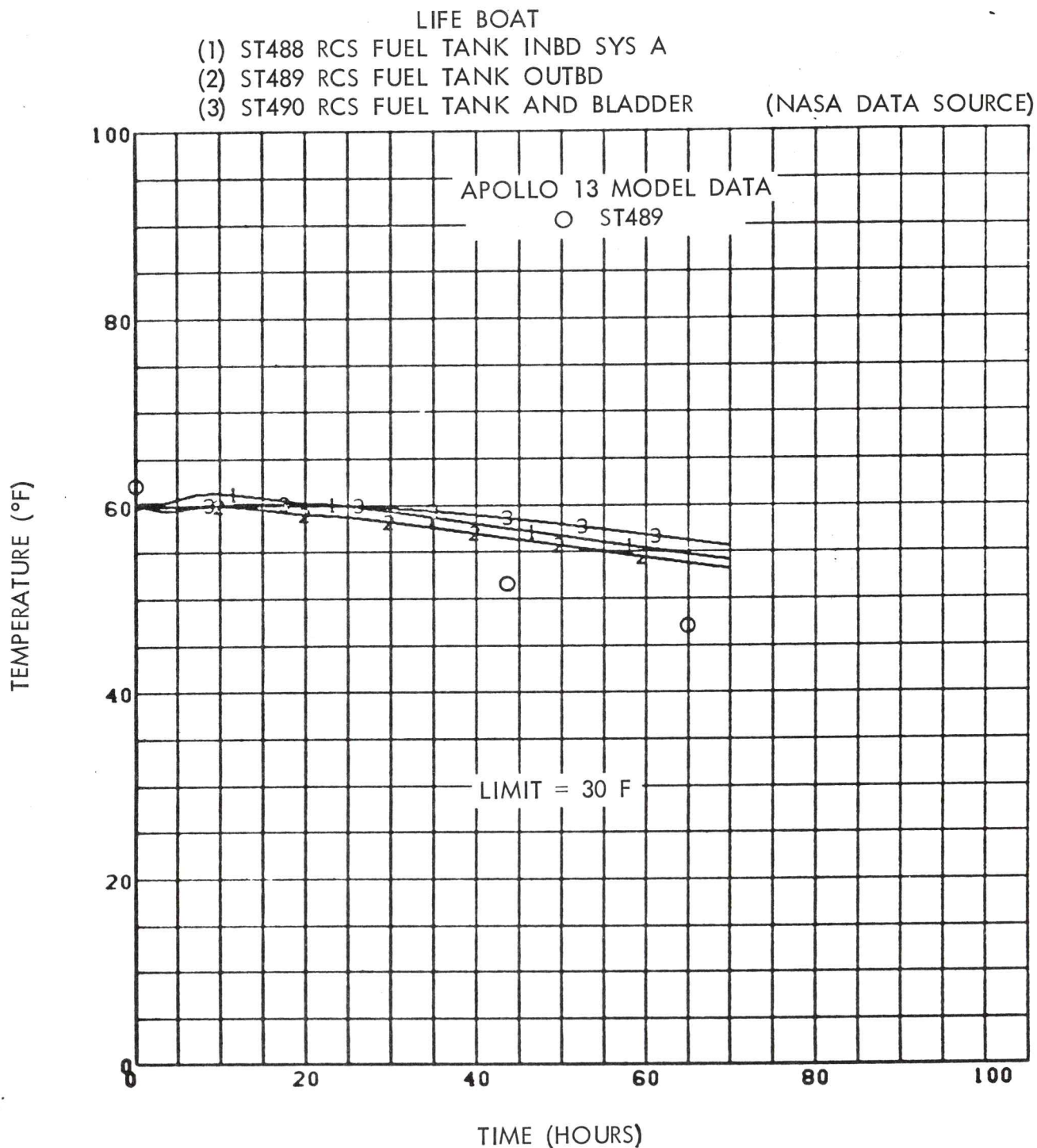


Figure 3.11-14. RCS Fuel Tank A Predicted Temperature Response
(See Paragraph 3.11.3)

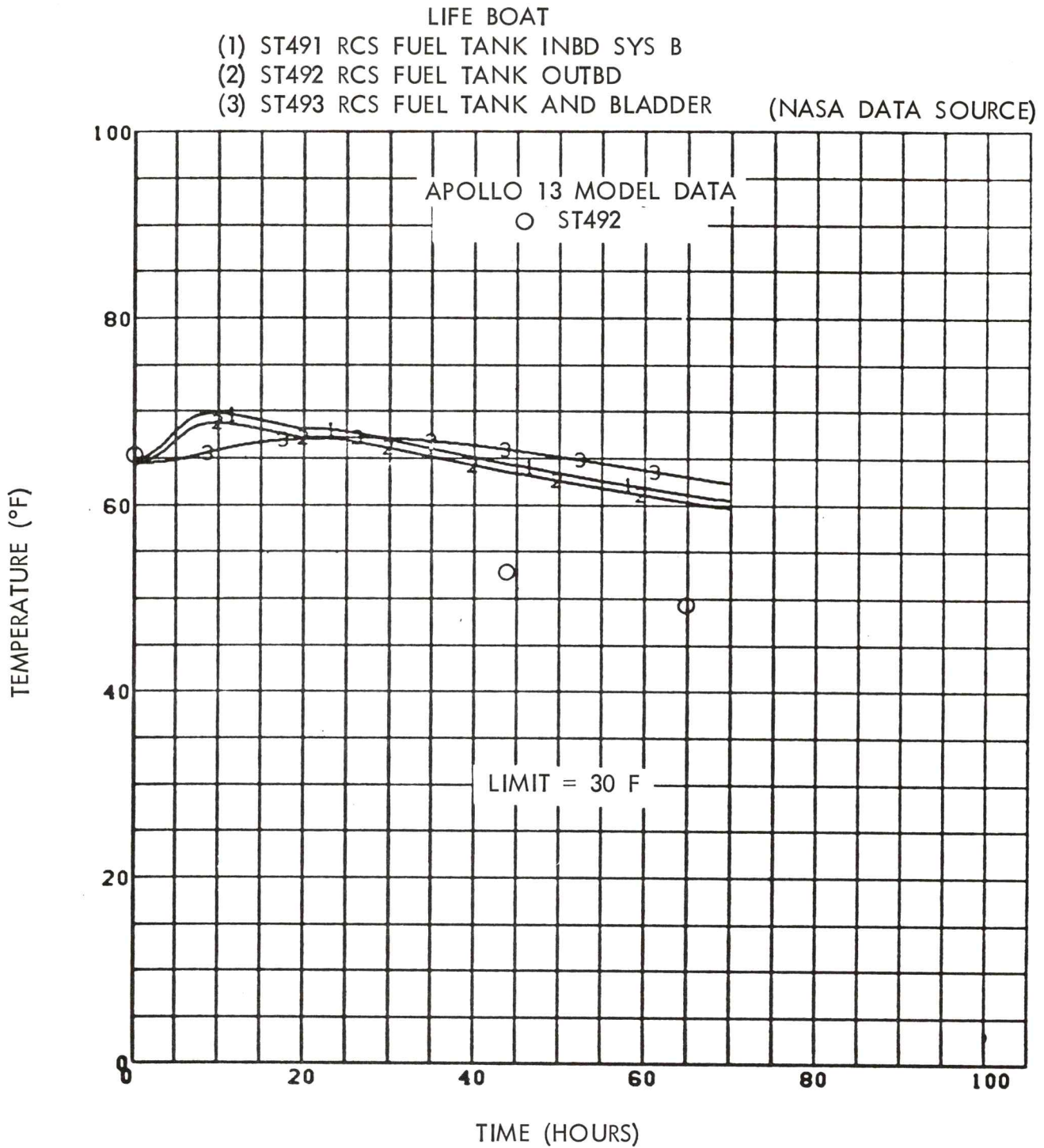


Figure 3.11-15. RCS Fuel Tank B Predicted Temperature Response
(See Paragraph 3.11.3)

LIFE BOAT

- (1) TT230 INVERTER NO. 1 (CC0175T)
- (2) TT231 INVERTER NO. 2 (CC0176T)
- (3) TT232 INVERTER NO. 3 (CC0177T)

(NASA DATA SOURCE)

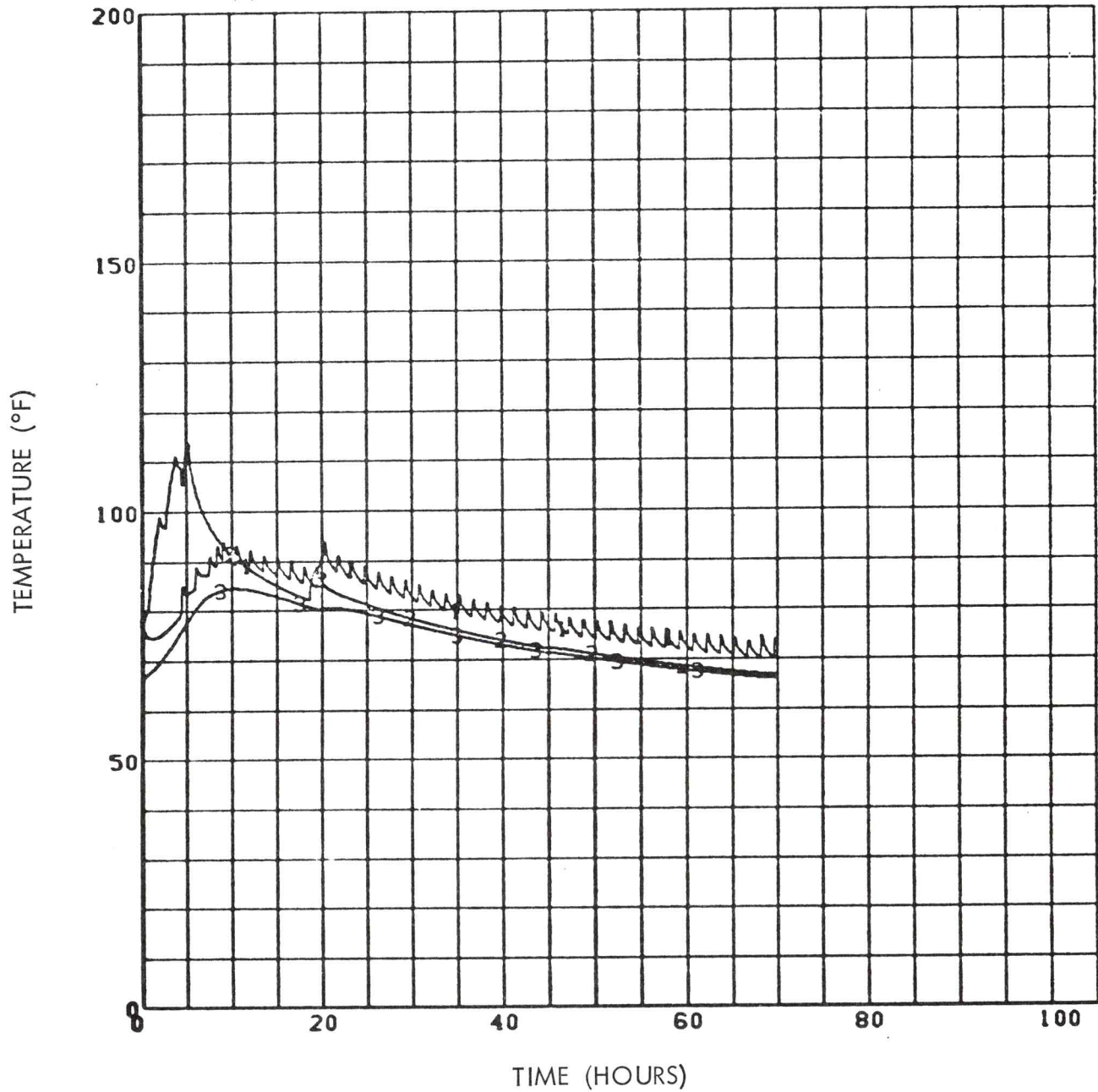


Figure 3.11-16. Inverters Predicted Temperature Response
(See Paragraph 3.11.3)

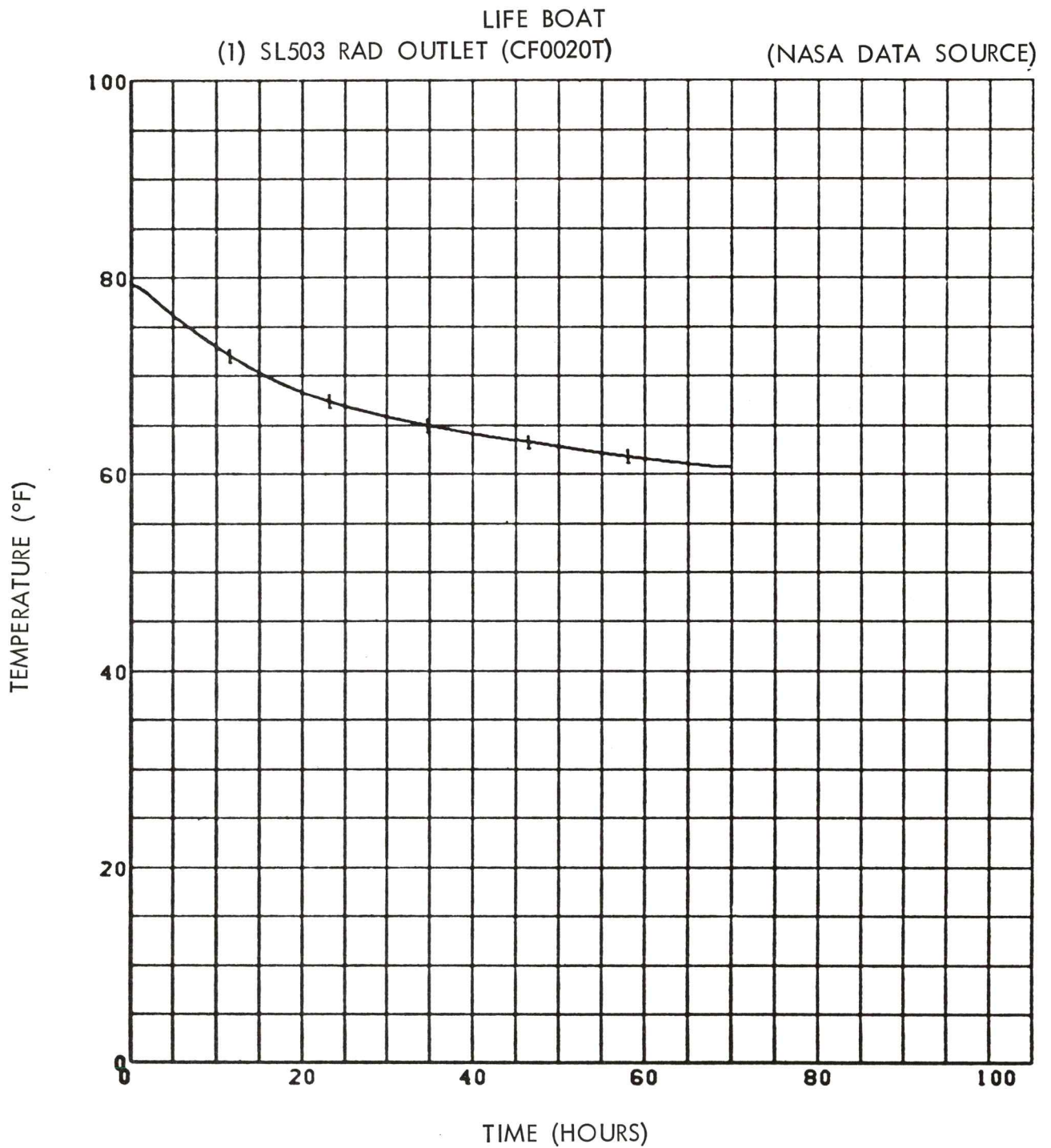


Figure 3.11-17. Radiator Outlet Predicted Temperature Response
(See Paragraph 3.11.3)

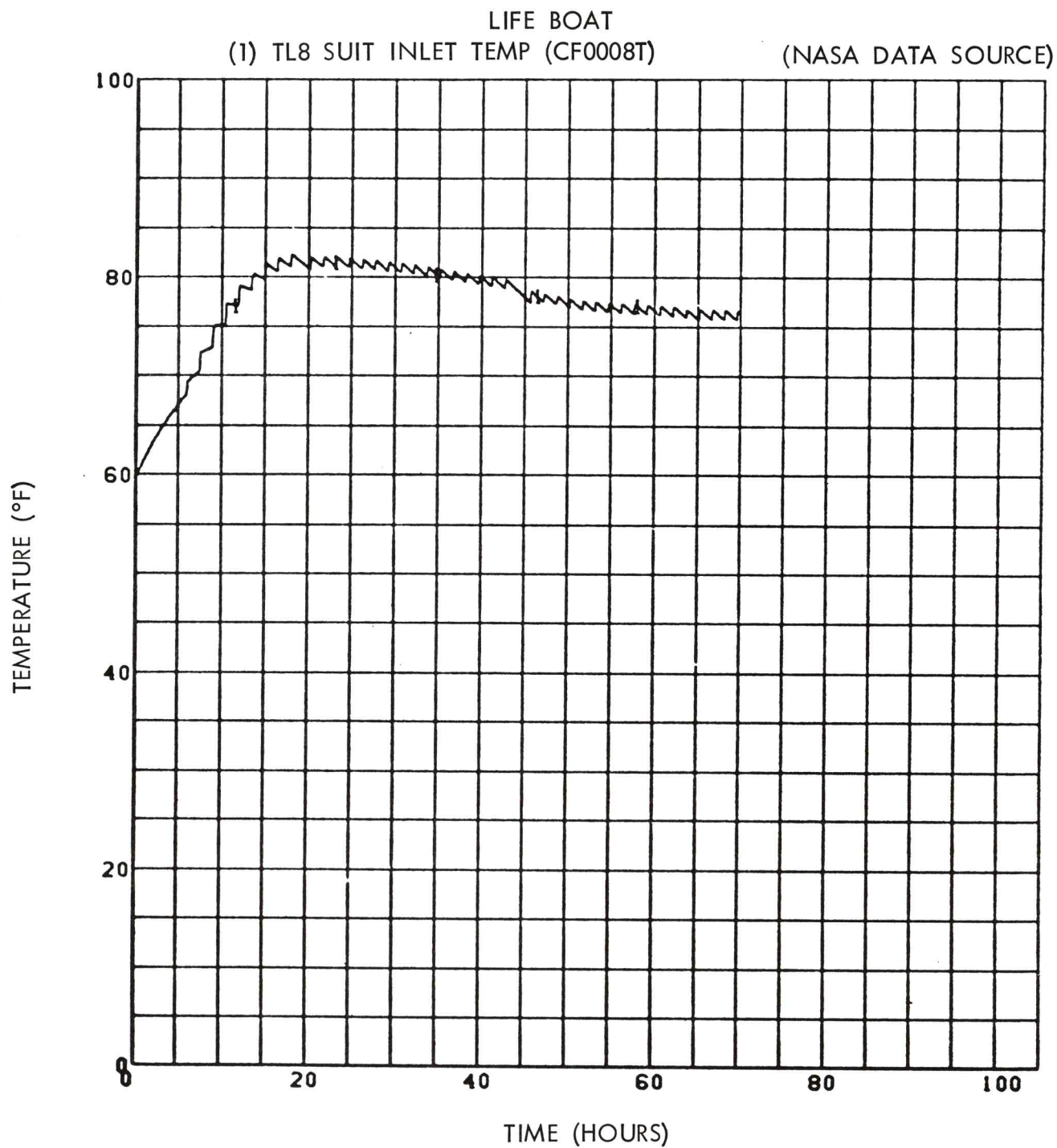


Figure 3.11-18. Suit Inlet Predicted Temperature Response
(See Paragraph 3.11.3)

4.0 SUBSYSTEM PERFORMANCE AND OPERATIONAL DATA

4.1 ELECTRICAL POWER SUBSYSTEM

4.1 EPS

4.0 SUBSYSTEM PERFORMANCE AND OPERATIONAL DATA

4.1 ELECTRICAL POWER SUBSYSTEM

CONTENTS

Paragraph No.	Description
4.1.1	POWER REQUIREMENTS AND PARAMETRIC DATA
4.1.1.1	Main Bus Voltage Allowable Range
4.1.1.2	Main Bus Voltage Performance
4.1.1.3	EPS Bus Structure Resistance Model
4.1.1.4	SPS Gimbal-Actuator Power Requirements
4.1.1.5	Power Level Change Operational Procedure
4.1.1.6	Logic Bus Alternate Power Source
4.1.2	FUEL CELL OPERATION
4.1.2.1	Module Performance
4.1.2.2	Module Temperature Range
4.1.2.3	Module Heat Rejection
4.1.2.4	Radiator Performance
4.1.2.5	Fuel-Cell Failure Mode Operation
4.1.2.5.1	Module Performance Without Cooling
4.1.2.5.2	Fuel-Cell Response After Failure of Primary or Secondary Bypass Valve
4.1.2.5.3	Fuel-Cell Response After Failure of Glycol Pump
4.1.2.5.4	Fuel-Cell Response After Failure of Hydrogen Pump or With Hydrogen Pump Off
4.1.2.5.5	Fuel-Cell Response With No Water Discharge
4.1.2.5.6	Fuel-Cell Life With Reactant Valves Closed
4.1.2.6	Module Isolation and Shutdown
4.1.2.7	Module Operation After CM-SM Separation
4.1.2.8	Module Disconnect Requirements
4.1.3	CRYOGENICS MANAGEMENT
4.1.3.1	Reactant Pressure/Quantity Relation
4.1.3.2	Hydrogen and Oxygen Tank Heater Power Dissipation
4.1.3.3	Tank Heat Input Parametric Data
4.1.3.4	Tank Terminal Pressure Decay
4.1.3.5	Oxygen Availability
4.1.3.6	Hydrogen Consumption Rate

Paragraph No.	Description
4.1.3.7	Oxygen Consumption Rate
4.1.3.8	Cryogenic Pressure Rise/Decay Rates
4.1.3.9	Cryogenic Tank Characteristics
4.1.3.10	Oxygen Tank Heat Leak Expulsion
4.1.3.11	Oxygen Tank Terminal Pressure Decay
4.1.4	BATTERIES AND BATTERY CHARGER
4.1.4.1	CSM Battery Energy Capacity
4.1.4.2	Battery Discharge Characteristics
4.1.4.3	Charger Characteristics
4.1.4.4	In-Flight Battery Charging Cutoff
4.1.4.5	Auxiliary Battery (415 amp-hr) Performance Characteristics
4.1.4.5.1	Auxiliary Battery Temperature Profile
4.1.4.6	Entry and Auxiliary Battery Load-Sharing Characteristics
4.1.4.7	Fuel-Cell and Entry Battery Load-Sharing Characteristics
4.1.5	AC OPERATION
4.1.5.1	Inverter Efficiency
4.1.5.2	Inverter Performance Without Cooling
4.1.5.3	Over/Under Voltage Sensing
4.1.6	MISCELLANEOUS
4.1.6.1	Master Electrical Equipment List
4.1.6.2	Diode Characteristics
4.1.6.3	Circuit Breaker and Fuse Overload Characteristics
4.1.6.4	Heat Dissipation of Electrical Equipment

4.0 SUBSYSTEM PERFORMANCE AND OPERATIONAL DATA

4.1 ELECTRICAL POWER SUBSYSTEM

4.1.1 POWER REQUIREMENTS AND PARAMETRIC DATA

4.1.1.1 Main Bus Voltage Allowable Range

Spacecraft systems have been designed to accept a maximum steady-state voltage of 30 volts and a 1-second transient of 32 volts, as defined at the load. Because of the designed-in minimum voltage drop between the main dc buses and certain systems, it is recommended that a maximum steady-state bus voltage of 30 volts be observed. Under no circumstances should the steady-state voltage be allowed to rise above 31 volts.

On the lower side of the voltage range spacecraft systems have been designed to a minimum steady-state voltage of 25 volts and 1-second transients to 21 volts, as defined at the load. However, because of ripple voltage, the G&N system should be supplied a minimum steady-state voltage of 25.8 volts, 24.0 volts under transient conditions. Special provisions have been made to minimize the line drop to the G&N system in order to satisfy these voltage requirements. As defined at the main dc buses, it is recommended that steady-state voltage be maintained above 26.5 volts and the transient voltage above 25.0 volts, to ensure proper operation of spacecraft systems. Severe degradation of system performance, however, is not anticipated as long as the steady-state voltage is maintained above 25.5 volts.

Operating near voltage limits requires consideration of the voltage regulation characteristics of the fuel cells and the effects of load changes, either intentionally switched or automatically cycled. The voltage regulation characteristic of a fuel cell is a function of temperature as well as load. At higher stack temperatures, the range of loads that the fuel cell can handle within voltage limits is greater than that at lower temperatures; i.e., $\Delta V/\Delta I$ decreases with increasing fuel-cell temperatures. In addition, the entire range of acceptable loads shifts upward with increasing stack temperatures. This characteristic is shown for three- and two-fuel-cell operation in Figures 4.1-1 and 4.1-2. Moreover, unlike the electrical loads that are switched on and off instantaneously, fuel-cell temperature is dependent upon the time history of the loads applied previous to the specific time in question. Although the fuel cell will seek the steady-state temperature associated with the loads being supplied, the response is relatively slow. The Block II qualification test indicates that the fuel cells will change temperature in an exponential manner, covering about two-thirds of the temperature change per hour. This rather slow response in temperature makes it possible to operate at almost any combination of fuel-cell temperature and load. Consequently, operation close to the voltage limits, either high or low, is to be expected. Since it is generally not feasible to predict the on and off times or duty cycles for automatically cycling loads, particularly those influenced by unknowns such as spacecraft attitude (thermal radiation incident upon the spacecraft), the only

practical means of precluding a possible over- or under-voltage condition is through avoidance of the minimum and maximum voltage areas by real-time power management. For example, with a maximum allowable steady-state main bus voltage of 31.0 volts and a minimum of 25.5 volts, maintaining the bus voltage between 26.5 volts and 30.0 volts will greatly reduce the probability of an over- or under-voltage condition.

This recommended operating range is shown as a function of load levels and fuel-cell temperature in Figures 4.1-1 and 4.1-2. This 1-volt caution area, while providing some cushion, will not protect against the simultaneous cycling of several of the larger automatic loads. The voltage cushion required to provide such a worst-case protection would be unduly restrictive on the allowable operating range. The caution area for fuel-cell temperatures below 390 F has been extended on the low-voltage side because of the added potential of the fuel-cell in-flight heater cycle in this temperature region. The approximate load levels and operating criteria for several of the major automatic cycling equipment items are listed in Table 4.1-1.

Because the critical temperatures and pressures associated with the operation of these cyclic loads can be monitored in real time by both the crew and Manned Space Flight Network (MSFN), their duty cycles can be anticipated. The MSFN can offer the crew considerable help in this area.

Qualification testing of the Block II fuel cells indicates that the thermodynamic control characteristics are significantly improved over the Block I fuel cell. Based on these tests, operation of the in-flight heaters is not expected at power levels above 1300 watts for three fuel cells. In addition, the ECS in-line heaters (primary system) are not expected to operate in a low earth orbit mission. The radiator outlet glycol temperature required to activate the heaters requires both a low electrical load (minimum heat input) and a cold radiator orientation. For a low earth orbit mission, the minimum thermal flux incident upon the radiator panels for any significant time is estimated to be in the range of 15 to 20 Btu/hr/ft² (average of both panels). At this thermal flux level, electrical loads would have to be reduced below 1400 watts (<48 amperes) before the radiator outlet temperature should reach the level required for heater operation (-15 F). However, the narrow control band of the secondary ECS loop could cause its heaters to operate under normal electric loads should the secondary system be activated. Consequently, the secondary loop, specifically secondary heater, should only be checked out when operating at a fuel-cell temperature and electrical load range where a 32-ampere load increase can be sustained. Simultaneous operation of both the primary and secondary radiators is not recommended; therefore, the primary and secondary heater will not be operating concurrently.

Figures 4.1-1 and 4.1-2 can be used to estimate the amount of cyclic loads which can be sustained without an over- or under-voltage condition. Entering the appropriate curve with the existing stack temperature (average of the fuel cells) and the total load (sum of the fuel-cell currents) will identify the present operating point with respect to the allowable range. The distance, at constant temperature, to the voltage limits indicates the size of the cyclic or transient load which can be sustained without exceeding these limits. If the operating point falls within the fuel-cell steady-state range, the operating conditions should remain fairly stable, i.e., the fuel-cell temperature should not change appreciably with time. On the other hand, should the operating

point fall outside the steady-state range, the point will drift toward the steady-state band. Operating lines which are a constant Δ current (as measured at 28 volts) away from the low-voltage warning light (26.25 volts) are shown as faint hidden lines. Constant Δ voltage lines are not shown for the upper limit.

Should either main bus voltage inadvertently fall below 26.25 ± 0.1 volts, illuminating the low-voltage warning light, it is recommended that an entry battery be placed on the line until loads can be reduced or until the fuel cells recover in temperature. If bus voltage approaches the 31-volt level, electrical loads should be added to the line to prevent an overvoltage condition.

4.1.1.2 Main Bus Voltage Performance

Figures 4.1-3 through 4.1-8 show command module main bus voltage as a function of fuel cell output current and temperature. Figures 4.1-3 through 4.1-5 reflect one-, two-, and three-fuel-cell operation at sea-level conditions, and Figures 4.1-6 through 4.1-8 reflect one-, two-, and three-fuel-cell operation under vacuum conditions.

The curves assume equal load sharing among the fuel cells.

4.1.1.3 EPS Bus Structure Resistance Model

Figure 4.1-12 shows the power sources, bus configuration, and line resistances of the electrical power distribution subsystem. The resistance values of other power distribution subsystem components such as connectors, switches, current shunts, and circuit breakers are included in the resistance values shown in the schematic.

4.1.1.4 SPS Gimbal-Actuator Power Requirements

Table 4.1-2 presents the SPS gimbal-actuator-motor power matrix. These data together with Figure 4.1-13 can be used to determine motor power requirements (specification and development test values). The power requirements may vary significantly between motors as well as between channels. Accordingly, specification values should be used until such time as test values for specific actuators become available.

4.1.1.5 Power Level Change Operational Procedure

When changing power levels, the permissible rate for powering the spacecraft up or down is primarily a function of the fuel-cell stack initial temperature and the rate at which the stack changes its temperature. Powering up or down, therefore, is more dependent upon the longer term electrical power averages than the precise power and orientation conditions from which the power change starts. Voltage regulation of the command module main dc bus is a primary concern during the power change operations, and the dc bus voltage reading should be used to determine the permissible step in power. During power down, the bus voltage should not be allowed to rise above 31 volts; when powering up, it would not drop below 26.5 volts. For example, when powering down, equipment may be turned off until the bus voltage reads 31 volts. This operating configuration should be maintained until the voltage drops to approximately 30.5 volts. Additional equipment may then be turned off until the bus again reaches the 31-volt limit. The procedure can be repeated until the desired power level is achieved. The spacecraft should be powered up similarly. Under normal operation with three fuel cells, the bus voltage will be high and fewer power steps will be required to power up than to power down.

4.1.1.6 Logic Bus Alternate Power Source

The redundant sequential events control system (SECS) draws power from SECS logic buses A and B, which normally are powered by entry batteries A and B, respectively. Loss of entry battery A or B or an open circuit between either battery and its respective bus would render the respective logic bus inoperative with a consequent loss of redundancy. To avoid the necessity for early mission termination due to the loss of SECS redundancy, a backup source for logic power is available.

If a failure of either battery A or B occurs, battery C may be connected to the bus of the failed battery by closing a circuit breaker (CB) on battery circuit breaker panel assembly 250. The closing of CB 15 will connect battery C to battery bus A, whereas closing CB 24 connects battery C to battery bus B, thereby re-establishing battery bus power, logic bus power, and SECS redundancy.

4.1.2 FUEL-CELL OPERATION

4.1.2.1 Module Performance

The fuel-cell voltage-current characteristics are shown in Figures 4.1-9, 4.1-10, and 4.1-11. Figures 4.1-9 and 4.1-10 indicate single fuel-cell performance, showing terminal voltage, current, and temperature under sea-level and vacuum conditions, respectively. Since the operational mode is

with three fuel cells operating under vacuum conditions, Figure 4.1-11 shows CM bus voltage, single fuel-cell load (assumes each fuel cell shares the load equally), and temperature characteristics under these conditions. It is noted that the VI characteristic of the fuel cell does not change between the sea-level and vacuum operation curve; i.e., the nominal steady-state terminal voltage under a given load (amperes) is the same for both sea-level and vacuum operation. The difference in the sensed surface temperature noted between the two curves reflects the cooling effects of the sea-level environment on the temperature transducer. In general, the sensed temperature during sea-level operation will run 10 to 15 F below the value sensed under vacuum operation for identical load conditions.

For instantaneous load changes, the fuel-cell VI characteristic will follow a constant-temperature line and will then recover to the steady-state condition corresponding to the new load. As the fuel cell recovers, its terminal voltages (and consequently CM main bus voltage) will change, which in turn will cause the load to change slightly. The time-temperature characteristics of the fuel cell are shown in Figure 4.1-14. This curve gives the time required for the fuel cell to reach its new steady-state condition as a result of a change in load.

The fuel-cell in-line heater located inside the pressure vessel is designed to maintain the stack at a temperature corresponding to a surface temperature of 380 to 385 F. Heater control actuation is based on the fuel-regenerator bypass valve inlet temperature, which is relatable to stack temperature. Figure 4.1-15 gives the estimated in-line heater duty cycle (vacuum operation) as a function of the fuel-cell load and external environment.

The condenser exit temperature as a function of fuel-cell current for various fixed secondary bypass valve positions is given in Figures 4.1-16, 4.1-17, and 4.1-18. Figure 4.1-16 is for cislunar coast with X-axis perpendicular to sun line and with roll of 1.5 revolutions per hour. Figure 4.1-17 is for quasi-steady-state lunar orbit maximum temperatures (light-side operation), 60-nautical-mile orbit, and X-axis parallel to the velocity vector. Figure 4.1-18 is the same as Figure 4.1-17 except for minimum temperatures (dark-side operation).

Figure 4.1-19 provides fuel-cell voltage decrease as a function of purge interval and cryogenic oxygen purity. Data are based upon 25-ampere load per fuel cell.

Figure 4.1-19.1 is an electrolyte concentration nomograph which presents fuel-cell water concentration in the electrolyte as a function of module temperature, current, and condenser exit temperature.*

Power plant voltage versus blanket pressure from 15 to 51.5 psia is shown for three power levels in Figure 4.1-19.2.*

* (NASA DATA SOURCE)

4.1.2.2 Module Temperature Range

The fuel-cell design is based on a minimum temperature limit of 380 F and a maximum of 500 F, as sensed at the middle cell of the 31-cell stack. The normal operating range, however, is between 390 and 440 F. Below 360 F, the cooler end cells of the 31-cell stack become less able to sustain the chemical reaction, resulting in degraded performance. Continued temperature decrease will result in eventual failure. An in-line heater located inside the pressure vessel is designed to maintain the stack temperature above 380 F by heating the incoming hydrogen should the fuel-cell temperature drop too low. Heater control actuation is based on the fuel regenerator bypass valve inlet temperature, which is relatable to stack temperature. If a fuel cell is being permanently removed from the bus, its heater can be deactivated by a switch on the main display panel to prevent heater operation as the fuel cell cools. On the high side of the range, the following temperatures may be used as guidelines:

- 440 F Maximum normal operating temperature associated with steady-state output of maximum power (1420 watts).
- 450 F Indicative of possible fuel-cell radiator malfunction.
- 500 F Maximum design temperature of the fuel cell. Above this temperature, the intercell sealing is marginal, resulting in potential KOH contamination of the oxidizer, fuel, and water.
- 550 F Above this temperature, electrolyte boiling can occur, resulting in a rapid buildup of gas in the KOH and subsequent fuel-cell flooding.

It is recommended that the fuel cell be removed from the bus should its temperature reach 500 F. However, in an emergency, the power plant can be operated above 500 F with increasingly degraded performance until failure. In all cases, circumstantial factors that can only be judged in real time may necessitate actions at other than the above temperatures. (See Table 3.11-1)

The fuel-cell glycol pump is designed to circulate glycol through the EPS radiators at a minimum temperature of -30 F. Below this temperature the pressure drop becomes excessive because of the increased glycol viscosity, and the pump may not be capable of maintaining flow. It is recommended that the radiator return temperature be maintained above -30 F by vehicle reorientation and/or load increase.

Heat transfer to the glycol loop from the primary (hydrogen) loop occurs at the condenser. The hydrogen exit temperature from the condenser is normally controlled to 160 ± 5 F. Exit temperatures greater than 225 F could result in excessive water buildup in the fuel cell. It is recommended that the condenser exit temperature be maintained below 225 F by reduced loads, open circuit operation, or vehicle reorientation.

4.1.2.3 Module Heat Rejection

Heat is rejected from the fuel cell by two modes. The primary mode of heat rejection involves the two active fuel-cell coolant loops and the EPS radiator subsystem. The second mode of heat rejection involves the heat lost from the fuel cell by conduction and radiation to the service module structure. Figure 4.1-20 shows the fuel-cell heat rejection to the EPS radiator subsystem, and Figure 4.1-21 illustrates the fuel-cell heat loss to structure for the minimum, maximum, and nominal fuel-cell structure temperatures expected for Apollo LOR missions. These structure temperatures represent averages for the fuel-cell compartment with ± 30 F variation for local extremes. The scales shown for the figures are in terms of one fuel cell, which is operating in parallel with two other fuel cells.

4.1.2.4 Radiator Performance

The EPS radiator transient performance in earth and lunar orbits can be related closely to the water-glycol temperature measurements at the radiator inlet and outlet ports and the fuel-cell current measurements from which the radiator heat rejection rate can be estimated. Figure 4.1-22, which shows the radiator inlet and outlet temperatures as a function of fuel-cell current, and Figure 4.1-23, which shows the nominal radiator heat rejection capability as a function of radiator inlet temperature, apply for a 100-nm earth orbit with the CSM X-axis parallel to the velocity vector. Figures 4.1-24 and 4.1-25 depict the same relationships for a 60-nm equatorial lunar orbit with the CSM X-axis parallel to the velocity vector. In Figure 4.1-24, which depicts maximum and minimum radiator inlet and outlet temperatures as two curves, the maximum and minimum fuel-cell heat rejection rates already defined have been taken into account. With respect to the temperature values shown in the figures no allowance has been made for measurement system error. The heat rejection and current scales shown for the figures are in terms of one fuel cell operating in parallel with two other fuel cells and with full radiator area.

4.1.2.5 Fuel-Cell Failure Mode Operation

The following paragraphs present fuel-cell performance characteristics for various failure modes.

4.1.2.5.1 Module Performance Without Cooling

Excess heat resulting from the chemical reaction in the fuel cell must be removed from the cell and rejected by the EPS radiators, which use water-glycol as the transport fluid. Should loss of cooling occur, the fuel cell will ultimately fail from overtemperature as described in paragraph 4.1.2.2.

If cooling is lost to only one fuel cell, that cell may accept a greater share of the total load as its temperature rises above the others. It should be removed from the spacecraft load before reaching a temperature of 500 F. Loss of a single fuel cell is not necessarily cause for an abort, because the remaining two power plants are capable of meeting mission power requirements.

If cooling is lost to all three power plants, it is estimated that the fuel cells will have a remaining useful life of two to four hours. The specific time before failure will be dependent upon stack temperature at the time of coolant failure, water concentration in the electrolyte at the time of failure, and power demand on the fuel cells and their tolerance to overtemperature. It may be possible to slow the temperature increase by extended purging of the hydrogen side of the electrodes. During hydrogen purges, steam expelled from the fuel cell through the purge vent line effects some cooling. Should cooling be lost to all three fuel cells, the following procedures are recommended:

1. Remove all nonessential loads from the buses.
2. Initiate single-inverter operation.
3. Initiate H₂ purge within the constraint of fuel-cell stack temperature and H₂ pressure.
4. Deorbit as soon as possible.

4.1.2.5.2 Fuel-Cell Response after Failure of the Primary or Secondary Bypass Valve *

The effect of primary or secondary bypass valve failure (in the zero or 100 percent position) on condenser exit temperature and module skin temperature is shown as a function of time for diagnostic purposes in Figures 4.1-25.1 through 4.1-25.4.

Figure 4.1-25.5 shows the maximum available operating time after a secondary bypass valve failure and a water removal blockage for various initial conditions as a function of powerplant load. The maximum allowable T_{CE} steady-state and transient limits for safe operation are also shown as a function of powerplant load.

4.1.2.5.3 Fuel-Cell Response after Failure of the Glycol Pump *

Figure 4.1-25.6 shows the effect of glycol pump failure on condenser exit temperature and module skin temperature as a function of time.

4.1.2.5.4 Fuel-Cell Response after Failure of the Hydrogen Pump or with Hydrogen Pump Off *

The effect of hydrogen pump failure on condenser exit temperature and module skin temperature is shown as a function of time in Figure 4.1-25.7. The rate of module skin temperature increase versus gross power is shown for the no purge condition in Figure 4.1-25.8.

* (NASA DATA SOURCE)

4.1.2.5.5 Fuel-Cell Response with No Water Discharge *

Fuel-cell available operating time with no water discharge versus fuel-cell current is shown in Figure 4.1-25.9.

Figure 4.1-25.10 presents the expected response of voltage, module skin temperature, and fuel-cell current as a function of time after water discharge blockage.

4.1.2.5.6 Fuel-Cell Life With Reactant Valves Closed

Life of an open-circuit fuel cell depends upon cell stack cooldown rate rather than pressure decay, as the leakage rates through the shut-off valves exceed the leakage rates of the fuel cell. Limited flight experience indicates this cooldown rate to be approximately 4 to 5 F per hour. Pump operation is not expected to significantly affect cooldown rates due to a minimum amount of heat being rejected. To assure fuel-cell operable condition, the module surface temperature should be maintained above 380 F.

If cooldown is accomplished with reactant shutoff valves closed and the in-line heater switch positioned to ON, fuel-cell failure resulting from H₂ system pressure depletion will occur within approximately 140 seconds (O₂ depletion requires 9 minutes) after automatic heater actuation which takes place at a module surface temperature of approximately 365 F.

Should the H₂ or O₂ reactant shutoff valve inadvertently close, (assuming nominal spacecraft loads) fuel-cell failure will occur within 30 seconds for H₂ shutoff or 120 seconds for O₂ shutoff.

The above information is based upon the following assumptions.

1. High pressure H ₂ Volume	8.4 In ³
Low Pressure-Low Temp (80 F) H ₂ Volume	168.0 In ³
Low Pressure-High Temp (420 F) H ₂ Volume	73.0 In ³
2. High Pressure O ₂ Volume	6.5 In ³
Low Pressure-Low Temp (80 F) O ₂ Volume	10.0 In ³
Low Pressure-High Temp (420 F) O ₂ Volume	73.0 In ³

3. High H₂ Pressure - 230 psia
High O₂ Pressure - 875 psia
Regulated H₂ & O₂ Pressure - 63 psia
Final H₂ & O₂ Pressure - 56 psia
4. Usable H₂ - 0.000602 lbs.
Usable O₂ - 0.01814 lbs.

CAUTION

1. Pumps may not restart following wet (in-flight) shutdown due to insulation resistance degradation.
2. In-line heater operation without operating pumps will result in loss of heater due to lack of cooling.

4.1.2.6 Module Isolation and Shutdown

Under certain circumstances, it may be necessary to isolate a fuel cell from the service module buses temporarily or to shut down the fuel cell completely. Isolation would normally be used while suspected fuel-cell failures are investigated; whereas shutdown would normally be used when the malfunction is judged to jeopardize the mission success or crew safety.

Isolation of a fuel cell is accomplished by (1) disconnecting the malfunctioned fuel cell from the service module bus/buses, (2) leaving the fuel-cell reactant valves open, (3) leaving the fuel-cell coolant and hydrogen pumps on, and (4) leaving the fuel-cell in-line heater on. Abnormal operating conditions that may require fuel-cell isolation are as follows:

1. Fuel-cell skin temperatures >450 F
2. Fuel-cell condenser exit temperature >225 F
3. Suspected internal shorts
 - a. Low voltage in relation to the load and temperature
 - b. High reactant consumption in relation to load
4. Severe load-sharing differential

5. Suspected reactant leakage
6. Other suspected malfunctions

Fuel-cell shutdown is accomplished by (1) disconnecting the malfunctioned fuel cell from the service module bus/buses, (2) closing the fuel-cell reactant valves, (3) turning off the fuel-cell coolant and hydrogen pumps, and (4) turning off the fuel-cell in-line heater.

Malfunctions that may require fuel-cell shutdown are as follows:

1. Loss of fuel-cell performance
2. Water contamination by KOH
3. Fuel-cell-regulated pressures above safe limits

(N₂=70 psia, H₂ and O₂=75 psia)

4. Purge valve stuck open or other confirmed excessive reactant leakage
5. Pump failure
6. Other confirmed malfunctions

In all cases, circumstantial factors that can only be adequately judged in real time may necessitate actions other than those stated.

4.1.2.7 Module Operation After CM-SM Separation

During the CM-SM separation sequence, the oxygen lines from the cryogenic storage tank to the command module are severed. The remaining oxygen in the service module vents directly to space, with the exception of 4.64 cubic inches for each fuel cell trapped between the fuel-cell shutoff valve module and the pressure regulator. Assuming initial oxygen temperature of 80 F, initial pressure of 860 psia, and adiabatic expansion, each fuel cell is capable of producing a minimum of 1490 ampere-seconds.

The hydrogen line is not severed during separation and hence is not a limiting factor.

The average service module jettison controller and service module RCS load for the first 5.5 seconds after service module jettison initiation is 7.15 amperes; thereafter, the load drops to 5.06 amperes. This load is shared equally by service module main buses A and B. If the gimbal motors are left running during the separation sequence, an additional 10-ampere load is added to each bus. Assuming one fuel cell per bus and gimbal motors running, the oxygen supply would support the service module bus loads for approximately 118 seconds. Without gimbal motors running, the oxygen supply would last approximately 579 seconds.

4.1.2.8 Module Disconnect Requirements

The fuel-cell circuitry is designed so that an overload or reverse current will disconnect the fuel cells from the buses. Table 4.1-3 shows the delay and transfer times for various loads. The test data are from one test and are included to show representative time.

4.1.3 CRYOGENICS MANAGEMENT

4.1.3.1 Reactant Pressure/Quantity Relation

Figures 4.1-26 and 4.1-27 show the relationship between supply tank temperature, pressure, and quantity for hydrogen and oxygen. Tank quantity is given in percent of gauge. Zero percent corresponds to a density of 0.17 pound per cubic foot for hydrogen and 1.39 pounds per cubic foot for oxygen. One hundred percent corresponds to 4.31 pounds per cubic foot for hydrogen and 69.5 pounds per cubic foot for oxygen.

The capability to determine quantity remaining by pressure and temperature (PVT), was provided as backup to the direct quantity measurements in each of the cryogenic oxygen and hydrogen storage tanks. While an error in the pressure measurement results in a minor error in determining quantity, a large quantity determination error results from a temperature measurement error. The quantity error is shown in Figure 4.1-26.1 as a function of true tank quantity for ± 6 F error in hydrogen temperature measurement and in Figure 4.1-27.1 for ± 11 F error in oxygen temperature measurement. The ± 6 F error in the hydrogen temperature measurement and ± 11 F error in the oxygen temperature measurement are the maximum end-to-end instrumentation errors unless otherwise specified in the individual spacecraft appendix.

4.1.3.2 Hydrogen and Oxygen Tank Heater Power Dissipation

See the appropriate spacecraft appendix for hydrogen and oxygen tank heater power dissipation as a function of CM main dc bus voltage.

4.1.3.3 Tank Heat Input Parametric Data

Figures 4.1-30 and 4.1-31 present specific heat input to the oxygen and hydrogen tanks parametrically as a function of pressure and gas quantity remaining in each tank.

4.1.3.4 Tank Terminal Pressure Decay

As the reactants are removed from the cryogenic hydrogen and oxygen storage tanks, the fluid temperatures and pressures are usually raised by automatic cycling-on of the heaters. As the pressure increases to a pre-determined level, the pressure switches automatically deactivate the heater. However, at very low densities, the pressure will drop with the heaters ON. This condition is known as tank terminal pressure decay. Unless the flow is reduced, the heaters will not switch off automatically and the fluid, tank structure, and heater temperatures could continue to increase. Crew action may be required to deactivate the heaters to avoid exceeding the heater and/or fluid temperature limits. These limits are $+80^{\circ}\text{F}$ for the oxygen fluid temperature and $+350^{\circ}\text{F}$ for the oxygen heater temperature. Since there is no heater temperature measurement for the hydrogen tank heaters, only a fluid temperature limit, -200°F , is defined for the hydrogen storage system.

The density at which terminal pressure decay begins and the rate at which pressure decays is a direct function of reactant flow rate. Figure 4.1-32 depicts the terminal pressure decay functions for a single oxygen tank for flow rates of 1.0, 1.5, and 2.0 lb/hr. The oxygen tank heater deactivation shown in Figure 4.1-32 assumes one-element heater operation at the start of terminal pressure decay. At lower density it is necessary to go to heaters OFF (at 75 F), to avoid exceeding the +80 F fluid temperature limit. It is possible to return to one-element heater operation after a sufficient duration of heaters OFF operation, which results in reduced temperatures within the tank. The figure does not consider a return to one-element operation after the heaters are turned off. Figure 4.1-33 depicts the terminal pressure decay function for a single hydrogen tank for flow rates of 0.05, 0.10, 0.15, and 0.20 lb/hr. With the exception of the 0.05 lb/hr hydrogen demand, the heater remained on throughout the duration of terminal pressure decay as a result of the fluid temperature dropping as the pressure dropped. At 0.05 lb/hr, the fluid temperature rise to -200 F required heaters OFF. The analysis does not consider a return to heater ON operation following heater shutoff.

4.1.3.5 Oxygen Availability

Oxygen availability is shown in Volume III.

4.1.3.6 Hydrogen Consumption Rate

Hydrogen is consumed by the fuel cells for the production of electrical power and for periodic purging of impurities from the electrodes. The flow rate is the instantaneous summation of the two.

$$\dot{H}_2 \text{ (lb/hr)} = \dot{H}_2 \text{ elec} + \dot{H}_2 \text{ purge}$$

The hydrogen consumption rate ($\dot{H}_2 \text{ elec}$) for the generation of electrical power can be obtained directly from the curves described in paragraph 4.1.1, or it can be calculated by using the relation: $\dot{H}_2 \text{ elec (lb/hr)} = 2.57 \times 10^{-3} \text{ (lb/A-H)} I_{FC} \text{ (amperes)}$; this relation is the theoretical electrochemical conversion rate and is reflected in the curves. For mission planning purposes, the fuel cell hydrogen purge flow rate is specified as 0.7 lb/hr per fuel cell. Purging may be scheduled regularly or may be based on electrical load and cryogenic impurities. (See Figure 4.1-33.1.)

The total hydrogen consumed between any two points in the mission may be calculated by integrating the H_2 versus mission time-plot between the time points desired. The amount of cryogenic hydrogen available is shown in Volume III of SODB.

4.1.3.7 Oxygen Consumption Rate

The cryogenic oxygen consumption rate is computed as follows:

$$\begin{aligned} \dot{O}_2 \text{ (lb/hr)} = & \dot{O}_2 \text{ met} + \dot{O}_2 \text{ leak} + \dot{O}_2 \text{ waste mgmt} + \dot{O}_2 \text{ elec} \\ & + \dot{O}_2 \text{ FC purge} + \dot{O}_2 \text{ bleed} + \dot{O}_2 \text{ LM press} \end{aligned}$$

Metabolic oxygen requirements are a function of crew activity, physical size of the men, respiration quotient (RQ), etc. Figure 4.2-39 shows the various metabolic rates as a function of

metabolic heat load that have been used for this section. Based on Figure 4.2-39, the average metabolic oxygen consumption rates (O_2 met) for various activity levels are as follows:

Activity Level (See Figure 4.2-39)	Metabolic Oxygen Usage Rate Per Man (lb/hr)
Work	0.085
Rest	0.066
Sleep	0.053

Cabin leakage (O_2 leak) can occur up to a rate of 0.2 lb/hr at a nominal cabin pressurization of 5 psig. Oxygen leakage at other than the 5-psi pressure may be calculated using the linear relationship:

$$\dot{O}_2 \text{ leak (lb/hr)} = \frac{P_{\text{actual psig}} \times 0.2}{5 \text{ psig}}$$

Measured leakage rates (at 5 psig) for specific spacecraft may be substituted for 0.2 lb/hr.

For mission planning purposes, an average usage rate of 0.076 lb/hr per man is recommended.

Oxygen is vented overboard through the waste management system during urine dump, fecal odor removal, and cabin atmosphere enrichment operations. During these operations the cabin atmosphere is vented at 1.0 lb/hr and is replaced by oxygen via the cabin pressure regulators except during the first 1.5 hours of the cabin atmosphere enrichment while cabin pressure bleeds down from the relief pressure $-6.0 (+0.2, -0.4)$ psid to normal operation pressure -5.0 ± 0.3 psia.

The following waste management oxygen budget is recommended for mission planning purposes.

Function	Duration per Occurrence	No. of Occurrences
Fecal odor removal	30 sec	3 per day
Urine dump	2 min	9 per day
Cabin atmosphere enrichment	10 hr	1 per mission

Oxygen is continuously vented overboard through bleed holes from within the pressurizing bladders of the potable and waste water tanks to the urine dump line. Any hydrogen diffusing through the bladders from the water is swept out of the system by the oxygen flow. A combined O_2 flow rate of 0.032 lb/hr nominal (0.044 lb/hr maximum) is expected.

For mission planning purposes, the expected ECS oxygen requirements for all of the above should be based on a total average rate of 0.32 ± 0.08 pound per hour for three-crewman operations and $0.128 + 0.08$ pound per hour for solo operations. (Also see appropriate appendices.)

For mission planning purposes, the following fuel-cell oxygen purge flow rate should be used:

$$\dot{O}_2 \text{ FC purge (lb/hr)} = 0.6 \text{ (per fuel cell)}$$

Purging may be schedule regularly or may be based on electrical load and cryogenic impurities. (See Figure 4.1-33.2.)

The oxygen consumption rate for electrical power production $\dot{O}_2 \text{ elec}$ may be assumed to occur at the stoichiometrical combination ratio with the $\dot{H}_2 \text{ elec}$ determined from paragraph 4.1.3.6 Hydrogen Consumption Rate.

$$\dot{O}_2 \text{ elec (lb/hr)} = 7.94 \times \dot{H}_2 \text{ elec (lb/hr)}$$

or

$$\dot{O}_2 \text{ elec (lb/hr)} = 2.04 \times 10^{-2} \text{ lb/AH} \times \text{amperes}$$

The oxygen requirement for pressurization of the LM ($\dot{O}_2 \text{ LM press}$) is primarily a function of the LM residual internal pressure at the time of pressurization. Because the LM pressure dump valve is left open during boost, venting the LM to ambient, a complete pressurization of the LM tunnel and cabin is required after transposition and docking. This pressurization requires approximately 0.3 lb for the tunnel and 6.6 lb for the LM cabin. The LM cabin and tunnel are expected to leak down to near ambient during translunar coast such that another complete pressurization (6.9 lb) will be required prior to the crew entering the LM for checkout in lunar orbit. While maintaining tunnel and LM cabin pressure from the CSM, a makeup oxygen usage rate of 0.3 lb/hr (0.2 lb/hr for LM cabin and 0.1 lb/hr for tunnel leakage) is recommended for mission planning purposes. After rendezvous and docking, a tunnel pressurization using 0.3 lb of oxygen is required. For nominal CM and LM cabin pressure regulator characteristics, no LM cabin pressurization will be required after docking.

Pressurization of the CM from 0.0 to 5.0 psia at 70 F requires 8.9 lb of oxygen. For pressurizations to other than the nominal conditions, the weight of oxygen required can be assumed to be directly proportional to the ratio of absolute pressure (psia) and inversely proportional to the absolute temperature ($^{\circ}\text{R}$).

4.1.3.8 Cryogenic Pressure Rise/Decay Rates*

The pressure in the cryogenic oxygen and hydrogen tanks is maintained within specified limits through the use of heaters and/or fans which operate in either an automatic or manual mode. The pressure rise/decay rates, dP/dt , have been determined in Figures 4.1-34 through 4.1-45 with the following simplifying assumptions about the system. The analysis assumed that the fluid is homogeneous and in thermodynamic equilibrium. The effects of pressure vessel stretch, tankwall thermal expansion and fluid compression in the plumbing line were accounted for in the analysis. The tank heat leak was considered as a function of mass outflow and quantity in the tank.

* NASA Data Source

The analysis of pressure rise/decay rates is based on single-tank performance. The results for oxygen for various heater powers and hydrogen for various fan and/or heater powers are presented in parametric form to include the range of probable operational conditions. The mass flow rate discharged from the tank and the percent quantity in the tank are the parameters. The single-tank results can be applied to multiple-tank usage for a combination of the included parameters. The results are based on nominal heater power, tank heat leak, and fan power dissipation values. These presented data can be used to estimate heater and/or fan cycling times which may be used in estimating mission EPS requirements.

4.1.3.9 Cryogenic Tank Characteristics

See the appropriate spacecraft appendix for cryogenic hydrogen and oxygen tanks average flow rate data, relief valve operation data, and pressure switch activation limits.

4.1.3.10 Oxygen Tank Heat Leak Expulsion

Figure 4.1-45.1, shows the heat leak expulsion in an environment of 70 F. These data were calculated from XTA0019 test results. While these data are not for the worst conditions of 140 F and maximum specification heat leak, it is representative of expected Apollo flight performance. The XTA0019 quantity vs. flowrate data is tabulated below:

Quant. (%)	Flow (lb/hr)	Quant. (%)	Flow (lb/hr)	Quant. (%)	Flow (lb/hr)
97.5	0.220	60	0.398	30	0.545
90	0.234	55	0.434	25	0.513
85	0.247	50	0.467	20	0.442
80	0.263	45	0.500	15	0.302
75	0.286	40	0.532	12	0.157
70	0.322	35	0.549	10.5	0.060
65	0.360	34	0.551	6.4	0.000

The ratio of flowrate at 140 F and 0 F to the flow at 70 F from XTA0019 test data at 930 psia and 35% quantity is:

Temperature, T	$(Flow)_T / (Flow)_{70}$
140 F	1.24
70 F	1.00
0 F	0.67

The correction can be calculated by the following equation:

$$\frac{(Flow)_T}{(Flow)_{70}} = -3.734 + 0.0138 (T + 460) - 9.184 \times 10^{-6} (T + 460)^2$$

4.1.3.11 Oxygen Tank Terminal Pressure Decay

Figure 4.1-45.2 shows the relationship between oxygen tank pressure and the quantity remaining during oxygen tank terminal pressure decay without the use of heaters. The isothermal curves represent limiting cases in which the withdrawal rate is so slow that the oxygen remains at ambient temperature. The adiabatic curve represents a limiting case where the pressure decay begins at 70 F and 900 psia, and the withdrawal rate is so fast that there is no effective energy addition by heat transfer from the tank mass or from the surroundings. Actual cases will fall between the adiabatic and isothermal curves. Below 150 psia, proper ECS and fuel-cell regulation cannot be maintained.

4.1.3.12 Oxygen Heater Temperature Predictions*

Figures 4.1-45.3 through 4.1-45.10 are provided for predicting the temperature of the oxygen tank heater. The heater wattage was picked at a nominal value of 80 watts and 120 watts with two and three active elements, respectively, for calculating the figures. Typical "g" levels for CSM passive thermal control (3.0×10^{-6} "g"), lunar orbit (5.0×10^{-7} "g") and attitude hold (7.2×10^{-8} "g") were used to compute the heater temperature. The figures present estimates substantiated by correlating calculations using oxygen tank quantity, "g" level, and heater "on" time within the ranges of 97% to 15%, 3×10^{-6} "g" to 7×10^{-8} "g" and 5 to 60 minutes, respectively, from the Apollo 14 flight. The correlation showed heater temperature estimates to be within 50 F with an average deviation of 20 F and a standard deviation of 22 F. This accuracy is applicable only when the heater is at the bulk fluid temperature prior to each heater "on" period.

Figure 4.1-45.3 provides single tank flow capability versus the heater sensor temperature (heater "on" continually) for various quantities. The curves enable selecting configuration of heater elements (40, 80 or 120 watts) to maintain the heater temperature below the 350 F maximum redline limit. The total oxygen flow can be estimated by summing the ECS and fuel-cell flows. The fuel-cell flow is calculated by multiplying the total fuel-cell current by 2.04×10^{-2} . By considering the oxygen tank pressures and heater control mode (on-off-auto) the flow from each tank can be estimated. The flow demand at the tank quantity and the chosen heater elements configuration uniquely specify the estimated heater temperature for an attitude hold "g" level of 7.2×10^{-8} .

Figure 4.1-45.4 predicts 120-watt heater maximum temperatures (three active elements) for various "g" levels and quantities providing estimates for "g" levels not included in Figures 4.1-45.3, 4.1-45.5, 4.1-45.6 and 4.1-45.7.

Figures 4.1-45.5 through 4.1-45.10 predict heater temperatures for various "on" times and either two or three active heater elements versus tank quantity. The flight attitude mode and the heater configuration determine the applicable figure. Heater "on" time (pressurizing period)

from flight data or from Figure 4.1-45.11 may be used to choose the "on"-time curve.

4.1.4 BATTERIES AND BATTERY CHARGER

4.1.4.1 CSM Battery (Cellophane-Type) Energy Capacity

Electrical energy for supporting the fuel cells during peak load periods and for entry and postlanding operations is supplied by three rechargeable silver oxide-zinc storage batteries. For mission planning purposes, the following battery capacity ratings should be used.

1. Flight Period. 40 ampere-hours
2. Postlanding Period. For postlanding operations, add 5 A-H per battery to the 40 A-H rating (based on Apollo 7 and Apollo 8 flight data).

4.1.4.2 Battery Discharge Characteristics

The discharge characteristics of the entry battery are shown in Figures 4.1-46 and 4.1-47. Figure 4.1-46 shows how the battery terminal voltage is affected when constant loads are applied to a fully-charged battery (>37.1 volts). Figure 4.1-47 depicts the battery volt-ampere characteristics as a function of temperature. Figure 4.1-48 presents battery voltage decline under small load conditions. Battery bus PCM voltage will read lower than battery terminal voltage due to the line resistance between battery terminals and battery bus, which may vary somewhat from spacecraft to spacecraft.

4.1.4.3 Charger Characteristics of Battery and Battery Charger

Figure 4.1-49 presents the battery charger input-output characteristics. The graph shows the input currents, ac and dc versus the output current and voltage. The curves were developed assuming constant input voltage of 28 Vdc and 116 Vac. Figure 4.1-50 presents the typical charging characteristics of the battery under partial discharge conditions. Figure 4.1-51 presents depth of battery discharge (ampere-hours out) versus the time required for the charger to fully recharge the partially discharged battery.

4.1.4.4 In-Flight Battery Charging Cutoff

A battery will be considered charged to its full capacity when one of the following conditions is satisfied (whichever occurs first):

1. The battery terminal voltage is ≥ 39.5 volts. Refer to the in-flight battery charging curves (Figure 4.1-52 of the spacecraft appendixes) to find the relationship between the battery charger current and the battery terminal voltage. (It is noted that the battery bus voltage should never exceed the acceptance test charger terminal voltage. However, at low-current values, the actual voltage difference between the battery charger terminals and the battery bus is small, and because of PCM data-bit resolution, battery bus PCM voltage may read higher than acceptance test data. The current for the individual spacecraft charger which corresponds to the maximum battery terminal voltage of 39.5 Vdc is determined by assuming a 0.5 ohm resistance from charger terminals to battery terminals.)
2. The amount of energy (A-H) taken out of the battery has been replaced.

4.1.4.5 Auxiliary Battery (415 Ampere-Hour) Performance Characteristics*

Figure 4.1-51.1 presents current/voltage characteristics for the 415 ampere-hour auxiliary battery. Tolerance lines (± 0.5 volt) about the average of the observed data points are included for reference. The basic curve was derived from raw ground and flight data and is only indicative of nominal battery performance. Figure 4.1-51.2 presents the V-I characteristics as a function of ampere-hours consumed.

4.1.4.5.1 Auxiliary Battery Temperature Profile

Figure 4.1-51.3 presents analytical data of the temperature response characteristics of the auxiliary battery as a function of battery load and time. The plots present the temperature response of the battery when operated in

*The data on the auxiliary battery were extracted from the Lunar Module Data Book, Volume II, Part 1, and reflect ground and flight data pertinent to the LM descent batteries.

environments of 40 and 85 F at loads of 10, 20, 30, 40, and 50 amperes. These two environments represent the lower and upper bounds of the average expected environment for a nominal mission.

Figures 4.1-51.4 and 4.1-51.5 represent the predicted temperature profiles for the 415 ampere-hour auxiliary battery during a 100-hour lunar orbit-to-earth contingency return for both the solo CSM and the CSM-LM A/S configurations. Figure 4.1-51.4 shows the profiles for the worst case or hot-soak boundary conditions, and Figure 4.1-51.5 shows the profiles for the nominal case or passive-thermal-control boundary conditions. By means of heating rate data derived from battery-current-usage profiles (provided by MPAD), curves were plotted, which were based on analyses conducted on the TRW enhancement battery thermal mathematical model in its correlation with thermal-vacuum test data.

4.1.4.6 Entry and Auxiliary Battery Load-Sharing Characteristics

Figure 4.1-51.6 presents plots of the load-sharing characteristics of the auxiliary and entry batteries under various load conditions. These plots reflect the circuit parameters presented in Figure 4.1-12 and the entry and auxiliary battery performance characteristics shown in Figures 4.1-47 and 4.1-51.1, respectively. In those cases where a SM bus load is indicated, the magnitude of the load in amperes can be determined by subtracting the CM bus load (horizontal scale) from the CSM battery load (vertical scale). The CSM battery load is the total current output of (1) the auxiliary battery or (2) the auxiliary battery plus one or more entry batteries.

4.1.4.7 Fuel Cell/Entry Battery Load-Sharing

Figure 4.1-51.7 sheets 1 thru 27 presents plots of the load-sharing characteristics of the fuel cells and entry batteries under various load conditions. F/C 1 load-sharing characteristics are representative of F/C 2 and F/C 3 operating under similar conditions. F/C 1/3 load-sharing characteristics are representative of F/C 1/2, and F/C 2/3 operating under similar conditions. These plots reflect the circuit parameters presented in Figure 4.1-12 and the fuel-cell and entry battery performance characteristics shown in Figures 4.1-10 and 4.1-47, respectively.

4.1.5 AC OPERATION

4.1.5.1 Inverter Efficiency

The curves presented in Figures 4.1-53 through 4.1-59 show inverter efficiency characteristics as a function of inverter input voltage, load (VA), and load power factor. The curves, which present data from inverter efficiency tests conducted by Westinghouse, are for lagging and leading power factors of 0.5, 0.7, 0.9, and unity (1.0) at input voltages of 25, 28, and 30 Vdc.

4.1.5.2 Inverter Performance Without Cooling

Inverters 1, 2, and 3 are cooled by coldplate assemblies V36-610035, 034, and 033, respectively. Loss of water-glycol flow to these plates could ultimately result in the loss of the inverters due to overtemperature. The inverter has a hot-spot design maximum temperature of 248 F. An inverter high-temperature warning light (and master alarm) will illuminate when the inverter temperature sensor, located on the bracket of the 65-ampere transistor case, exceeds 190 F.

Inverter hot-spot temperature can be monitored by MSFN on high bit rate up to its 248 F design limit. It is estimated that the inverter would continue to operate for approximately 20 to 35 minutes after reaching its design maximum temperature, depending on the ac load demands; however, operation above the 248 F design maximum temperature cannot be guaranteed.

The time required for the inverter to reach its design maximum temperature is dependent upon the ac load demands as well as the initial temperature conditions of inverter components and the coldplate at the time of coolant loss. Inverter operation without cooling was demonstrated in thermal-vacuum-chamber testing, and the test results indicate that substantial operating time is available after the loss of cooling. Inverter hot-spot temperature as a function of time from loss of cooling is shown in Figure 4.1-60. From an initial operating temperature of 90 F, the most highly loaded inverter rose approximately 50 F in three hours. The temperature rise rate during the latter two hours of the test was nearly linear at approximately 10 F per hour. Although the test was terminated after 3.25 hours, extrapolation of the data indicates that the inverter would reach the 190 F warning light level approximately eight hours after the loss of cooling. Inverter 3, which was not operating, had a linear temperature rise rate of approximately 9 F per hour. While this test did not represent a worst-case condition because of moderate initial temperature, nominal inverter loading, and convective cooling, it is indicative of the order of magnitude of time involved. Furthermore, in actual contingency cases, it may be possible to maintain inverter operation for extended periods without cooling by appropriate load management.

If loss of coolant flow to the inverter coldplates (primary and secondary) is detected during flight, the following procedures, which tend to maximize inverter operating time and maintenance of continuous ac power, are recommended.

1. Remove all nonessential ac loads from ac buses 1 and 2.
2. Balance loads on ac buses 1 and 2 to the extent possible and maintain dual-inverter operation.
3. If and when the first inverter reaches 190 F (light illumination if MSFN is not monitoring temperature), remove the inverter from its bus and power both buses with single inverter.
4. If and when the second inverter reaches 190 F, replace it with the redundant inverter.
5. Continue cycling inverters whenever the maximum temperature is reached. If the maximum temperature is reached in less than 30 minutes, switch at 30-minute intervals.

The rationale for the preceding recommended procedures is as follows:

1. Minimization and balancing of ac loads minimize the possibility of either inverter reaching its design maximum temperature.

2. Should the maximum temperature be reached at the reduced loads, then initiation of single-inverter operation maximizes inverter efficiency (minimizes heat generation per unit output).
3. Switchover at the C&W warning temperature (190 F) maximizes the heat dissipation and temperature decrease during its cool-off period when off-line.

4.1.5.3 Over/Under Voltage Sensing

The ac over/under-voltage sensing unit operating time is relatively insensitive to the magnitude of the over- or under-voltage condition. The unit operates for voltage conditions of greater than 130 ± 2 Vac and less than 95 ± 3 Vac. The operating time requirements are 25 to 40 milliseconds. The nominal operating time demonstrated by test is 30 milliseconds.

4.1.6 MISCELLANEOUS

4.1.6.1 Master Electrical Equipment List

The spacecraft electrical equipment that uses ac or dc power and the power levels for each piece of equipment are depicted in the master electrical equipment lists in the appendixes (Table 4.1-6). Each electrical equipment list reflects unit values of power for a specific spacecraft. For the IMU heater peak power and duty cycle see Figure 4.1-60.1.

4.1.6.2 Diode Characteristics

Two types of diodes are used in the power distribution subsystem. Characteristic curves for these diodes are shown in Figures 4.1-61 and 4.1-62.

4.1.6.3 Circuit Breaker and Fuse Overload Characteristics

Figure 4.1-63 shows the overload trip characteristics of the circuit breakers used in the spacecraft. The curves depict circuit breaker specification trip time limits for overload conditions of 200, 400, and 600 percent of nominal ampere rating.

Table 4.1-5 lists the overload blowing characteristics of fuses representative of those used in the spacecraft.

4.1.6.4 Heat Dissipation of Electrical Equipment

The heat dissipation of most CSM electrical and electronic equipment can be equated to the components electrical power consumption while operating. However, the communications and scientific systems do radiate some power in the form of RF energy from antennas and, therefore, dissipate heat at a somewhat lower rate than their respective power demands. The energy radiated from

the CSM lights, laser altimeter, etc., in the visible spectrum is not significant. CSM equipment electrical power requirements and general location are given in the Master Electrical Equipment List (MEEL), Table 4.1-6 of the appropriate CSM appendix. Since the power requirements (both ac and dc) are given in watts, they may be converted to thermal units by multiplying the power values by 3.41 Btu's/watt hour. To account for radiated RF energy the power requirements of the following equipment should be reduced by the indicated amount prior to converting to the thermal units.

MEEL CODE	DESCRIPTION	RADIATED POWER WATTS	CSM EFFECTIVITY	
			113	114
2108	S-BD Power Amp HI (#1)	11.2	X	X
2110	S-BD Power Amp LO (#1)	2.8	X	X
2112	S-BD Power Amp HI (#2)	11.2	X	X
2114	S-BD Power Amp LO (#2)	2.8	X	X
2120	VHF/AM XMIT (296.8)	5.0	X	X
2121	VHF/AM XMIT (259.7)	5.0	X	X
2130	Rendezvous Xponder	0.3	X	X
2143	VHF Recovery Beacon	3.0	X	X
*	Lunar Sounder (HF Mode)	11.2		X
*	Lunar Sounder (VHF Mode)	1.5		X

*MEEL Code Not Assigned

The heat dissipation of the CSM inverters (MEEL codes 1615, 1616, and 1617) is equivalent to the efficiency loss in converting the dc input power to ac output. Accordingly, the heat dissipation can be calculated using the efficiency curves of Figures 4.1-53 through 4.1-57, given the inverter loads, power factors and input dc voltages. Under normal operational conditions inverter 1 heat dissipation will average approximately 160 watts (545 Btu/hr) while inverter 2 averages approximately 135 watts (460 Btu/hr) based on average output power of 450 and 350 watts respectively, at 0.9 power factors (lagging) and with 28.0 Vdc applied to the inverters. Since inverter 3 is not normally energized during the mission it does not contribute to the electrical and electronic equipment heat dissipation. Should an inverter be energized but not loaded (idle mode) it will dissipate approximately 112 watts (382 Btu/hr).

The CM battery charger (MEEL Code 1613 and 1614) must be treated in a similar manner as the inverters. Heat dissipation from the charger can be calculated by subtracting the output power (dc) from the input power (ac and dc) using Figure 4.1-49 and assuming nominal input voltages of 28.0 Vdc and 115.0 Vac. However, a more simple treatment is to assume the charger operates at a constant efficiency of approximately 90% over its normal operating range or that it dissipates heat at an average rate of 5 watts (17 Btu/hr) during a typical battery charge cycle (average charge rate of 1 amp/hr per hour).

In all cases, the equipment operational modes and duty cycles must be considered.

Table 4.1-1. Major Automatic Cycling Equipment
(See Paragraph 4.1.1.1)

Equipment	Load (amperes)	Operating Criteria
MAJOR LOADS		
Fuel-cell in-line heaters Service module RCS quad heaters	6.6 per fuel cell 3.4 per quad	Fuel-cell temperature ≤ 385 F Temperature $\leq 120 \pm 5$ F (primary and secondary)
ECS radiator heaters (primary) ECS radiator heaters (secondary)	17.3 17.3 (first step) 17.3 (second step)	Primary radiator outlet ≤ -15 F Secondary radiator outlet ≤ 43 F Secondary radiator outlet ≤ 42 F
Cryogenic O ₂ heaters Cryogenic H ₂ heaters	11 (both tanks) 1.4 (both tanks)	≤ 865 psia (both tanks) ≤ 225 psia (both tanks)
OTHER MAJOR LOADS		
IMU CMC SCS	6.6 3.2 6.6	Powerup from standby Powerup from standby Powerup from warmup mode

4.1-17

Table 4.1-2. SPS Gimbal-Actuator-Motor Power Matrix (Mod II Actuator) (A)
(See Paragraph 4.1.1.4)

Condition	Motor	Channel I (watts) (B)		Channel II (watts) (B)		Total (watts) (B)	
		Specification	Test (C)	Specification	Test (C)	Specification	Test (C)
Idle (D)	Pitch	210	200	140	140	700	680
	Yaw	210	200	140	140		
Boost (E)	Pitch	245	224	140	140	770	728
	Yaw	245	224	140	140		
SPS thrusting (F)	Pitch	500	371	140	140	1280	1022
	Yaw	500	371	140	140		
Maximum (G)	Pitch	1000	(H) 910	140	140	2280	2100
	Yaw	1000	(H) 910	140	140		

Notes:

(A) 1. Effective on SC 017 and subsequent spacecraft.

(B) 2. Assumes Channel I operating and Channel II in STANDBY.

(C) 3. Specification MC287-0014.

4. Development Test Results 2-1-P CH I Ext.

(G) 5. All powers for 28 volts dc at load interface.

6. Initial abort transient.

7. Actuator force assumed to be:

(D) 0 lb (E) 100 lb (F) 500 lb (G) 1300 lb

(H) 8. Measured at 2000-lb force.

4.1-18

SNA-8-D-027(II), Rev 3

Table 4.1-3. Delay and Transfer Times for Various Loads
(See Paragraph 4.1.2.8)

Load (amp/ cell)	Required Disconnect Delay (sec)	Test Delay (sec)	Transfer Time (sec)
FUEL-CELL DISCONNECT OVERLOAD CURRENT DATA			
75	100 ampere minimum	No transfer	
112	25 to 300	80	0.046
150	8 to 150	38	0.046
300	2 to 8	5.81	0.046
450	1 to 2	1.07	0.046
600	0.62 to 1.2	0.776	0.046
750	0.42 to 0.76	0.572	0.046
1000	0.24 to 0.55	0.470	0.046
FUEL-CELL DISCONNECT REVERSE CURRENT DATA			
4	No trip	No transfer	
20	1 to 10	2.10	0.046
30	1 to 1.3	1.22	0.046
50	1 to 1.3	1.11	0.046

Table 4.1-4. Cryogenic Tank Characteristics

See Table 4.1-4 of the appropriate appendix.

Table 4.1-5. Fuse Time-Current Characteristics
(See Paragraph 4.1.6.3)

Current Rating (amperes)	Overload (amperes)	Blowing Time (seconds)
1. SPECIFICATION: ME451-0006 (FUSE, MICROMINIATURE)		
0.125	1.7	0.0003 to 0.0008
	0.5	0.003 to 0.008
	0.25	0.015 to 5.0
0.250	4.5	0.0003 to 0.0008
	1.3	0.003 to 0.008
	0.5	0.015 to 5.0
3.000	58.0	0.0003 to 0.0008
	17.0	0.003 to 0.008
	6.0	0.015 to 5.0
2. SPECIFICATION: ME451-0009 (FUSE, MINIATURE, CARTRIDGE)		
1.0	8.0	0.002 to 0.035
	3.8	0.020 to 0.075
	3.1	0.025 to 0.125
5.0	16.0	0.030 to 1.30
	8.6	12.00 to 3.00
	7.3	3600 max
10.0	40.0	0.380 to 0.620
	20.0	15.00 to 30.00
	17.0	25 to 300

Table 4.1-6. Master Electrical Equipment List

See Table 4.1-6 of the appropriate appendix.

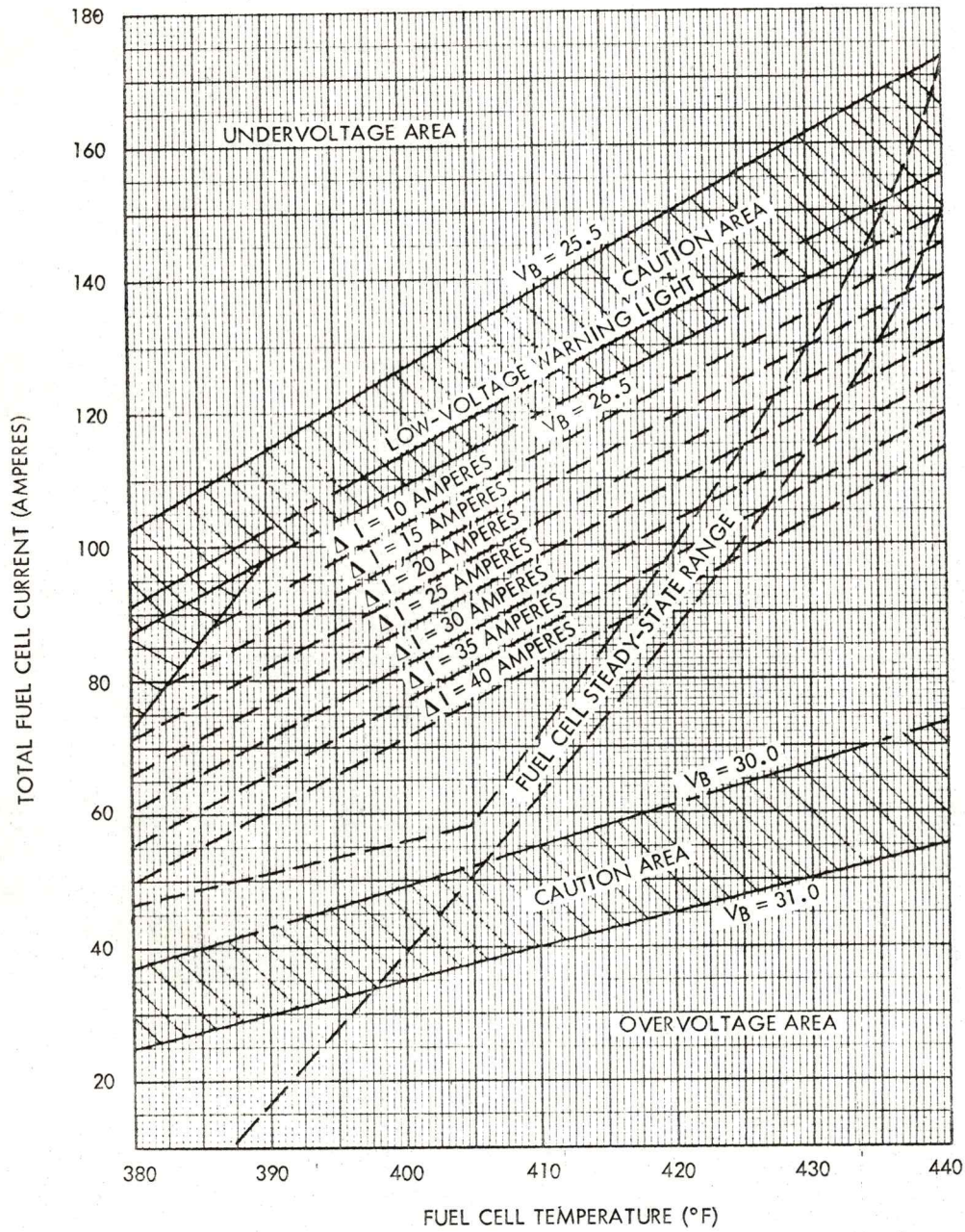


Figure 4.1-1. Allowable Operating Range (Three Fuel Cell) Vacuum Conditions

(See Paragraph 4.1.1.1)

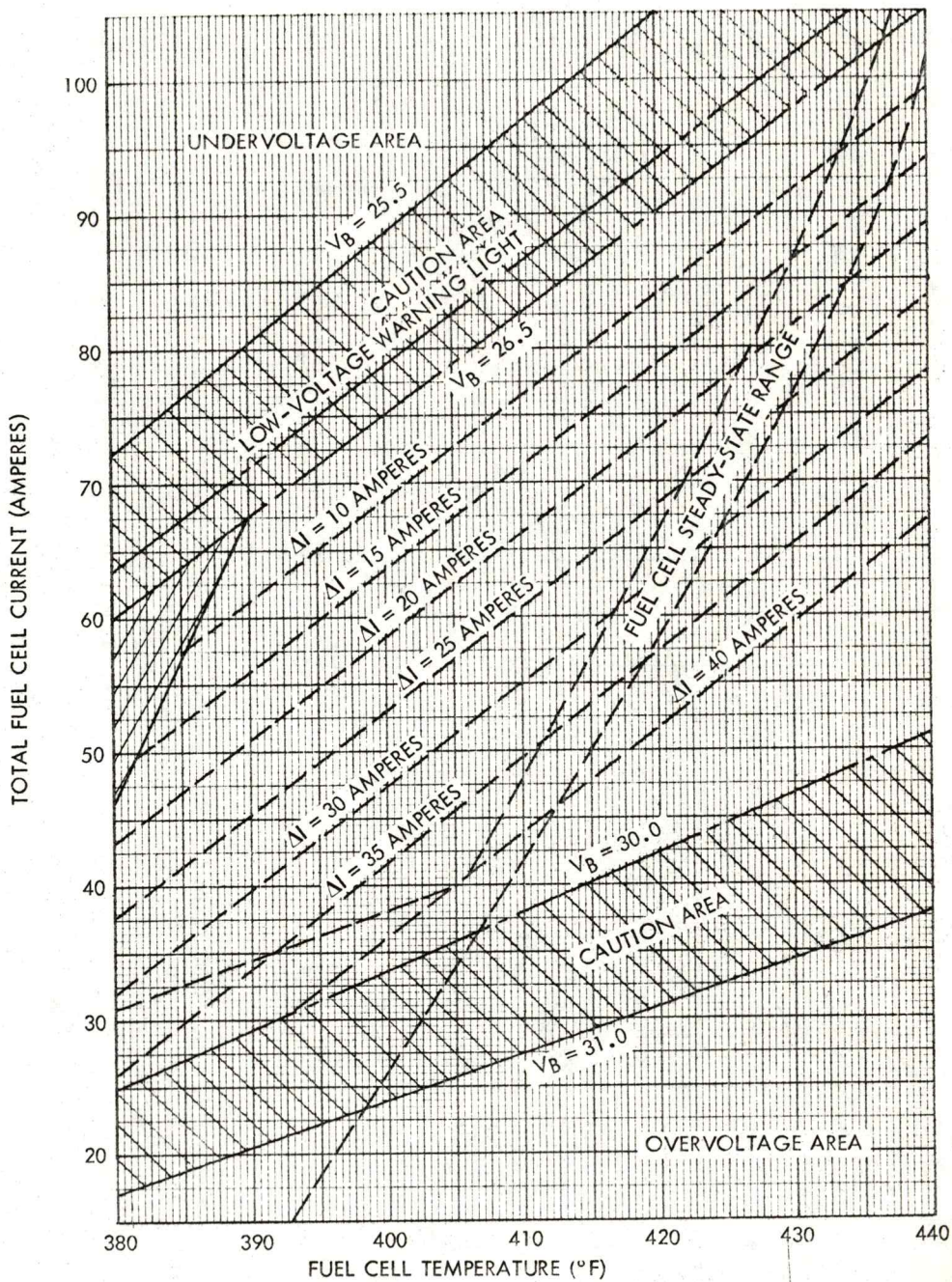


Figure 4.1-2. Allowable Operating Range (Two Fuel Cell) Vacuum Conditions
 (See Paragraph 4.1.1.1)

ONE FUEL CELL - SEA LEVEL

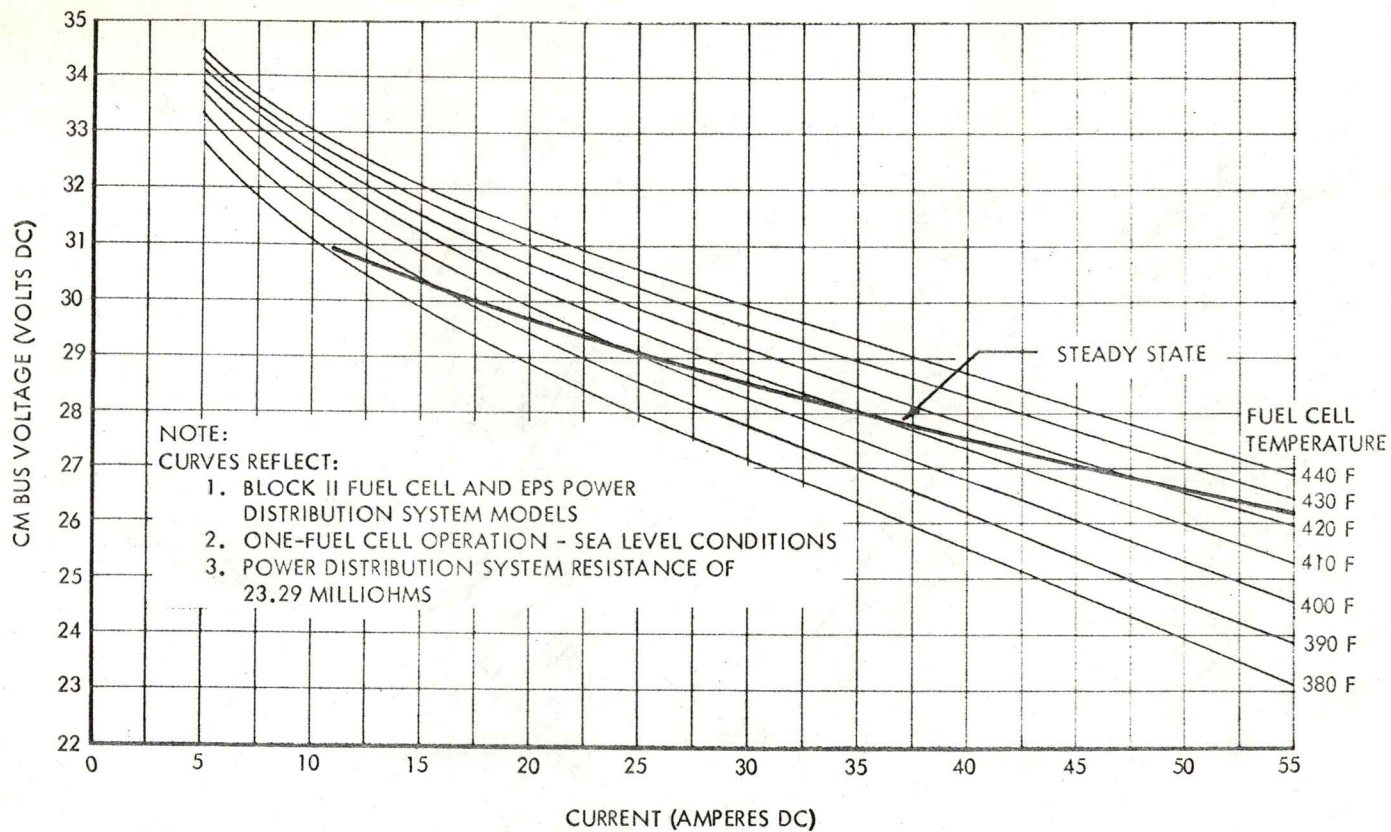


Figure 4.1-3. CM Main DC Bus Voltage as Function of Fuel Cell Current and Temperature

(See Paragraph 4.1.1.2)

4.1-23

SNA-8-D-027(I), Rev 3

TWO FUEL CELLS - SEA LEVEL

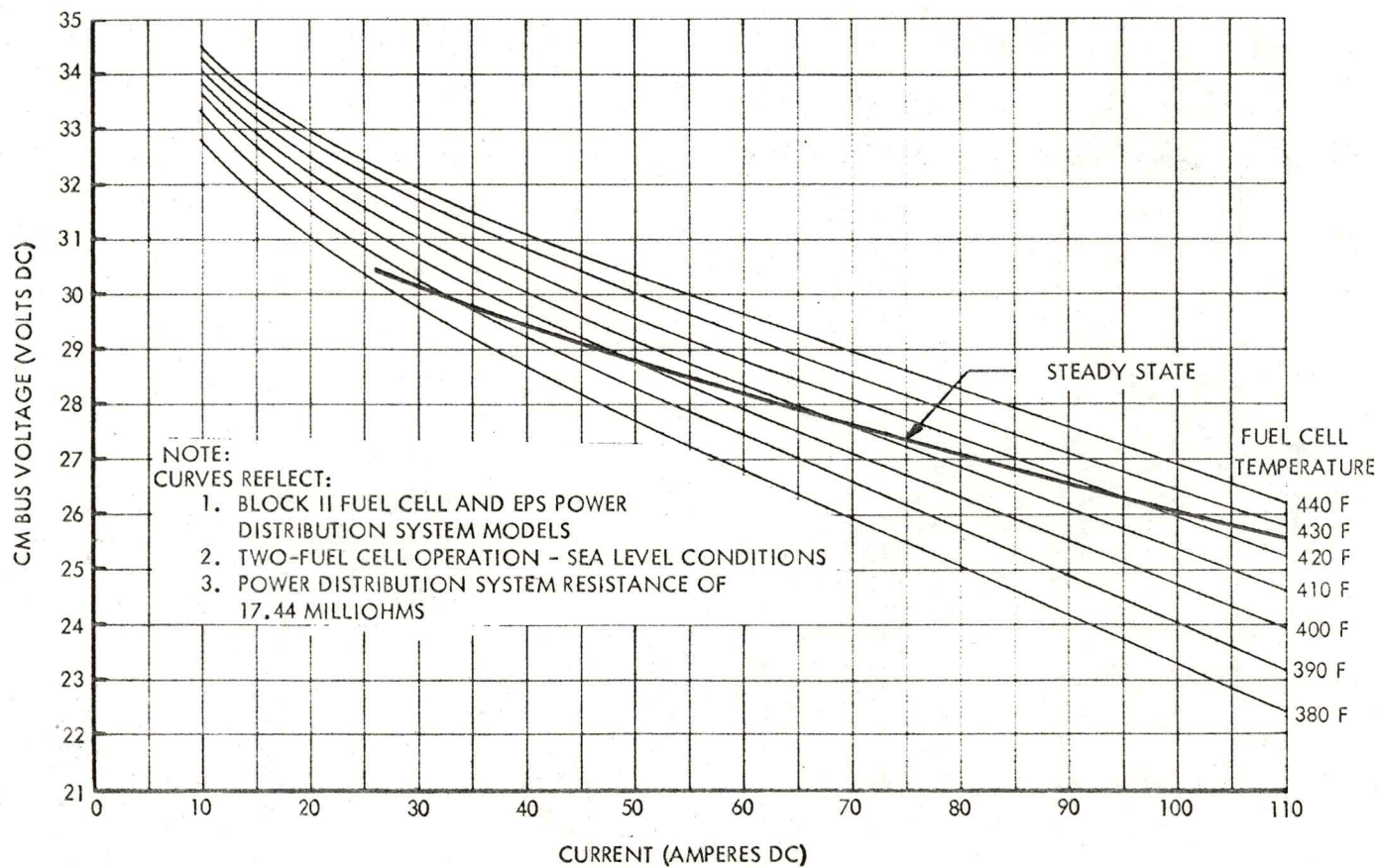


Figure 4.1-4. CM Main DC Bus Voltage as Function of Fuel Cell Current and Temperature

(See Paragraph 4.1.1.2)

THREE FUEL CELLS - SEA LEVEL

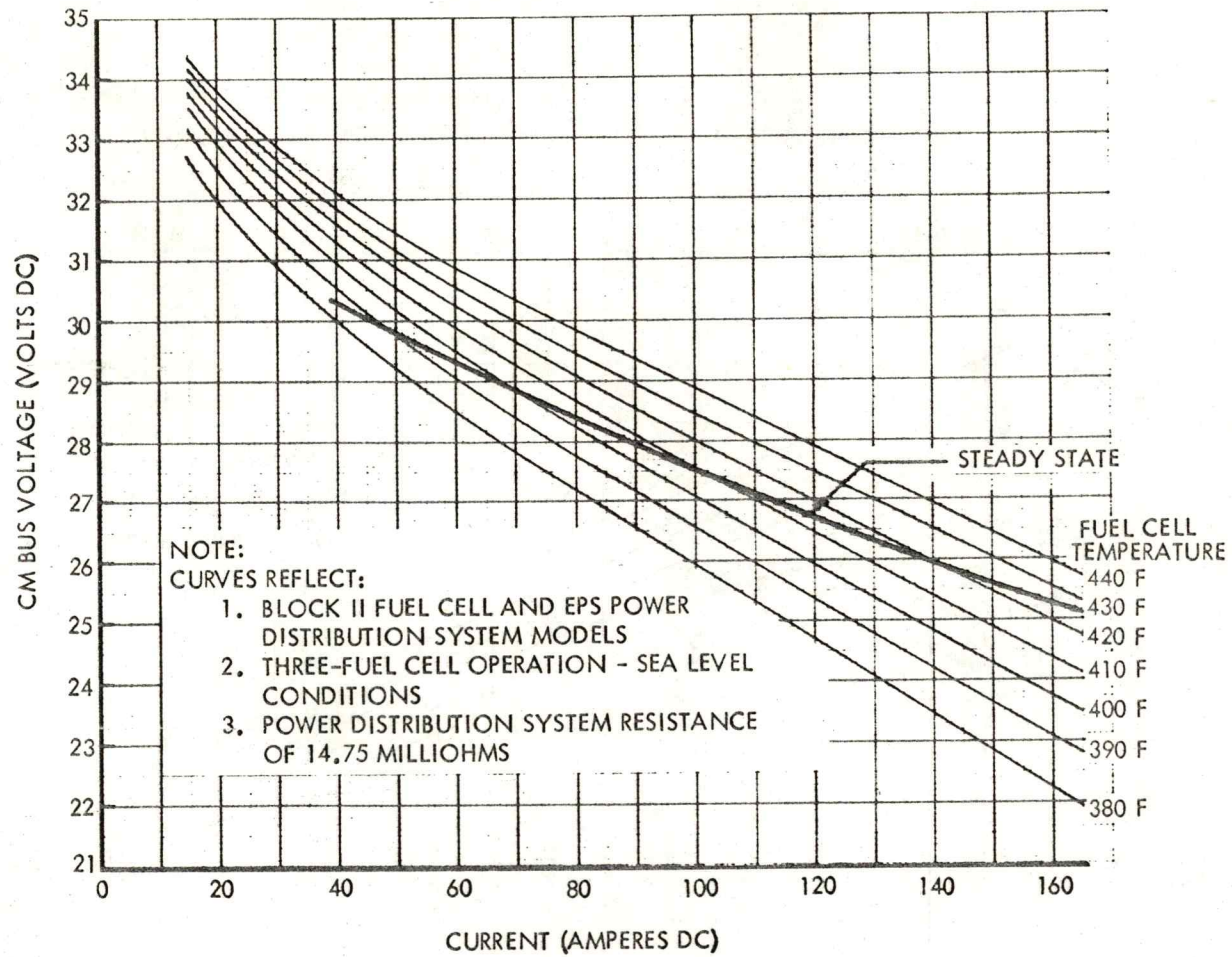


Figure 4.1-5. CM Main DC Bus Voltage as Function of Fuel Cell Current and Temperature

(See Paragraph 4.1.1.2)

4.1-25

SNA-8-D-027(I), Rev 3

ONE FUEL CELL - VACUUM CONDITIONS

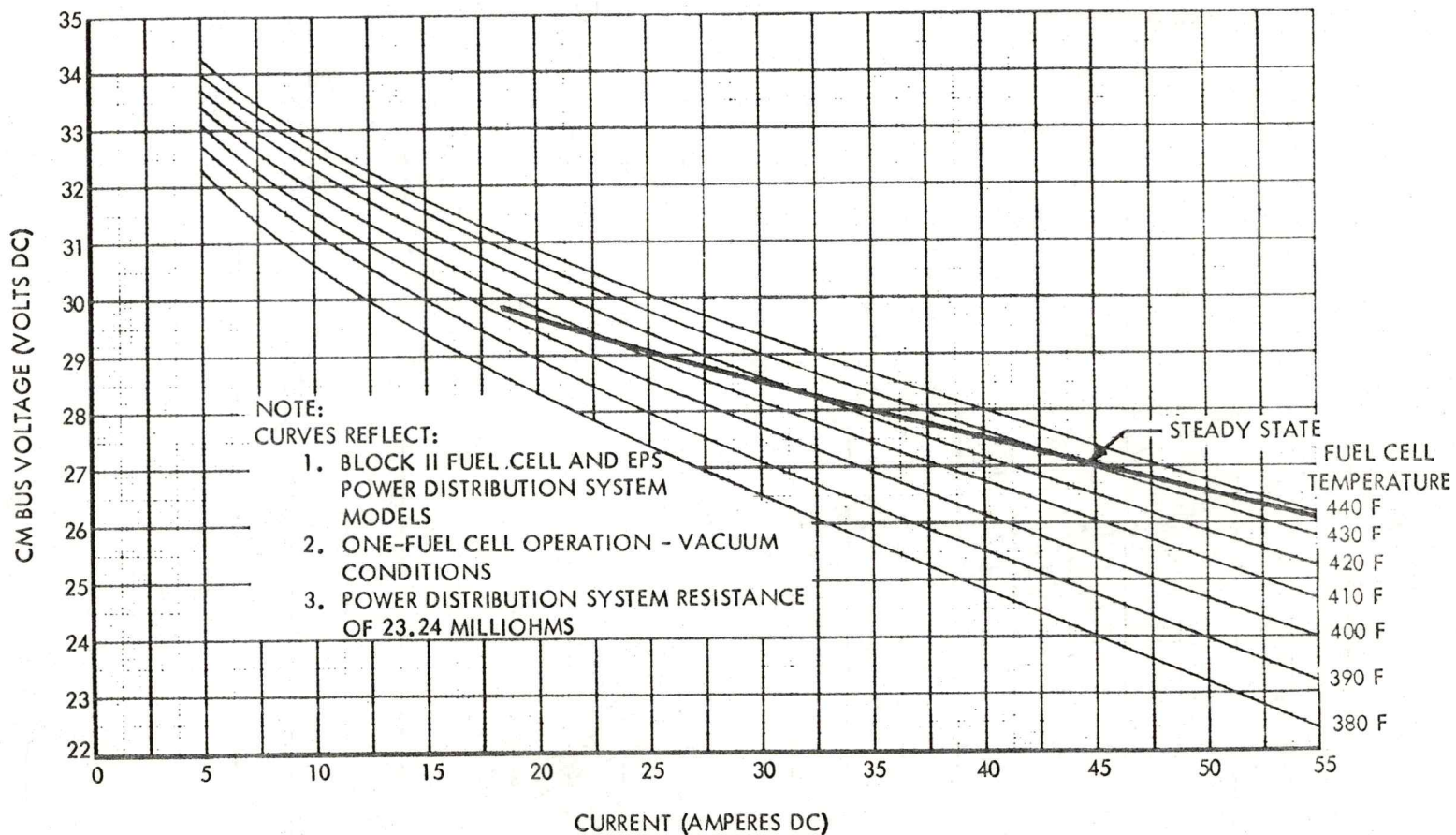


Figure 4.1-6. CM Main DC Bus Voltage as Function of Fuel Cell Current and Temperature

(See Paragraph 4.1.1.2)

4.1-26

SNA-8-D-027(I), Rev 3

TWO FUEL CELLS - VACUUM CONDITIONS

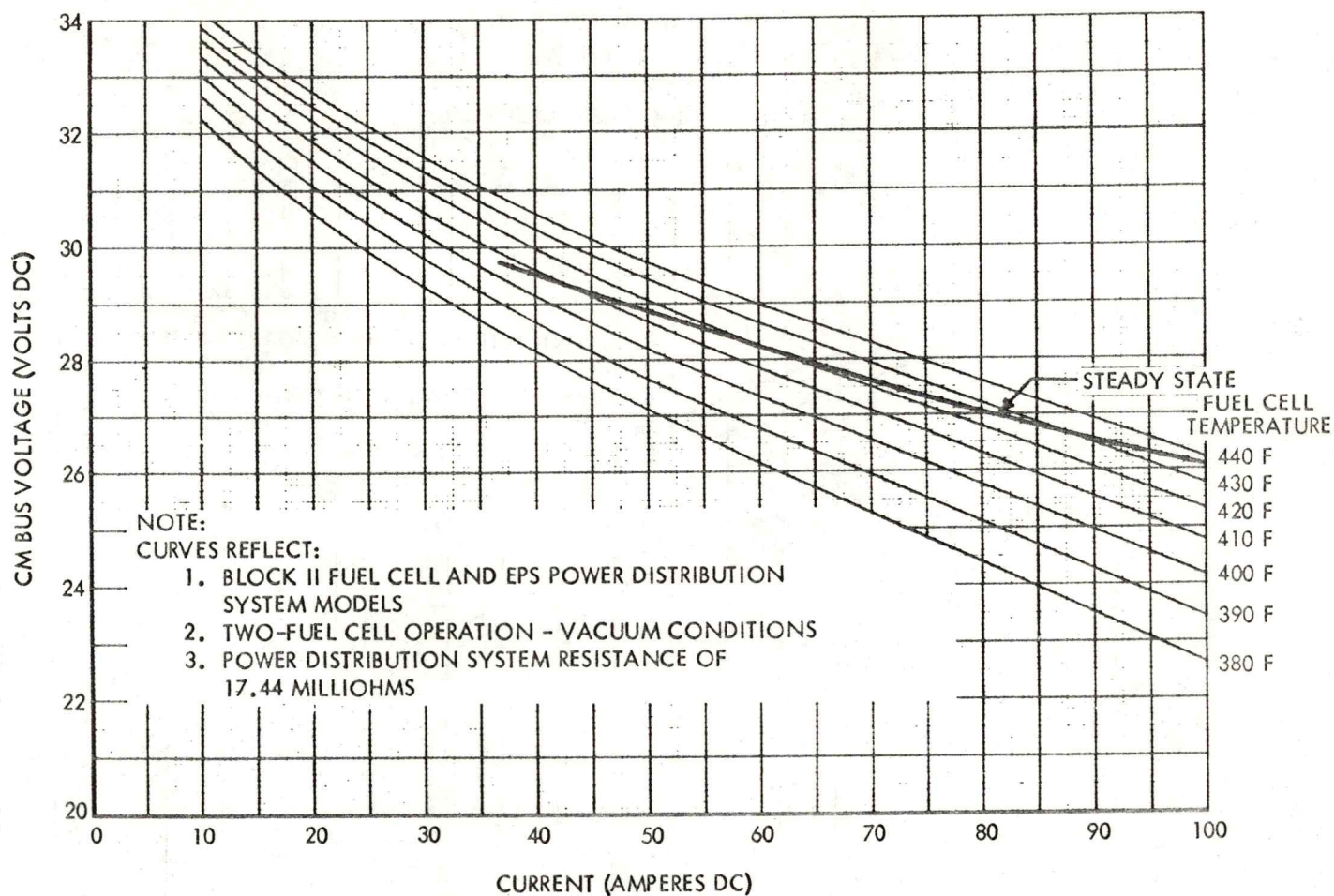


Figure 4.1-7. CM Main DC Bus Voltage as Function of Fuel Cell Current and Temperature

(See Paragraph 4.1.1.2)

4.1-27

SNA-8-D-027(I), Rev 3

THREE FUEL CELLS - VACUUM CONDITIONS

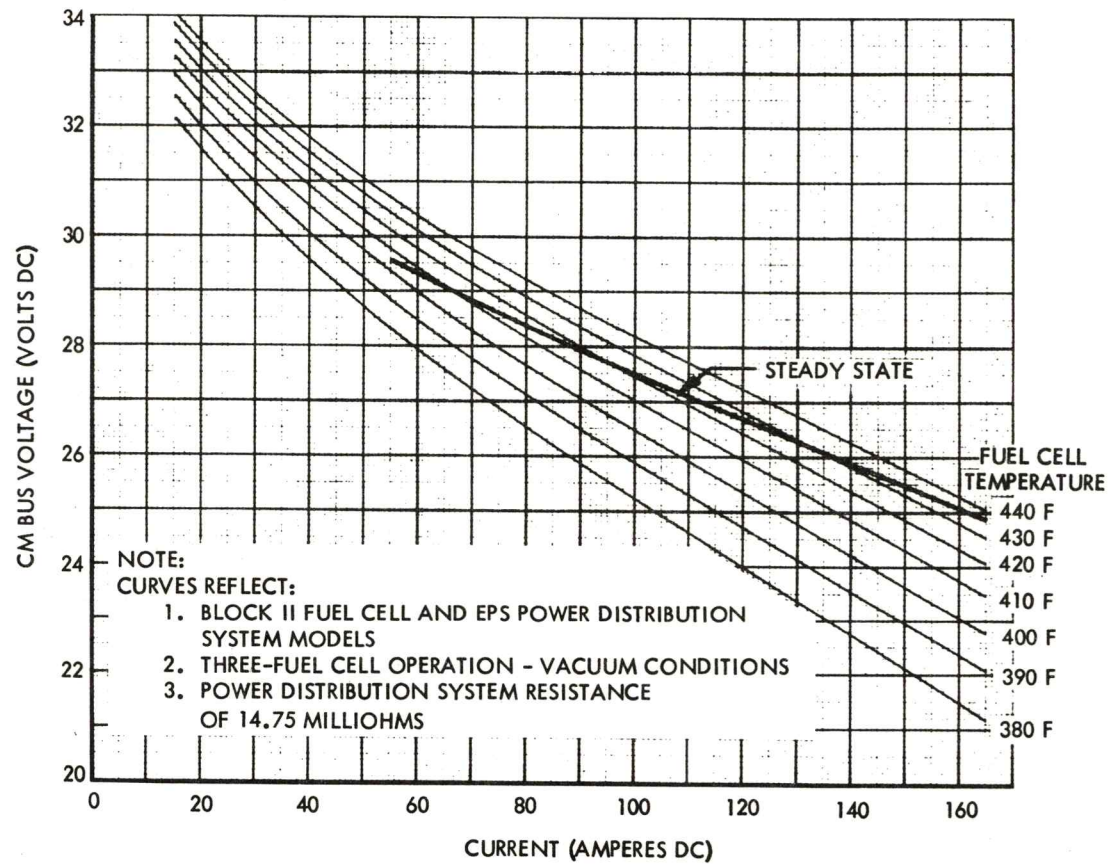


Figure 4.1-8. CM Main DC Bus Voltage as Function of Fuel Cell Current and Temperature

(See Paragraph 4.1.1.2)

4.1-28

SNA-8-D-027(I), Rev 3

4.1-29

SNA-8-D-027(I), Rev 3

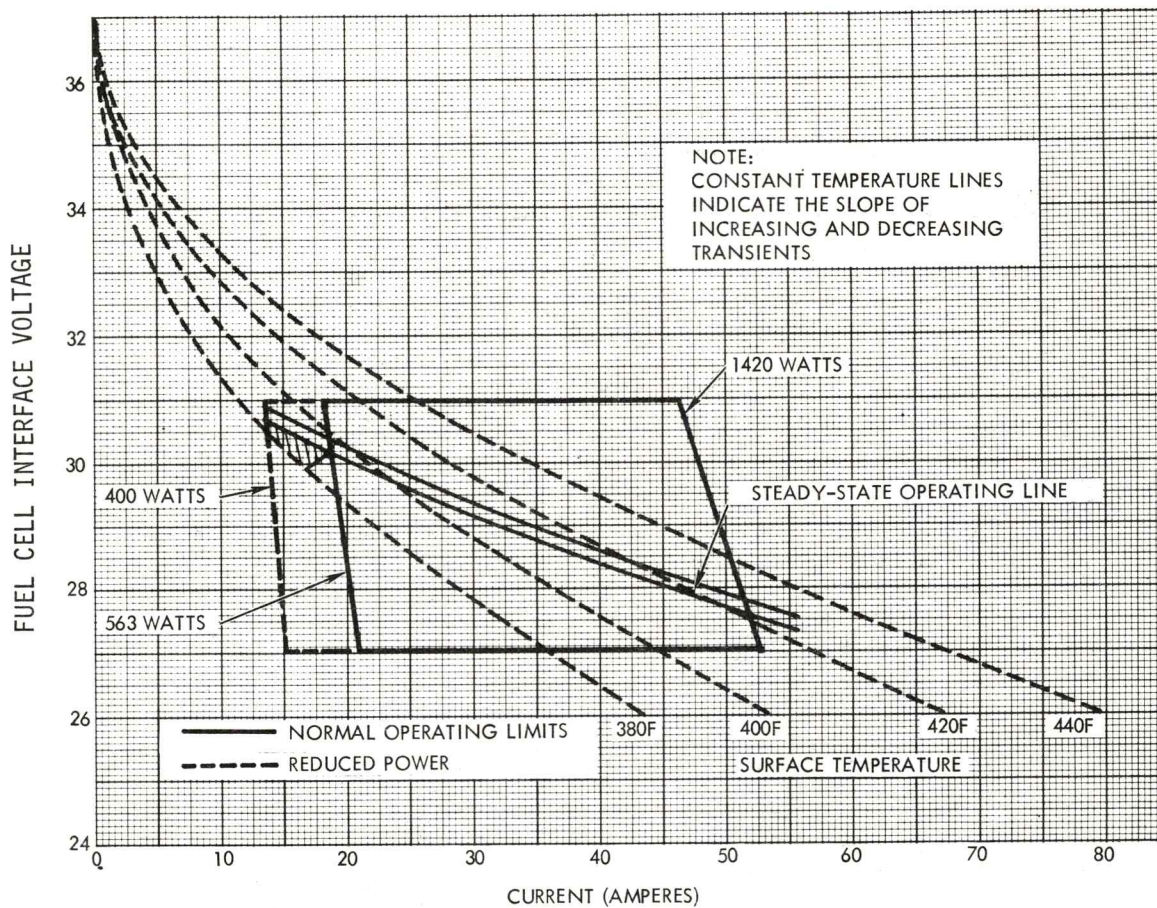


Figure 4.1-9. Fuel-Cell Performance Characteristics, Sea-Level Conditions

(See Paragraphs 4.1.1.2, 4.1.2.1)

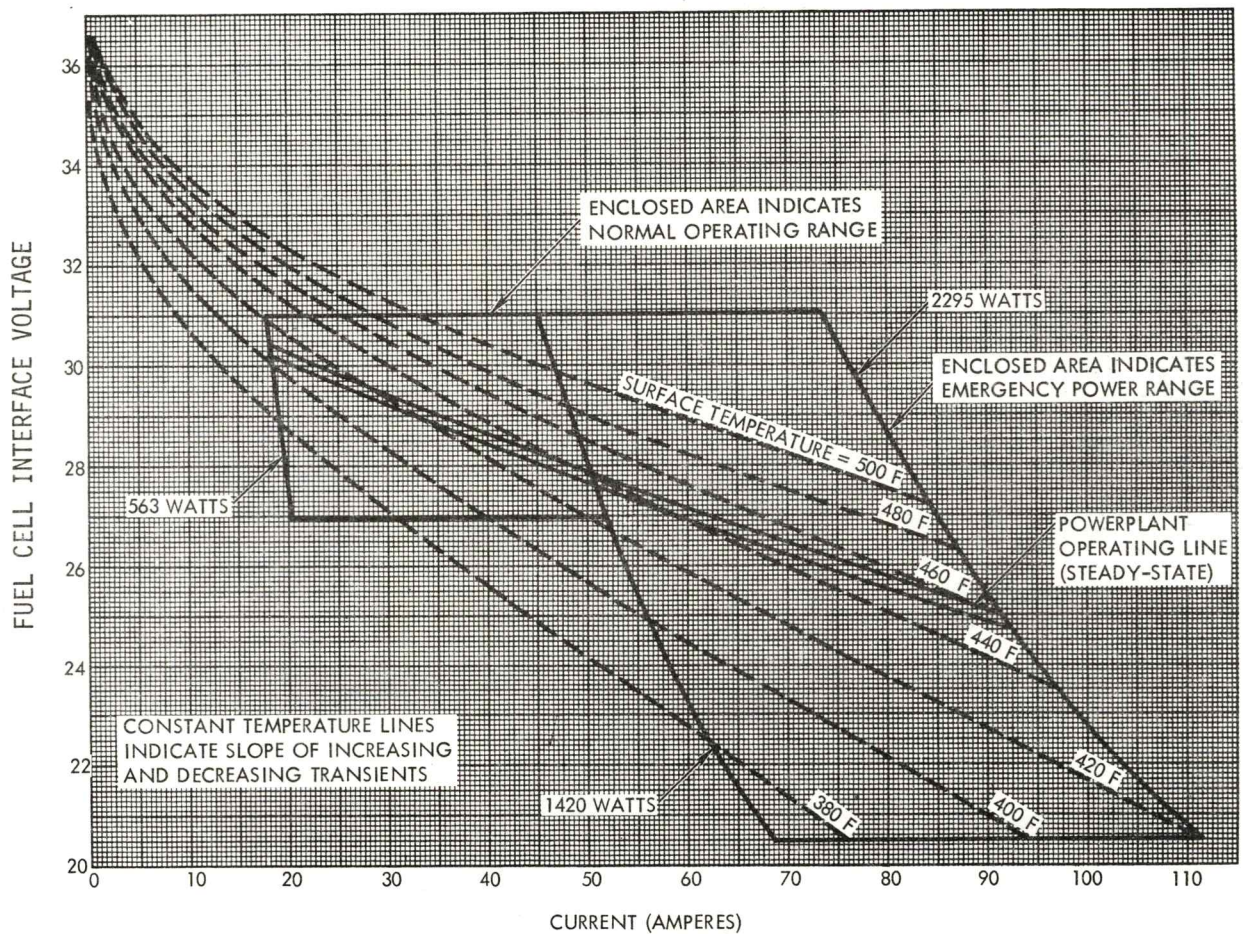


Figure 4.1-10. Fuel-Cell Powerplant PC3A-2E, Nominal Performance Characteristics During Normal And Emergency Power Operation Vacuum Conditions (See Paragraphs 4.1.1.2 and 4.1.2.1)

4.1-30

SNA-8-D-027(I), Rev 3

Amendment 92
3/27/72

4.1-31

SNA-8-D-027(I), Rev 3

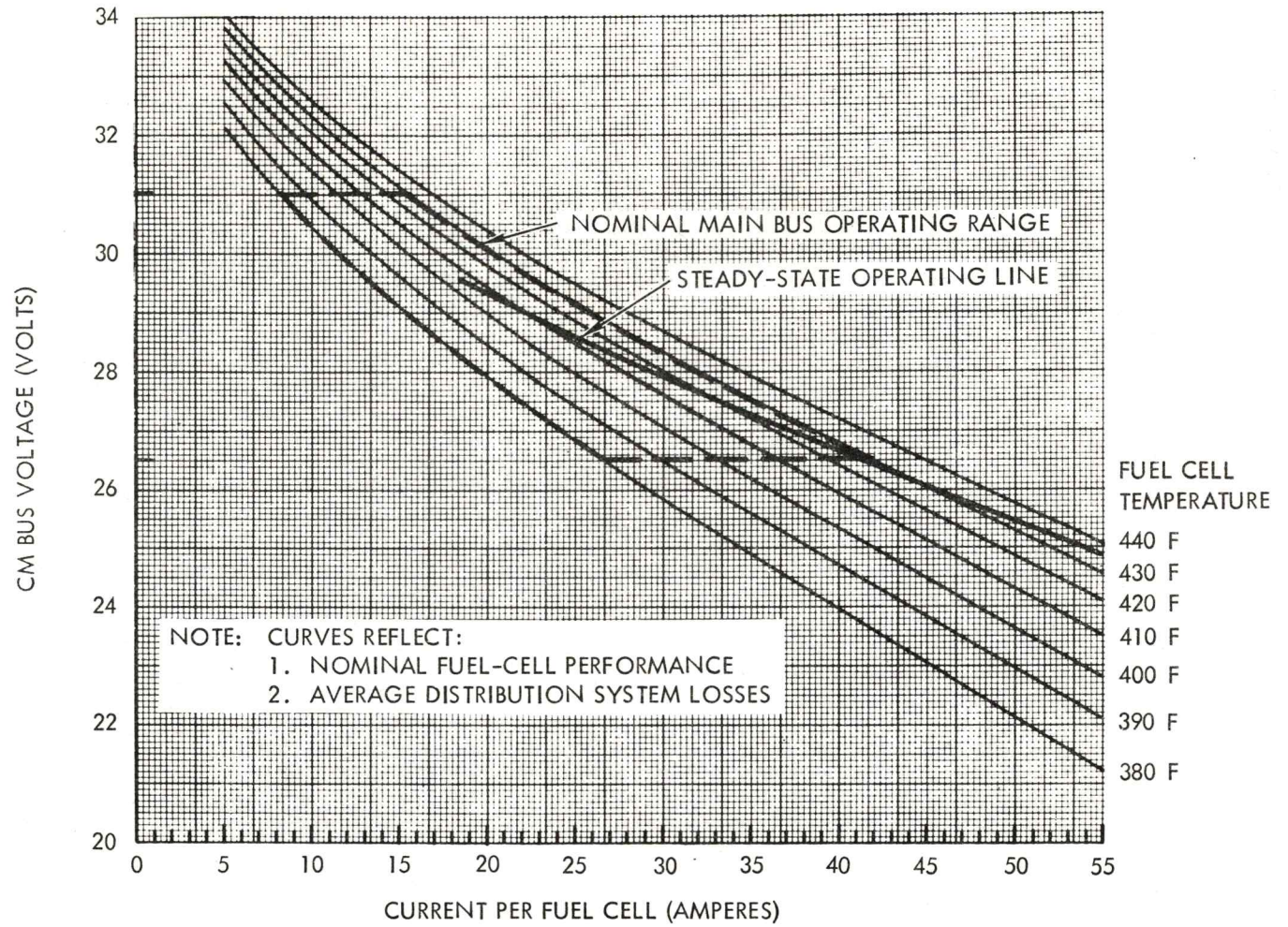


Figure 4.1-11. Command Module Main Bus Operating Range
(See Paragraph 4.1.2.1)

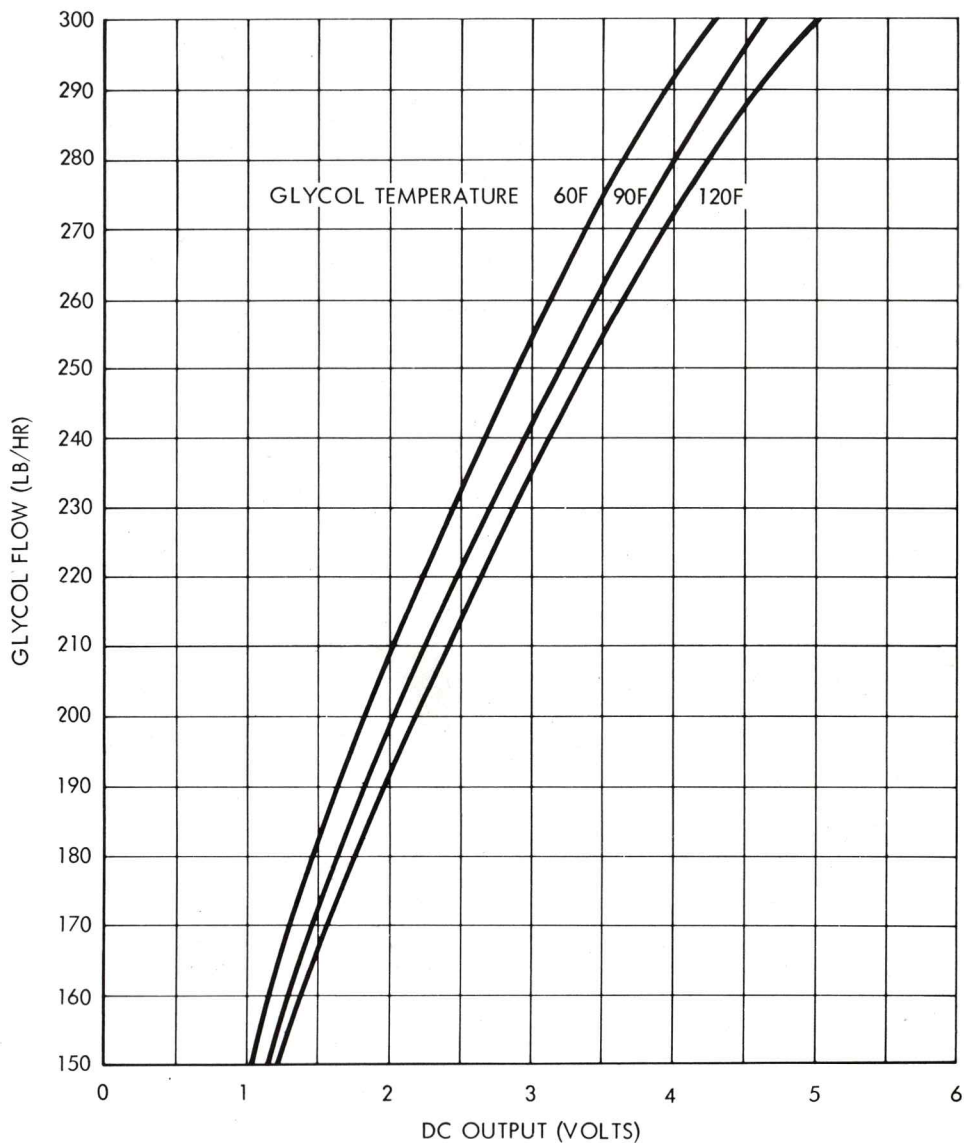


Figure 4.3-36. Primary Coolant Loop Flowmeter Calibration Curves (Typical)
 (See Paragraph 4.3.3.8)

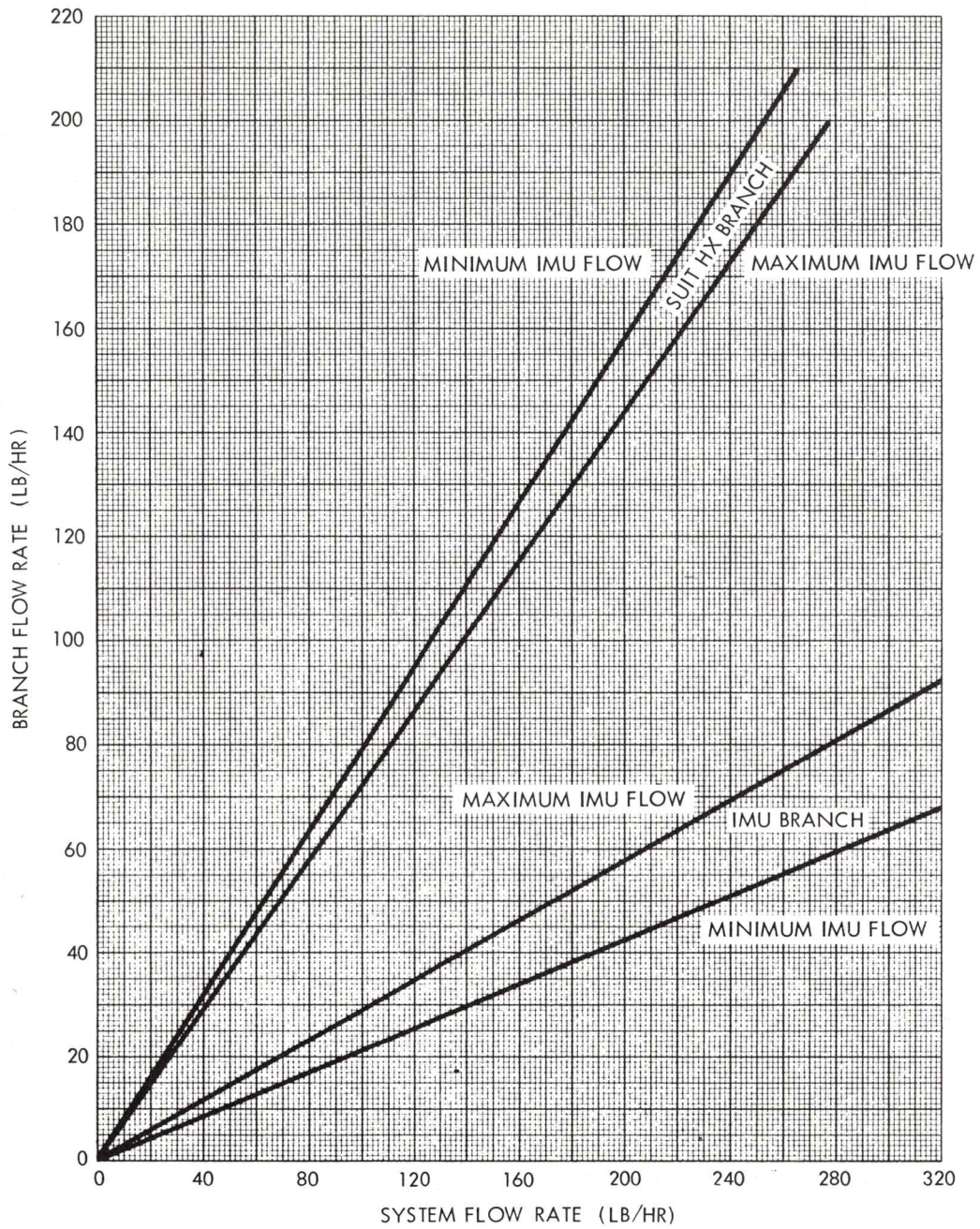


Figure 4.3-37. IMU Branch Flow Split Versus Glycol System Flow (See Paragraph 4.3.3.9)

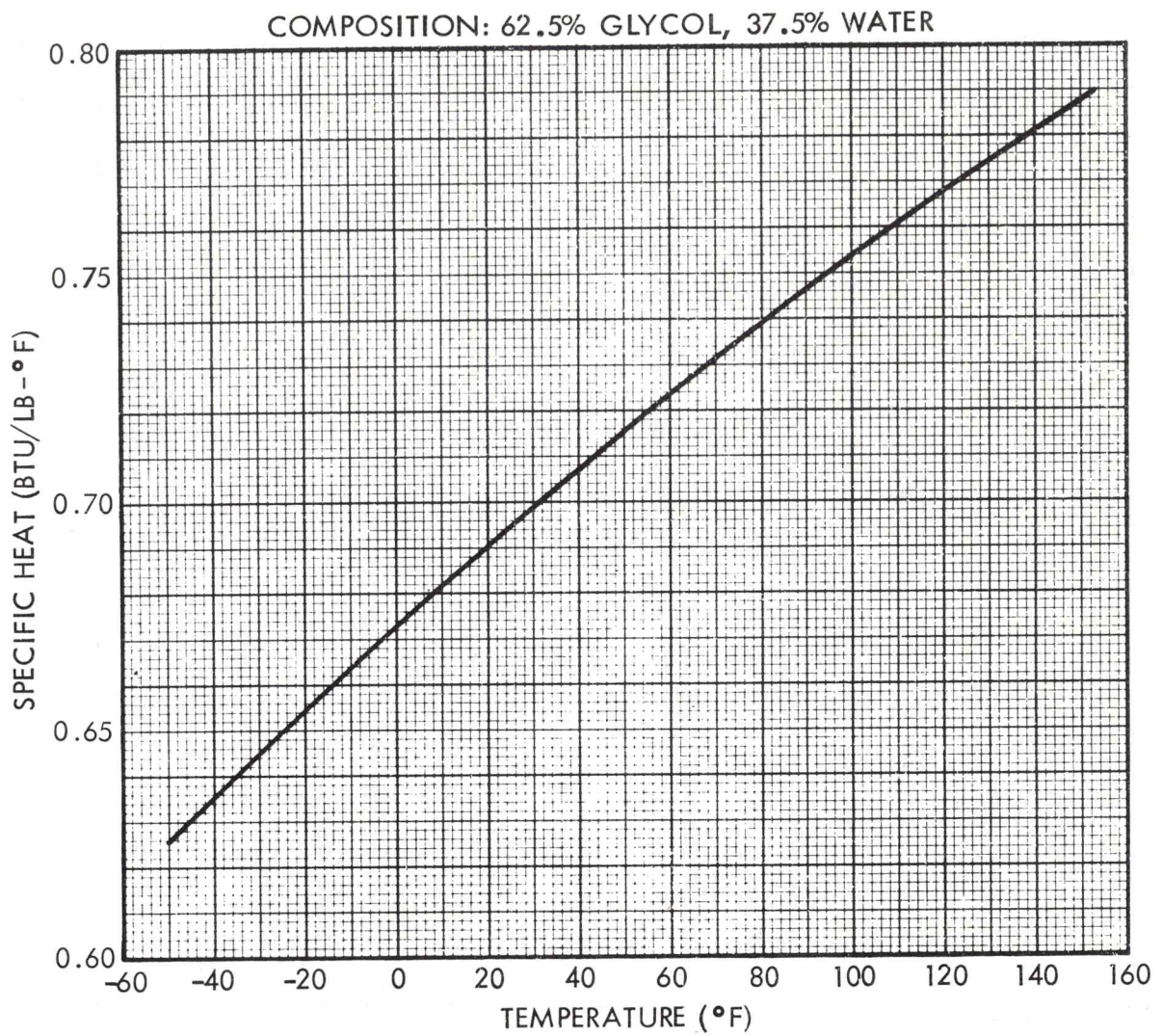


Figure 4.3-38. Specific Heat Aqueous Ethylene Glycol vs. Temperature
(See Paragraph 4.3.3.10)

4.3-68

MSC-07765 (Vol. 1)

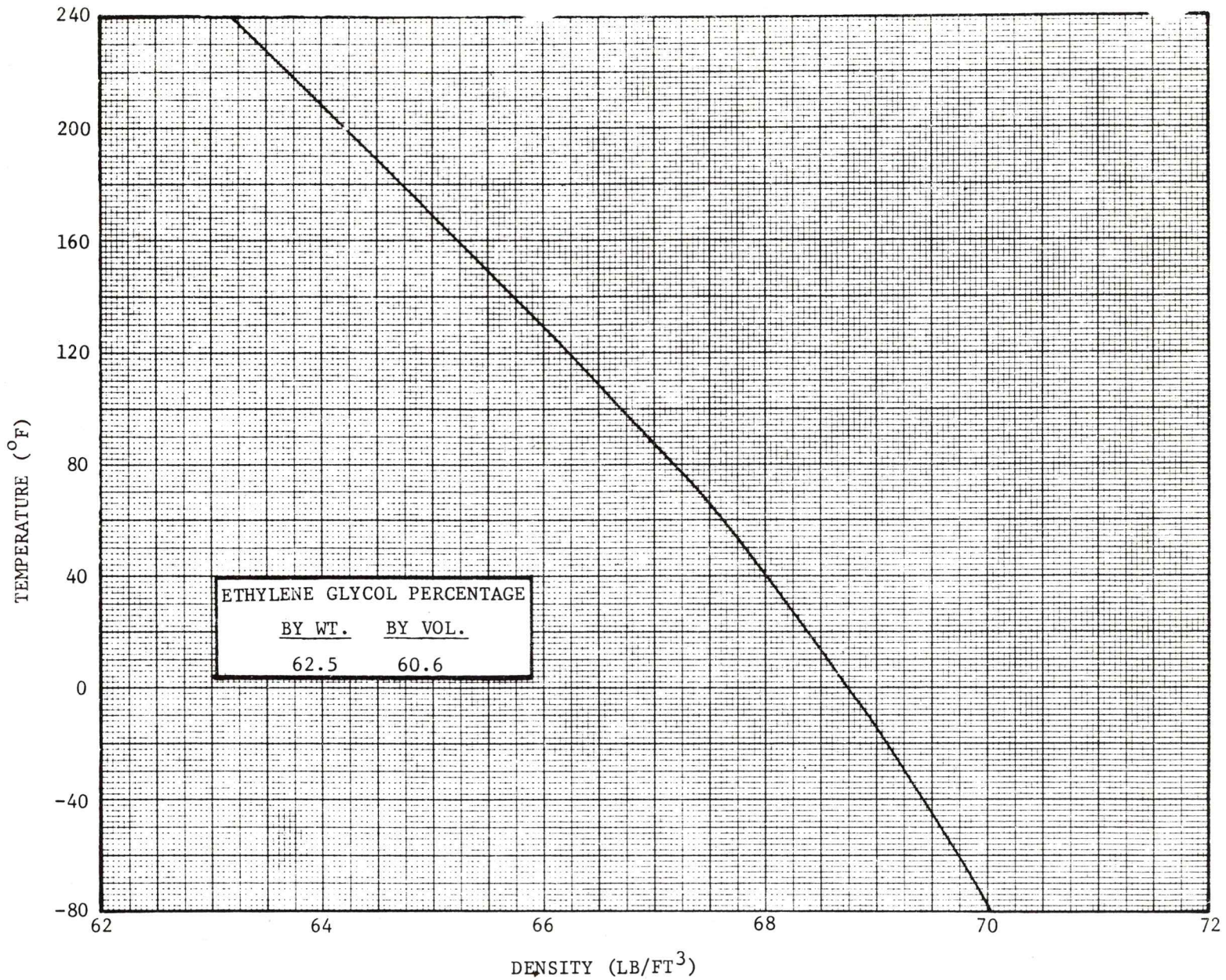


Figure 4.3-39. Density of Aqueous Ethylene Solutions
(See Paragraph 4.3.3.10)

4.3-69

MSC-07765 (Vol. I)

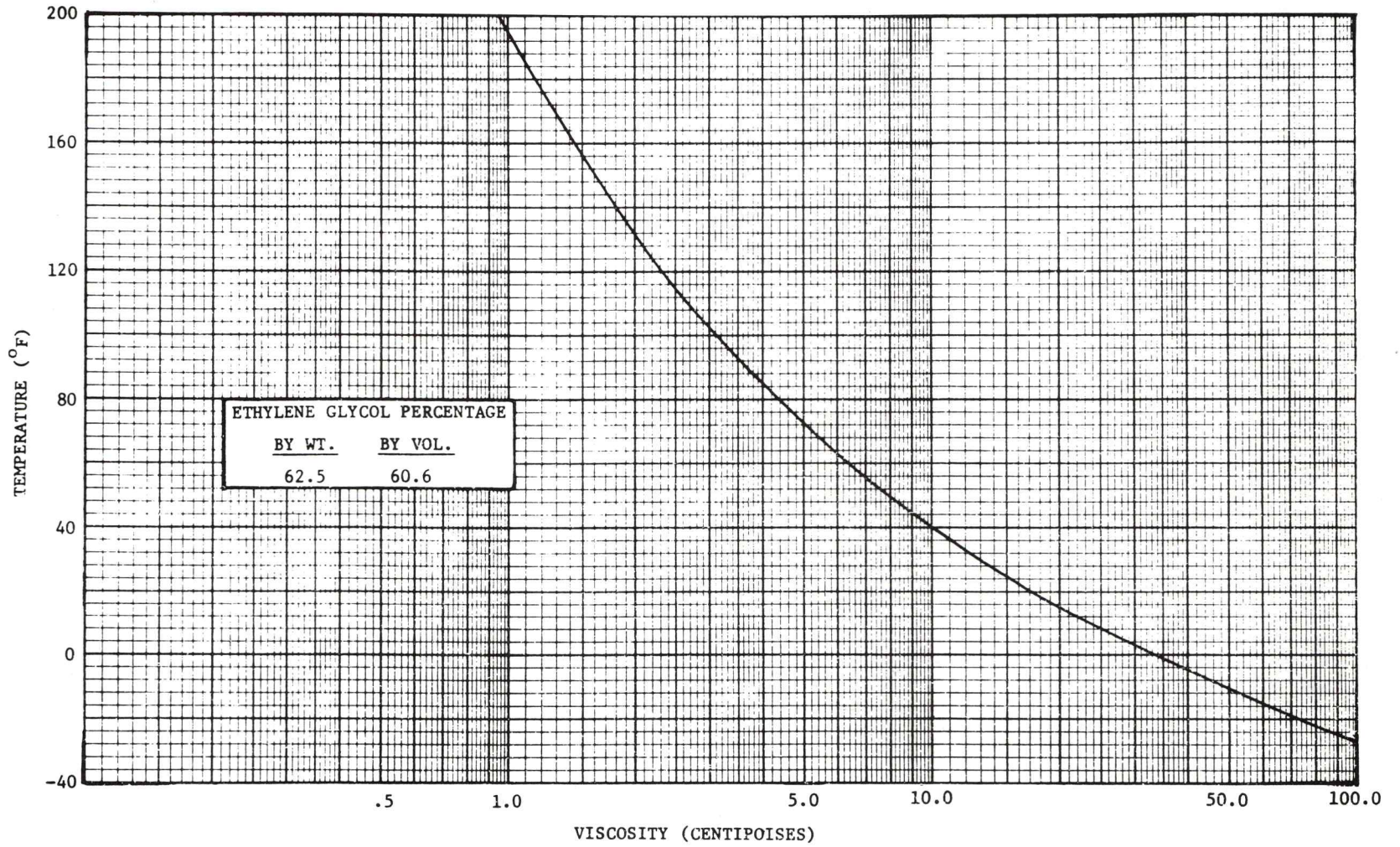


Figure 4.3-40. Viscosity of Aqueous Ethylene Glycol Solutions
(See Paragraph 4.3.3.10)

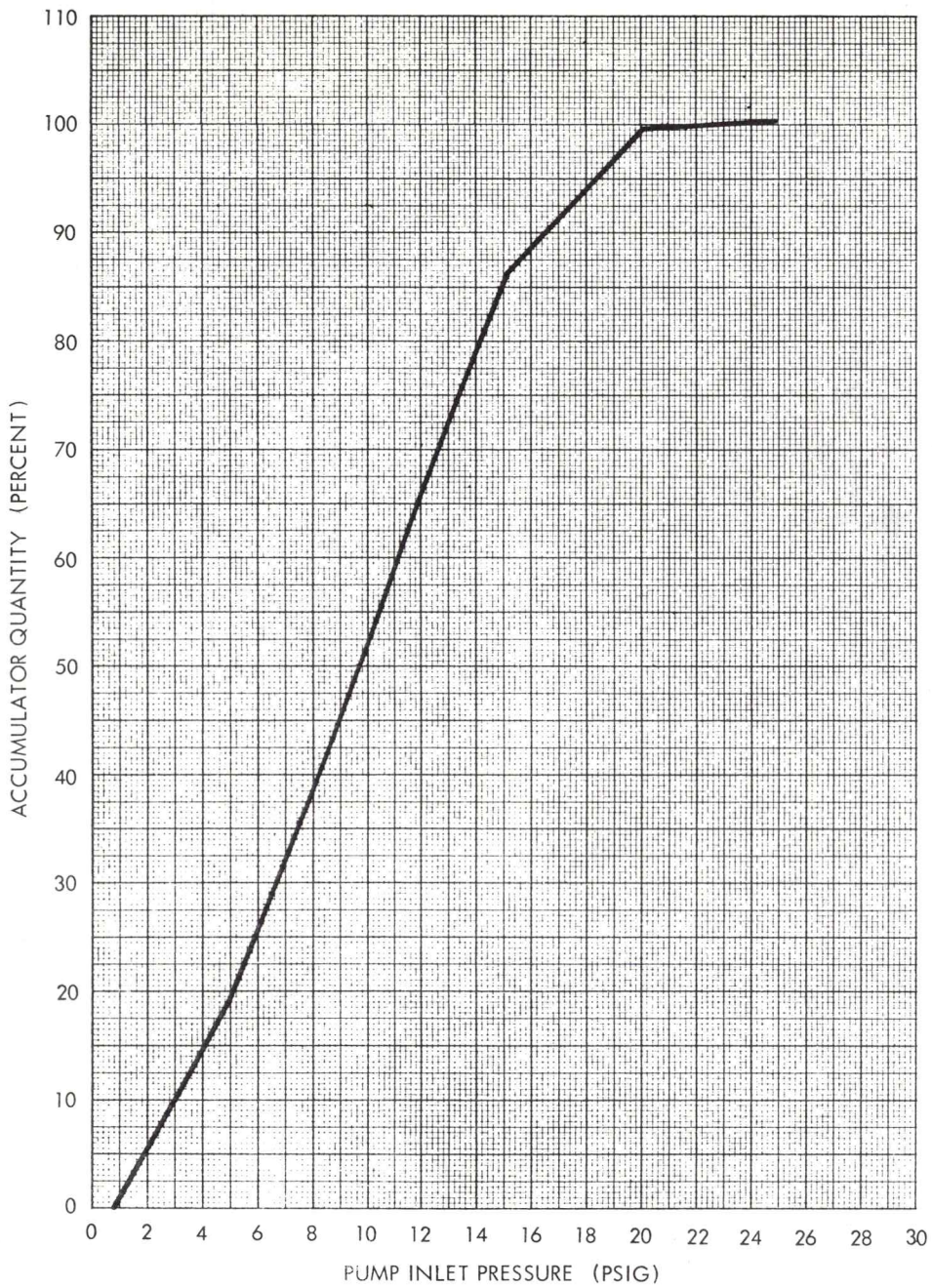


Figure 4.3-41. Secondary Glycol Accumulator Quantity Vs. Pump Inlet Pressure (Typical)
 (See Paragraph 4.3.4.3)

$\Delta T = \text{TEMPERATURE BAY 56} - \text{TEMPERATURE BAY 23}$

- LEGEND
① TOTAL FLOW 240 LB/HR
② TOTAL FLOW 200 LB/HR
③ TOTAL FLOW 180 LB/HR

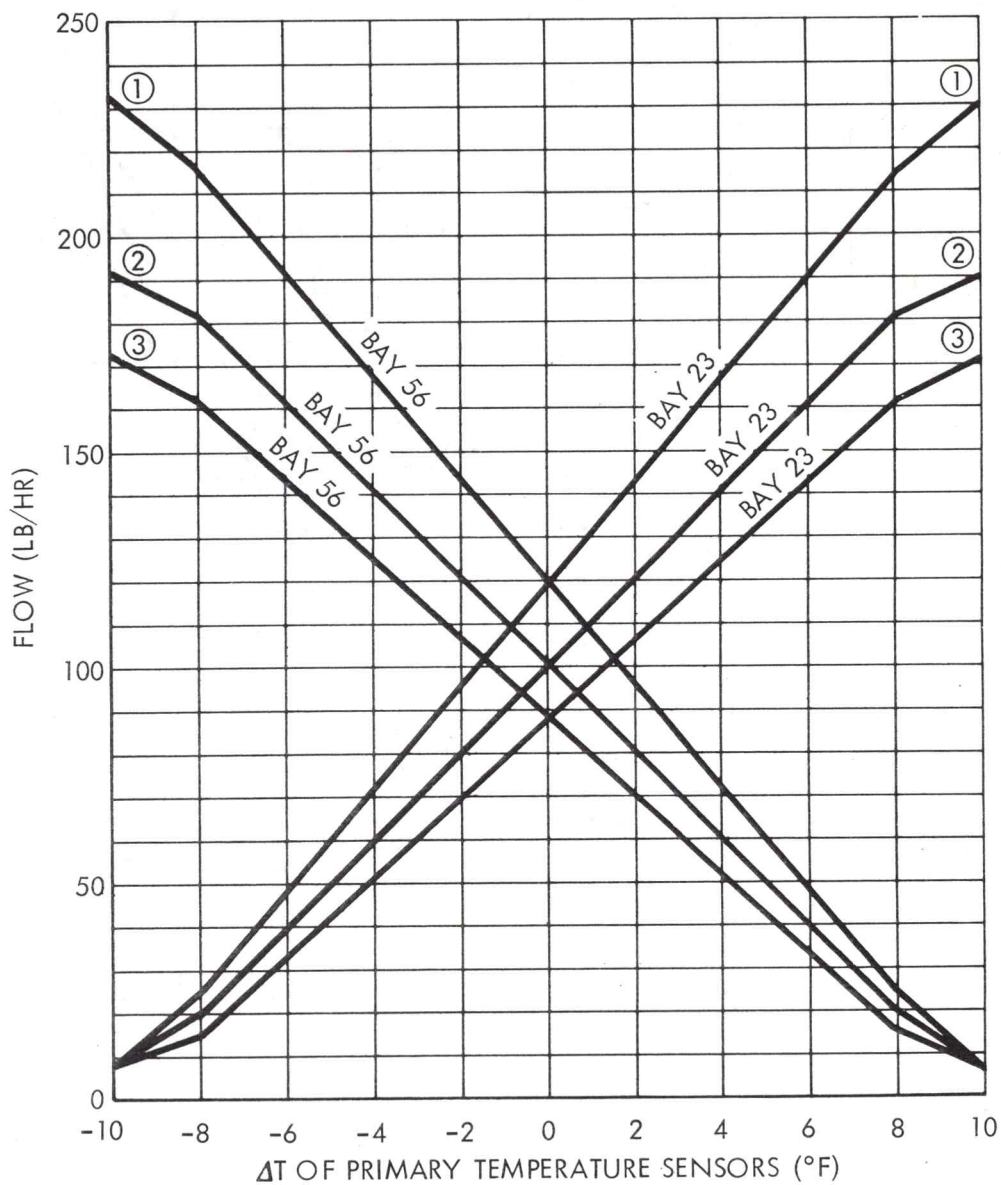


Figure 4.3-42. Proportioning Valve Characteristic
(See Paragraph 4.3.5.3)

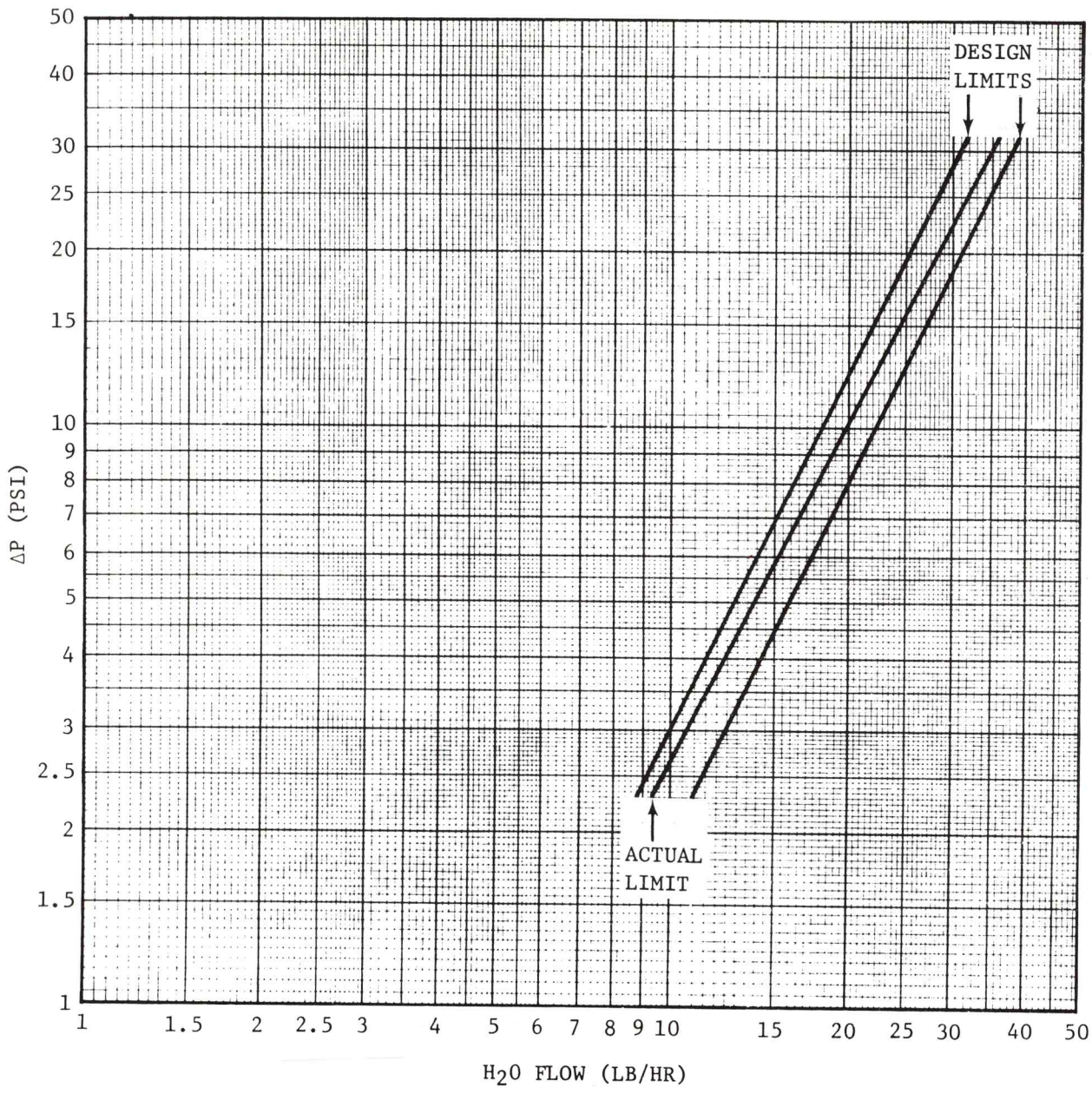


Figure 4.3-43. Glycol Evaporator Water Control Valve Vs. ΔP
 (See Paragraph 4.3.7.3)

4.3-73

MSC-07765 (Vol. I)

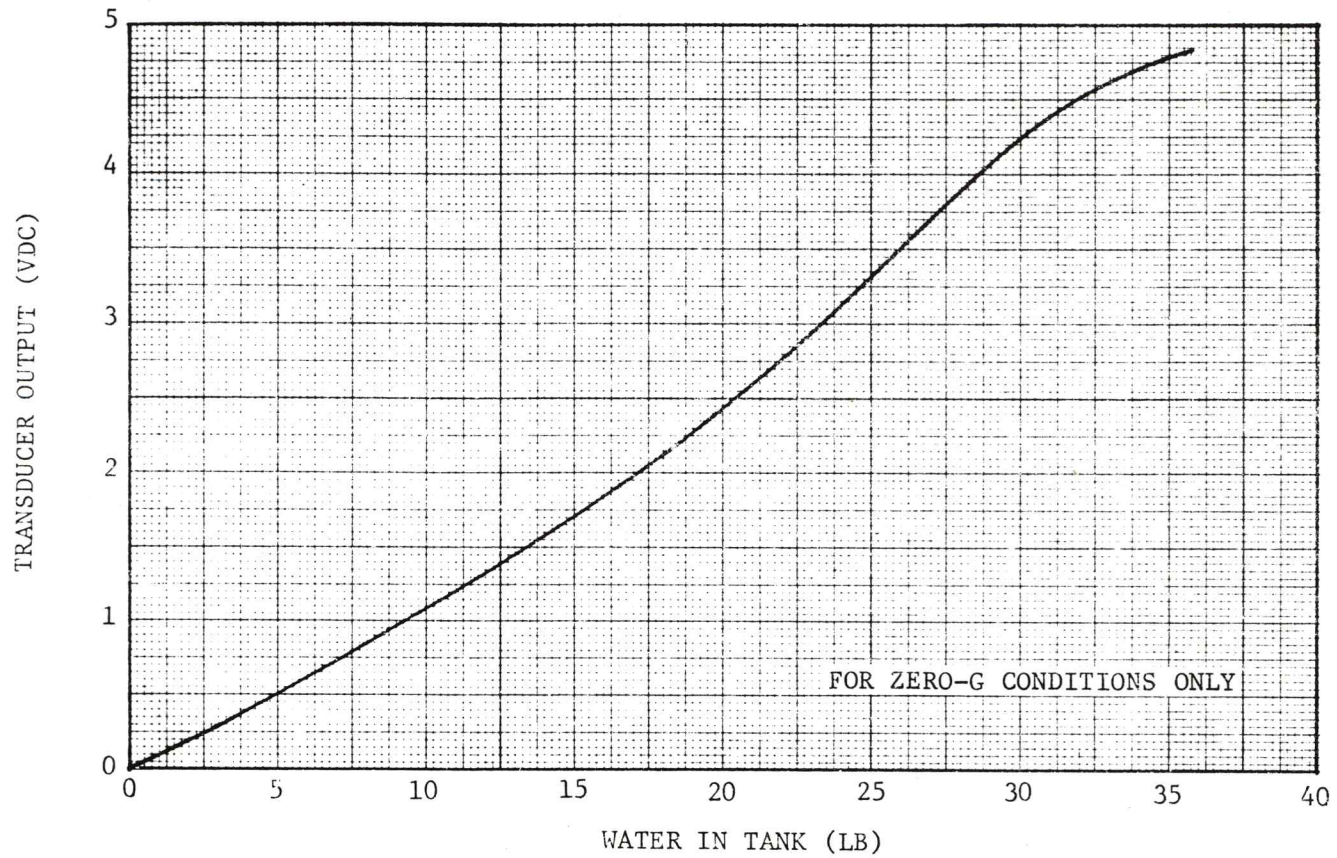


Figure 4.3-44. Potable Water Tank Calibration (Typical)
(See Paragraph 4.3.7.4)

4.3-74

MSC-07765 (Vol. I)

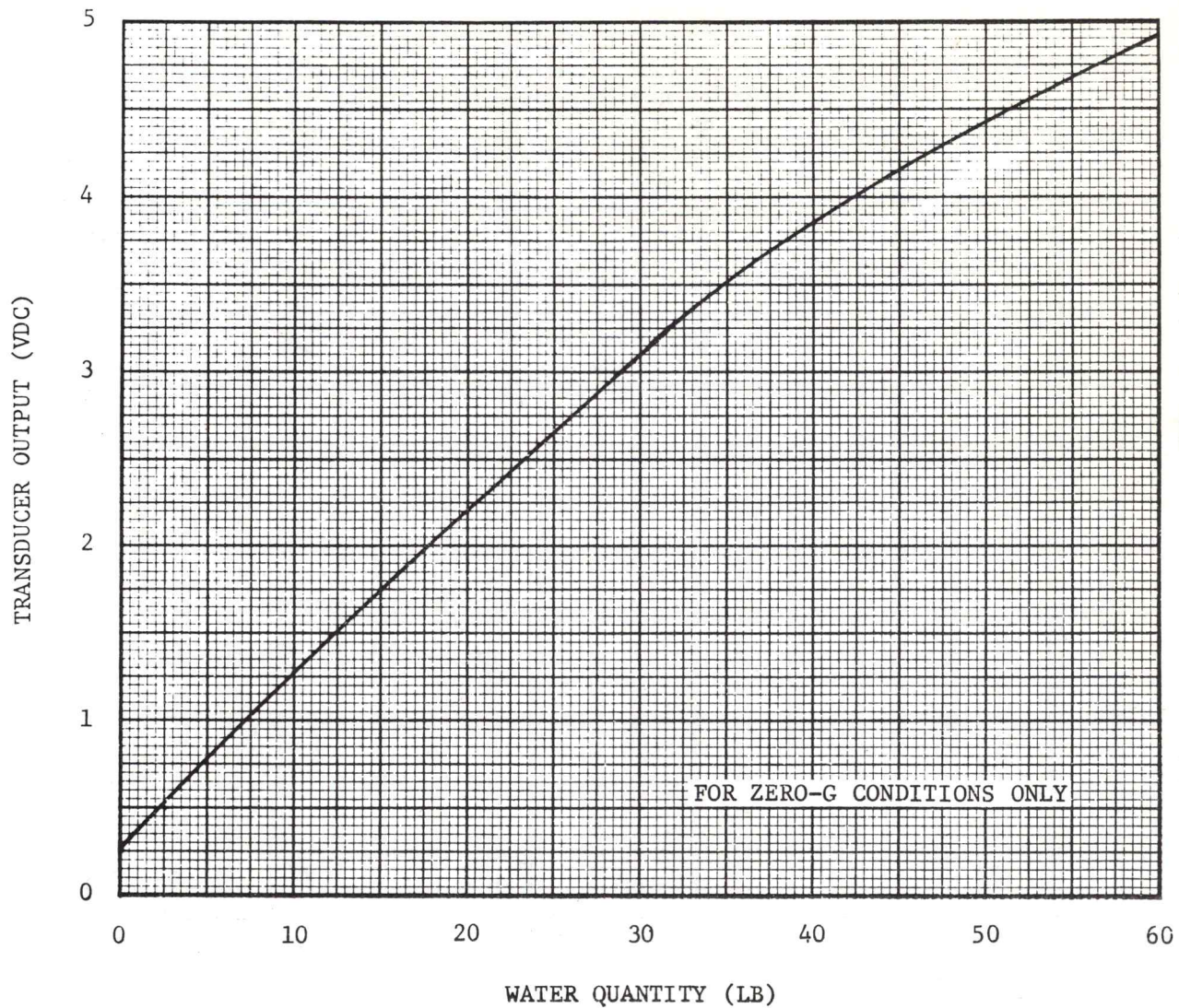


Figure 4.3-45. Waste Water Tank Quantity Calibration (Typical)
(See Paragraph 4.3.7.5)

GUIDANCE AND CONTROL (G&C) SUBSYSTEM

and Control Subsystem (GNCS)

ment Unit (IMU)

Axes Intersection Point

up Time

t

e Drift Rates

Subsystem

able Memory Constants

4.4 GUIDANCE AND CONTROL SUBSYSTEM (G&C)

4.4 GUIDANCE AND CONTROL (G&C) SUBSYSTEM

- 4.4.1 Guidance, Navigation and Control Subsystem (GNCS)
 - 4.4.1.1 Inertial Measurement Unit (IMU)
 - 4.4.1.1.1 Gimbal Axes Intersection Point
 - 4.4.1.1.2 IMU Warmup Time
 - 4.4.1.1.3 IMU Errors
 - 4.4.1.1.4 IMU Alignment
 - 4.4.1.1.5 IMU Temperature Drift Rates
 - 4.4.1.1.6 IMU Gimbal Lock
 - 4.4.1.2 Command Module Computer (CMC) Subsystem
 - 4.4.1.2.1 Guidance Computer Erasable Memory Constants
 - 4.4.1.3 Optical Subsystem (OSS)
 - 4.4.1.3.1 Optics Modes
 - 4.4.1.3.1.1 CMC Mode
 - 4.4.1.3.1.2 Zero Optics Mode
 - 4.4.1.3.1.3 Manual Optics Mode
 - 4.4.1.3.2 Optics Drive Rates
 - 4.4.1.3.3 Optical Coverage
 - 4.4.1.3.3.1 Undocked
 - 4.4.1.3.3.2 Docked
 - 4.4.1.3.4 Optical Blind Zone
 - 4.4.1.3.5 Optical Operational Limitations
 - 4.4.1.3.6 Pilot's Field of View
- 4.4.2 Stabilization and Control System (SCS)
 - 4.4.2.1 Body-Mounted Attitude Gyro (BMAG) Warmup Time
 - 4.4.2.2 Gyro Assembly (GA) - Gyro Display Coupler (GDC) Drift
 - 4.4.2.2.1 Gyro Assembly (GA)
 - 4.4.2.2.2 Gyro Display Coupler
 - 4.4.2.3 SCS Gimbal Lock Limits
 - 4.4.2.4 Flight Director Attitude Indicator (FDAI)
 - 4.4.2.4.1 Attitude Display Modes
 - 4.4.2.4.2 Attitude Error Display Modes
 - 4.4.2.4.3 Attitude Rate Display Modes
- 4.4.3 Entry Monitor Subsystem (EMS)
 - 4.4.3.1 EMS Software Design Data
 - 4.4.3.2 Scroll and Flight Monitor
 - 4.4.3.2.1 Scroll
 - 4.4.3.2.2 Flight Monitor
 - 4.4.3.3 Lift Vector Orientation Indicator
 - 4.4.3.4 Delta V/Range-to-go Indicator
 - 4.4.3.4.1 Delta V (ΔV)

- 4.4.3.4.1.1 Delta-V Counter Setting Determination
- 4.4.3.4.2 Range-to-go
- 4.4.3.4.3 Slew Switch (ΔV EMS Set)
- 4.4.3.4.4 VHF Range
- 4.4.3.4.5 Mode Selection Switch
- 4.4.3.4.6 Function Switch
- 4.4.3.5 Entry Threshold Indicator
- 4.4.4 Attitude Control
 - 4.4.4.1 Earth Orbit
 - 4.4.4.1.1 GNCS
 - 4.4.4.1.2 SCS
 - 4.4.4.1.3 SM RCS Thrust Vector and Control Moment Data
 - 4.4.4.1.3.1 Thrust Components and Moment Arm Definition
 - 4.4.4.1.3.2 Moment Equations
 - 4.4.4.1.3.3 Impingement Forces
 - 4.4.4.1.4 SM RCS Control Forces and Moments
 - 4.4.4.2 Entry
 - 4.4.4.2.1 GNCS
 - 4.4.4.2.2 SCS
 - 4.4.4.2.3 CM RCS Force and Moment Equations
 - 4.4.4.2.4 CM RCS Control Forces and Moments
- 4.4.5 Thrust Vector Control
 - 4.4.5.1 SPS Thrust Vector Location
 - 4.4.5.2 SPS Actuation System
 - 4.4.5.3 SPS TVC Error Sources
 - 4.4.5.4 SCS TVC Pointing Accuracy
- 4.4.6 Miscellaneous
 - 4.4.6.1 Command Module Aerodynamic Capture Envelope
 - 4.4.6.2 Crewman Optical Alignment Sight (COAS)
 - 4.4.6.3 G-Meter

4.4 GUIDANCE AND CONTROL (G&C) SUBSYSTEM

The G&C system consists of the guidance, navigation and control subsystem (GNCS); the stabilization and control subsystem (SCS); and the entry monitor subsystem (EMS). The GNCS contains rotational and translational sensors of attitude, attitude rate, and acceleration. The SCS senses attitude and attitude rate and the EMS senses acceleration along the +X axis. These sensors provide information to control electronics which operate on and condition the information into commands to spacecraft propulsion systems. For spacecraft attitude control, RCS jets are fired singly or as couples. For spacecraft translation, RCS jet pairs are fired along the desired axes. (Jet select logic for Apollo/Soyuz attitude control and translation will be defined at a later date.) Major spacecraft velocity changes are accomplished by commanding the firing and controlling the gimbaling of the SPS engine. The G&C provides these basic functions: (1) attitude reference, (2) attitude control, (3) thrust and thrust vector control, (4) navigation, and (5) guidance.

4.4.1 Guidance, Navigation and Control Subsystem (GNCS).

4.4.1.1 Inertial Measurement Unit (IMU). The IMU is a gimballed, three-degree-of-freedom, gyroscopically stabilized instrument.

4.4.1.1.1 Gimbal Axes Intersection Point. The following IMU navigation base position is expressed in the CM vehicle coordinate system.

X _c component	55.715 ±0.010 in.
Y _c component	0.0 ±0.010 in.
Z _c component	40.914 ±0.010 in.

The lateral tolerances relative to this point are not significant to analysis efforts. The three-sigma uncertainties of navigation base rotations with respect to the CM docking ring are as follows:

About X-axis ±24.18 arc minutes
About Y-axis ±38.18 arc minutes
About Z-axis ±32.62 arc minutes

4.4.1.1.2 IMU Warmup Time.† When the GNCS is powered up from stabilized standby condition, a warmup period must be observed before beginning the IMU alignment procedure. The warmup requirements are described in Section 3.4, Guidance and Control Subsystem constraints and limitations.

4.4.1.1.3 IMU Errors.† Inertial measurement unit errors are caused by instrument mounting errors and drift. The three types of drift are: (1) nonacceleration sensitive, (2) acceleration sensitive, and (3) acceleration squared sensitive. Important error terms are corrected by the

†NASA Data Source

application of CMC-determined compensation terms. Inertial measurement unit errors and CMC compensation capability per axis are presented in Table 4.4-1. The root mean square (rms) errors after compensation were taken from Table 3.2 of MEI No. 2015000, Part I. The compensation range and quantization were taken from MIT/IL Memorandum AG 852-66. The pre-flight and flight data are the result of an analysis of previous Apollo spacecraft and are presented in Table 4.4-1.

4.4.1.1.4 IMU Alignment.† Inertial measurement unit prelaunch alignment, orientation determination or realignment must be completed at some time prior to GNCS controlled translation or attitude maneuvers and landmark or rendezvous tracking. The time interval is dependent on the accuracy requirement for the particular event. The total IMU misalignment can be obtained by combining the drift term (NBD x time) indicated in Table 4.4-1 and the alignment error existing after an IMU alignment. Based on MEI No. 2015000, Part I, the rms alignment errors are:

Prelaunch azimuth	500 arc-sec
Vertical	50 arc-sec
Free fall, per axis	40 arc-sec

4.4.1.1.5 IMU Temperature Drift Rates.† An additional form of IMU drift results from temperature variances about the nominal IMU operating temperatures. Table 4.4-2 presents the temperature drift rates obtained by varying the component temperatures $\pm 4.5^\circ\text{F}$ about the nominal value. The nominal operating temperature for the accelerometers is 130°F . The nominal operating temperature for the gyros is 133°F . The temperature drift rates were taken from MIT/IL Apollo Guidance and Navigation System Test Group Memo No. 1231.

4.4.1.1.6 IMU Gimbal Lock.† The primary mode of spacecraft maneuvers is automatic guidance, navigation and control system (GNCS) supplemented by manual inputs through the computer display keyboard (DSKY). The maneuver rate is specified by the operator, and final gimbal angles are either specified by the operator or presented for his approval prior to maneuver initiation. G&C controlled maneuvers achieve the final gimbal angles with a single rotation about an arbitrary axis (fixed).

The IMU begins to lose its accuracy when the inner and outer axes approach within 20 degrees of each other (yaw angles greater than ± 70 degrees). At this point, the GNCS caution and warning lamp on the DSKY comes on. The inertial reference will be lost (IMU automatically goes to coarse align) if the yaw angle exceeds ± 85 degrees. From an operational viewpoint, attitude maneuvers that place the IMU in the gimbal-lock region should not be planned. If an attitude is required that places the IMU in the gimbal-lock region, the IMU must be realigned to a reference compatible with the required attitude. Maneuvers through this region must also be avoided.

†NASA Data Source

4.4.1.1.7 IMU Redlines.[†] The inertial components will require recalibration if the unit temperature exceeds 140°F or falls below 120°F (recalibration range). An accelerometer can be permanently damaged if the unit temperature exceeds 160°F or falls below 40°F.

4.4.1.2 Command Module Computer (CMC) Subsystem.[†] The CMC is a general-purpose digital device which processes and controls information to and from the IMU, the optics, and the two display and keyboard panels (DSKY's), and stores program and reference data.

The astronaut-computer communication link is by the DSKY via which the computer can display information to the crew or request the crew to perform some action. The crew, on the other hand, can enter information and/or instructions to the computer by means of the DSKY. Ground stations transmit and receive certain information to and from the computer directly via the telemetry uplink and downlink channels.

The CMC is a core memory machine with both fixed and erasable sections. The fixed, nonerasable memory contains 36,864 words and is used for permanent storage of navigation tables, trajectory parameters, programs, and constants. The erasable memory, which contains 2048 words, is used to store intermediate information, such as constants and equations which change during flight.

4.4.1.2.1 Guidance Computer Erasable Memory Constants.[†] The erasable memory constants are presented in Table 4.4-3.

4.4.1.3 Optical Subsystem (OSS). The optical subsystem is composed of a scanning telescope (SCT), a sextant (SXT), drive motors for positioning the SCT and SXT, parts of the power servo assembly (PSA), part of the controls and displays, and two channels of the coupling data unit (CDU). The SCT and SXT provide the capability to determine the spacecraft position and attitude in relation to landmarks and stars.

The sextant is a 28-power optical instrument that has two lines of sight. One line of sight is fixed along the SXT shaft axis, which in turn is fixed perpendicular to the navigation base. This defines the landmark line of sight (LLOS). The other line of sight, which may be varied, is the star line of sight (SLOS). The SLOS is varied to acquire the second sighting point by articulation of a mirror about the SXT trunnion and shaft axes.

The trunnion axis is perpendicular to the shaft axis. Rotation about the SXT shaft and trunnion axes is limited by mechanical stops. The orientation and limits of rotation are shown in Figure 4.4-1. The one-sigma SXT angular errors for unit vector determinations with respect to the IMU (rendezvous and orbital navigation and IMU alignment) are:

Noise = 0.2 mrad per axis
Bias = 0.2 mrad per axis

[†]NASA Data Source

The SCT is a one-power, refracting optical instrument with a 60-degree field-of-view (FOV). The shaft axis of the SCT is aligned parallel to the LLOS. The line of sight of the SCT is varied by rotation of a double-dove prism about the SCT trunnion and shaft axes. The trunnion axis is perpendicular to the shaft axis. The limits of rotation for the SCT are given in Figure 4.4-1, for the SCT coupled to SXT. The one-sigma SCT angular errors are:

Noise = 1.0 mrad per axis
Bias = 1.0 mrad per axis

4.4.1.3.1 Optics Modes. The command module optics may be operated in three different modes: the computer (CMC) mode, the zero-optics mode, and the manual mode. In all three modes, the shaft axis of the SCT is electrically slaved to the shaft axis of the SXT.

4.4.1.3.1.1 CMC Mode. In the computer (CMC) mode, the trunnion axis of the SCT is electrically slaved to the trunnion axis of the SXT.

4.4.1.3.1.2 Zero Optics Mode. In the zero-optics mode, both the SXT and SCT shaft and trunnion axes are driven to, and held in, the zero position. In the zero position, the shaft axis of the SXT is at 0-degree rotation and SLOS coincident with the LLOS (trunnion axis parallel to the spacecraft Y-axis) the SCT line of sight is parallel to the LLOS, and the shaft axis is at 0-degree rotation. Likewise, the CDU error and read counters are zeroed.

4.4.1.3.1.3 Manual Optics Mode. In the manual optics mode, there are three types of operation of the SCT trunnion (that correspond to three settings of the telescope trunnion select switch): slave-to-SXT, 0-degree, and 25-degree positions. In the slave-to-SXT position, the SCT trunnion is electrically slaved to the SXT trunnion. In the 0-degree position, the SCT trunnion is locked to the LLOS. In the 25-degree position, the SCT trunnion is offset 25 degrees with respect to the SCT shaft axis.

There are two modes, direct or resolved, available when the optics are in the manual mode. The direct mode enables manual control of the optics SLOS rate and direction, in a shaft and trunnion coordinate system, directly from the optics hand controller. The resolved mode resolves the shaft and trunnion input commands from the hand controller so that the SLOS moves in an X, Y coordinate system with respect to the operator, and connects the shaft commands through a drive rate resolution circuit so that equal input commands result in equal image motion in the optical field-of-view.

4.4.1.3.2 Optics Drive Rates. The following table defines the nominal rotational rates for the optics when in the direct mode. All drive rates in the table have a ± 20 percent tolerance. The rotational rate capability

of the optics when in the resolved mode is dependent on the trunnion angle. When the optics are in the resolved mode, the shaft axis rotational rates can be higher than when in the direct mode. The resolved mode cannot be used when the trunnion angle is less than 5 degrees.

Optics Drive Rates

Drive Rate for Direct Mode (deg/sec)

<u>Axis</u>	<u>High</u>	<u>Medium</u>	<u>Low</u>
Trunnion	10.0	1.0	0.1
Shaft	19.5	2.0	0.2

4.4.1.3.3 Optical Coverage.

4.4.1.3.3.1 Undocked (Figures 4.4-2 and 4.4-3). Each line of sight of the SXT has a 1.8-degree true field of view. By means of the trunnion and shaft axis rotations, the SXT can scan a hemisphere about the shaft axis. However, due to physical obstructions (the optical assembly ablative covers), the effective field of view of the SXT is 45 to 50 degrees (cone half-angle). The design field of view of the SCT is 60 degrees. Because of obstruction, the effective field of view of the SCT is 36 to 44 degrees (cone half-angle).

4.4.1.3.3.2 Docked. TBS

4.4.1.3.4 Optical Blind Zone. Because of the shaft angle rate limit of the scanning telescope, there are certain zones in orbital navigation where the line-of-sight of the scanning telescope cannot keep up with the landmark as the earth goes by. These blind zones are circles, with an additional area required for catchup. Figure 4.4-4 presents the blind zones for the shaft axis down the local vertical (spacecraft pitched down 33 degrees). Because the shaft axis has a 19.5 deg/sec ± 20 percent rate capability, Figure 4.4-4 reflects the nominal 19.5 deg/sec rate and the worst case, 15.6 deg/sec rate.

4.4.1.3.5 Optical Operational Limitations. An adequate portion of the star field must be visible through the scanning telescope in order that navigational stars can be recognized. The optics shaft-drive axis must be pointed at least 30° above the local sunlit earth horizon and at least 20° above the local dark earth horizon. The minimum angle between sextant lines of sight to the moon's edge and a star is 5°.

To prevent sun interference with use of the optics, the minimum angle from the sextant landmark line of sight to the vehicle sunline is 15°. The minimum angle from the telescope line of sight to the sun is 60°.

In order to maintain the shaft drive rate within the maximum during landmark tracking, the optics line of sight to the landmark must be more than 8.5 degrees from the optics shaft drive axis ground track at the closest point of approach of the landmark to the shaft axis ground track.

4.4.1.3.6 Crewman's Field of View (Reference Figure 4.4-5). The crewman's field of view is dependent upon the particular command module, couch, and pressure garment in use. The left-hand rendezvous window fields of view for 50th and 80th percentile man are shown in Figure 4.4-6 as determined for CM 103. The fields of view through the heat-shield, side-hatch window for 50th and 80th percentile man are presented in Figure 4.4-7 as determined for CM 103. The field of view for the left-hand side window is presented in Figure 4.4-8 as determined for CM 103.

4.4.2 Stabilization and Control System (SCS).

4.4.2.1 Body-Mounted Attitude Gyro (BMAG) Warmup Time. The BMAG's require 40-minutes warmup time. The "OUT OF TEMP" lights indicate when the BMAG's are not at operating temperature. Rate and attitude error accuracy are impaired if BMAG's are operated at off-nominal temperatures.

4.4.2.2 Gyro Assembly (GA) - Gyro Display Coupler (GDC) Drift. The attitude reference in the SCS is composed of two identical gyro assemblies (GA) and the GDC.

4.4.2.2.1 Gyro Assembly (GA). GA 1 is normally operated in the (uncaged) attitude mode to provide attitude error signals to control and display circuits. In this mode, the gyro serves as an attitude error source for control and display for SCS maneuvers with the RCS and SPS. It is automatically caged during rotation control-commanded maneuvers and may be manually caged by axis by panel switch selection. It may also be used in place of GA 2 as the rate gyro by individual axis by appropriate positioning of the same panel switches. In this event, there is no longer an attitude error source.

The BMAG's of GA 2 are always caged (rate mode) and are normally connected to the system for rate control and damping, rate display, and to provide rate signals for GDC computation of total attitude.

Table 4.4-4 summarizes the 3 σ drift characteristics of the BMAG for three different environmental conditions expected in flight: zero g, acceleration, and vibrations induced during thrusting. These drifts are, in general, only meaningful as applied to the attitude mode or uncaged condition of the BMAG.

4.4.2.2.2 Gyro Display Coupler. The function of the GDC is to convert body rates from the rate GA into Euler (inertial) angles for display on the flight director attitude indicator (FDAI). The GDC will normally be used as a backup to the IMU and will be aligned or realigned to it just

prior to any critical maneuver. If the IMU is inoperative, the G&N optics or the COAS, along with STDN, are sufficient to align the GDC.

Because of the inherent drifts and errors resulting from the GDC analog type of transformation from body rates to Euler attitude, the GDC is not capable of providing an accurate attitude reference for extended periods without realignment. To illustrate, a summary of some of the drift data accumulated to date is presented in Table 4.4-5. The data assume a nonmaneuvering state of the vehicle. There is no procurement specification requirement on GDC drift. In the design of the SCS, a portion of the total drift tolerance was allotted to the GDC on a 3σ basis for mission time extreme environment (MTEE) conditions. Mission time extreme environment conditions reflect the effects (either estimated or based on test results) on the start-of-life tolerances of operating and nonoperating aging plus the possible mission environments defined in the procurement specification. This is the allocation provided in columns 2 and 3 (3σ) of Table 4.4-5.

4.4.2.3 SCS Gimbal Lock Limits. The flight director attitude indicator (FDAI) has the plus and minus yaw poles marked in red, indicating the gimbal-lock areas. The two red areas are for yaw angles of $\pm 75^\circ$ or greater. These markings provide the astronaut with a visual indication when the gimbal-lock region is being approached. However, this is an "electronic gimbal lock" only. In addition, the GDC computational error becomes excessive for yaw angles greater than ± 60 degrees.

4.4.2.4 Flight Director Attitude Indicator (FDAI). The CSM attitude displays are divided into three categories: attitude, attitude error, and attitude rate. Table 4.4-6 provides a summary of FDAI rate and attitude display characteristics. In the following paragraphs, modes of operation and accuracies are described under the three categories mentioned above. Accuracies and uncertainties quoted are exclusive of G&N errors and read-out errors. There are two FDAI's; G&N and SCS attitude reference and attitude errors may be displayed simultaneously, or either FDAI may be enabled alone and then display either G&N or SCS attitude and attitude error. Only SCS rates are displayed.

4.4.2.4.1 Attitude Display Modes. The primary mode uses the IMU gimbal angle resolvers to drive the commander's (left-hand) FDAI attitude ball. As a backup, the ball can be driven by the BMAG's operating through the GDC. IMU attitude may also be displayed on the right-hand FDAI. During vehicle reentry, the roll attitude about the stability axis of the vehicle can be displayed on the roll axis of the FDAI's. In this mode, the ball is disabled in pitch and yaw. In normal (primary mode) operation, roll drive comes from the GDC for the right-hand FDAI and from the IMU for the left-hand FDAI.

The attitude ball is capable of displaying the following angles:

Pitch	0° to 360°
Roll	0° to 360°
Yaw	270° through 0° to 90°

The accuracy of attitude display when driven by the IMU resolvers is ± 1.5 degrees. When driven by the GDC, the accuracies are as follows:

- a) Low Rate Maneuvers

Pitch and yaw	$\pm 1.5^\circ (3\sigma)$
Roll	$\pm 2.5^\circ (3\sigma)$
- b) Large Angle Maneuvers

All axes	$\pm 5^\circ (3\sigma)$
----------	-------------------------
- c) Single Axis Maneuvers

All axes	± 0.9 degree plus 0.723% of the maneuver (3σ)
----------	--
- d) High Rate Maneuvers

All axes	$\pm 1.05^\circ (3\sigma)$
----------	----------------------------
- e) Preentry Maneuvers

All axes	$\pm 5.0^\circ (3\sigma)$
----------	---------------------------
- f) Entry Maneuvers

Stability roll $\pm 4^\circ$ to 14° , depending on duration of entry mode and cumulative maneuver angle

4.4.2.4.2 Attitude Error Display Modes. Four sources of attitude error are available:

- a) The primary mode is used for displaying attitude plus steering errors in all three axes. These errors are generated within the CMC using IMU information. The error signals are sent through the CDU and applied to the FDAI attitude error indicators.
- b) The output of the BMAG's (uncaged) can be applied directly to the attitude error meters. In the SCS attitude hold mode, the attitude deviation from the gyro uncaged attitude is displayed.
- c) The difference between angles set in on the attitude set control panel (ASCP) and the G&N IMU inertial angles.

- d) The difference between the Euler attitude integrated by the GDC and the set-in attitude, converted to body axes.

Full-scale deflection on the attitude error needles is presented in Table 4.4-6 for the various mission phases.

The uncertainty of attitude error display is as follows:

- a) G&N Attitude Source
 - 1) Less than 0.2° plus 3.3% of indication when on 5° scale
 - 2) Less than 0.6° plus 3.3% of indication when on 15° scale
 - 3) Less than 2.0° plus 3.3% of indication when on 50° scale
- b) CMC Backup Attitude Source
 - 1) Less than 0.33° plus 5% of indication when on 5° scale
 - 2) Less than 1.0° plus 6.5% of indication when on 15° scale
- c) G&N Backup Attitude Source
 - 1) Less than 0.2° plus 7.4% of indication when on 5° scale
 - 2) Less than 0.6° plus 7.4% of indication when on 15° scale

4.4.2.4.3 Attitude Rate Display Modes. Attitude rate is derived from BMAG 2 in the primary mode and from BMAG 1 in the backup mode.

- a) Rate scales available are:
 - 1) All axes 1 deg/sec
 - 2) All axes 5 deg/sec
 - 3) Pitch and yaw 10 deg/sec
 - Roll 50 deg/sec

b) The uncertainty of the rate display is:

- 1) Less than 0.07 deg/sec plus 4% of indication on 1 deg/sec scale
- 2) Less than 0.2 deg/sec plus 4% of indication on 5 deg/sec scale
- 3) Less than 0.4 deg/sec plus 4% of indication on 10 deg/sec scale
- 4) Less than 2.0 deg/sec plus 4% of indication on 50 deg/sec scale

4.4.3 Entry Monitor Subsystem (EMS).[†] The EMS displays consist of a lift-vector orientation indicator, delta \bar{V} /range-to-go indicator, entry threshold indicator, corridor verification indicator, VHF range display, mode select switch, function select switch, slew switch, SPS annunciator and a flight monitor.

The acceleration and velocity display data are derived from a single longitudinal axis accelerometer. The EMS accelerometer is aligned along the spacecraft X-body axis and monitors accelerations during entry and powered flight burns.

4.4.3.1 EMS Software Design Data. The parameters used to design the EMS software are given below.

- | | |
|-----------------|--|
| a) Planet | Rotating, oblate spheroid (earth) |
| b) Atmosphere | 1962 U.S. Standard with ± 3 -sigma, 30°N density deviations |
| c) Aerodynamics | Operating range: $0.250 \leq L/D \leq 0.375$
Coefficient data: Refer to Section 5.0, ($M \geq 29.5$) |
| *d) RCS | Single system: +3.73 degrees/second ²
-3.51 degrees/second ² |
| *e) SCS | Maximum stick command = 22.5 degrees/second
Minimum output = 20.5 degrees/second
Delta θ = 180° in 14.47 seconds
(12.43953 degrees/second) |

[†] NASA Data Source

* RCS, SCS performance and vehicle inertias are set to achieve worst-case maneuver performance and, therefore, are not to be interpreted as representative of any given CSM configuration.

	System	Delta \emptyset Time (seconds)
	Single proportional	14.47
	Dual proportional	11.71
	Single direct	14.06
	Dual direct	9.94
*f) Vehicle	W = 13,500 pounds I _{xx} = 7380 slug - ft ² I _{yy} = 6530 slug - ft ² I _{zz} = 5760 slug - ft ²	A _{ref} = 129.4 ft ²

†g) Earth return conic

Latitude: 30° N

h) Trajectory

Limit case for maximum compatibility with G&N

i) Mathematical

$$\text{Velocity, } V = V_o - K_D \int_{t_{0.05g}}^t A_x dt$$

$$\text{Range-to-go, } R_{TG} = R_o - K_R \int_{t_{0.05g}}^t V dt$$

V_o = initial velocity (feet/second)

R_o = initial range (n mi)

A_x = acceleration in X-body direction (feet/second²)

†K_D = 0.947 (see Figure 4.4-9)

K_R = 0.000162 (range scale factor) (n mi/ft)

4.4.3.2 Scroll and Flight Monitor.

4.4.3.2.1 Scroll. Flight limit design criteria are as follows:

a) Onset limits Maximum g = 10.0

* RCS, SCS performance and vehicle inertias are set to achieve worst-case maneuver performance and, therefore, are not to be interpreted as representative of any given CSM configuration.

† NASA Data Source

- | | | |
|----|-----------------------------|---|
| b) | Offset limits | Non-exit
Maximum range = 3500 n mi
Minimum g = 0.20

3500-n mi range limit
Maximum range = 3500 n mi
Constant g flight mode
Positive lift exits
Zero-lift reentries |
| c) | Circular velocity line | All patterns

Established for altitude coincident with g = 0.20 and shifted consistent with velocity error budget |
| d) | Terminal ranging capability | Longitudinal ranging capability between end of scroll pattern (V = 4000 feet per second) and drogue deployment given in Figure 4.4-10 |

4.4.3.2.2 Flight Monitor. The flight monitor is a rectilinear display of the entry acceleration load factor, g, as a function of inertial velocity. It presents an entry trajectory trace, in terms of g and V, to the pilot for continuous comparison with a monitoring pattern which defines limiting acceleration onset and offset rates.

- | | | |
|----|------------------------|---|
| a) | Design range | Inertial velocity, 37,000 feet per second $\geq V \geq$ 4000 feet per second
Acceleration load factor, $0 \leq G \leq 10$ |
| b) | Maximum load factor | Hardware will not lose information at G's up to 14 |
| c) | Maximum g-rate | 2 g/sec |
| d) | Maximum g-acceleration | 0.27 g/sec^2 |
| e) | Accelerometer | Resolution factor, K_D , set to minimize velocity errors for expected L/D range (see Figure 4.4-9) |
| f) | Velocity error | Total budget = 300 feet per second in first 11,500 feet per second delta V. (Refer to Table 4.4-7 for error sources and nominal RSS Delta V error.) |

g) Initialization

V_0 set for ground communication
(GNCS backup) prior to 0.05 g

Maximum uncertainty $\Delta V = \pm 48$
feet per second (Figure 4.4-11)

Altitude for 0.05-g point is in
erasable memory. Current on-board
value is $h=297,431$ feet

h) Operation

Monitoring patterns printed on the
obverse of a mylar tape scroll having
an emulsion-coated back are driven
horizontally from right to left (high
to low velocity). A scribe mechanism
located behind the scroll removes
emulsion as it is driven vertically.

Scroll rate - proportional to command
module velocity change

Scribe rate - proportional to changes
in total acceleration load factor, G_T

4.4.3.3 Lift Vector Orientation Indicator. This display provides visual indication of the roll attitude of the CM about the stability axis. Each revolution of the indicating needle represents 360° of vehicle rotation; however, the display is capable of continuous rotation in either direction. The needle-up position (0°) indicates maximum lift-up vector (full positive lift), and the needle-down position (180°) indicates maximum lift-down vector (negative lift). The earth roll indicator follows signals corresponding to the following: roll rates up to 60° per second, and roll accelerations up to 15° per second. The overall accuracy with respect to the input signal is $\pm 3^\circ$. The corridor verification annunciator lamps located at the top (zero degrees) and bottom (180°) of the lift vector orientation indicator are to be ignored. Corridor verification is a lunar function only and cannot be relied on for earth orbital entries.

4.4.3.4 Delta V/Range-to-go Indicator. The delta V/range-to-go indicator is comprised of a six-digit, digital numeric display with associated electronics. In addition to performing delta V remaining during delta-V thrusting operations and range-to-go during entry, the counter is mechanized to display VHF range.

4.4.3.4.1 Delta V (ΔV). The ΔV indicator consists of a digital display and right-hand annunciator lamp located immediately below the flight

monitor. The annunciator lamp illuminates when the SPS engine fire command is given.

The digital display is capable of displaying velocity from 0.1 to 99,999.9 feet per second. The desired ΔV is preset into the EMS. The ΔV counter electronics integrate acceleration and decrement the ΔV preset in the counter. When the proper ΔV is obtained (ΔV on counter = 0), a thrust termination signal is provided for SCS controlled ΔV .

The ΔV indicator logic is designed for unidirectional incrementing through 0.0 and can display false ΔV indications if acceleration is reversed when the counter is displaying 0.0 or -0.0. Starting ΔV 's at $\Delta V = 0.0$ or ending ΔV 's with a planned 0.0 for ΔV_c residual, before or after RCS +/-X trim, should be avoided.

The specified accuracy of the EMS in the ΔV mode is ± 1.3 percent or ± 0.7 feet per second, whichever is greater, for the following acceleration levels: +0.004 to 0.02 g for a maximum of 25 seconds, and +0.2 to 1.3 g for a maximum of 7 minutes. The latter tolerance (± 0.7 foot per second) would normally preclude the use of the EMS when performing very small RCS delta V's. However, use of the following procedure should render the EMS effective for the low-level RCS delta V's.

- a) Conduct at least three EMS accelerometer bias checks in a quiescent zero-g environment, i.e., no RCS activity and minimum crew activity. If the results of the bias checks are repeatable within a tolerance spread, the delta V value present into the Delta V/RANGE display may be adjusted to minimize the effects of null bias.
- b) Observe the ΔV /RANGE display to determine the direction/sense of the first pulse count (0.1 foot per second) during each RCS ΔV . If the first count is in the wrong direction (a phenomenon which may occur in any ΔV operation but which is not significant in SPS thrusting), terminate the RCS thrusting 0.2 feet per second before attaining the planned terminal value in the ΔV /RANGE display.

The null bias anomaly is 0.1 foot per second for initial counter jump.

4.4.3.4.1.1 Delta-V Counter Setting Determination. This section contains the performance data relative to an SCS-controlled short SPS burn. Data are provided for both two- and four-jet ullage operations. (Figures 4.4-12 and 4.4-13 are independent of ullage duration.)

Definitions - The following definitions apply to the data contained in this section and in Figures 4.4-12 and 4.4-13.

- 1) ΔV_c - Initial ΔV counter setting

- 2) ΔV_F - ΔV counter reading used for ignition cue
- 3) ΔV_U - ΔV ullage
- 4) ΔV_S - ΔV occurring after ΔV_F
- 5) ΔV_T - Total ΔV desired ($\Delta V_S + \Delta V_U$)

Assumptions - The data contained in Figures 4.4-12 and 4.4-13 assume that ullage is continued beyond the ignition cue (ΔV_F) until SPS ignition occurs. The calculations assumed a 0.3-second pilot-reaction time and 0.5-second system delay to exist between ignition cue (ΔV_F) and SPS ignition. The delta V occurring during this period (0.8 sec.) is included in the term delta V_S along with the delta V derived from the SPS engine. In using these data, it is further assumed that spacecraft weight, ΔV_T , and ΔV_U are known or can be calculated external to these data. This permits an arbitrary selection of ullage time and configuration to be employed.

Data Explanation - Figures 4.4-12 and 4.4-13 are plots of ΔV_S ($\Delta V_T - \Delta V_U$) and ΔV_F for various spacecraft weights ranging from 24,000 to 40,000 pounds. For other than depicted values, interpolation may be employed. The single purpose of the data contained in these figures is to provide the ΔV counter reading to be used as the cue for SPS ignition (ΔV_F). Having determined ΔV_F , the initial ΔV counter setting (ΔV_C) is calculated by adding ΔV_U to ΔV_F (i.e., $\Delta V_C = \Delta V_F + \Delta V_U$).

Procedurally, the data are employed as follows:

- 1) Given SC weight, ΔV_T and ΔV_U
- 2) Determine ΔV_S ($\Delta V_S = \Delta V_T - \Delta V_U$)
- 3) Determine ΔV_F (using ΔV_S and SC weight in figures)
- 4) Calculate ΔV_C ($\Delta V_C = \Delta V_F + \Delta V_U$)

4.4.3.4.2 Range-to-go. During the range-to-go mode, range-to-go information is displayed on the digital display in terms of nautical miles from 0 to 3500. The overall accuracy of the range-to-go display is ± 3 percent of the integral of velocity along the spacecraft velocity vector for acceleration inputs up to 14 g's and ranges between 1000 and 3500 nautical miles. Initial and predicted display errors are provided in Tables 4.4-8 and 4.4-9, respectively.

4.4.3.4.3 Slew Switch (ΔV EMS Set). The slew switch is a rocker type used to preset the ΔV thrust requirement, the initial range-to-go, and the scroll velocity requirement. The rocker switch has five positions: null, slow increase, fast increase, slow decrease, and fast decrease. The rates that may be selected are as follows:

<u>Slew Switch Speed</u>	<u>G-V Display Rate 1827 ft/sec = 1 inch of scroll (ft/sec/sec)</u>	<u>ΔV/RTG Rate (counts/sec)</u>
Slow	30	2.5
Fast	480	1275.0

4.4.3.4.4 VHF Range. The maximum range of the VHF ranging system between the CSM and a target vehicle is 300 nautical miles with an accuracy of ± 450 feet between 500 feet and 300 nautical miles. This range includes bias error (± 270 feet) and random error (± 180 feet). The display resolution of the entry monitor subsystem is 0.01 nautical mile. The decimal is blanked out in the VHF ranging mode. Loss of the VHF ranging "data good" signal will be presented to the crewman as blanking of the EMS display with the exception of the last two digits on the right-hand side which will show zero. See Section 4.9.1.2 for VHF ranging limitations.

4.4.3.4.5 Mode Selection Switch. The three-position mode selection toggle switch is manually operated and labeled as shown in Figure 4.4-14. Position and corresponding function are listed in Table 4.4-10.

4.4.3.4.6 Function Switch. The 12-position function switch is manually operated and labeled as shown in Figure 4.4-14. Position and corresponding function are listed in Table 4.4-11.

4.4.3.5 Entry Threshold Indicator. The entry threshold indicator provides the first visual indication of total acceleration (G_T) sensed at the entry threshold (approximately 290,000 feet altitude). The lamp illuminates not less than 0.5 second, or more than 1.5 seconds, after G_T reaches 0.05 (± 0.005) g and turns off when the acceleration drops below 0.02 (± 0.005) g.

4.4.4 Attitude Control.

4.4.4.1 Earth Orbit.

4.4.4.1.1 GNCS. The attitude deadband and attitude rate limits available through the GNCS are a function of the command module computer (CMC) program. The following deadbands and rates have been proposed for CSM attitude control.

- a) Attitude deadbands 0.2°, 0.5°, 5.0° and erasable deadband*
- b) Attitude rates 2.0°, 0.5°, 0.2° and 0.05°/sec and erasable rate

4.4.4.1.2 SCS. The earth orbit attitude control limits (for all axes) available through automatic SCS control are presented in Table 4.4-12. Figure 4.4-15 shows the change in spacecraft angular rate per pulse in each axis during these modes of operation.

†Manual control through the SCS provides a choice of:

- a) Acceleration command. Enables the rotation controller to fire RCS jets while inhibiting all other command inputs; jets remain on as long as controller is displaced beyond breakout
- b) Rate command. Provides proportional-rate control from the rotation controller; rates available are 0.65 deg/sec in pitch, yaw, and roll
- c) Minimum impulse. Inhibits all SCS attitude and rate inputs; provides one RCS minimum impulse for each closure of the rotation control breakout switch
- d) Direct. Provides acceleration command using secondary RCS coils when control is displaced beyond soft stop

Each of the manual modes is selective on an individual axis basis.

4.4.4.1.3 SM RCS Thrust Vector and Control Moment Data. The data provided herein define thrust vector locations, moment arm definition, engine locations, engine impingement data, and moment equations. Engine thrust levels are presented in Section 4.6. Engine locations for each quad and RCS notation are shown in Figure 4.4-16. The engines are numbered in accordance with the NASA system for RCS engine identification.

4.4.4.1.3.1 Thrust Components and Moment Arm Definition. The geometry of the thrust application points is shown in Figures 4.4-17 and 4.4-18. Figure 4.4-19 shows the components of thrust for each engine, and Figure 4.4-20 illustrates the moment arms. The thrust components and the moment arms are defined in Tables 4.4-13 and 4.4-14. The components of thrust and the moment arms are left in a general form so that changes in location of the reaction jets will not require a new derivation of the equation. Each reaction jet quad is designated by an unsubscripted capital letter (A, B, C, or D).

* Tentatively, it is specified that there will be an astronaut option for loading an arbitrary deadband and rate. The maneuver rate erasable option will be in the range of 0.0 to 4.0 deg/sec.

† NASA Data Source

The capital letters (A_1 , B_1 , etc.) are equivalent to the thrust developed by that particular engine of the quad. Capital letters with a double subscript (A_{2y} , B_{1z} , etc.) designate the component of thrust from a particular engine along the particular axis used in the subscript. No direction, either plus or minus, is implied from the subscripts.

The moment arms are subscripted to designate the length from the geometric center of the engine attach points in a quad to the c.g. parallel to a particular axis (l_{Ay} , l_{Bz} , etc.) or to designate the length from a single engine to the c.g. parallel to a particular axis (l_{C2y} , l_{D4z} , etc.). For the moment arms parallel to the X-axis, the designations l_{x1} , l_{x2} , l_{x3} , and l_{x4} are used and are the x-distance from the engine, denoted by the number in the subscript, to the c.g. No quad differentiation is required since all the engines with a common number subscript are mounted in a plane perpendicular to the X-axis.

4.4.4.1.3.2 Moment Equations (See Table 4.4-15). The moments as given are about the CSM axis system. The expressions are for the major thrust of the engines and do not include the moment due to jet impingements. The expressions take into account the 10-degree cant angle of the jet nozzle from the local tangent plane to the surface, and the 7.25-degree rotation of the jet quads from the CSM axis system. The jet symbols (A_1 , A_2 , A_3 , A_4) in the moment equations are the absolute value of the thrust. The sign of the moment is taken into account in the coefficient expression.

4.4.4.1.3.3 Impingement Forces. The simplest explanation of impingement forces is that the spacecraft appears to the thrust as an extension of part of the nozzle. Thus, the jet impingement produces a force normal to the surface of the spacecraft. The magnitude of the force depends on the geometry and location of the jet. The jets may be divided into three groups: the roll jets, the forward thrust jets, and the after thrust jets. The impingement forces involved are defined in Figure 4.4-21, and the engine vectors are shown in Figure 4.4-22. The letter F, as used in these figures, denotes an engine and the appropriate engine letter; i.e., A_1 , A_2 , ... D_3 , D_4 , may be substituted for F. Thrust vector locations are shown in Figures 4.4-23 and 4.4-24.

4.4.4.1.4 SM RCS Control Forces and Moments. RCS control forces and moments for a heavy CSM (31,800 pounds), light CSM (23,200 pounds) and docked with the DM and Soyuz are presented in Tables 4.4-16 through 4.4-20.

4.4.4.2 Entry

4.4.4.2.1 GNCS.† The entry DAP is described in the Apollo Guidance and Navigation Document, "Guidance Systems Operations Plan for Manned CM Earth Orbital and Lunar Missions Using Program Colossus 2, Section 3, Digital Autopilots", R-577, MIT/IL.

4.4.4.2.2 SCS. The entry attitude control limits available through automatic SCS control are given in Table 4.4-12. Figure 4.4-25 shows the change in command module angular rate per pulse in each axis during these modes of operation.

†Manual attitude control through the SCS is limited to the following rates:

Pitch and Yaw Rate	7°/sec
Roll Rate	20.5°/sec

4.4.4.2.3 CM RCS Force and Moment Equations. The CM RCS engine locations and thrusting geometry are shown in Figure 4.4-26. The parameters shown in the figure are defined as follows:

β = Angle between a projected center line of either engine No. 13 or No. 23 on a $Y_c - Z_c$ plane and the Z_c axis, and also between a center line of either engine No. 15, No. 26, No. 25 or No. 16 and the $Y_c - X_c$ plane in degrees.

γ = Angle between a center line of either engine No. 13 or No. 23 and the $Y_c - Z_c$ plane and also between a center line of either engine No. 15, No. 26, No. 25 or No. 16 and $Y_c - Z_c$ plane in degrees.

μ = Angle between a center line of either engine No. 11 or No. 22 and Y_c axis in degrees.

λ = Angle between a center line of either engine No. 21 or No. 12 and Z_c axis in degrees.

ρ = Angle between a projected center line of either engine No. 14 or No. 24 on a $Y_c - Z_c$ plane and the Z_c axis in degrees.

X_c, Y_c, Z_c = Coordinate axes fixed in command module.

The engines are numbered in accordance with the NASA system for RCS engine identification.

†NASA Data Source

The numerical values for these parameters in the present CM configuration are given in Table 4.4-21.

The RCS engine nozzle extensions are scarfed as a result of the CM geometry. This scarfing results in a misalignment of the engine thrust vector and the engine centerline. The misalignment angle and the effective point of thrust application due to scarfing vary with altitude. The values for the scarf angles and the variations due to altitude are defined in Paragraph 4.7.4.2. The effects of the engine nozzle scarfing are indicated in the force and moment equations by the parameters defined as follows:

<u>CM RCS Engine</u>	<u>Misalignment Angle</u>	<u>Thrust Vector Location</u>
Positive Pitch Engines (13 & 23)	$\Delta\theta_1$	$\Delta\ell_{pp}$
Negative Pitch Engines (14 & 24)	$\Delta\theta_2$	$\Delta\ell_{np}$
Yaw Engines (15 & 26 and 25 & 16)	$\Delta\psi$	$\Delta\ell_{yaw}$
Long Roll Engines (11 & 22)	$\Delta\phi_1$	$\Delta\ell_{lr}$
Short Roll Engines (21 & 12)	$\Delta\phi_2$	$\Delta\ell_{sr}$

The CM RCS force equations are given in Table 4.4-22. The moment arms are illustrated in Figure 4.4-27 and defined in Table 4.4-23. The moment arm changes resulting from thrust vector variations with altitude are given in Table 4.4-24. The CM RCS moment equations are given in Table 4.4-25. The force and moment arm equations are left in a general form so that changes in the locations of the reaction jets will not require a new derivation of the equations. The CM RCS moment equations are given for the spacecraft configuration.

4.4.4.2.4 CM RCS Control Forces and Moments. Command module RCS control forces and moments are presented in Tables 4.4-26 and 4.4-27.

4.4.5 Thrust Vector Control

4.4.5.1 SPS Thrust Vector Location. The SPS thrust vector point of application lies at $X_{A6} = 833.2$ and is coincident with the X-axis at that plane ± 0.25 inch translational and at ± 0.5 degree angular. The gimbal plane is also at $X_{A6} = 833.2$. The nominal gimbaling capability is shown in

Figure 4.4-28. Table 4.4-28 illustrates the variation of gimbaling capability with four values of CSM weight.

4.4.5.2 SPS Actuation System. The SPS engine-actuation system consists of three basic elements: the actuator, the gimbal assembly, and the servo electronics. The actuator is controlled by a two-loop servo system employing the sensing of actuator extension or retraction (representing engine angular position) and actuator extension or retraction rate. An engine angular position, with respect to the spacecraft, may be commanded by electrical input to the servoamplifier.

The actuator dynamics data are presented in Table 4.4-29. The SPS actuation system gimbal range is restricted by the capabilities of the integral components. The component limit data are presented in Table 4.4-30.

4.4.5.3 SPS TVC Error Sources. Errors inherent in the SPS TVC System arise from the following sources:

- a) Thrust Vector Uncertainty. Factors contributing to this error source are tabulated below:

<u>Factor</u>	<u>Value</u>	<u>Type</u>
Thrust to gimbal offset	1/8 sec	Specification
Misalignment of thrust with engine centerline	1/2 deg	Specification
Gimbal to spacecraft offset	1/32 sec	3 σ
Gimbal mounting misalignment	0 deg	(Taken out with final alignment procedure)

- b) Center of Gravity Uncertainty. The lateral uncertainty in the known position of the center of gravity is assumed to have a 3 σ value of 2 inches in both the Y and Z axes.
- c) Thrust-Yaw Coupling Uncertainty. The uncertainty in the yaw gimbal position rotation due to thrust - yaw coupling is ± 30 percent of the nominal.
- d) Stability Requirements. The thrust vector control system must meet the following stability requirements:
- 1) Small Signal Stability Not less than 30 degrees phase margin and 6 dB gain margin over the linear range of operation.

- | | |
|--|---|
| 2) Large Signal Stability | Vehicle pitch and yaw rates shall converge to 2 degrees/second within 10 seconds. |
| 3) Limit Cycling (Engine Angular Position) | Shall not produce a limit cycle of amplitude in excess of 1/10 deg at frequencies less than 2 Hz. No limit cycling at frequencies above 2 Hz. |

4.4.5.4 SCS TVC Pointing Accuracy. Selection of automatic or manual SCS TVC is possible on an individual axis basis. The peak total delta velocity pointing error for burn times less than 80 seconds is 5.7°.

4.4.6 Miscellaneous

4.4.6.1 Command Module Aerodynamic Capture Envelope. The capture envelope is the locus of allowable angles of attack and side-slip which result in aerodynamic stabilization of the command module, heat shield forward, after the control mode is changed from attitude hold about the three axes to rate damping in pitch and yaw and attitude hold in roll. The control mode change occurs at an aerodynamic pressure (q) equivalent to the 0.05-g point. Points outside of the envelope at 0.05 g may result in the stabilization of the command module apex forward. The definition of the aerodynamic capture envelope is of interest in the determination of allowable attitude excursions from trim prior to entry into the sensible atmosphere.

Dynamic capture envelopes are presented in Figure 4.4-29. The smaller envelope represents the maximum capture envelope allowable at 0.05 g when no RCS control is considered. The only damping present in this case is the stabilizing effect of the increasing dynamic pressure. The larger envelope includes the stabilizing effect of a single system RCS and represents the nominal design case.

It is recommended that an envelope no greater than the smaller envelope shown in Figure 4.4-29 be used for crew training. This will allow heat-shield-forward capture under any conditions. Failure of the operational RCS at 0.05 g does not allow sufficient time to reactuate the redundant RCS in time to avoid apex-forward capture under certain conditions of α and β represented by the larger envelope shown in Figure 4.4-29.

4.4.6.2 Crewman Optical Alignment Sight (COAS). The function of the COAS is to provide the crewman with a fixed line-of-sight attitude reference image which appears to be the same distance away as the target. This image is boresighted parallel to the X-axis of the command module. The image consists of a 10° circle, vertical and horizontal cross hairs with 1° marks, and an elevation scale of -10° to +31.5°. The COAS functions as an aid to the flight crew to accomplish docking.

A constant angle on a star during a delta V maneuver can be maintained by use of the elevation scale. The barrel of the COAS may be rotated around the X-axis for this operation. Rotation of the COAS barrel is limited to $\pm 35^\circ$.

The COAS may be used to align the spacecraft inertial reference. Errors in alignment using the COAS are tabulated below.*

X-axis - 0.073 degree

Y-axis - 0.060 degree

Z-axis - 0.085 degree

4.4.6.3 G-Meter. The g-meter, a continuously active mechanical accelerometer, displays the acceleration load-factor measured along the command module X structural axis. The conversion equation is $g = a_x/32.174$. The meter is calibrated in 1.0-g increments from -1.0 to 15.0 g 's. Its accuracy is as follows:

<u>True Acceleration</u>	<u>Allowable Deviation</u>
Less than 4.0 g	± 0.2 g
Greater than 4.0 g	± 5 percent of true

* Errors are flight data for the Apollo 9 mission.

Table 4.4-1. IMU Errors (See Paragraphs 4.4.1.1.3 and 4.4.1.1.4) (Sheet 1 of 2)

<u>Item (Symbol)</u>	<u>RMS Error After Compensation</u>	<u>Error Units</u>	<u>CMC Compensation Range (and Quantization)</u>
Accelerometer Errors			
Bias error (ACB)	0.20	cm/sec ²	±9.14 (0.01)
Scale factor error (SFE)	116	ppm	±1953 (10)
Acceleration squared error (NC)	10	μg/g ²	NA
Input axis misalignment (α)	20	arc-sec	NA
Gyro Errors			
Bias drift (NBD)	2	meru	±128 (0.01)
Input axis acceleration sensitive drift (ADIA)	8	meru/g	±862 (1.0)
Spin reference axis acceleration sensitive drift (ADSRA)	5	meru/g	±862 (1.0)
Input axis acceleration squared sensitive drift (A ² DIA)	0.6	meru/g ²	NA
Spin reference axis acceleration squared sensitive drift (A ² DSRA)	0.6	meru/g ²	NA
IRIG scale factor (SF)	500	ppm	NA
Input axis misalignment about spin reference axis (α SRA)	300	arc-sec	NA
Input axis misalignment about output axis (α OA)	300	arc-sec	NA

Table 4.4-1. IMU Errors (See Paragraphs 4.4.41.1.3 and 4.4.1.1.4) (Sheet 2 of 2)

<u>Item (Symbol)</u>	<u>Preflight Test Data</u>	<u>Apollo Flight Analysis Data*</u>	<u>Error Units</u>
Accelerometer Errors			
Bias error (ACB)	0.1	0.067	cm/sec ²
Scale factor error (SFE)	57		ppm
Gyro Errors			
Bias drift (NBD)	1.3	1.2	meru
Input axis acceleration sensitive drift (ADIA)	7.7		meru/g
Spin reference axis acceleration sensitive drift (ADSRA)	3.5		meru/g
IRIG scale factor (SF)	157		ppm
Output axis acceleration sensitive drift (ADOA)	0.7		meru/g

*Can only be expected if temperature and voltage are held near nominal

Table 4.4-2 IMU Temperature Drift Rates (See Paragraph 4.4.1.1.5)

<u>Item (Symbol)</u>	<u>Temperature Drift Rates</u>	<u>Drift Rate Units</u>
Accelerometer Drift Rates		
Bias (ACB)	0.014	cm/sec ² /°F
Scale factor (SF)	280	ppm/°F
Gyro Drift Rates		
Bias drift (NBD)	0.2	meru/°F
Input axis acceleration sensitive drift (ADIA)	0.5	meru/g/°F
Spin reference axis acceleration sensitive drift (ADSRA)	0.5	meru/g/°F
IRIG scale factor (SF)	250	ppm/°F

Table 4.4-3. Erasable Memory Constants
(See Paragraph 4.4.1.2.1)

TBS

Table 4.4-4. SCS BMAG Drift Values
(See Paragraph 4.4.2.2.1)

<u>Type of Drift</u>	<u>Axis</u>	<u>Maximum Drift</u>
Nonacceleration sensitive drift	X	1.73 deg/hr
	Y	1.73 deg/hr
	Z	1.73 deg/hr
Acceleration sensitive drift	X	*4.0 deg/hr/g
	Y	*4.0 deg/hr/g
	Z	*4.0 deg/hr/g
Acceleration squared sensitive drift	X	**6.0 deg/hr/g ²
	Y	**7.0 deg/hr/g ²
	Z	**7.0 deg/hr/g ²

*Maximum for each of spin reference, input, and output axes. The maximum drift for vector sum of spin reference, input, and output axes for each of X, Y, and Z gyros is 4 deg/hr/g. The value of acceleration-sensitive drift is defined as the vector sum of maximum 3-sigma drift due to input axis mass unbalance and that due to spin-axis mass unbalance. Separate values are not specified for the components.

**Maximum for each of spin reference, input, and output axes for X, Y, and Z axes.

Table 4.4-5. GDC Drift (See Paragraph 4.4.2.2.2)

Axis	GDC Drift (3 σ) (Design Limit)*		GDC Drift - Lab System; Room Ambient Conditions (deg/hr)**	Combined BMAG and GDC Drift Rates (SC 2 TV-1)***			
	Yaw = 0 deg/hr	Yaw = 60 deg/hr		Test 1 (deg/hr)	Test 2 (deg/hr)	Test 3 (deg/hr)	Test 4 (deg/hr)
R	9.45	10.0	0.4	5.43	5.43	6.03	6.03
P	8.75	9.35	0.5	1.08	1.08	1.68	1.68
Y	8.45	8.85	2.0	2.76	2.46	3.36	4.66

*This is MTEE (3 σ) drift allocated to the GDC in Honeywell's Technical Development Specification 1005. Values for 0-, 0-, and 0-degree, and 0-, 0-, and 60-degree alignments are given to illustrate effect of yaw angles on drift rates. Pitch and roll have no effect.

**Results of a GDC drift test performed at NR on an engineering model of the GDC. (Reference G&C Lab Notebook EM5, Activity Book 1, Page M208721, 19 November 1966.) The GDC was aligned initially to 0-, 0-, 0-degrees, and the drift was measured after 2 hours, 36 minutes with BMAG spin motors off to eliminate BMAG drift.

***These drift values represent combined BMAG and GDC drift rates that were recorded at NR on SC 2TV-1. Tests 1 and 2 were recorded 20 minutes after the GDC was aligned to 0-, 0-, and 0-degrees, and tests 3 and 4 were recorded 5 minutes after the GDC was aligned to 0-, 0-, and 0-degrees, then extrapolated out to drift/hour. Earth rate was subtracted from each axis. The tests were performed on one GDC only. No such tests were run on any subsequent spacecraft.

4.4-28

MSC-07765 (Vol. I)

Table 4.4-6. FDAI Display Capability
(See Paragraphs 4.4.2.4 and 4.4.2.4.2)

Switch Position	Flight Phase	Attitude Error		Rate	
		CMC	SCS	CMC	SCS
5/1	Boost and entry	20-deg roll 5-deg pitch and yaw	5-deg pitch, yaw and roll	Not applicable	1-deg/sec
	All other	5-deg pitch, yaw and roll	5-deg pitch, yaw and roll	Not applicable	1-deg/sec
5/5	Boost and entry	20-deg roll 5-deg pitch and yaw	5-deg pitch, yaw and roll	Not applicable	5-deg/sec
	All other	5-deg pitch, yaw and roll	5-deg pitch, yaw and roll	Not applicable	5-deg/sec
50/15/50/10	Boost and entry	50-deg roll 15-deg pitch and yaw	50-deg roll 15-deg pitch and yaw	Not applicable	50-deg/sec roll 10-deg/sec pitch and yaw
	All other	12.5-deg roll 15-deg pitch and yaw	50-deg roll 15-deg pitch and yaw	Not applicable	50-deg/sec roll 10-deg/sec pitch and yaw

NOTE: Rate scale indexed at null; $\pm 1/5$, $\pm 2/5$, $\pm 3/5$, $\pm 4/5$ of full scale; and full scale.
Attitude scale indexed at null; $\pm 1/3$, $\pm 2/3$ of full scale; and full scale for pitch and yaw.
Roll attitude scale indexed at null; $\pm 1/2$ full scale; and full scale.

Table 4.4-7. EMS Velocity Error Budget
 (See Paragraph 4.4.3.2.2)

<u>Error Sources</u>	<u>3σ ΔV Error (feet per second)</u>
Aerodynamic trim deviations ($0.25 \leq L/D \leq 0.375$, $161.6 \text{ deg} \geq \alpha \geq 155.8 \text{ deg}$)	160.4
Alignment	17.8
V_o determination	15.0
V_o setting	50.0
Earth gravity and rotation	56.0
Hardware (measurement, integration, and display)	<u>100.0</u>
3 σ RSS ΔV	204.7
Total ΔV error budget	300.0

$V_o = 37,000$ feet per second

$\Delta V = 11,500$ feet per second

Table 4.4-8. Range-To-Go Three-Sigma Time and Range Tolerances at 0.05 g (See Paragraph 4.4.3.4.2)

<u>Error Source</u>	<u>Δt (sec)</u>	<u>ΔR (n mi)</u>
Atmospheric density deviations ($\pm 3\sigma$, 30°N deviations about 1962 USSA)	± 5.8	± 25
Aerodynamic trim uncertainties ($\Delta L/D = \pm 0.05$)	± 1.0	± 4
Sensing tolerances ($\Delta g = \pm 0.005$)	<u>± 2.8</u>	<u>± 12</u>
RSS	± 6.5	± 28

Table 4.4-9. Range-To-Go Three-Sigma Ranging Accuracy, Representative SPS Deorbit (See Paragraph 4.4.3.4.2)

<u>Error Source</u>	<u>ΔR (n mi)</u>
Initial range, R_0	± 28
Initial velocity	± 4
Aerodynamic trim (Integral, $\int V dt$)	± 15
Hardware (0.30 percent ΔV)	± 4
R_{TG} counter (null by crew)	<u>± 15</u>
RSS	± 35.6

Table 4.4-10. EMS Mode Toggle Switch
(See Paragraph 4.4.3.4.5)

Applicable Spacecraft	Position	Function (EMS Electronics On)	
		Entry	Delta-V
106 and subsequent	NORMAL	Inhibits integrator until 0.05 g	Integrator on; com- parators and G-servo inhibited
All	STBY	Inhibits comparators, integrators, and G-servo	Inhibits comparators integrators, and G-servo
106 and subsequent	<u>BACKUP</u> VHF RNG	Comparators deactivated. Range integrator and G-servo on	Comparators, range integrator, and G-servo inhibited ΔV /RANGE indicator displays VHF range data supplied from external source.

Table 4.4-11. EMS Function Switch
(See Paragraph 4.4.3.4.6)

Position	Function
OFF	All power off except SPS thrust lamp circuitry
EMS TEST	
1	Threshold comparator - lower trip point (0.043 g)
2	Threshold comparator - upper trip point (0.0572 g)
3	Roll annunciator lamp - lower trip point (0.245 g for SC 106 and subsequent)
4	Velocity integration circuitry, G-servo circuitry, G-V plotter, and range (to-go) (accelerometer torqued to 9 g for 10.053 sec)
5	Roll annunciator lamp - upper trip (0.279 g for SC 106 and subsequent)
RNG SET	Permits slewing range counter for operational entry mode
V _o SET	Permits slewing G-V scroll prior to operational entry mode
ENTRY	Operational monitoring mode for entry
ΔV TEST	Operational mode for ΔV circuitry self-test
ΔV SET VHF RNG	MODE switch in NORMAL or STBY - establishes circuitry for slewing ΔV /RANGE display to desired values for opera- tional modes and ΔV self-test MODE switch in BACKUP/VHF RNG - provides digital display for VHF ranging
ΔV	Operational mode for monitoring ΔV maneuvers

Table 4.4-12. SCS RCS Automatic-Control Modes and Deadbands
(See Paragraphs 4.4.4.1.2 and 4.4.4.2.2)

SCS RCS Attitude Hold Mode	Control-Panel Switches and Positions			Attitude Deadband (degree)	Rate Deadband (°/sec)	Pseudo Rate Feedback	Recommended Mission Applicability
	Limit Cycle Switch	Rate Switch	Attitude Deadband Switch				
1	ON	LOW	MIN.	0.2	0.2	In	Earth Orbit
2	ON	LOW	MAX.	4.2	0.2	In	Earth Orbit
3	ON	HIGH	MIN.	4.0	2.0	In	Earth Orbit and Preentry
4	ON	HIGH	MAX.	8.0	2.0	In	Earth Orbit and Preentry
5	OFF	LOW	MIN.	0.2	0.2	Out	None *
6	OFF	LOW	MAX.	4.2	0.2	Out	None *
7	OFF	HIGH	MIN.	4.0	2.0	Out	Entry (after 0.05 g)
8	OFF	HIGH	MAX.	8.0	2.0	Out	Entry (after 0.05 g)

* SCS attitude hold without pseudo-rate feedback is normally not recommended because of excessive propellant consumption.

4.4-34

MSC-07765 (Vol. I)

Table 4.4-13. Thrust Component Definitions (Pounds-Force)
 (See Paragraph 4.4.4.1.3.1)

$A_{3x} = A_3 \cos \alpha$	$B_{3x} = B_3 \cos \alpha$
$A_{3y} = A_3 \sin \alpha \sin \beta$	$B_{3y} = B_3 \sin \alpha \cos \beta$
$A_{3z} = A_3 \sin \alpha \cos \beta$	$B_{3z} = B_3 \sin \alpha \sin \beta$
$A_{2x} = 0$	$B_{2x} = 0$
$A_{2y} = A_2 \cos (\alpha+\beta)$	$B_{2y} = B_2 \sin (\alpha+\beta)$
$A_{2z} = A_2 \sin (\alpha+\beta)$	$B_{2z} = B_2 \cos (\alpha+\beta)$
$A_{4x} = A_4 \cos \alpha$	$B_{4x} = B_4 \cos \alpha$
$A_{4y} = A_4 \sin \alpha \sin \beta$	$B_{4y} = B_4 \sin \alpha \cos \beta$
$A_{4z} = A_4 \sin \alpha \cos \beta$	$B_{4z} = B_4 \sin \alpha \sin \beta$
$A_{1x} = 0$	$B_{1x} = 0$
$A_{1y} = A_1 \cos (\alpha-\beta)$	$B_{1y} = B_1 \sin (\alpha-\beta)$
$A_{1z} = A_1 \sin (\alpha-\beta)$	$B_{1z} = B_1 \cos (\alpha-\beta)$
$C_{4x} = C_4 \cos \alpha$	$D_{4x} = D_4 \cos \alpha$
$C_{4y} = C_4 \sin \alpha \sin \beta$	$D_{4y} = D_4 \sin \alpha \cos \beta$
$C_{4z} = C_4 \sin \alpha \cos \beta$	$D_{4z} = D_4 \sin \alpha \sin \beta$
$C_{2x} = 0$	$D_{2x} = 0$
$C_{2y} = C_2 \cos (\alpha+\beta)$	$D_{2y} = D_2 \sin (\alpha+\beta)$
$C_{2z} = C_2 \sin (\alpha+\beta)$	$D_{2z} = D_2 \cos (\alpha+\beta)$
$C_{3x} = C_3 \cos \alpha$	$D_{3x} = D_3 \cos \alpha$
$C_{3y} = C_3 \sin \alpha \sin \beta$	$D_{3y} = D_3 \sin \alpha \cos \beta$
$C_{3z} = C_3 \sin \alpha \cos \beta$	$D_{3z} = D_3 \sin \alpha \sin \beta$

Table 4.4-13. Thrust Component Definitions (Pounds-Force)
 (See Paragraph 4.4.4.1.3.1) (Concluded)

$C_{1x} = 0$	$D_{1x} = 0$
$C_{1y} = C_1 \cos (\alpha-\beta)$	$D_{1y} = D_1 \sin (\alpha-\beta)$
$C_{1z} = C_1 \sin (\alpha-\beta)$	$D_{1z} = D_1 \cos (\alpha-\beta)$

$$A_i = B_i = C_i = D_i = 102.8 \text{ lb force} \quad i = 1, 2, 3, \text{ and } 4$$

(nominal)

α = cant angle measured from the plane of the engine attach points (positive angle away from vehicle) = 10 deg

β = rotation of the reaction jet quad center with respect to the body reference system (positive rotation clockwise looking aft) = 7.25 deg

$\sin \alpha = 0.17365$	$\sin (\alpha+\beta) = 0.29654$
$\sin \beta = 0.12620$	$\sin (\alpha-\beta) = 0.04798$
$\cos \alpha = 0.98481$	$\cos (\alpha+\beta) = 0.95502$
$\cos \beta = 0.99200$	$\cos (\alpha-\beta) = 0.99885$

$$\sin \alpha \sin \beta = 0.021915$$

$$\sin \alpha \cos \beta = 0.17226$$

Table 4.4-14. Moment Arm Definition (Ft)
 (See Paragraph 4.4.4.1.3.1)

$l_{Az} = l \cos \beta + Z_{cg}$	$l_{Ay} = l \sin \beta + Y_{cg}$
$l_{Bz} = l \sin \beta + Z_{cg}$	$l_{By} = l \cos \beta - Y_{cg}$
$l_{Cz} = l \cos \beta - Z_{cg}$	$l_{Cy} = l \sin \beta - Y_{cg}$
$l_{Dz} = l \sin \beta - Z_{cg}$	$l_{Dy} = l \cos \beta + Y_{cg}$
$l_{A_2z} = l_{Az} + K \sin \beta$	$l_{A_2y} = l_{Ay} - K \cos \beta$
$l_{A_1z} = l_{Az} - K \sin \beta$	$l_{A_1y} = l_{Ay} + K \cos \beta$
$l_{B_2z} = l_{Bz} - K \cos \beta$	$l_{B_2y} = l_{By} + K \sin \beta$
$l_{B_1z} = l_{Bz} + K \cos \beta$	$l_{B_1y} = l_{By} - K \sin \beta$
$l_{C_2z} = l_{Cz} + K \sin \beta$	$l_{C_2y} = l_{Cy} - K \cos \beta$
$l_{C_1z} = l_{Cz} - K \sin \beta$	$l_{C_1y} = l_{Cy} + K \cos \beta$
$l_{D_2z} = l_{Dz} - K \cos \beta$	$l_{D_2y} = l_{Dy} + K \sin \beta$
$l_{D_1z} = l_{Dz} + K \cos \beta$	$l_{D_1y} = l_{Dy} - K \sin \beta$
$l_{x_1} = X_{cg} - X_{01}$	$l_{x_3} = X_{cg} - X_{03}$
$l_{x_2} = X_{cg} - X_{02}$	$l_{x_4} = X_{cg} - X_{04}$

Table 4.4-14. Moment Arm Definition (See Paragraph
4.4.4.1.3.1) (Concluded)

-
- ℓ - radial distance to reaction jet attach point plane = 6.9633 feet
(83.56 in.)
- β - rotation of reaction jet quad center = 7.25° ($\sin \beta = 0.12620$,
 $\cos \beta = 0.99220$)
- K - half the circumferential distance between the attach points of the
roll jets - 0.2604 ft (3.125 in.)
- X_{01} - location of the plane containing minus X translation thruster
(A3, B3, C4, D4) attach point = 80.47667 ft (station 965.72)
- X_{02} - location of the plane containing minus roll thruster (A2, B2, C2, D2)
attach points = 79.9925 ft (station 959.91)
- X_{03} - location of the plane containing plus X translation thruster (A4,
B4, C3, D3) attach points = 79.35167 ft (station 952.22)
- X_{04} - location of the plane containing plus roll thruster (A1, B1, C1, D1)
attach points = 79.83583 ft (station 958.03)
- X_{cg} - x center of gravity (ft)
- Y_{cg} - y center of gravity (ft)
- Z_{cg} - z center of gravity (ft)

The above stations are in the Apollo reference system as shown in Section 2,
Configuration.

Table 4.4-15. CSM Moment Equations
(See Paragraph 4.4.4.1.3.2)

ROLL MOMENTS

$$\begin{aligned}
 A1 & A1 \left\{ \cos(\alpha-\beta) [\ell \cos\beta - K \sin\beta + Z_{cg}] - \sin(\alpha-\beta) [\ell \sin\beta + K \cos\beta + Y_{cg}] \right\} \\
 A2 & A2 \left\{ -\cos(\alpha+\beta) [\ell \cos\beta + K \sin\beta + Z_{cg}] - \sin(\alpha+\beta) [\ell \sin\beta - K \cos\beta + Y_{cg}] \right\} \\
 A3 & A3 [\sin\alpha (Z_{cg} \sin\beta - Y_{cg} \cos\beta)] \\
 A4 & A4 [\sin\alpha (Z_{cg} \sin\beta - Y_{cg} \cos\beta)] \\
 B1 & B1 \left\{ \cos(\alpha-\beta) [\ell \cos\beta - K \sin\beta - Y_{cg}] - \sin(\alpha-\beta) [\ell \sin\beta + K \cos\beta + Z_{cg}] \right\} \\
 B2 & B2 \left\{ -\cos(\alpha+\beta) [\ell \cos\beta + K \sin\beta - Y_{cg}] - \sin(\alpha+\beta) [\ell \sin\beta - K \cos\beta + Z_{cg}] \right\} \\
 B3 & B3 [-\sin\alpha (Y_{cg} \sin\beta + Z_{cg} \cos\beta)] \\
 B4 & B4 [-\sin\alpha (Y_{cg} \sin\beta + Z_{cg} \cos\beta)] \\
 C1 & C1 \left\{ \cos(\alpha-\beta) [\ell \cos\beta - K \sin\beta - Z_{cg}] - \sin(\alpha-\beta) [\ell \sin\beta + K \cos\beta - Y_{cg}] \right\} \\
 C2 & C2 \left\{ -\cos(\alpha+\beta) [\ell \cos\beta + K \sin\beta - Z_{cg}] - \sin(\alpha+\beta) [\ell \sin\beta - K \cos\beta - Y_{cg}] \right\} \\
 C3 & C3 [\sin\alpha (Y_{cg} \cos\beta - Z_{cg} \sin\beta)] \\
 C4 & C4 [\sin\alpha (Y_{cg} \cos\beta - Z_{cg} \sin\beta)] \\
 D1 & D1 \left\{ \cos(\alpha-\beta) [\ell \cos\beta - K \sin\beta + Y_{cg}] - \sin(\alpha-\beta) [\ell \sin\beta + K \cos\beta - Z_{cg}] \right\} \\
 D2 & D2 \left\{ -\cos(\alpha+\beta) [\ell \cos\beta + K \sin\beta + Y_{cg}] - \sin(\alpha+\beta) [\ell \sin\beta - K \cos\beta - Z_{cg}] \right\} \\
 D3 & D3 [\sin\alpha (Y_{cg} \sin\beta + Z_{cg} \cos\beta)] \\
 D4 & D4 [\sin\alpha (Y_{cg} \sin\beta + Z_{cg} \cos\beta)]
 \end{aligned}$$

ℓ	= 6.9633 ft.	$\sin \alpha$	= 0.17365	$\sin (\alpha+\beta)$	= 0.29654
K	= 0.2604 ft	$\sin \beta$	= 0.12620	$\sin (\alpha-\beta)$	= 0.04798
X_{01}	= 80.47667 ft	$\cos \alpha$	= 0.98481	$\cos (\alpha+\beta)$	= 0.95502
X_{02}	= 79.9925 ft	$\cos \beta$	= 0.99200	$\cos (\alpha-\beta)$	= 0.99885
X_{03}	= 79.35167 ft				
X_{04}	= 79.83583 ft	$\sin \alpha \sin \beta$	= 0.021915		
		$\sin \alpha \cos \beta$	= 0.17226		

Table 4.4-15. CSM Moment Equations (See Paragraph
4.4.4.1.3.2) (Concluded)

PITCH MOMENTS

A1	$A1[\sin(\alpha-\beta)(X_{cg}-X_{04})]$
A2	$A2[\sin(\alpha+\beta)(X_{cg}-X_{02})]$
A3	$A3[\cos\alpha(\ell\cos\beta+Z_{cg})+\sin\alpha\cos\beta(X_{cg}-X_{01})]$
A4	$A4[\sin\alpha\cos\beta(X_{cg}-X_{03})-\cos\alpha(\ell\cos\beta+Z_{cg})]$
B1	$B1[\cos(\alpha-\beta)(X_{cg}-X_{04})]$
B2	$B2[-\cos(\alpha+\beta)(X_{cg}-X_{02})]$
B3	$B3[\cos\alpha(\ell\sin\beta+Z_{cg})+\sin\alpha\sin\beta(X_{cg}-X_{01})]$
B4	$B4[-\cos\alpha(\ell\sin\beta+Z_{cg})+\sin\alpha\sin\beta(X_{cg}-X_{03})]$
C1	$C1[-\sin(\alpha-\beta)(X_{cg}-X_{04})]$
C2	$C2[-\sin(\alpha+\beta)(X_{cg}-X_{02})]$
C3	$C3[\cos\alpha(\ell\cos\beta-Z_{cg})-\sin\alpha\cos\beta(X_{cg}-X_{03})]$
C4	$C4[-\cos\alpha(\ell\cos\beta-Z_{cg})-\sin\alpha\cos\beta(X_{cg}-X_{01})]$
D1	$D1[-\cos(\alpha-\beta)(X_{cg}-X_{04})]$
D2	$D2[\cos(\alpha+\beta)(X_{cg}-X_{02})]$
D3	$D3[\cos\alpha(\ell\sin\beta-Z_{cg})-\sin\alpha\sin\beta(X_{cg}-X_{03})]$
D4	$D4[-\cos\alpha(\ell\sin\beta-Z_{cg})-\sin\alpha\sin\beta(X_{cg}-X_{01})]$

YAW MOMENTS

A1	$A1[-\cos(\alpha-\beta)(X_{cg}-X_{04})]$
A2	$A2[\cos(\alpha+\beta)(X_{cg}-X_{02})]$
A3	$A3[-\cos\alpha(\ell\sin\beta+Y_{cg})-\sin\alpha\sin\beta(X_{cg}-X_{01})]$
A4	$A4[\cos\alpha(\ell\sin\beta+Y_{cg})-\sin\alpha\sin\beta(X_{cg}-X_{03})]$
B1	$B1[\sin(\alpha-\beta)(X_{cg}-X_{04})]$
B2	$B2[\sin(\alpha+\beta)(X_{cg}-X_{02})]$
B3	$B3[\cos\alpha(\ell\cos\beta-Y_{cg})+\sin\alpha\cos\beta(X_{cg}-X_{01})]$
B4	$B4[\sin\alpha\cos\beta(X_{cg}-X_{03})-\cos\alpha(\ell\cos\beta-Y_{cg})]$
C1	$C1[\cos(\alpha-\beta)(X_{cg}-X_{04})]$
C2	$C2[-\cos(\alpha+\beta)(X_{cg}-X_{02})]$
C3	$C3[\sin\alpha\sin\beta(X_{cg}-X_{03})-\cos\alpha(\ell\sin\beta-Y_{cg})]$
C4	$C4[\cos\alpha(\ell\sin\beta-Y_{cg})+\sin\alpha\sin\beta(X_{cg}-X_{01})]$
D1	$D1[-\sin(\alpha-\beta)(X_{cg}-X_{04})]$
D2	$D2[-\sin(\alpha+\beta)(X_{cg}-X_{02})]$
D3	$D3[\cos\alpha(\ell\cos\beta+Y_{cg})-\sin\alpha\cos\beta(X_{cg}-X_{03})]$
D4	$D4[-\cos\alpha(\ell\cos\beta+Y_{cg})-\sin\alpha\cos\beta(X_{cg}-X_{01})]$

Table 4.4-16. SM RCS Control Forces and Moments
(See Paragraph 4.4.4.1.4)

TBS

Table 4.4-17. SM RCS Control Forces and Moments
(See Paragraph 4.4.4.1.4)

TBS

Table 4.4-18. SM RCS Control Forces and Moments
(See Paragraph 4.4.4.1.4)

TBS

Table 4.4-19. SM RCS Control Forces and Moments
(See Paragraph 4.4.4.1.4)

TBS

Table 4.4-20. SM RCS Control Forces and Moments
(See Paragraph 4.4.4.1.4)

TBS

Table 4.4-21. Fixed Parameters for CM RCS Moments
(See Paragraph 4.4.4.2.3)

NR Engine Number	NASA Engine Number	Control Axis	X_C (ft)	Y_C (ft)	Z_C (ft)	β (deg)	γ (deg)	α (deg)	μ (deg)	λ (deg)	ρ (deg)
1	13	+ Pitch	2.3063	0.3684	-6.0237	3.50	47.0	47.0533	-	-	-
2	14	- Pitch	7.0933	0.3274	-2.9645	-	-	-	-	-	6.3025
3	23	+ Pitch	2.3063	-0.3684	-6.0237	3.50	47.0	47.0533	-	-	-
4	24	- Pitch	7.0933	-0.3274	-2.9645	-	-	-	-	-	6.3025
5	15	+ Yaw	2.3063	6.0237	-0.3684	3.50	47.0	47.0533	-	-	-
6	26	- Yaw	2.3063	-6.0237	-0.3684	3.50	47.0	47.0533	-	-	-
7	25	+ Yaw	2.3063	6.0237	0.3684	3.50	47.0	47.0533	-	-	-
8	16	- Yaw	2.3063	-6.0237	0.3684	3.50	47.0	47.0533	-	-	-
9	11	+ Roll	2.6917	4.3319	-4.1955	-	-	-	79.5421	-	-
10	22	- Roll	2.6917	-4.3319	-4.1955	-	-	-	79.5421	-	-
11	21	+ Roll	2.6917	-4.3319	-4.1955	-	-	-	-	87.6806	-
12	12	- Roll	2.6917	4.3319	-4.1955	-	-	-	-	87.6806	-

4.4-46

MSC-07765 (Vol. I)

Table 4.4-22. CM RCS Force Equations
(See Paragraph 4.4.4.2.3)

<u>Forces Along X-Body Axis</u>	<u>Forces Along Y-Body Axis</u>
$F_{x13} = -FS(\gamma - \Delta\theta_1)$	$F_{y13} = -FC(\gamma - \Delta\theta_1)S(\beta)$
$F_{x14} = -FS(\Delta\theta_2)$	$F_{y14} = -FC(\Delta\theta_2)S(\rho)$
$F_{x23} = -FS(\gamma - \Delta\theta_1)$	$F_{y23} = +FC(\gamma - \Delta\theta_1)S(\beta)$
$F_{x24} = -FS(\Delta\theta_2)$	$F_{y24} = +FC(\Delta\theta_2)S(\rho)$
$F_{x15} = -FS(\gamma - \Delta\psi)$	$F_{y15} = -FC(\gamma - \Delta\psi)C(\beta)$
$F_{x26} = -FS(\gamma - \Delta\psi)$	$F_{y26} = +FC(\gamma - \Delta\psi)C(\beta)$
$F_{x25} = -FS(\gamma - \Delta\psi)$	$F_{y25} = -FC(\gamma - \Delta\psi)C(\beta)$
$F_{x16} = -FS(\gamma - \Delta\psi)$	$F_{y16} = +FC(\gamma - \Delta\psi)C(\beta)$
$F_{x11} = -FS(\Delta\phi_1)S(32.5^\circ)$	$F_{y11} = +F [C(\Delta\phi_1)C(\mu) - S(\Delta\phi_1)S(\mu)C(32.5^\circ)]$
$F_{x22} = -FS(\Delta\phi_1)S(32.5^\circ)$	$F_{y22} = -F [C(\Delta\phi_1)C(\mu) - S(\Delta\phi_1)S(\mu)C(32.5^\circ)]$
$F_{x21} = -FS(\Delta\phi_2)S(32.5^\circ)$	$F_{y21} = +F [C(\Delta\phi_2)S(\lambda) + S(\Delta\phi_2)C(\lambda)C(32.5^\circ)]$
$F_{x12} = -FS(\Delta\phi_2)S(32.5^\circ)$	$F_{y12} = -F [C(\Delta\phi_2)S(\lambda) + S(\Delta\phi_2)C(\lambda)C(32.5^\circ)]$
<u>Forces Along Z-Body Axis</u>	
$F_{z13} = +FC(\gamma - \Delta\theta_1)C(\beta)$	<p>NOTE:</p> <p>F \equiv Engine Thrust Value</p> <p>C \equiv Cosine</p> <p>S \equiv Sine</p>
$F_{z14} = +FC(\Delta\theta_2)C(\rho)$	
$F_{z23} = +FC(\gamma - \Delta\theta_1)C(\beta)$	
$F_{z24} = +FC(\Delta\theta_2)C(\rho)$	
$F_{z15} = +FC(\gamma - \Delta\psi)S(\beta)$	
$F_{z26} = +FC(\gamma - \Delta\psi)S(\beta)$	
$F_{z25} = -FC(\gamma - \Delta\psi)S(\beta)$	
$F_{z16} = -FC(\gamma - \Delta\psi)S(\beta)$	
$F_{z11} = +F [C(\Delta\phi_1)S(\mu) + S(\Delta\phi_1)C(\mu)C(32.5^\circ)]$	
$F_{z22} = +F [C(\Delta\phi_1)S(\mu) + S(\Delta\phi_1)C(\mu)C(32.5^\circ)]$	
$F_{z21} = -F [C(\Delta\phi_2)C(\lambda) - S(\Delta\phi_2)S(\lambda)C(32.5^\circ)]$	
$F_{z12} = -F [C(\Delta\phi_2)C(\lambda) - S(\Delta\phi_2)S(\lambda)C(32.5^\circ)]$	

Table 4.4-23. CM RCS Moment Arms
(See Paragraph 4.4.4.2.3)

$$l_{x13} = X_{13} - X_{cg} + \Delta X_{13}$$

$$l_{x14} = X_{14} - X_{cg} + \Delta X_{14}$$

$$l_{x23} = X_{23} - X_{cg} + \Delta X_{23}$$

$$l_{x24} = X_{24} - X_{cg} + \Delta X_{24}$$

$$l_{x15} = X_{15} - X_{cg} + \Delta X_{15}$$

$$l_{x26} = X_{26} - X_{cg} + \Delta X_{26}$$

$$l_{x25} = X_{25} - X_{cg} + \Delta X_{25}$$

$$l_{x16} = X_{16} - X_{cg} + \Delta X_{16}$$

$$l_{x11} = X_{11} - X_{cg} + \Delta X_{11}$$

$$l_{x22} = X_{22} - X_{cg} + \Delta X_{22}$$

$$l_{x21} = X_{21} - X_{cg} + \Delta X_{21}$$

$$l_{x12} = X_{12} - X_{cg} + \Delta X_{12}$$

$$l_{y13} = Y_{13} - Y_{cg} + \Delta Y_{13}$$

$$l_{y14} = Y_{14} - Y_{cg} + \Delta Y_{14}$$

$$l_{y23} = Y_{23} - Y_{cg} + \Delta Y_{23}$$

$$l_{y24} = Y_{24} - Y_{cg} + \Delta Y_{24}$$

$$l_{y15} = Y_{15} - Y_{cg} + \Delta Y_{15}$$

$$l_{y26} = Y_{26} - Y_{cg} + \Delta Y_{26}$$

$$l_{y25} = Y_{25} - Y_{cg} + \Delta Y_{25}$$

$$l_{y16} = Y_{16} - Y_{cg} + \Delta Y_{16}$$

$$l_{y11} = Y_{11} - Y_{cg} + \Delta Y_{11}$$

$$l_{y22} = Y_{22} - Y_{cg} + \Delta Y_{22}$$

$$l_{y21} = Y_{21} - Y_{cg} + \Delta Y_{21}$$

$$l_{y12} = Y_{12} - Y_{cg} + \Delta Y_{12}$$

$$l_{z13} = Z_{13} - Z_{cg} + \Delta Z_{13}$$

$$l_{z14} = Z_{14} - Z_{cg} + \Delta Z_{14}$$

$$l_{z23} = Z_{23} - Z_{cg} + \Delta Z_{23}$$

$$l_{z24} = Z_{24} - Z_{cg} + \Delta Z_{24}$$

$$l_{z15} = Z_{15} - Z_{cg} + \Delta Z_{15}$$

$$l_{z26} = Z_{26} - Z_{cg} + \Delta Z_{26}$$

$$l_{z25} = Z_{25} - Z_{cg} + \Delta Z_{25}$$

$$l_{z16} = Z_{16} - Z_{cg} + \Delta Z_{16}$$

$$l_{z11} = Z_{11} - Z_{cg} + \Delta Z_{11}$$

$$l_{z22} = Z_{22} - Z_{cg} + \Delta Z_{22}$$

$$l_{z21} = Z_{21} - Z_{cg} + \Delta Z_{21}$$

$$l_{z12} = Z_{12} - Z_{cg} + \Delta Z_{12}$$

NOTE:

X_i \equiv X location of engine No. i

Y_i \equiv Y location of engine No. i

Z_i \equiv Z location of engine No. i

X_{cg} \equiv X center of gravity

Y_{cg} \equiv Y center of gravity

Z_{cg} \equiv Z center of gravity

Table 4.4-24. Delta Moment Arms
(See Paragraph 4.4.4.2.3)

$\Delta X_{13} = \Delta l_{pp} S(\gamma)$	$\Delta Y_{13} = \Delta l_{pp} C(\gamma) S(\beta)$
$\Delta X_{14} = 0.0$	$\Delta Y_{14} = \Delta l_{np} S(\rho)$
$\Delta X_{23} = \Delta l_{pp} S(\gamma)$	$\Delta Y_{23} = -\Delta l_{pp} C(\gamma) S(\beta)$
$\Delta X_{24} = 0.0$	$\Delta Y_{24} = -\Delta l_{np} S(\rho)$
$\Delta X_{15} = \Delta l_{yaw} S(\gamma)$	$\Delta Y_{15} = \Delta l_{yaw} C(\gamma) C(\beta)$
$\Delta X_{26} = \Delta l_{yaw} S(\gamma)$	$\Delta Y_{26} = -\Delta l_{yaw} C(\gamma) C(\beta)$
$\Delta X_{25} = \Delta l_{yaw} S(\gamma)$	$\Delta Y_{25} = \Delta l_{yaw} C(\gamma) C(\beta)$
$\Delta X_{16} = \Delta l_{yaw} S(\gamma)$	$\Delta Y_{16} = -\Delta l_{yaw} C(\gamma) C(\beta)$
$\Delta X_{11} = 0.0$	$\Delta Y_{11} = -\Delta l_{lr} C(\mu)$
$\Delta X_{22} = 0.0$	$\Delta Y_{22} = \Delta l_{lr} C(\mu)$
$\Delta X_{21} = 0.0$	$\Delta Y_{21} = -\Delta l_{sr} S(\lambda)$
$\Delta X_{12} = 0.0$	$\Delta Y_{12} = \Delta l_{sr} S(\lambda)$
$\Delta Z_{13} = -\Delta l_{pp} C(\gamma) C(\beta)$	
$\Delta Z_{14} = -\Delta l_{np} C(\rho)$	
$\Delta Z_{23} = -\Delta l_{pp} C(\gamma) C(\beta)$	
$\Delta Z_{24} = -\Delta l_{np} C(\rho)$	
$\Delta Z_{15} = -\Delta l_{yaw} C(\gamma) S(\beta)$	
$\Delta Z_{26} = -\Delta l_{yaw} C(\gamma) S(\beta)$	
$\Delta Z_{25} = \Delta l_{yaw} C(\gamma) S(\beta)$	
$\Delta Z_{16} = \Delta l_{yaw} C(\gamma) S(\beta)$	
$\Delta Z_{11} = -\Delta l_{lr} S(\mu)$	
$\Delta Z_{22} = -\Delta l_{lr} S(\mu)$	
$\Delta Z_{21} = \Delta l_{sr} C(\lambda)$	
$\Delta Z_{12} = \Delta l_{sr} C(\lambda)$	

Table 4.4-25. CM RCS Moment Equations
(See Paragraph 4.4.4.2.3)

$$\begin{aligned}
 L_{13} &= FC(47-\Delta\theta_1) [-0.99813Y_{cg}-0.06105Z_{cg}] \\
 L_{14} &= FC(\Delta\theta_2) [-0.99396Y_{cg}-0.10973Z_{cg}] \\
 L_{23} &= FC(47-\Delta\theta_1) [-0.99813Y_{cg}+0.06105Z_{cg}] \\
 L_{24} &= FC(\Delta\theta_2) [-0.99396Y_{cg}+0.10973Z_{cg}] \\
 L_{15} &= FC(47-\Delta\psi) [-0.06105Y_{cg}-0.99813Z_{cg}] \\
 L_{26} &= FC(47-\Delta\psi) [-0.06105Y_{cg}+0.99813Z_{cg}] \\
 L_{25} &= FC(47-\Delta\psi) [0.06105Y_{cg}-0.99813Z_{cg}] \\
 L_{16} &= FC(47-\Delta\psi) [0.06105Y_{cg}+0.99813Z_{cg}] \\
 L_{11} &= F [C(\Delta\phi_1) (5.02159-0.98338Y_{cg}+0.18155Z_{cg}) \\
 &\quad +S(\Delta\phi_1) (-2.81632-0.84339\Delta l_{lr}-0.15312Y_{cg}-0.82937Z_{cg})] \\
 L_{22} &= F [C(\Delta\phi_1) (-5.02159-0.98338Y_{cg}-0.18155Z_{cg}) \\
 &\quad +S(\Delta\phi_1) (2.81632+0.84339\Delta l_{lr}-0.15312Y_{cg}+0.82937Z_{cg})] \\
 L_{21} &= F [C(\Delta\phi_2) (4.36742+0.04048Y_{cg}+0.99918Z_{cg}) \\
 &\quad +S(\Delta\phi_2) (-3.50726-0.85583\Delta l_{sr}-0.8427Y_{cg}+0.03414Z_{cg})] \\
 L_{12} &= F [C(\Delta\phi_2) (-4.36742+0.04048Y_{cg}-0.99918Z_{cg}) \\
 &\quad +S(\Delta\phi_2) (3.50726+0.85583\Delta l_{sr}-0.8427Y_{cg}-0.03414Z_{cg})] \\
 \\
 M_{13} &= F [S(47-\Delta\theta_1) (6.0237+0.68072\Delta l_{pp}+Z_{cg}) \\
 &\quad -C(47-\Delta\theta_1) (2.30199+0.72998\Delta l_{pp}-0.99813X_{cg})] \\
 M_{14} &= F [S(\Delta\theta_2) (2.9647+0.99396\Delta l_{np}+Z_{cg}) \\
 &\quad -C(\Delta\theta_2) (7.05046-0.99396X_{cg})] \\
 M_{23} &= F [S(47-\Delta\theta_1) (6.0237+0.68072\Delta l_{pp}+Z_{cg}) \\
 &\quad -C(47-\Delta\theta_1) (2.30199+0.72998\Delta l_{pp}-0.99813X_{cg})] \\
 M_{24} &= F [S(\Delta\theta_2) (2.9647+0.99396\Delta l_{np}+Z_{cg}) \\
 &\quad -C(\Delta\theta_2) (7.05046-0.99396X_{cg})] \\
 M_{15} &= F [S(47-\Delta\psi) (0.3684+0.04164\Delta l_{yaw}+Z_{cg}) \\
 &\quad -C(47-\Delta\psi) (0.1408+0.04465\Delta l_{yaw}-0.06105X_{cg})] \\
 M_{26} &= F [S(47-\Delta\psi) (0.3684+0.04164\Delta l_{yaw}+Z_{cg}) \\
 &\quad -C(47-\Delta\psi) (0.1408+0.04465\Delta l_{yaw}-0.06105X_{cg})]
 \end{aligned}$$

Table 4.4-25. CM RCS Moment Equations (See Paragraph 4.4.4.2.3) (Continued)

$$M_{25} = F [S(47-\Delta\psi)(-0.3684-0.04164\Delta l_{yaw}^{+Z_{cg}}) + C(47-\Delta\psi)(0.1408+0.04465\Delta l_{yaw}^{-0.06105X_{cg}})]$$

$$M_{16} = F [S(47-\Delta\psi)(-0.3684-0.04164\Delta l_{yaw}^{+Z_{cg}}) + C(47-\Delta\psi)(0.1408+0.04465\Delta l_{yaw}^{-0.06105X_{cg}})]$$

$$M_{11} = F [S(\Delta\phi_1)(1.84209+0.52837\Delta l_{lr}^{+0.5373Z_{cg}+0.15312X_{cg}}) - C(\Delta\phi_1)(2.64696-0.98338X_{cg})]$$

$$M_{22} = F [S(\Delta\phi_1)(1.84209+0.52837\Delta l_{lr}^{+0.5373Z_{cg}+0.15312X_{cg}}) - C(\Delta\phi_1)(2.64696-0.98338X_{cg})]$$

$$M_{21} = F [S(\Delta\phi_2)(-0.01406-0.02175\Delta l_{sr}^{+0.5373Z_{cg}+0.8427X_{cg}}) + C(\Delta\phi_2)(0.10896-0.04048X_{cg})]$$

$$M_{12} = F [S(\Delta\phi_2)(-0.01406-0.02175\Delta l_{sr}^{+0.5373Z_{cg}+0.8427X_{cg}}) + C(\Delta\phi_2)(0.10896-0.04048X_{cg})]$$

$$N_{13} = F [C(47-\Delta\theta_1)(-0.14080-0.04465\Delta l_{pp}^{+0.06105X_{cg}}) + S(47-\Delta\theta_1)(0.3684+0.04164\Delta l_{pp}^{-Y_{cg}})]$$

$$N_{14} = F [C(\Delta\theta_2)(-0.77835+0.10973X_{cg}) + S(\Delta\theta_2)(0.3274+0.10973\Delta l_{np}^{-Y_{cg}})]$$

$$N_{23} = F [C(47-\Delta\theta_1)(0.14080+0.04465\Delta l_{pp}^{-0.06105X_{cg}}) - S(47-\Delta\theta_1)(0.3684+0.04164\Delta l_{pp}^{+Y_{cg}})]$$

$$N_{24} = F [C(\Delta\theta_2)(.77835-0.10973X_{cg}) - S(\Delta\theta_2)(0.3274+0.10973\Delta l_{np}^{+Y_{cg}})]$$

$$N_{15} = F [C(47-\Delta\psi)(-2.30199-0.72998\Delta l_{yaw}^{+0.99813X_{cg}}) + S(47-\Delta\psi)(6.0237+0.68072\Delta l_{yaw}^{-Y_{cg}})]$$

$$N_{26} = F [C(47-\Delta\psi)(2.30199+0.72998\Delta l_{yaw}^{-0.99813X_{cg}}) - S(47-\Delta\psi)(6.0237+0.68072\Delta l_{yaw}^{+Y_{cg}})]$$

$$N_{25} = F [C(47-\Delta\psi)(-2.30199-0.72998\Delta l_{yaw}^{+0.99813X_{cg}}) + S(47-\Delta\psi)(6.0237+0.68072\Delta l_{yaw}^{-Y_{cg}})]$$

$$N_{16} = F [C(47-\Delta\psi)(2.30199+0.72998\Delta l_{yaw}^{-0.99813X_{cg}}) - S(47-\Delta\psi)(6.0237+0.68072\Delta l_{yaw}^{+Y_{cg}})]$$

Table 4.4-25. CM RCS Moment Equation (See Paragraph 4.4.4.2.3) (Concluded)

$$N_{11} = F [C(\Delta\phi_1)(0.48868 - 0.18155X_{cg}) - S(\Delta\phi_1)(0.09511 - 0.09755\Delta l_{lr} + 0.82937X_{cg} - 0.5373Y_{cg})]$$

$$N_{22} = F [C(\Delta\phi_1)(-0.48868 + 0.18155X_{cg}) + S(\Delta\phi_1)(0.09511 + 0.09755\Delta l_{lr} - 0.82937X_{cg} - 0.5373Y_{cg})]$$

$$N_{21} = F [C(\Delta\phi_2)(2.68949 - 0.99918X_{cg}) + S(\Delta\phi_2)(-2.23564 - 0.53686\Delta l_{sr} - 0.03414X_{cg} - 0.5373Y_{cg})]$$

$$N_{12} = F [C(\Delta\phi_2)(-2.68949 + 0.99918X_{cg}) + S(\Delta\phi_2)(2.23564 + 0.53686\Delta l_{sr} + 0.03414X_{cg} - 0.5373Y_{cg})]$$

NOTE:

F ≡ Engine Thrust Value

C ≡ Cosine

S ≡ Sine

L_i ≡ Roll moment due to engine No. i

M_i ≡ Pitch moment due to engine No. i

N_i ≡ Yaw moment due to engine No. i

Table 4.4-26. CM RCS Control Forces and Moments
(See Paragraph 4.4.4.2.4)

TBS

Tables 4.4-27. CM RCS Control Forces and Moments
(See Paragraph 4.4.4.2.4)

TBS

Table 4.4-28. SPS Engine Gimbaling Capability
(See Paragraph 4.4.5.1)

CSM Weight (lb)	Actual Center-of-Gravity Angles*(deg)		Center-of-Gravity Gimbal Angles**(deg)		Nominal Maximum Gimbal Authority (deg)				Acceleration Coefficients* F _I /I (sec ⁻²)	
	Pitch	Yaw	Pitch	Yaw	Pitch		Yaw		Pitch	Yaw
					Positive	Negative	Positive	Negative		
30,141	-0.97	1.28	1.18	0.33	3.32	-5.68	4.17	-4.83	4.26	4.19
28,713	-0.94	1.07	1.21	0.12	3.29	-5.71	4.38	-4.62	4.66	4.65
27,705	-0.59	1.44	1.56	0.49	2.94	-6.06	4.01	-4.99	4.85	4.83
26,423	-0.57	1.26	1.58	0.31	2.92	-6.08	4.19	-4.81	5.49	5.53

*Based on preliminary mass properties and X-station thrust-application point of 833.2 inches in CSM coordinates

**Based on actuator installation biases as follows:

	<u>Pitch (deg)</u>	<u>Yaw (deg)</u>
Bias set in during installation	-1.50	0.00
Distortion due to firing	<u>-0.65</u>	<u>0.95</u>
Null angle of firing engine	-2.15	0.95
Nominal maximum gimbaling capability from the X-axis	2.35 to -6.65	5.45 to -3.55

4.4-55

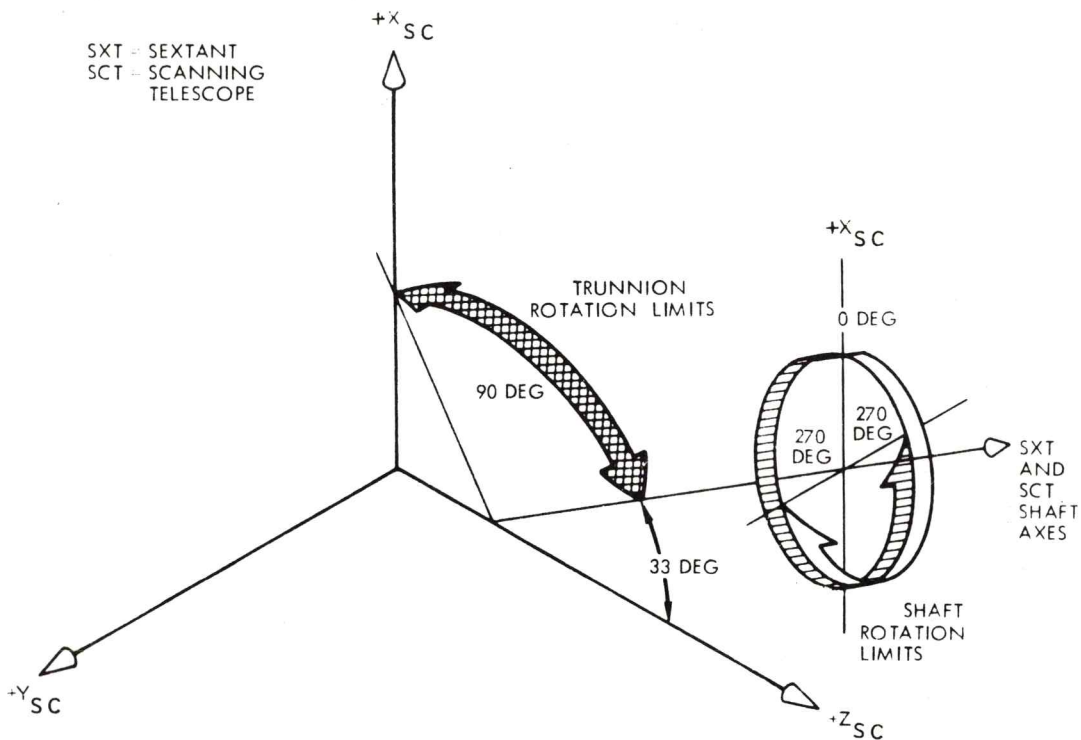
Table 4.4-29. Actuator Dynamics Data
(See Paragraph 4.4.5.2)

<u>Description</u>	<u>Value</u>	<u>Unit</u>
Servo amplifier gain	20	amps/rad
Actuator clutch gain		
Average	3635	ft-lb/amp
Range	1750 to 5280	ft-lb/amp
Position feedback gain	1.0	nondimensional
Rate feedback gain	0.09	sec
*Engine exhaust jet damping	171	ft-lb-sec/rad
*Hose stiffness	285	ft-lb/rad
*Snubber spring stiffness	23,000	ft-lb/deg
Engine inertia about gimbal axis		
Pitch	236.0	slug-ft ²
Yaw	245.0	slug-ft ²
Actuator inertia (reflected to engine)	65.1	slug-ft ²
Engine mass		
Pitch	20.5	slugs
Yaw	25.4	slugs
Engine moment arm (distance from c.g. to gimbal axis)		
Pitch	0.342	ft
Yaw	0.200	ft
Actuator internal spring constants	2,340,000	lb/ft
	195,000	lb/in
Spring constant external to actuator	531,600	lb/ft
	44,300	lb/in
		} pitch
Total actuator system stiffness	36,099 (pitch)	lb/in
	27,931 (yaw)	lb/in
Effective lever arm of actuator	0.988 (pitch)	ft
	1.0318 (yaw)	ft
Damping across engine bearings	686.0	ft-lb-sec

*These parameters were not used in the NR actuator simulation models because they were not considered to be dynamically significant.

Table 4.4-30. Actuator and CDU Limit Data
(See Paragraph 4.4.5.3)

<u>Description</u>	<u>Value</u>	<u>Unit</u>
Optics D/A limit (optics error counter)	384	pulse count
Scale factor: pulse count to gimbal angle command	1.42	arc min per pulse
Pulse train rate	3200	pulses/sec
Clutch torque limit	1800	ft-lb
Gimbal rate limit	0.15 nom. 0.12 min.	rad/sec rad/sec
Gimbal position limit	4.5	deg
Engine gimbal mounting offset-pitch	-2.15	deg
Engine gimbal mounting offset-yaw	0.95	deg



ROTATION LIMITS - SHAFT ANGLE $+270 \text{ DEG}$ $(-0, +10)$ to -270 DEG $(-10, +0)$
TRUNNION ANGLE 0 DEG $(+0, -10)$ to 90 DEG $(+10, -0)$

NOTES: SXT SHAFT AND TRUNNION MOTION IS LIMITED, AS GIVEN ABOVE, BY MECHANICAL STOPS.

WHEN THE SCT IS SLAVED TO THE SXT IN THE COMPUTER MODE, THE SXT LIMITS APPLY TO THE SCT.

FOR BOTH SXT AND SCT, THE TRUNNION AXIS IS PERPENDICULAR TO THE SHAFT AXIS.

THE SXT AND SCT SHAFT AXES ARE FIXED IN THE SPACECRAFT X-Z PLANE AT 33 DEG ABOVE THE SPACECRAFT Z-AXIS (PERPENDICULAR TO THE NAVIGATION BASE AND SPACECRAFT EXTERIOR) AND DEFINE THE LANDMARK LINE OF SIGHT (LLOS).

IN THE "ZERO OPTICS MODE", BOTH THE SXT AND SCT TRUNNION AXES ARE PARALLEL TO THE SPACECRAFT Y-AXIS, THE STAR LINE OF SIGHT (SLOS) IS COINCIDENT WITH THE LLOS, AND BOTH THE SXT AND SCT SHAFT AXES ARE AT 0 DEG ROTATION.

Figure 4.4-1. CM Optics Rotation Limits
(See Paragraph 4.4.1.3)

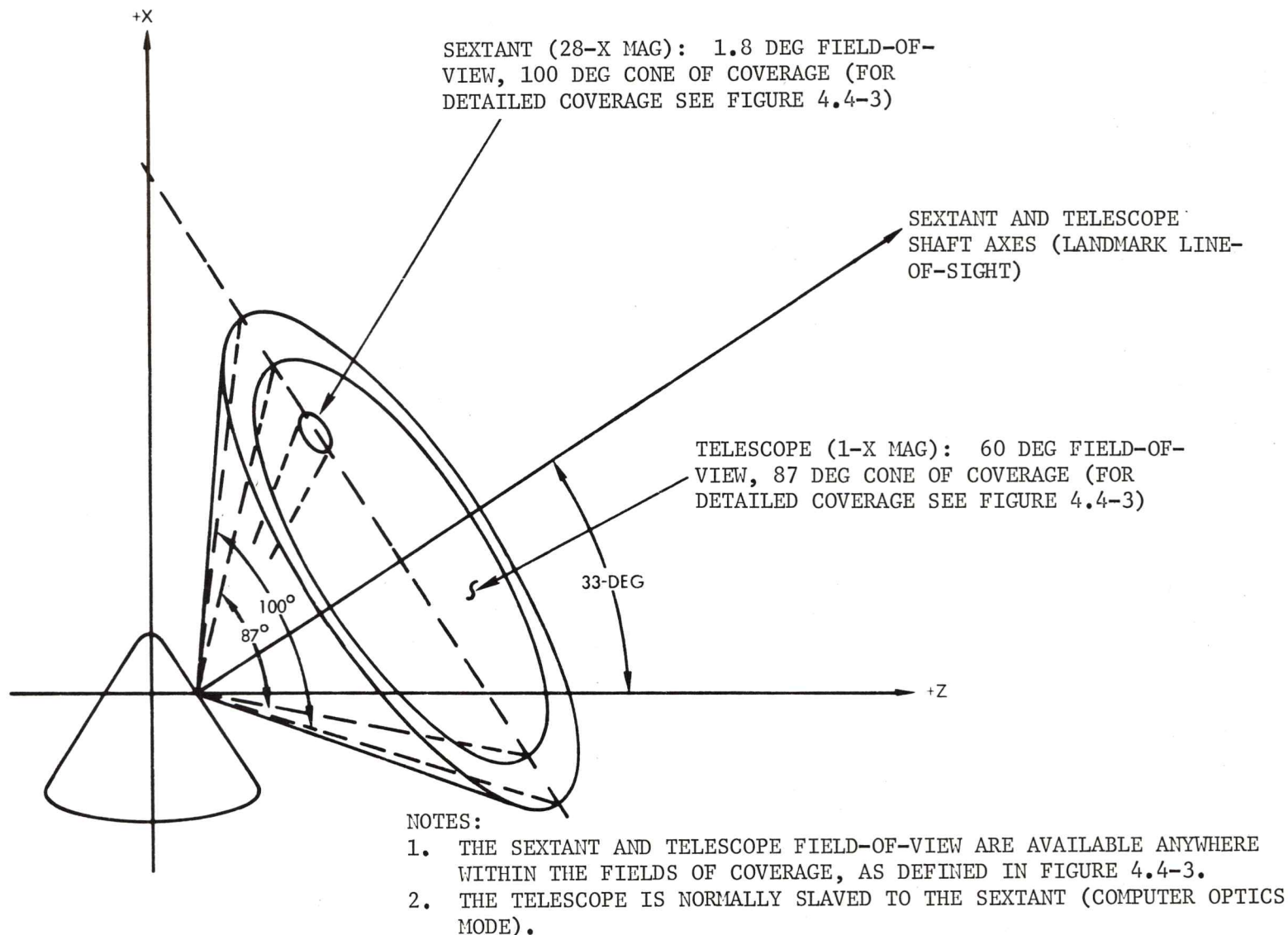
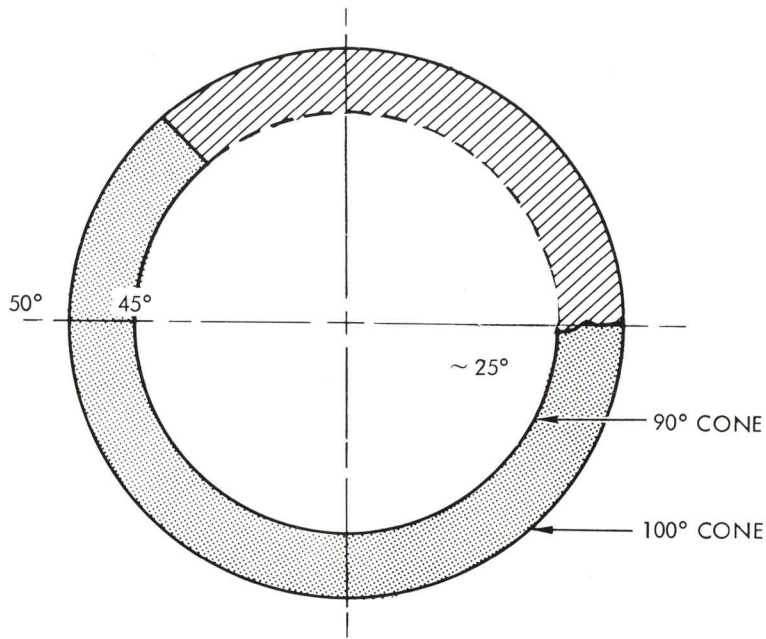
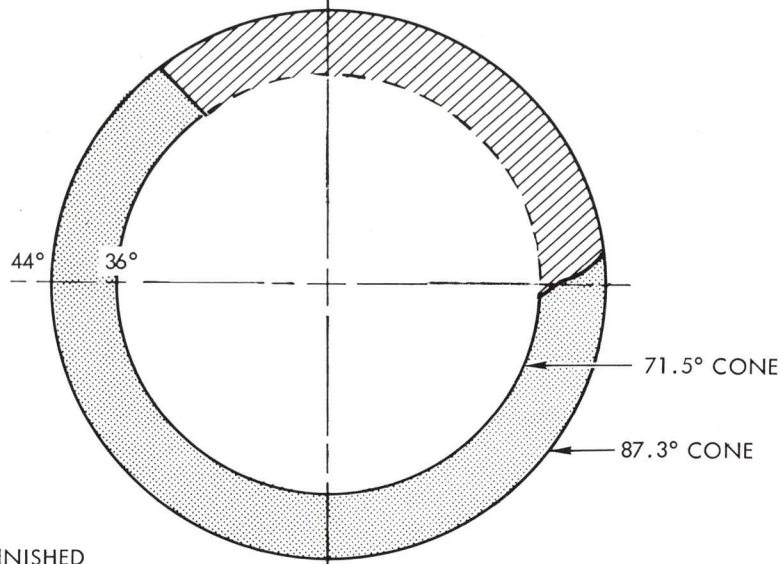


Figure 4.4-2. General Command Module Optics Field of Coverage
(See Paragraph 4.4.1.3.3.1)



(b) SEXTANT



(a) SCANNING TELESCOPE

AREA OF DIMINISHED
BRIGHTNESS DUE TO
VIGNETTING

Figure 4.4-3. Command Module Optics Coverage
(See Paragraph 4.4.1.3.3.1)

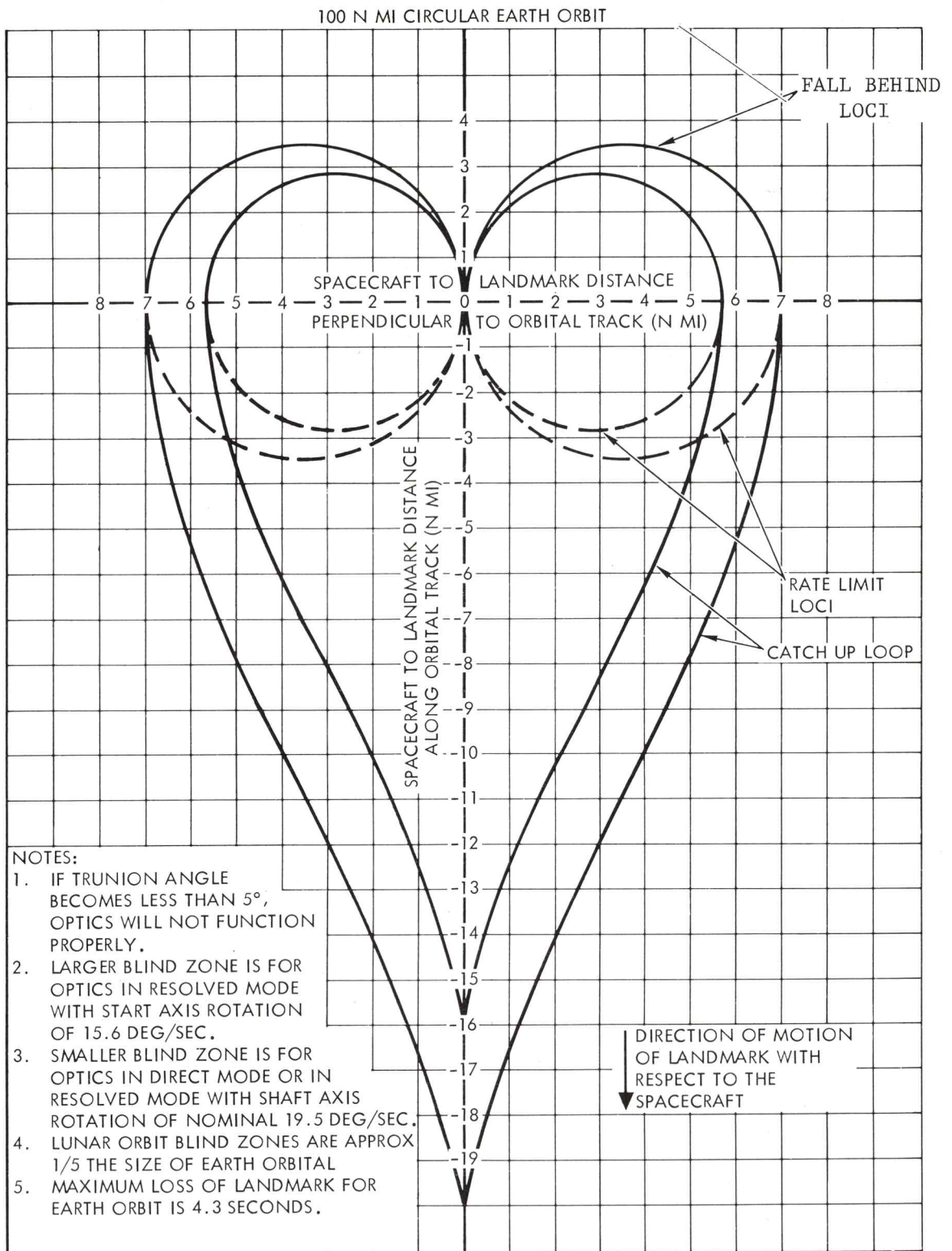


Figure 4.4-4. Scanning Telescope Optics Blind Zone
(See Paragraph 4.4.1.3.4)

4.4-62

MSC-07765 (Vol. 1)

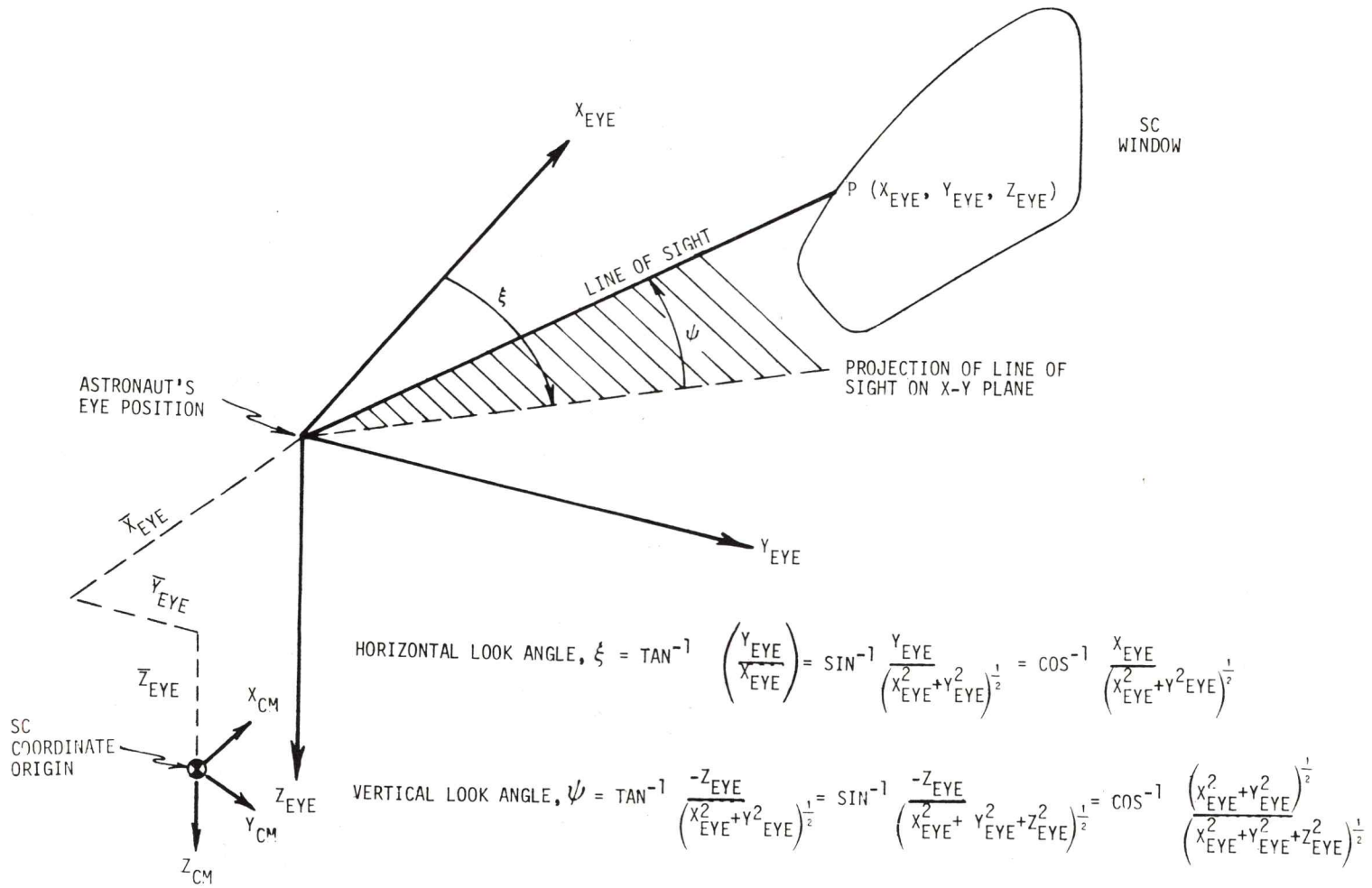


Figure 4.4-5. Look Angle Definition (No Scale)
(See Paragraph 4.4.1.3.6)

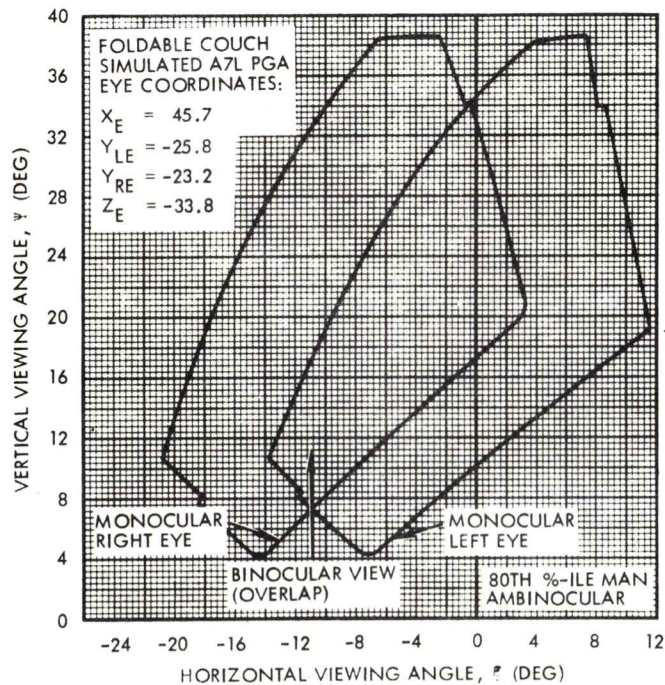
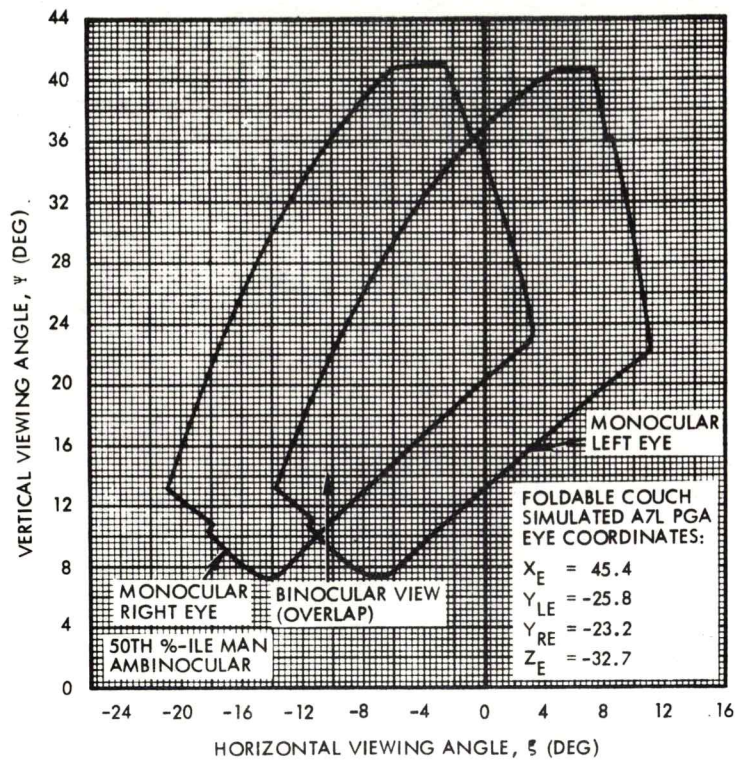


Figure 4.4-6. Crewman's FOV Through Left-Hand Rendezvous Window
(See Paragraph 4.4.1.3.6)

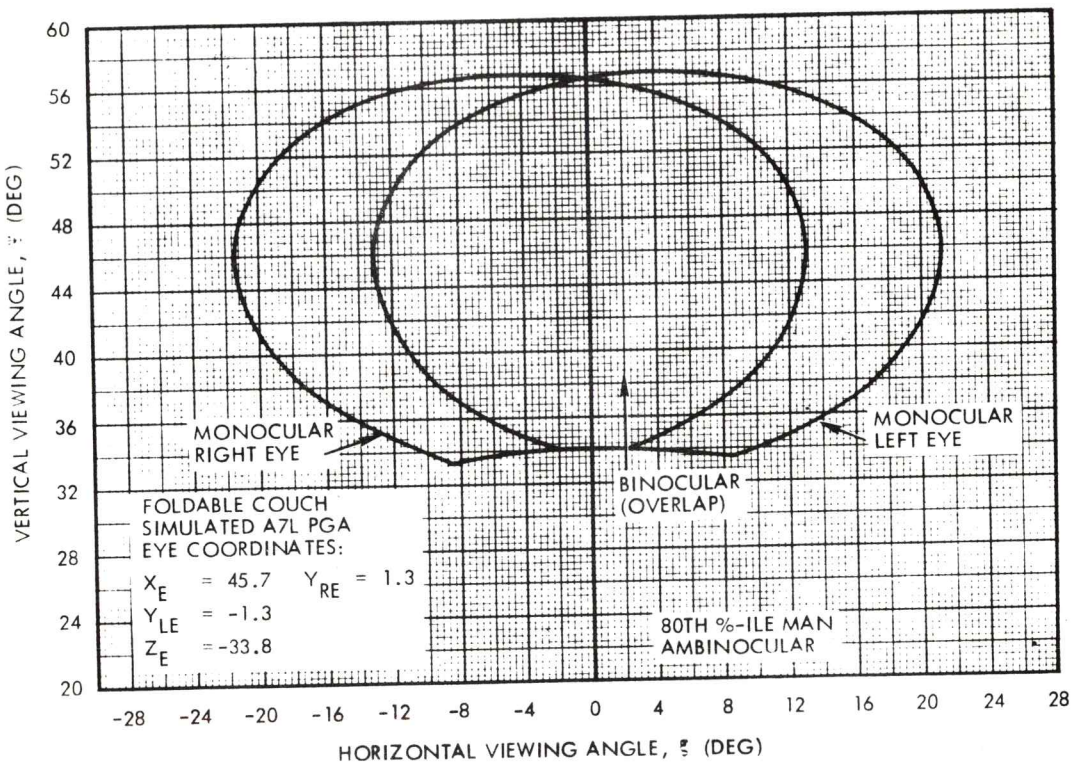
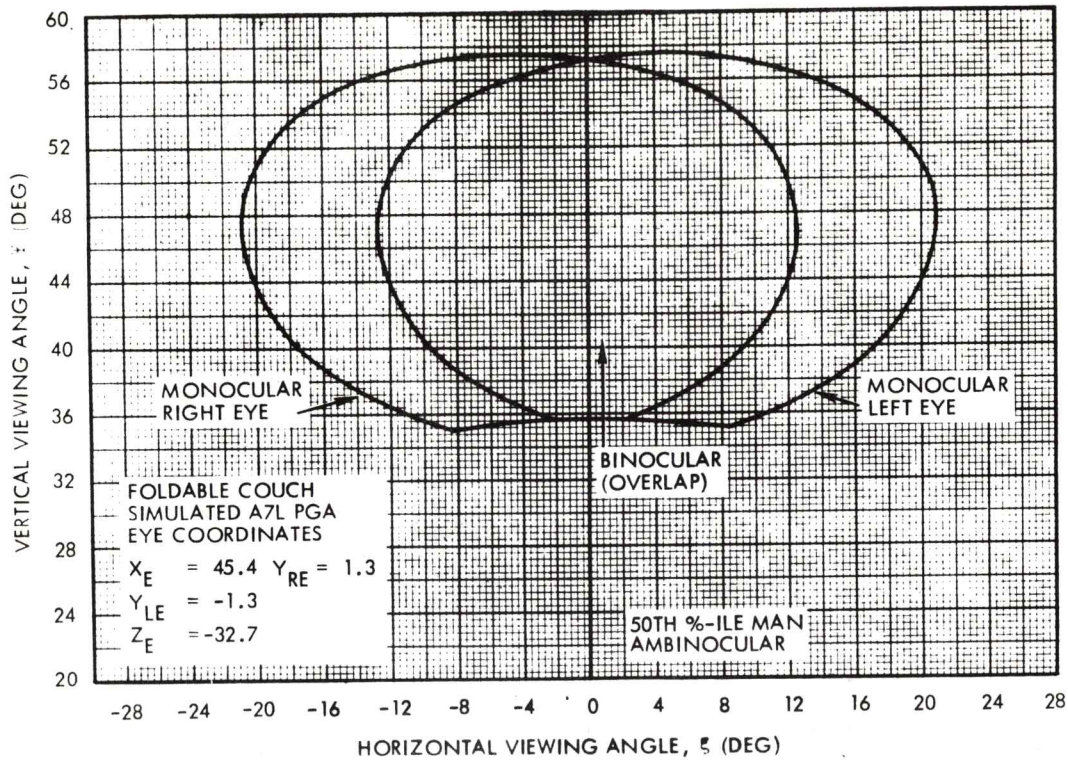


Figure 4.4-7. Heat Shield Hatch Window FOV (CM 103)
(See Paragraph 4.4.1.3.6)

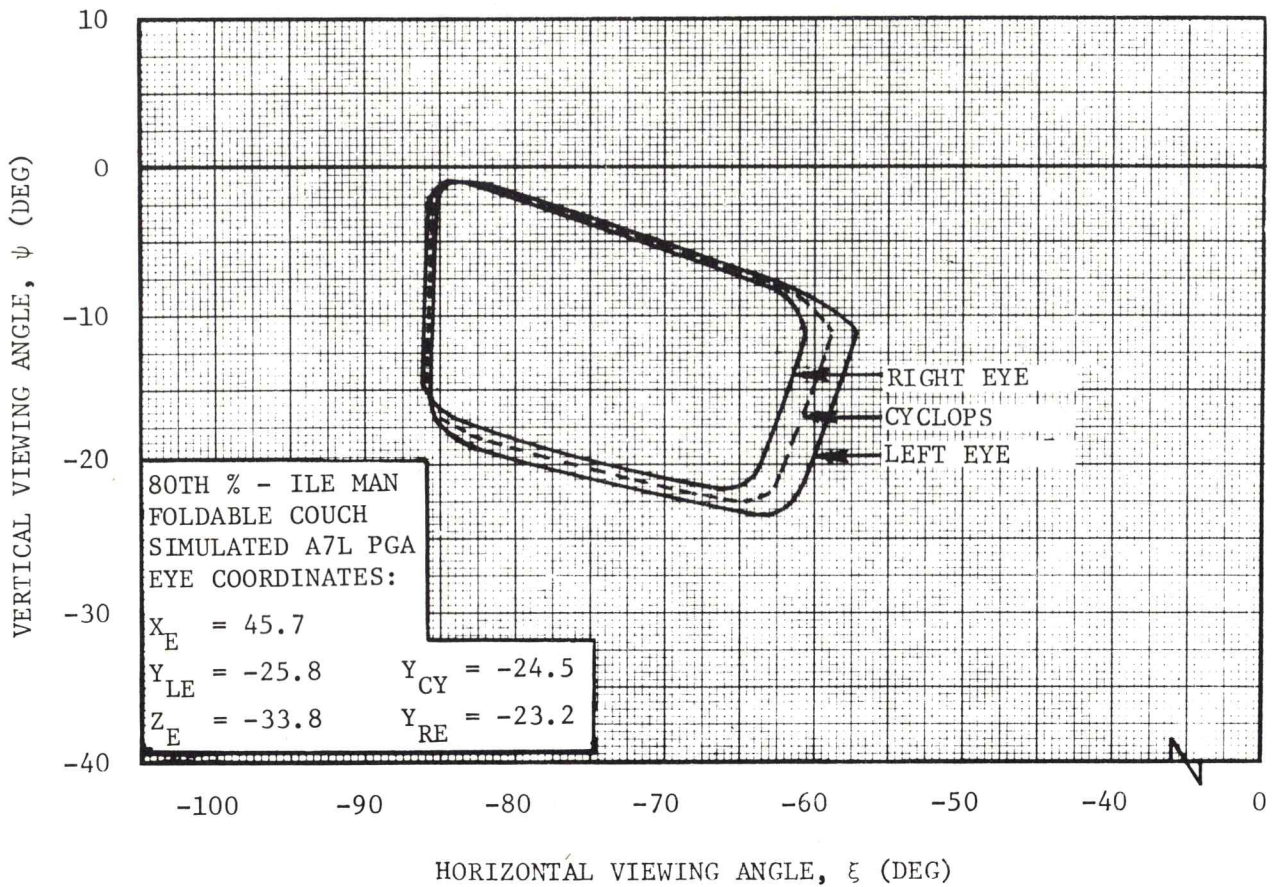


Figure 4.4-8. FOV, Left-Hand Side Window
 (See Paragraph 4.4.1.3.6)

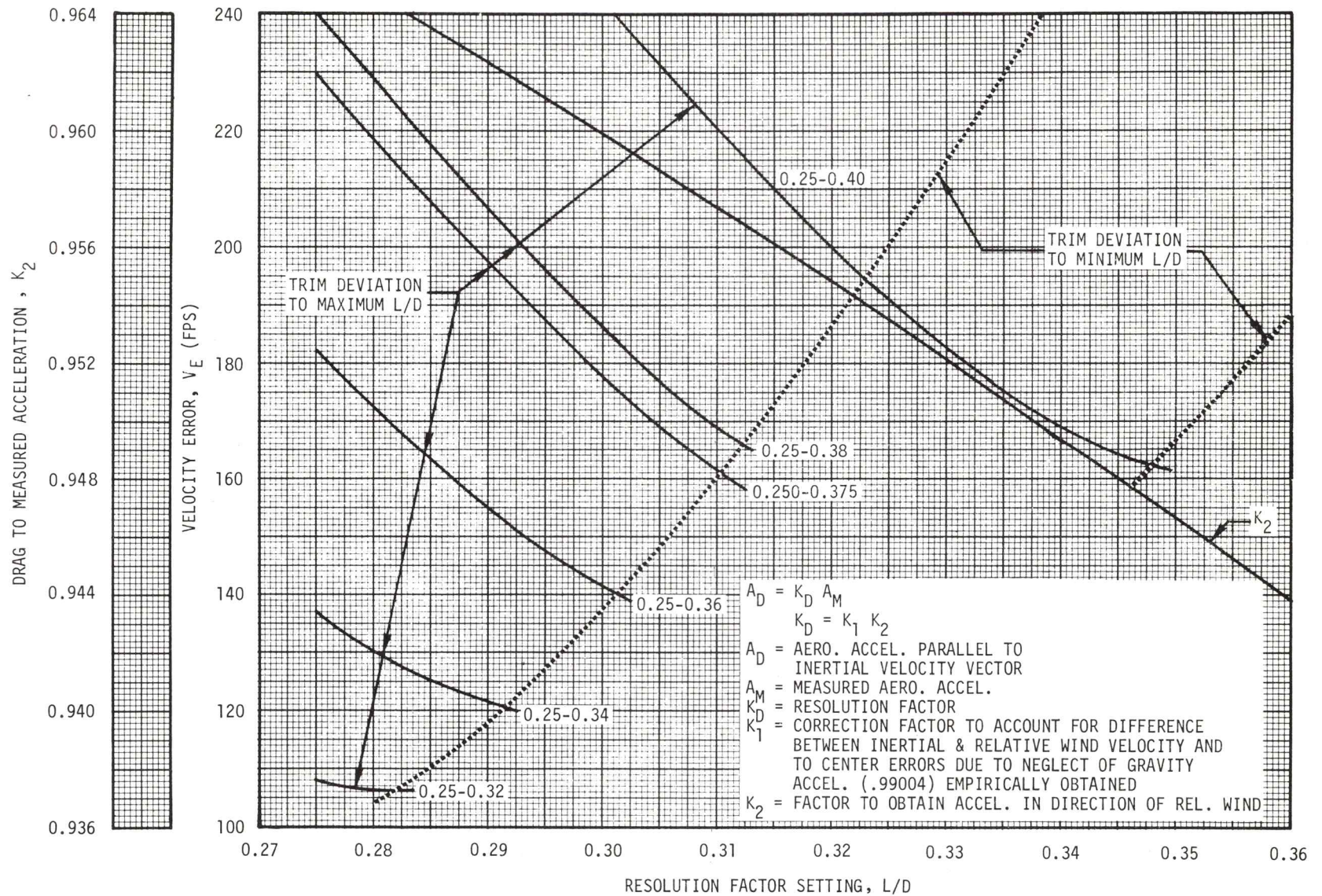


Figure 4.4-9. EMS Accelerometer Errors
(See Paragraphs 4.4.3.1 and 4.4.3.2.2)

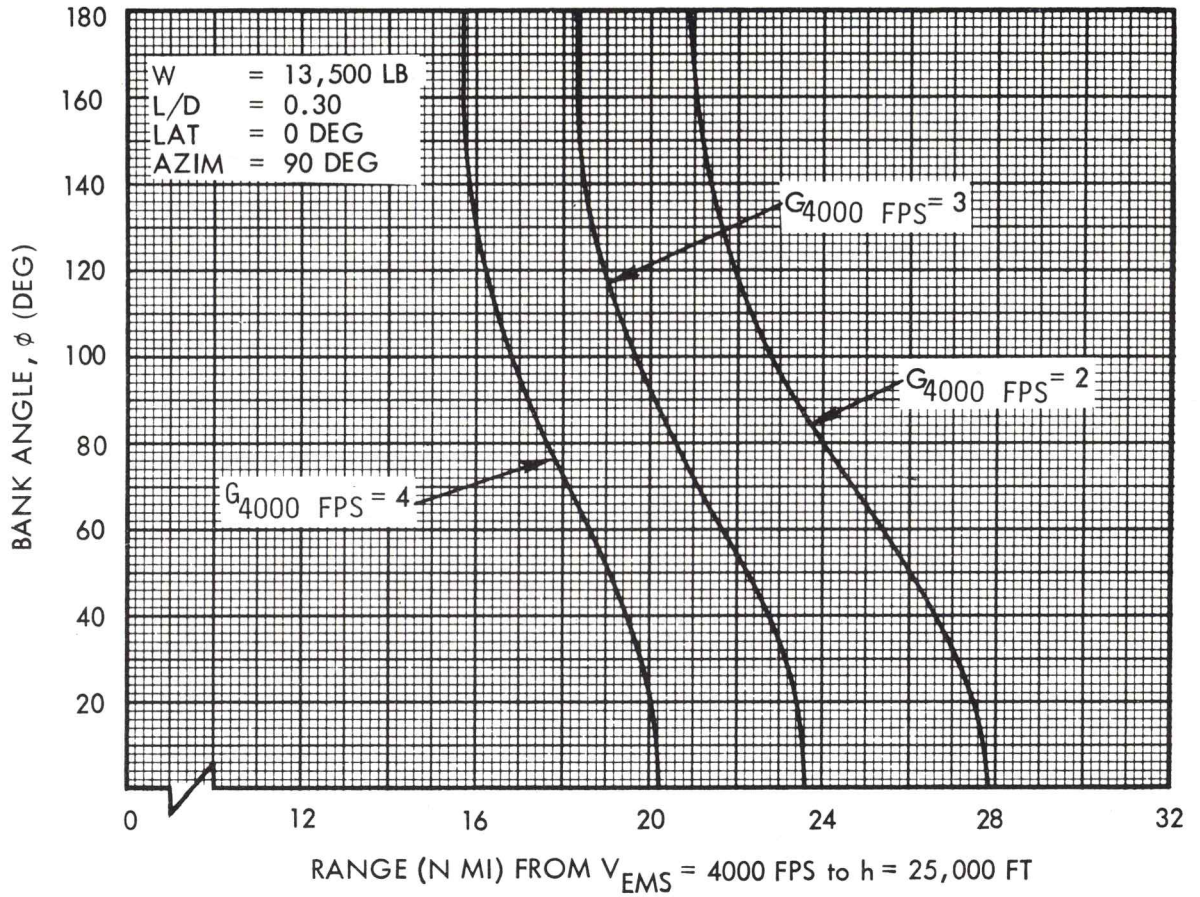


Figure 4.4-10. Terminal EMS Ranging Capability
 (See Paragraph 4.4.3.2.1)

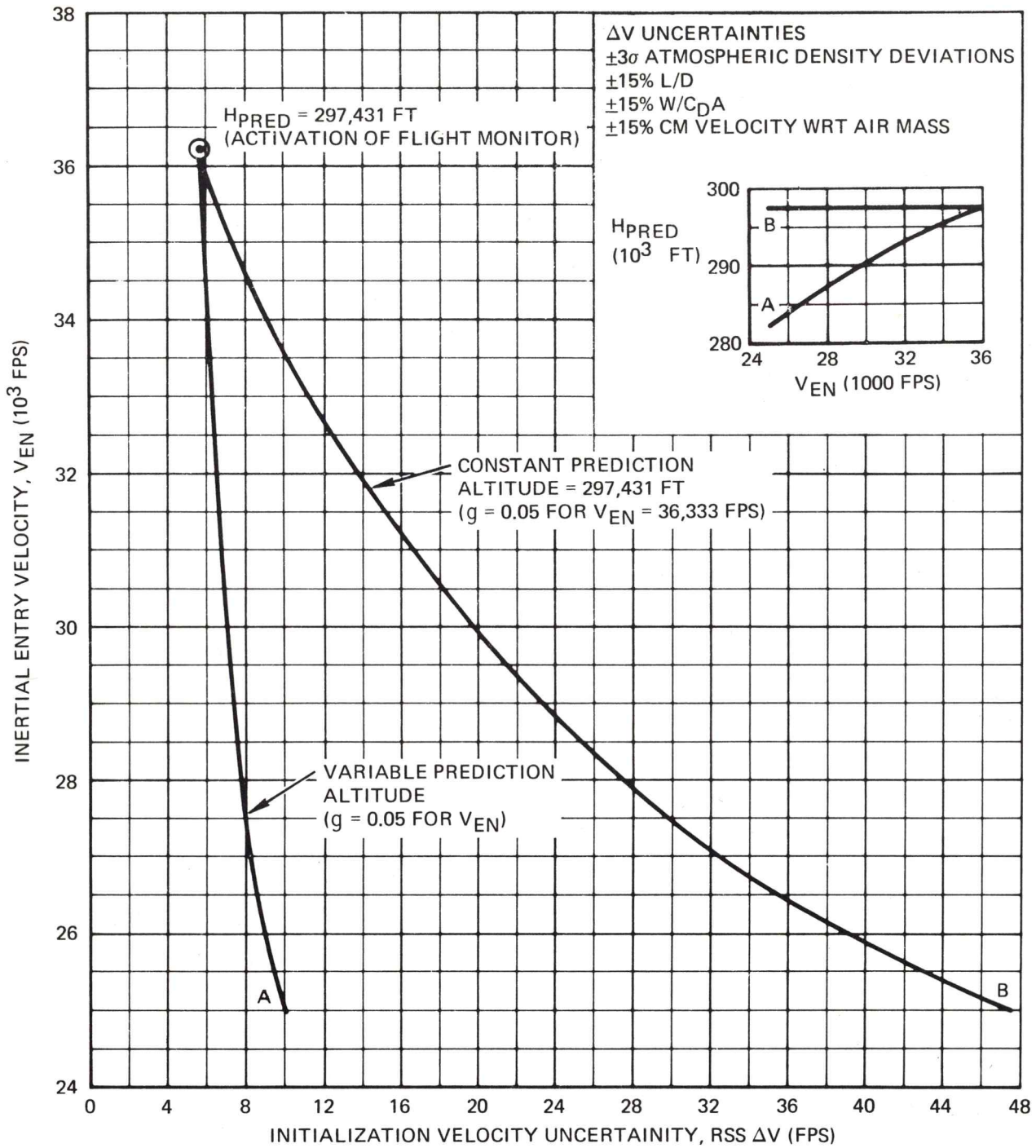


Figure 4.4-11. EMS Initialization Velocity Uncertainty at 0.05 g
 (See Paragraph 4.4.3.2.2)

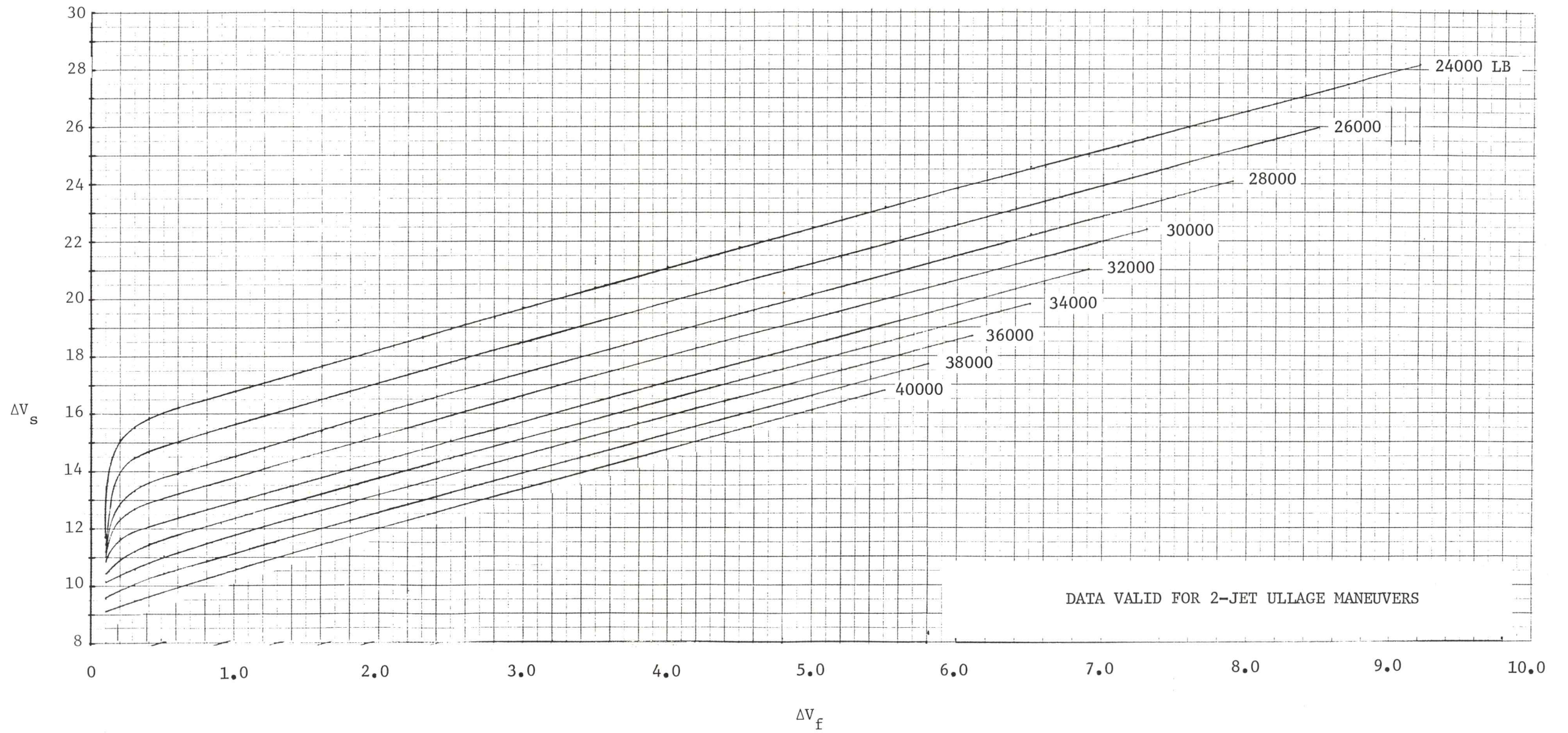


Figure 4.4-12. Small Impulse SPS/SCS Burn (2-Jet Ullage)
 (See Paragraph 4.4.3.4.1.1)

4.4-69/4.4-70

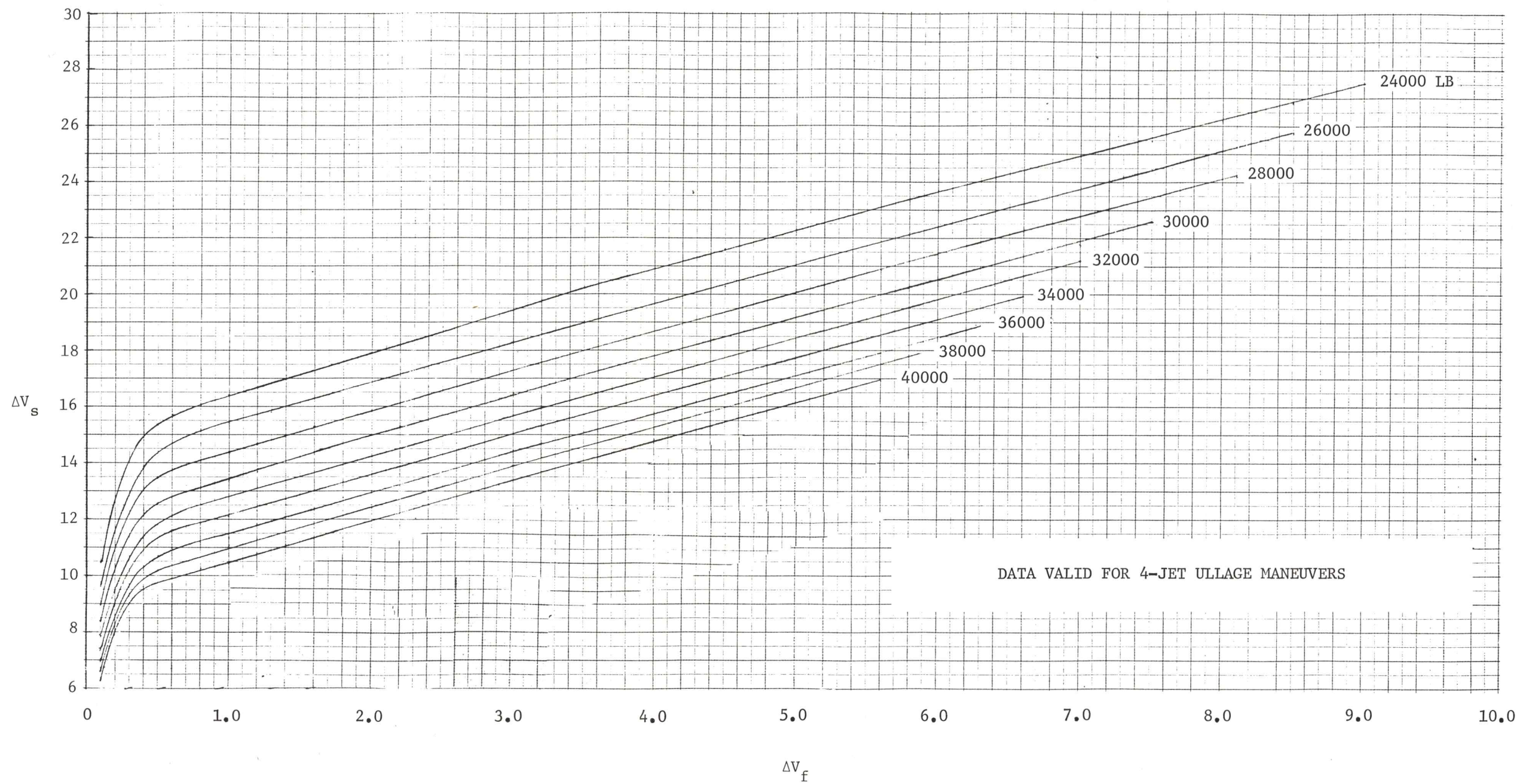
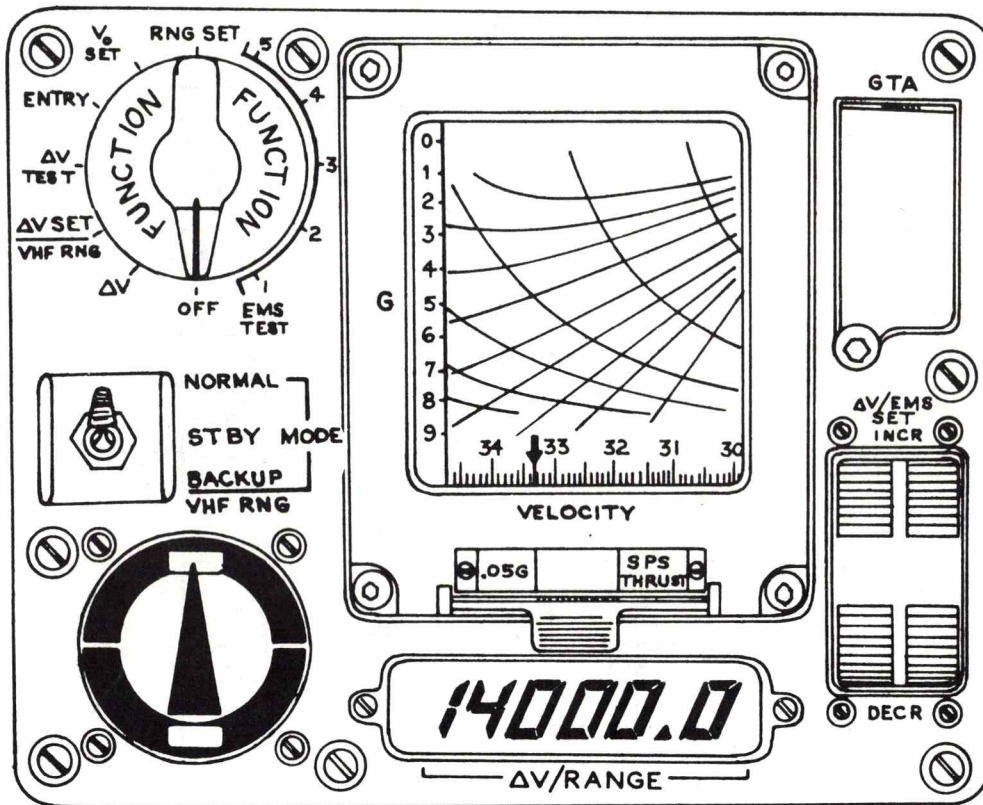


Figure 4.4-13. Small Impulse SPS/SCS Burn (4-Jet Ullage)
 (See Paragraph 4.4.3.4.1.1)



FRONT PANEL

Figure 4.4-14. EMS Display Panel (See Paragraphs 4.4.3.4.5 and 4.4.3.4.6)

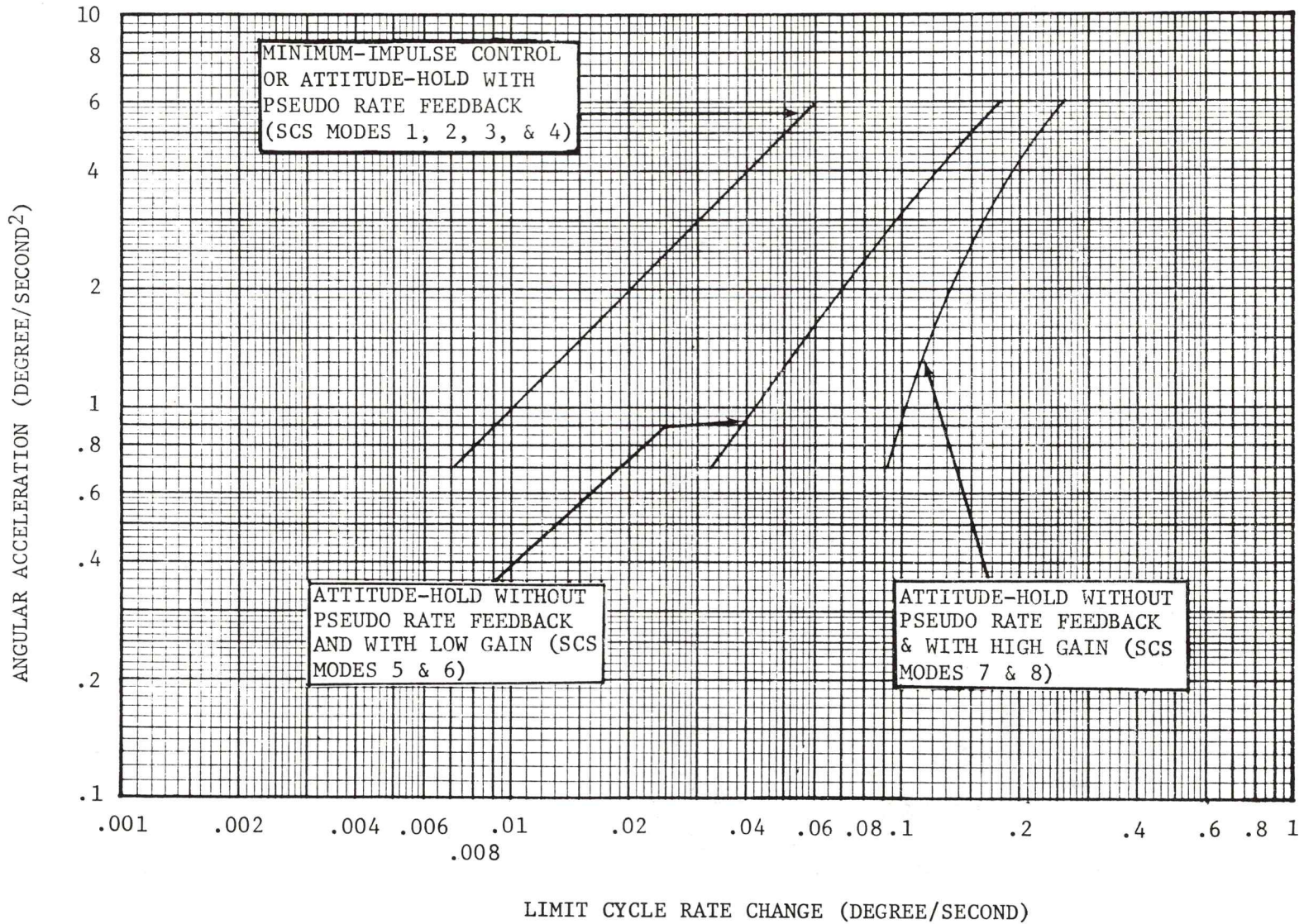
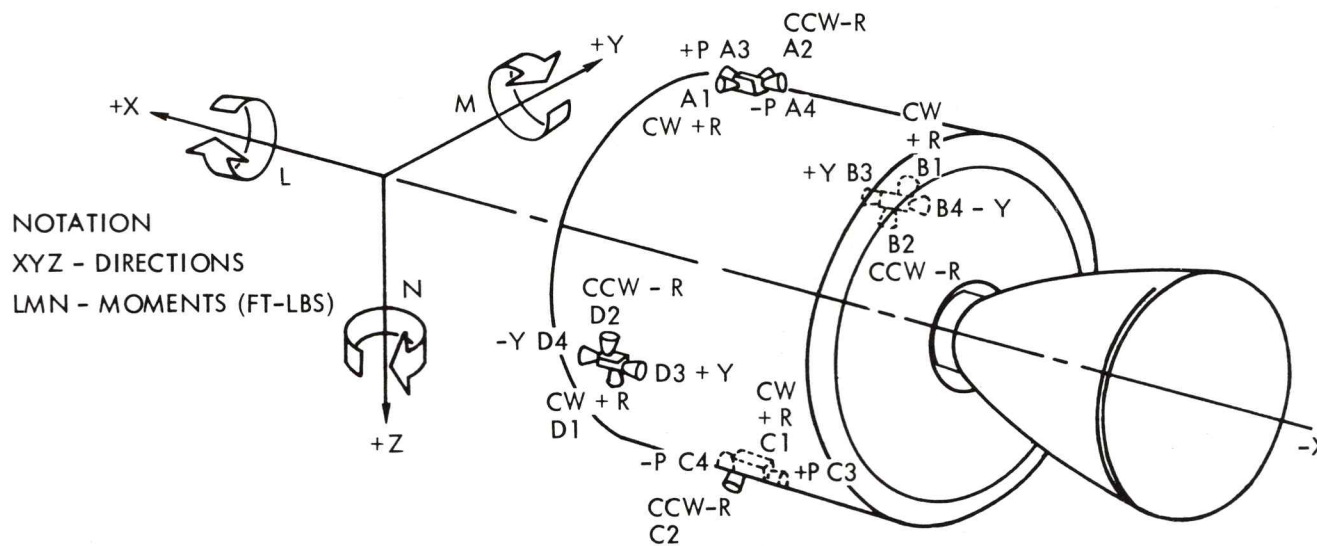


Figure 4.4-15. SCS SM RCS Attitude-Hold Limit Cycle Rate Changes (CSM Vehicle) (See Paragraph 4.4.4.1.2)

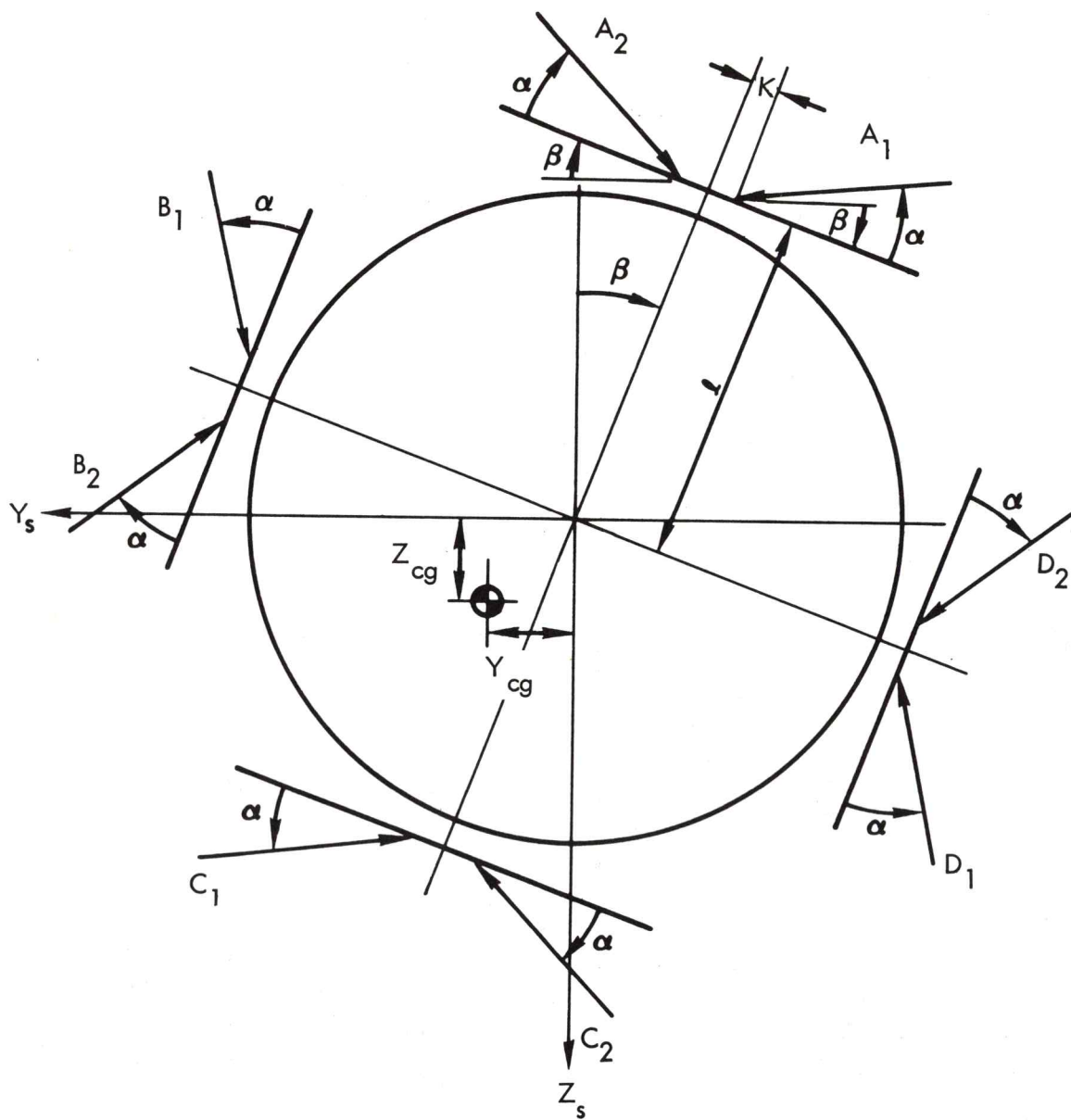


JET	TRANSLATION	ROTATION	JET	TRANSLATION	ROTATION
A ₁	+Y	+φ	C ₁	-Y	+φ
A ₂	-Y	-φ	C ₂	+Y	-φ
A ₃	-X	+θ	C ₃	+X	+θ
A ₄	+X	-θ	C ₄	-X	-θ
B ₁	+Z	+φ	D ₁	-Z	+φ
B ₂	-Z	-φ	D ₂	+Z	-φ
B ₃	-X	+ψ	D ₃	+X	+ψ
B ₄	+X	-ψ	D ₄	-X	-ψ

A = SM RCS QUAD A
 B = SM RCS QUAD B
 C = SM RCS QUAD C
 D = SM RCS QUAD D

NOTE: SM RCS ENGINES ARE NUMBERED IN ACCORDANCE WITH RCS ENGINE ENABLE (AUTO RCS SELECT) SWITCHES ON THE CM CONTROL PANEL.

Figure 4.4-16. SM RCS Engine Definition
 (See Paragraph 4.4.4.1.3)



VIEW LOOKING AFT

Figure 4.4-17. Geometry of Roll Thrust Application Points
(See Paragraph 4.4.4.1.3.1)

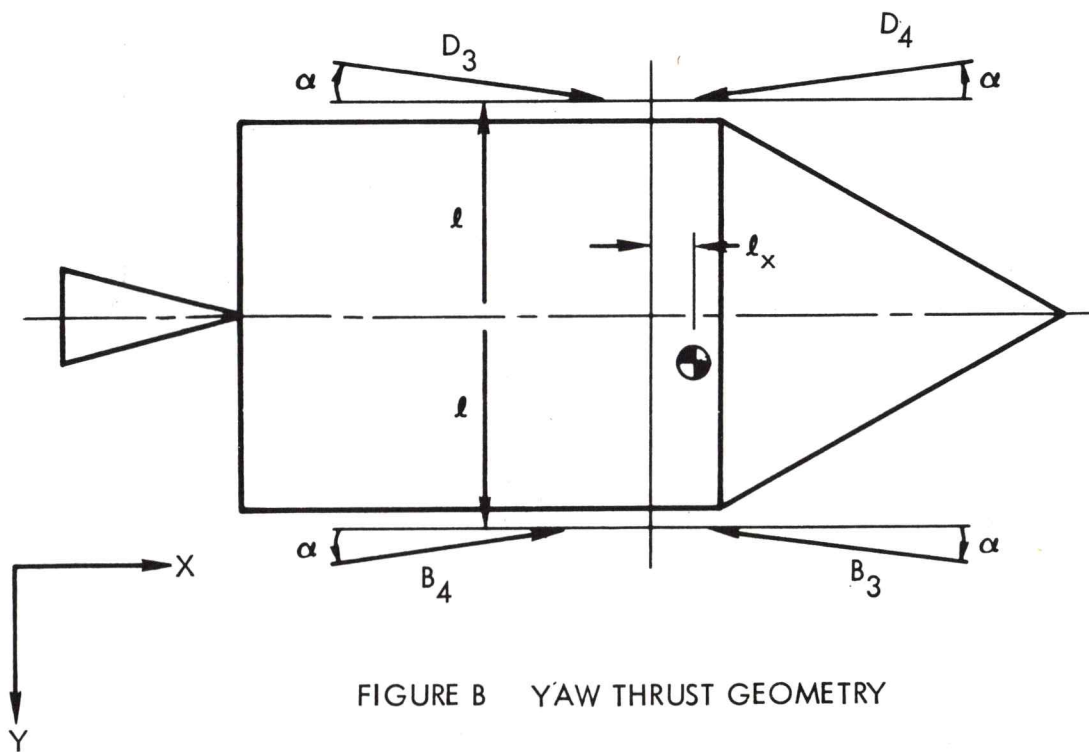
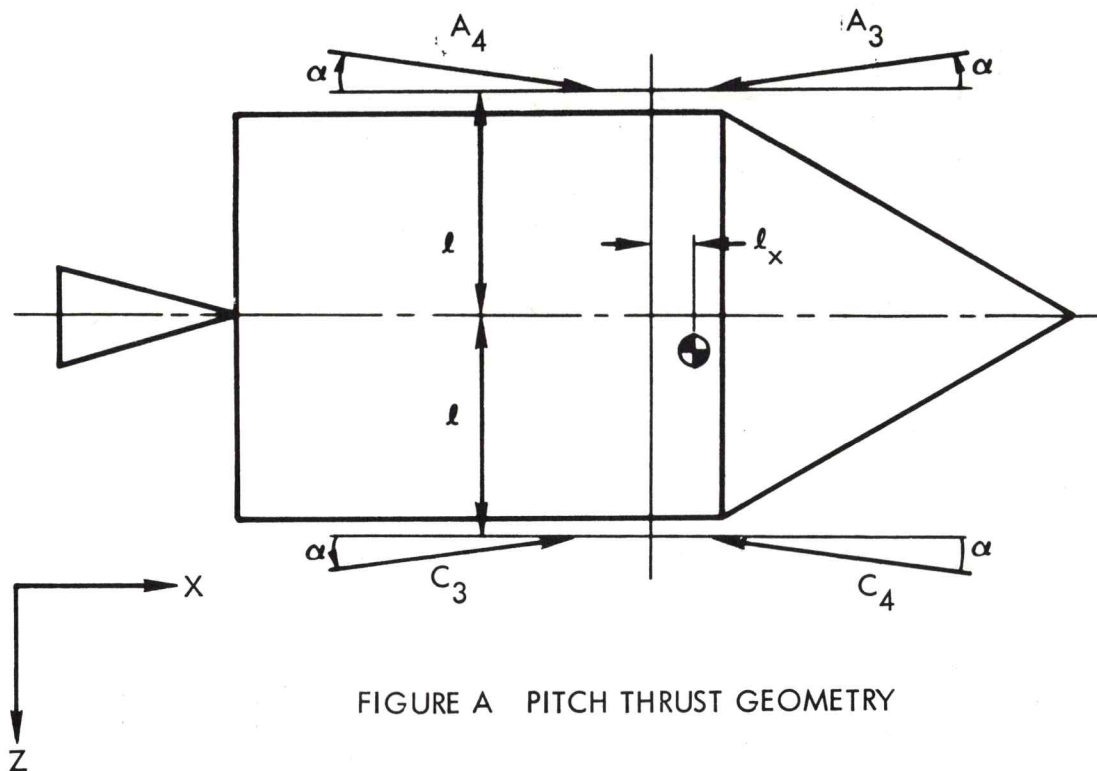


Figure 4.4-18. Geometry of Pitch and Yaw Thrust Application Points
(See Paragraph 4.4.4.1.3.1)

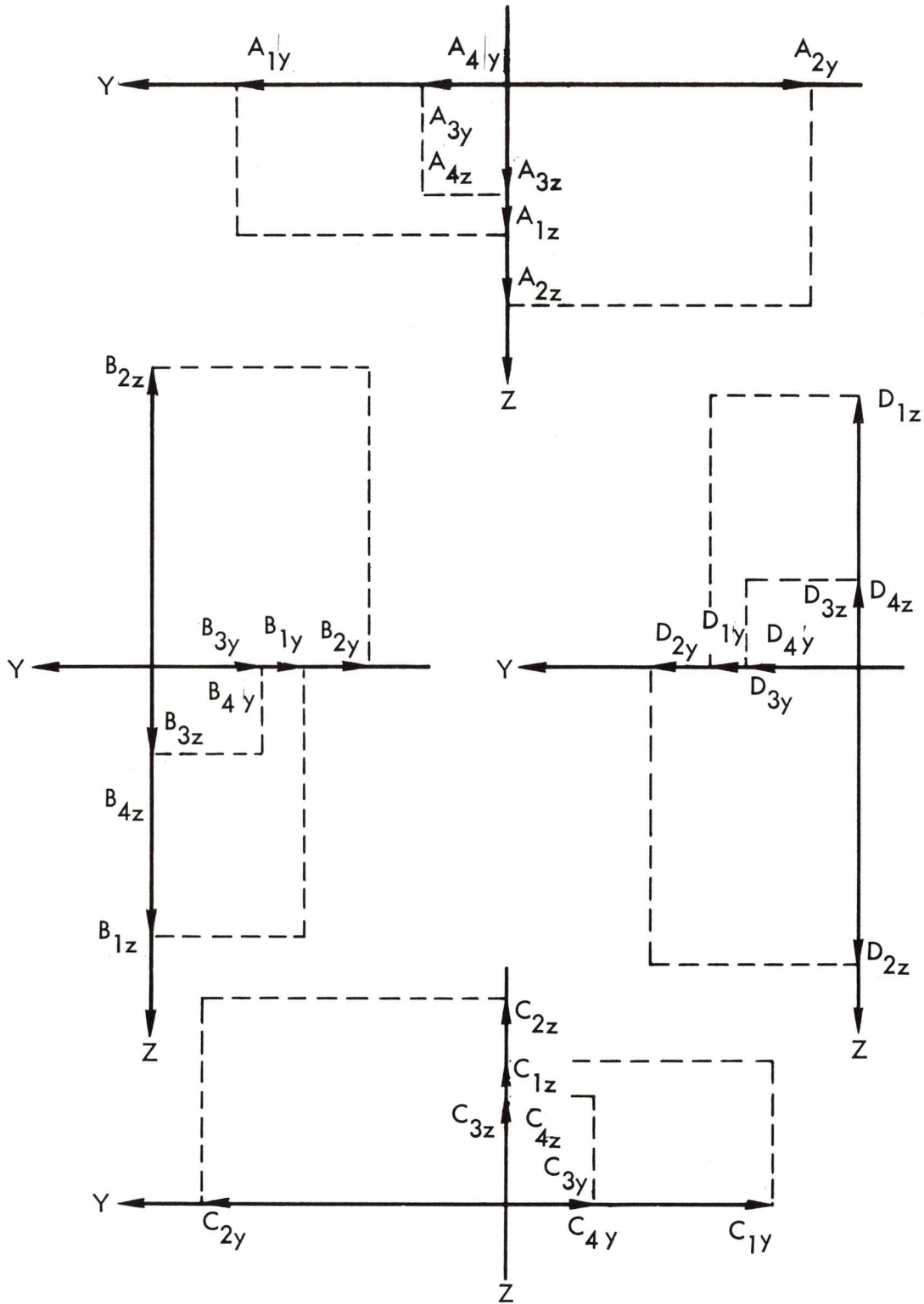
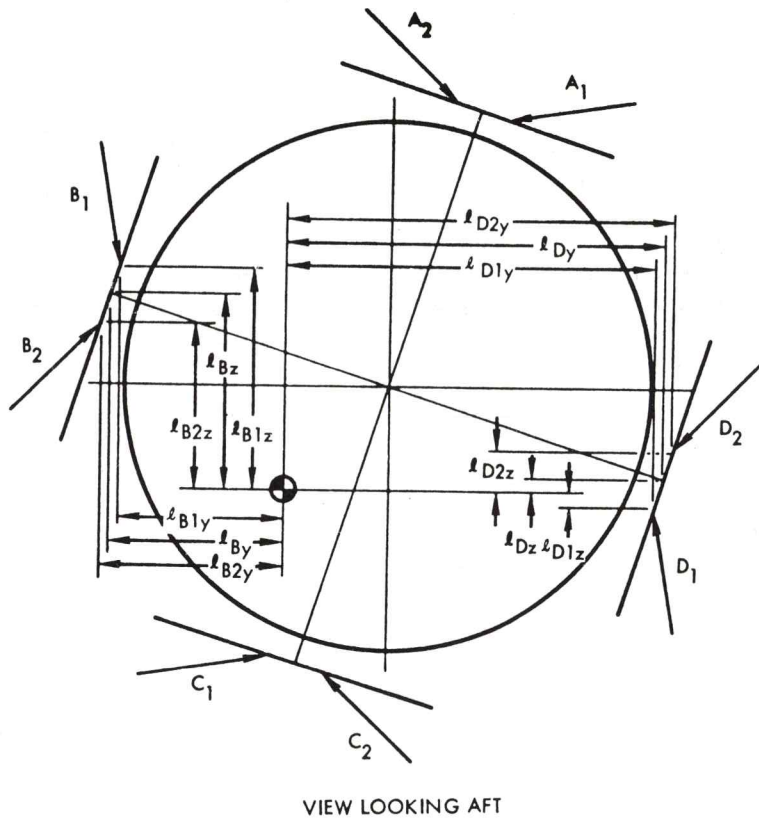
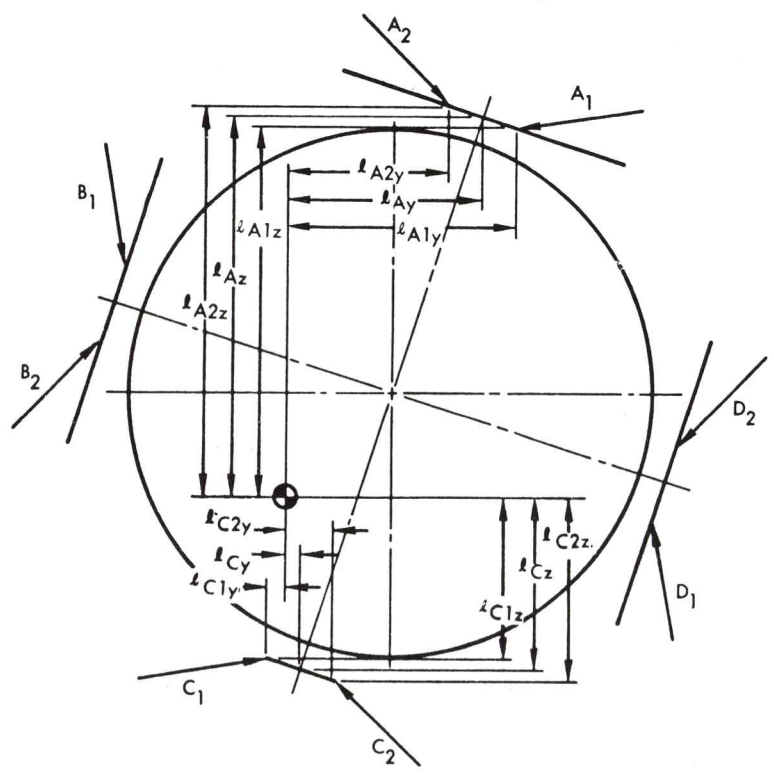


Figure 4.4-19. SM RCS Components of Thrust
(See Paragraph 4.4.4.1.3.1)



VIEW LOOKING AFT



VIEW LOOKING AFT

Figure 4.4-20. SM RCS Moment Arm Diagram
(See Paragraph 4.4.4.1.3.1)

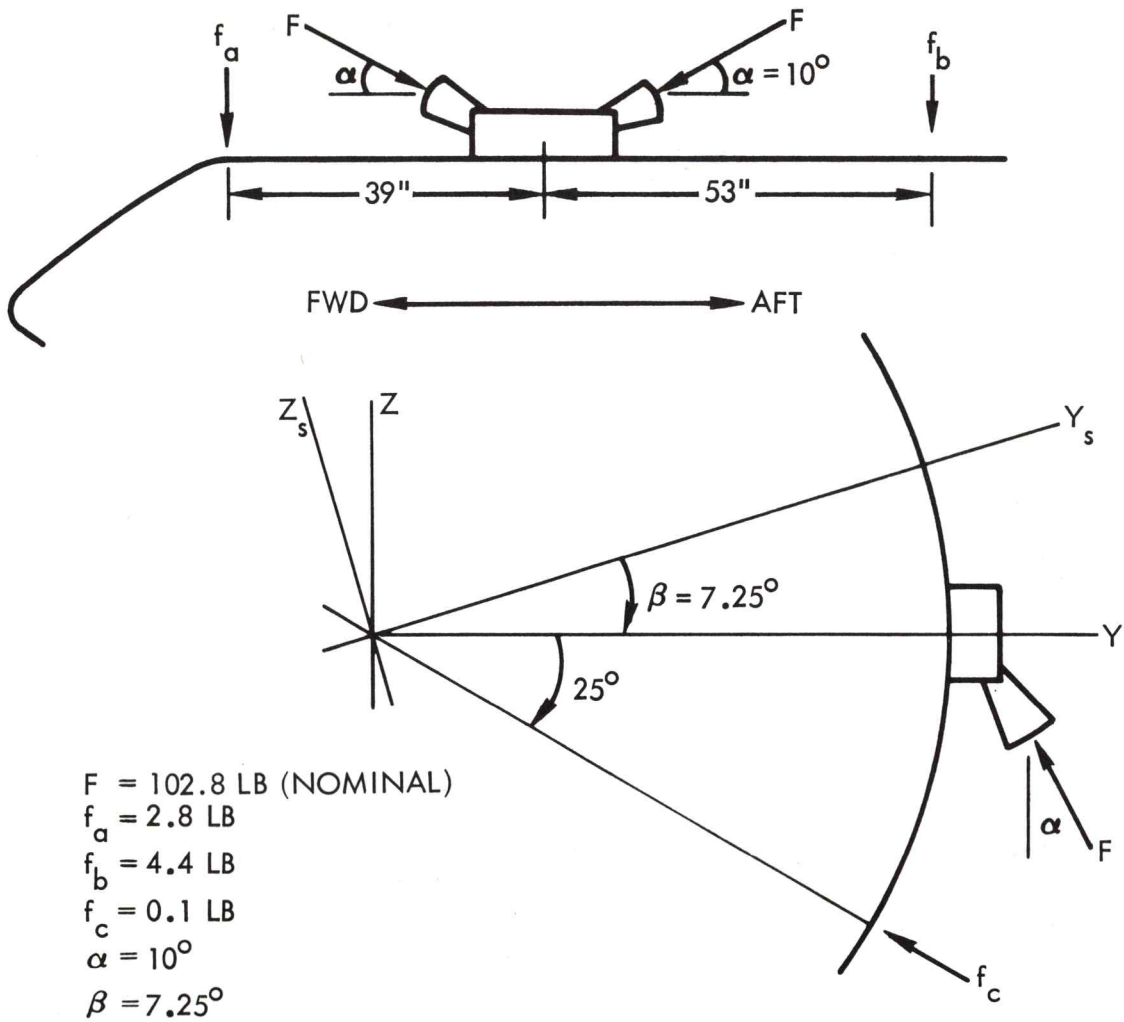
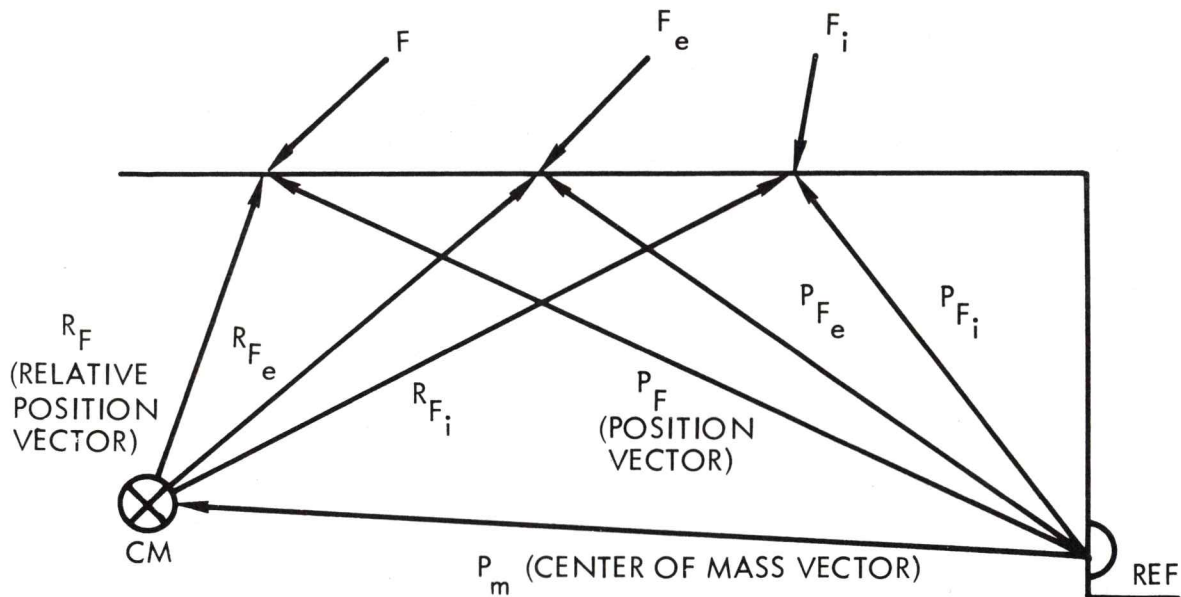


Figure 4.4-21. SM RCS Engine Impingement Data
(See Paragraph 4.4.4.1.3.3)



WHERE SUBSCRIPTS ARE
i - IMPINGEMENT
e - EFFECTIVE
F - THE ENGINE ($A_1, A_2, \dots, D_3, D_4$)

Figure 4.4-22. SM RCS Engine Vectors
(See Paragraph 4.4.4.1.3.3)

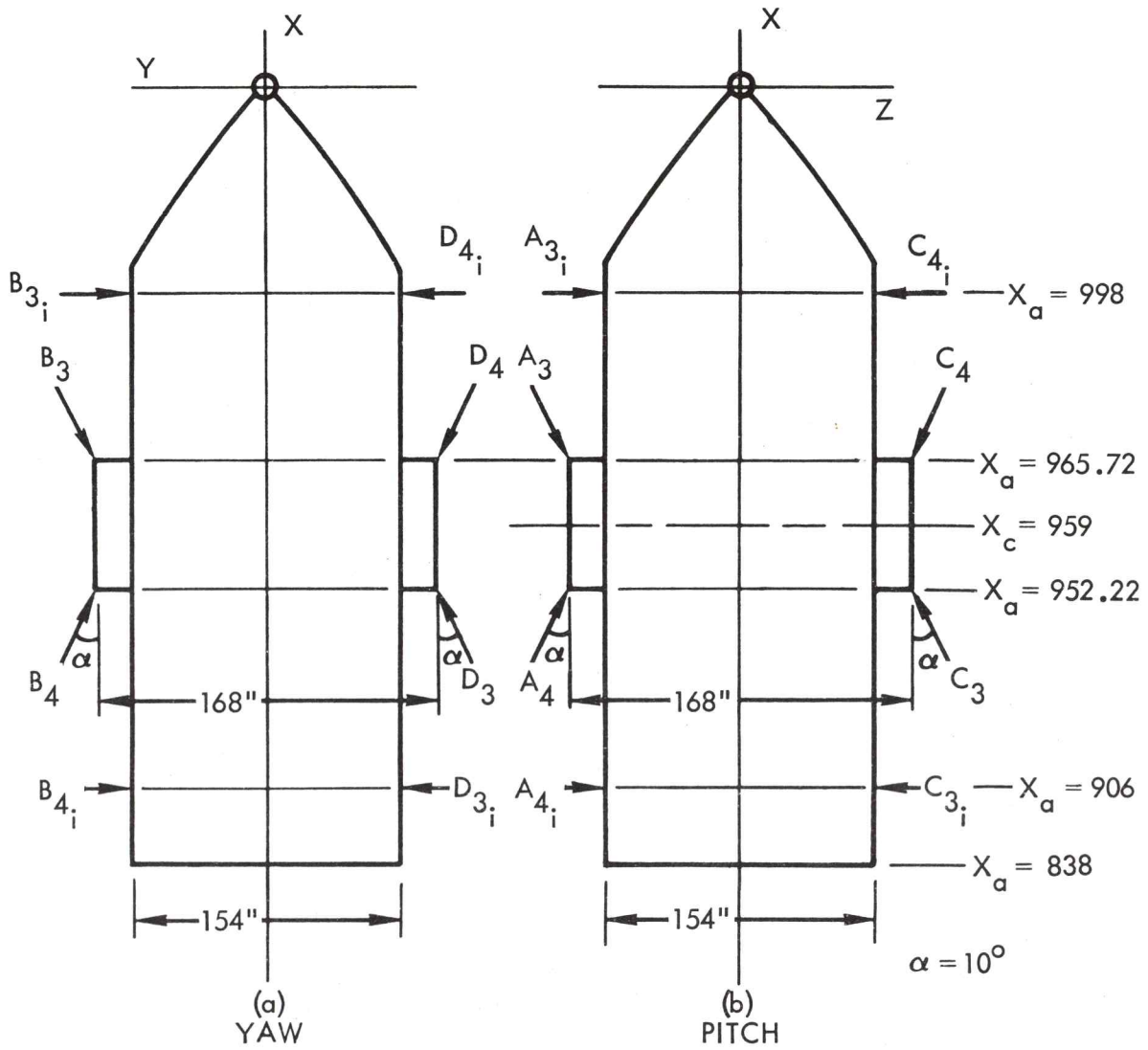
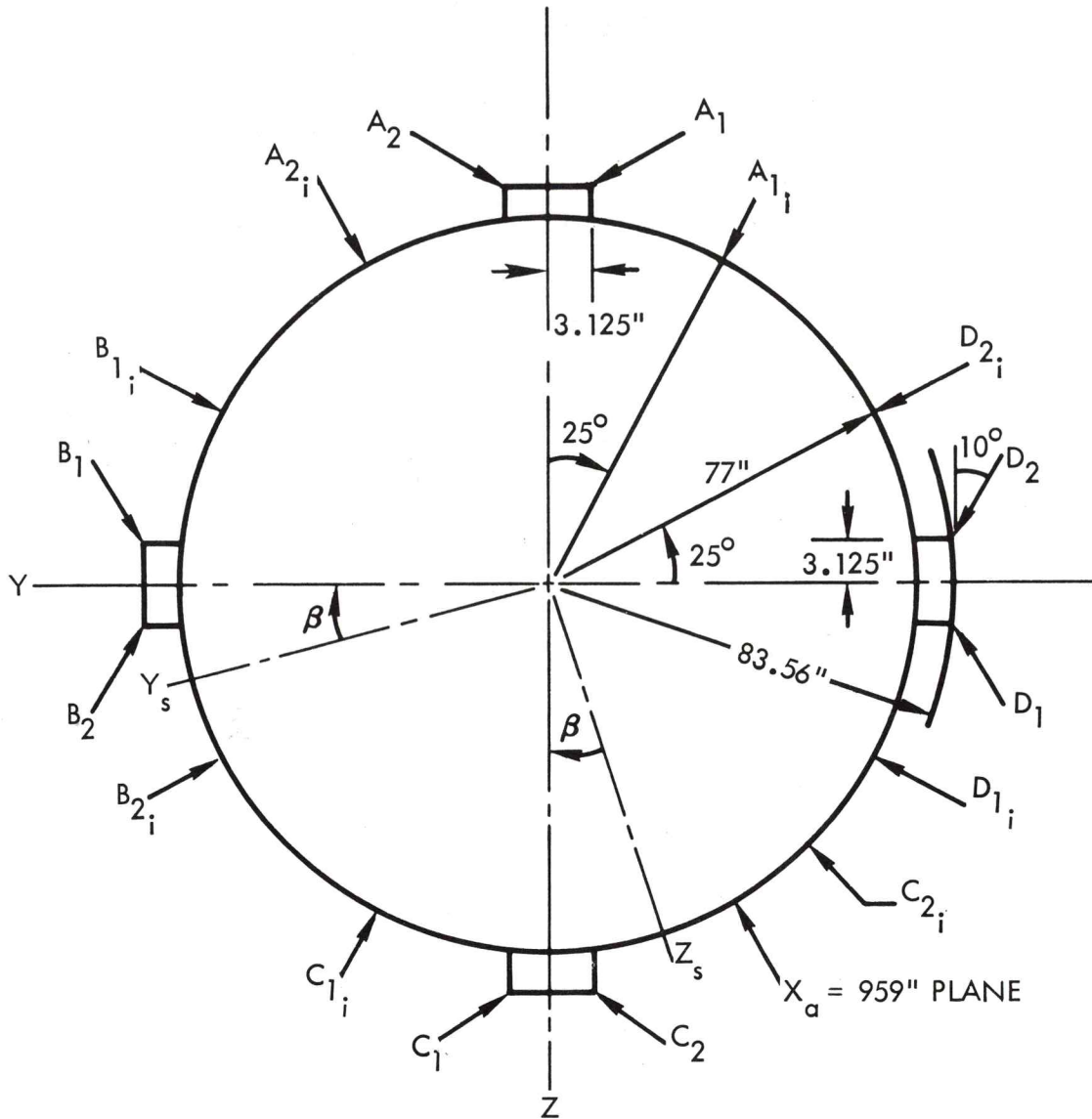


Figure 4.4-23. SM Jet Thrust Vector Locations
(See Paragraph 4.4.4.1.3.3)



$\beta = 7^\circ 15'$

Figure 4.4-24. SM Roll Jet Thrust Vector Locations
(See Paragraph 4.4.4.1.3.3)

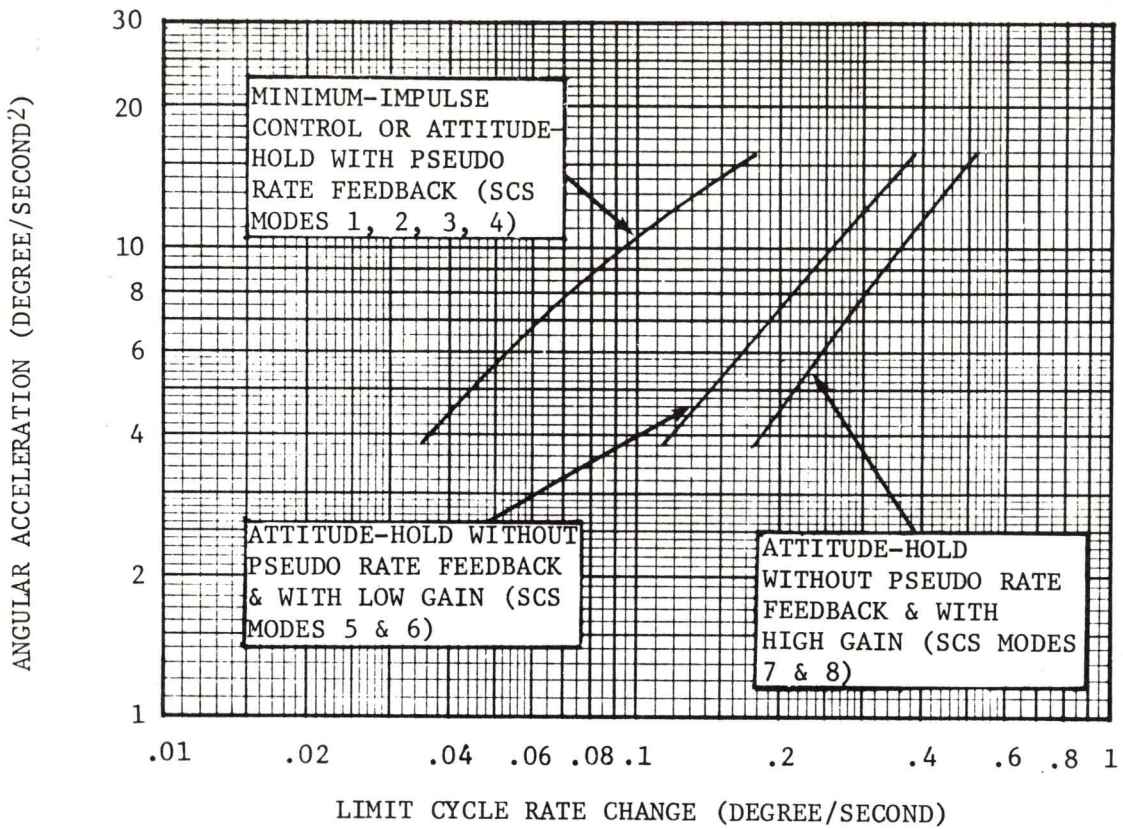


Figure 4.4-25. SCS CM RCS Preentry Attitude-Hold Limit Cycle Rate Changes (CM Vehicle)
(See Paragraph 4.4.4.2.2)

4.4-85

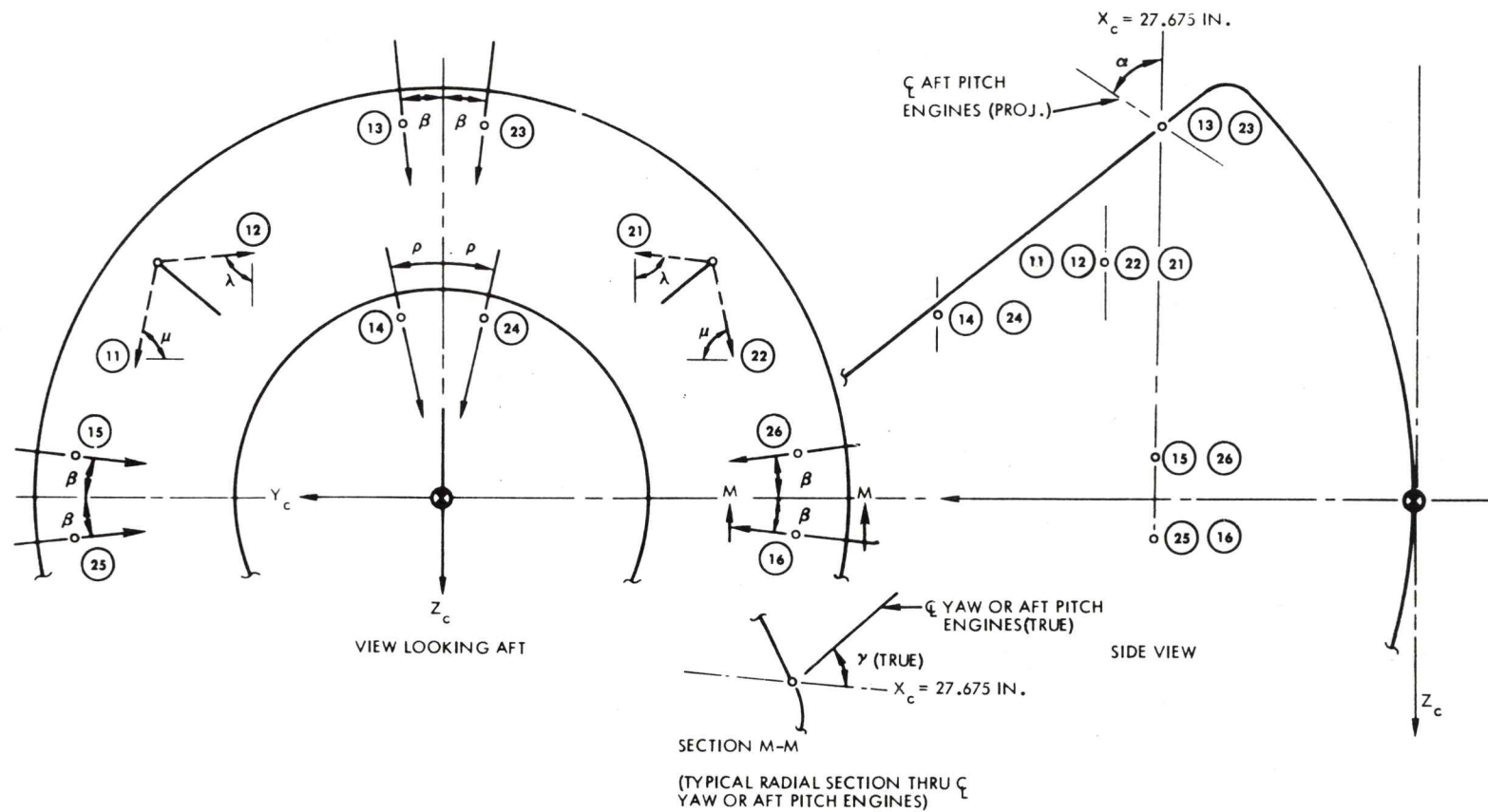


Figure 4.4-26. CM Engine Location Diagram
(See Paragraph 4.4.4.2.3)

4.4-86

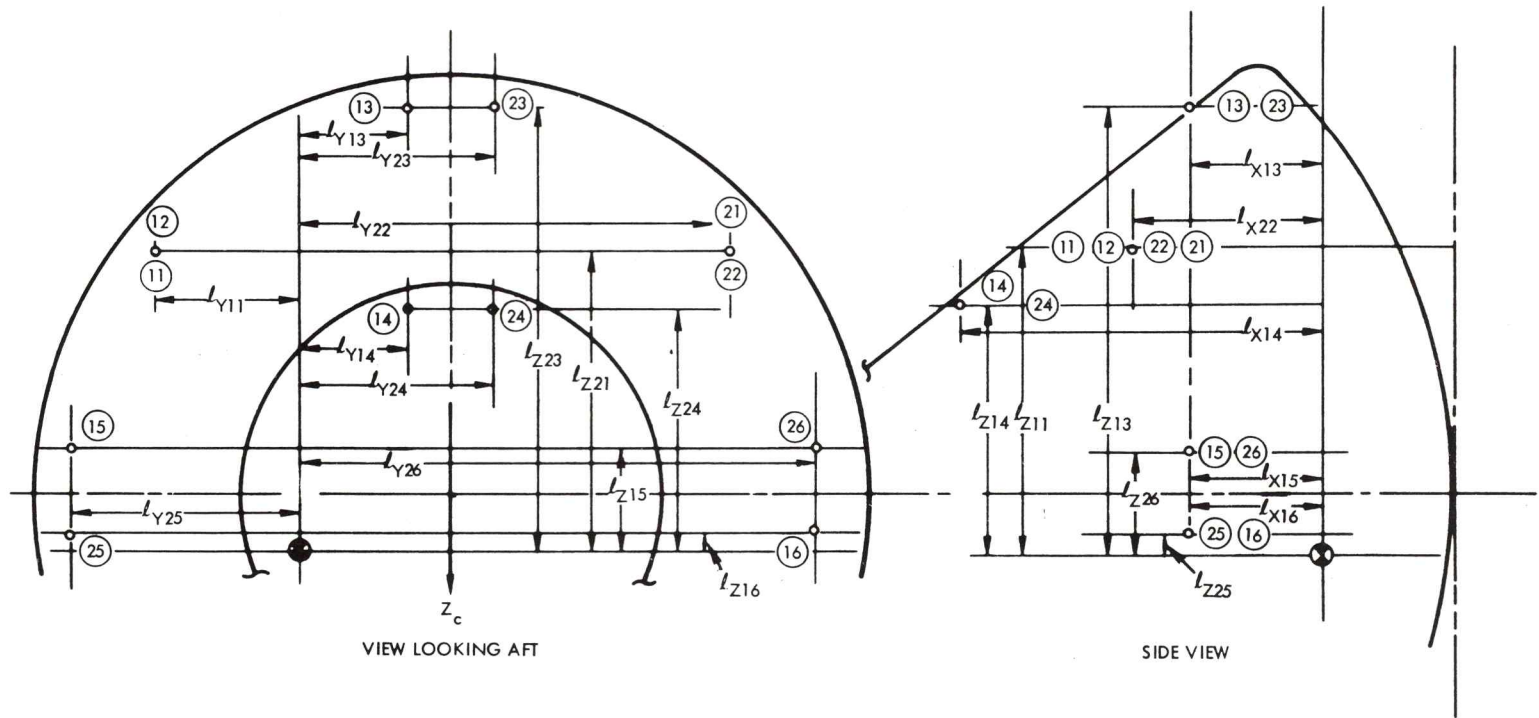


Figure 4.4-27. CM RCS Moment Arm Definition
(See Paragraph 4.4.4.2.3)

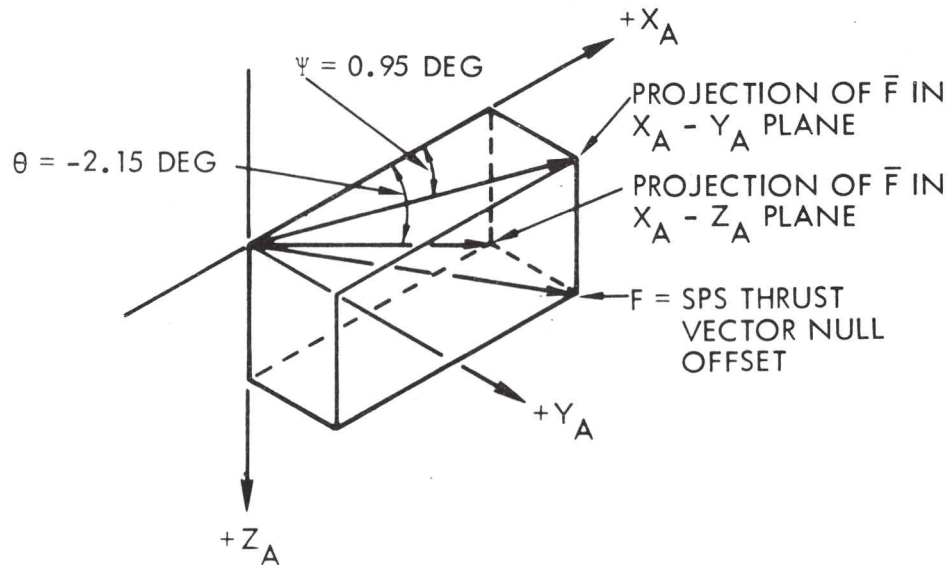
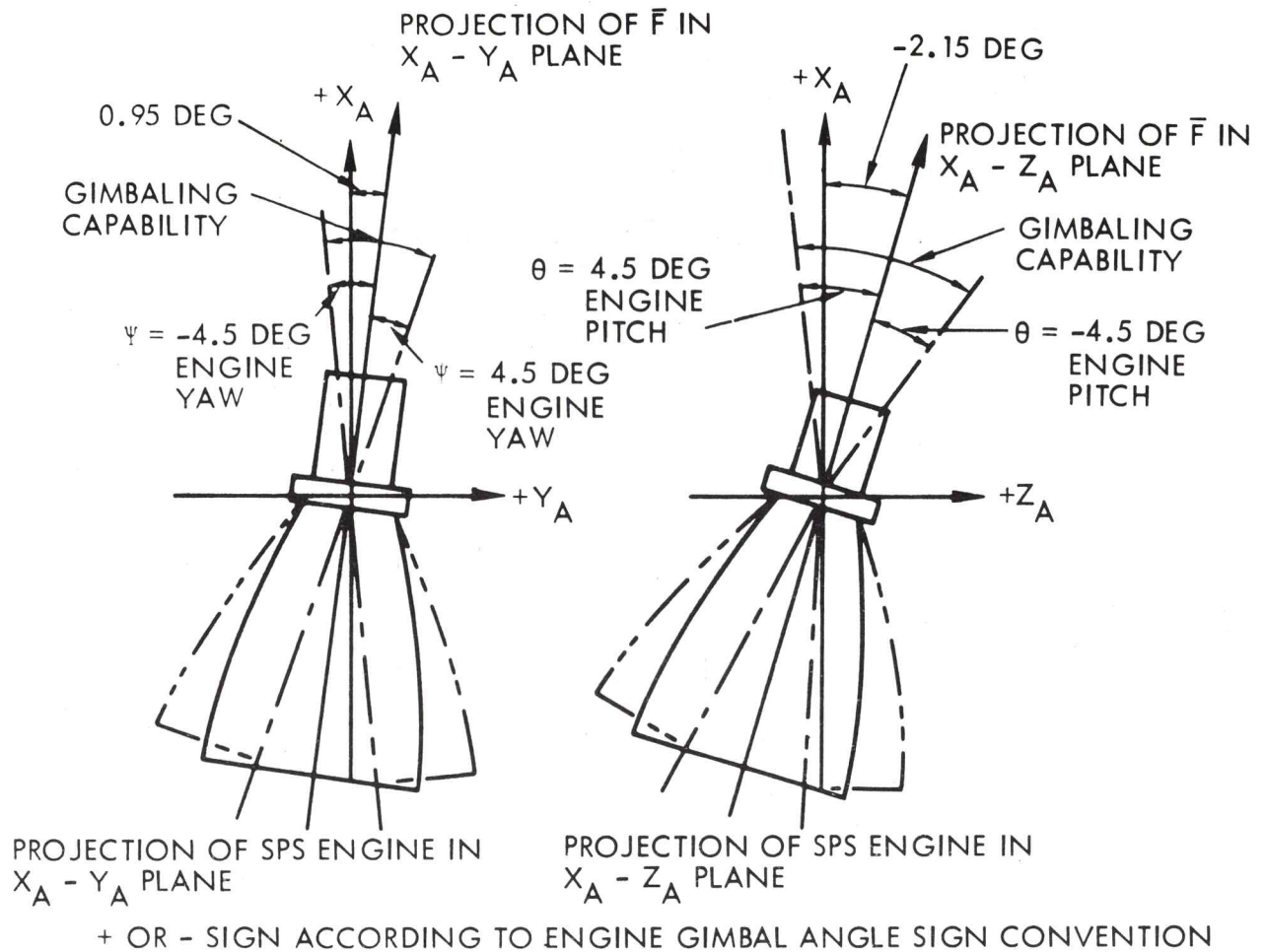


Figure 4.4-28. SPS Gimballing Capability
(See Paragraph 4.4.5.1)

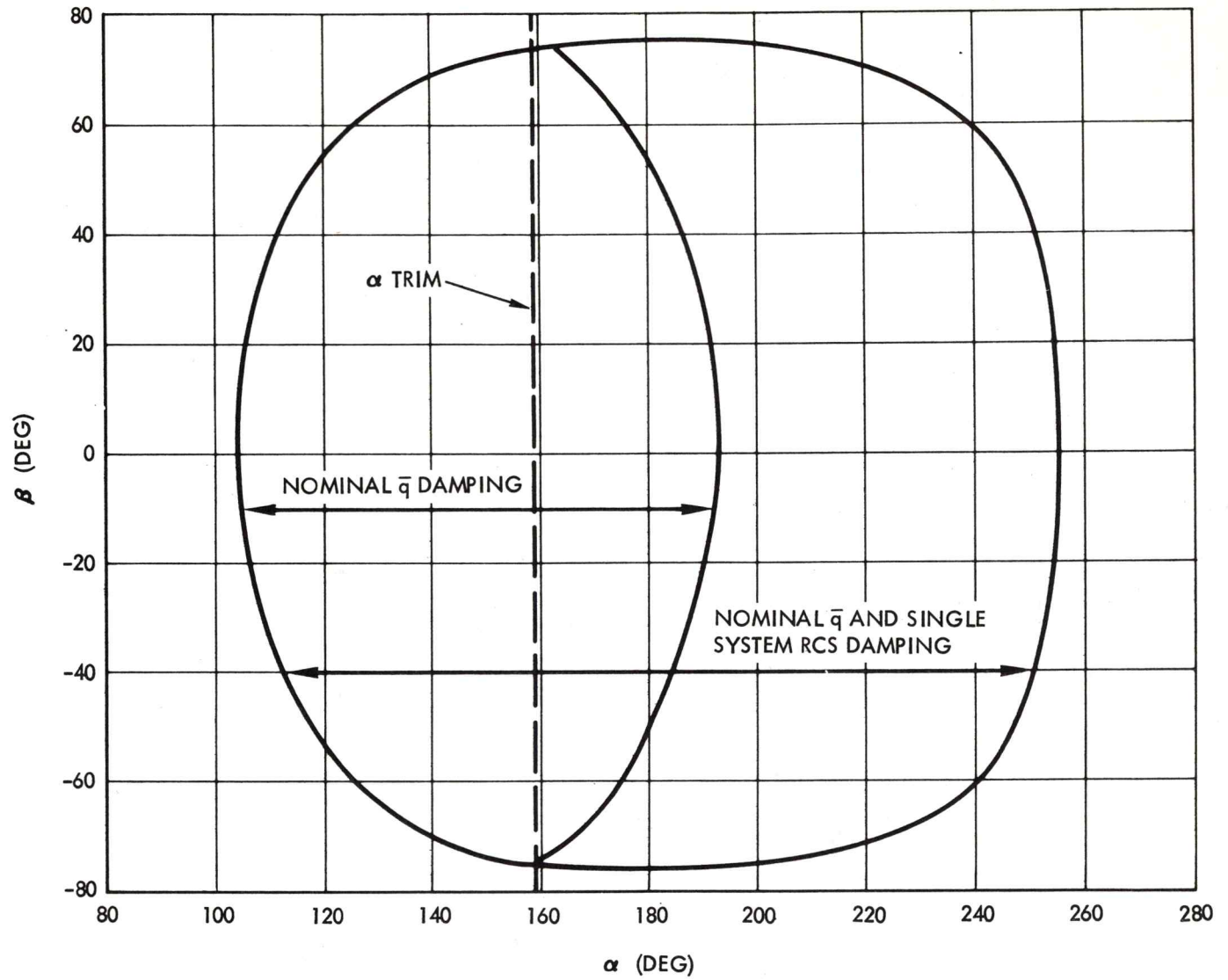


Figure 4.4-29. Block II $\alpha - \beta$ Capture Envelope at 0.05 g
(See Paragraph 4.4.6.1)

4.5 SERVICE PROPULSION SUBSYSTEM (SPS)

s and Propellant Storage System
dizer

lant Tank Capacity and Trapped Quantities
Requirements

Nominal Ullage

Contingency Ullage

ure Limits

emperature Limits

Pressure-Temperature Limits

Flow Rates

istance

rop Flow Rate Data

terface Pressure Drop

Chamber Pressure Drop

Gaging System (PUGS)

t the Engine Interface

formance Parameters

imits

ities

4.5 SERVICE PROPULSION SUBSYSTEM (SPS)

4.5 SERVICE PROPULSION SUBSYSTEM (SPS)

- 4.5.1 Propellants and Propellant Storage System
 - 4.5.1.1 Oxidizer
 - 4.5.1.2 Fuel
 - 4.5.1.3 Propellant Tank Capacity and Trapped Quantities
 - 4.5.1.4 Ullage Requirements
 - 4.5.1.4.1 Nominal Ullage
 - 4.5.1.4.2 Contingency Ullage
 - 4.5.1.5 Ullage Pressure Limits
 - 4.5.1.6 Propellant Temperature Limits
 - 4.5.1.7 Propellant Tank Pressure-Temperature Limits
- 4.5.2 Propellant Feed System
 - 4.5.2.1 Fuel and Oxidizer Flow Rates
 - 4.5.2.2 Propellant Flow Resistance
 - 4.5.2.3 Propellant Pressure Drop Flow Rate Data
 - 4.5.2.3.1 Ullage-to-Interface Pressure Drop
 - 4.5.2.3.2 Interface-to-Chamber Pressure Drop
 - 4.5.2.4 Propellant Utilization and Gaging System (PUGS)
 - 4.5.2.5 Propellant Pressure Limits at the Engine Interface
 - 4.5.2.6 Blowdown Capability
- 4.5.3 Helium Pressurization System
 - 4.5.3.1 Helium Pressurization System Performance Parameters
 - 4.5.3.2 Helium Pressure and Temperature Limits
 - 4.5.3.3 Helium Loading Window
 - 4.5.3.4 Pressure Loss Budget
- 4.5.4 Nitrogen Pressurization System
 - 4.5.4.1 Nitrogen Tank Capacity and Trapped Quantities
 - 4.5.4.2 Nitrogen Pressure System Characteristics
 - 4.5.4.3 Nitrogen Tank Pressure Loading Limits
 - 4.5.4.4 Nitrogen Tank Temperature Loading Limits
- 4.5.5 SPS Engine Performance
 - 4.5.5.1 SPS Engine Design Characteristics
 - 4.5.5.2 SPS Engine Performance Characteristics
 - 4.5.5.3 Minimum Impulse
 - 4.5.5.4 Start and Shutdown Thrust Transients
 - 4.5.5.5 Minimum Chamber Pressure
 - 4.5.5.6 Chamber Pressure Overshoot Limit
 - 4.5.5.7 Time Between Starts
 - 4.5.5.8 Blowdown Performance
- 4.5.6 SPS Thermal Control System (TCS)
 - 4.5.6.1 Attitude Constraints
 - 4.5.6.2 TCS Operation
 - 4.5.6.3 Propellant Temperature
- 4.5.7 Miscellaneous
 - 4.5.7.1 Gimbal Motor and Clutch Temperature Characteristics
 - 4.5.7.2 CSM Angular Acceleration by SPS Hardover

4.5 SERVICE PROPULSION SUBSYSTEM (SPS)

The SPS is a nonthrottleable pressure fed system using hypergolic propellants and an ablative thrust chamber with a radiant cooled nozzle extension. The SPS is used to provide thrust for X-axis velocity changes after separation from the S-IVB booster up to CM/SM separation. The system also supports the SPS abort capability during the launch phase after the launch escape tower has been jettisoned. The thrust chamber is installed in the SM such that the thrust vector passes through the intersection of the Y_{A6} and Z_{A6} axes at station $X_{A6} = 833.2 \pm 0.25$ inches. The SPS effective nozzle expansion ratio is 60:1. The SPS consists of the following subsystems:

- a) Helium pressurization
- b) Propellant storage and delivery
- c) Engine assembly
- d) Thermal control

The propellant utilization and gaging system (PUGS) has been rendered inoperative by removal of the PUGS control unit. Thrust vector alignment and component arrangement are shown in Figures 4.5-1 and 4.5-2, respectively.

4.5.1 Propellants and Propellant Storage System. The storable, hypergolic propellants utilized by the SPS are nitrogen tetroxide (oxidizer) and Aerozine 50 (A50) (fuel).

4.5.1.1 Oxidizer. The SPS oxidizer is inhibited nitrogen tetroxide (N_2O_4) (0.60 to 1.00 percent nitric oxide) which conforms to NASA Specification MSC-PPD-2B, August 1, 1968, or subsequent revisions.

4.5.1.2 Fuel. The SPS fuel is Aerozine 50 (A50) which is a mixture of hydrazine (N_2H_4) and unsymmetrical dimethylhydrazine (UDMH) in approximately equal proportions by weight that conforms to the military specification "Propellant, Hydrazine-unsymmetrical Dimethylhydrazine (50% N_2H_4 - 50% UDMH)", MIL-P-27402B (USAF), May 27, 1969, or subsequent revisions.

4.5.1.3 Propellant Tank Capacity and Trapped Quantities. The SPS propellant system capacities for sump tanks loaded to the top of the standpipe (139.2 inches) are shown in Table 4.5-1. The residual trapped quantities which are considered unusable are included in this table. Figures 4.5-3 and 4.5-4 present mixture ratio allowance and pre-load loading uncertainty, respectively, as a function of load percent. Figure 4.5-3 is based on the assumption that the mission mixture ratio was 1.60 with an uncertainty of ± 0.024 . The pre-load loading uncertainty curve of Figure 4.5-4 is based on the following uncertainties:

- a) Tank volume variations (manufacturing tolerances)
- b) Temperature gage error ($\pm 2.0^\circ F$)
- c) Point sensor height
- d) Propellant gage error ($\pm 0.35\%$ of gageable)
- e) Batch density variation (oxidizer $\pm 0.30\%$ loaded; fuel $\pm 0.60\%$ loaded)

- f) Loading pressure variation (± 5.0 psi)
- g) Load specification (gage reading)

4.5.1.4 Ullage Requirements. Before the SPS engine is started in a zero-g environment, propellant settling periods are required. Propellant settling is accomplished by firing the SM RCS engines to accelerate the spacecraft and cause the propellants to settle at the aft end of the propellant tanks.

4.5.1.4.1 Nominal Ullage. The primary mode of propellant settling is four-jet ullage. The two-jet ullage settling maneuver is a backup mode of operation for use in the event of a service module RCS quad failure, unpredicted depletion of the SM RCS quad failure, unpredicted depletion of the SM RCS propellant budget, or failure of the control systems to initiate a four-jet ullage maneuver. Propellant settling periods for two- and four-jet ullages are presented in Figures 4.5-5 and 4.5-6, respectively. The data are applicable to any spacecraft burnout weight (total spacecraft weight less usable SPS propellant).

Data and criteria considered in the generation of Figures 4.5-5 and 4.5-6 are as follows:

- a) settling time requirements as a function of acceleration and distance from the top of settled propellant to the top of the tank
- b) distance from the top of settled propellant to the top of tank as a function of SPS propellant remaining
- c) average acceleration thrust by service module RCS:

Two-jet = 187.5 pounds
Four-jet = 375.0 pounds

4.5.1.4.2 Contingency Ullage. When the anticipated service module RCS propellants are computed to be inadequate to complete the mission, the following settling maneuvers are acceptable.

- a) Before SPS burns of less than 4 seconds or more than 20 seconds duration, a five-second, two-jet propellant settling maneuver is acceptable.
- b) A maximum of four short-duration SPS burns (each less than 4 seconds) may be performed in succession when each burn is preceded by the relevant five-second propellant-settling maneuver. Subsequent SPS burns must be preceded by a full-duration propellant-settling maneuver, as defined by Figures 4.5-5 and 4.5-6, as applicable.

The initial long-duration SPS burn following any short-duration burns, when one or more of these short-duration burns utilized the five-second propellant-settling maneuver, must be for a minimum duration of 40 seconds.

- c) A 40-second SPS burn will allow a repeat of the four short-duration burn series, each utilizing the five-second settling maneuver. If no more than three short-duration SPS burns were made in succession with each burn preceded by the five-second settling maneuver, it is permissible to utilize the five-second settling maneuver for the initial long-duration burn following the series.

4.5.1.5 Ullage Pressure Limits. The SPS system is normally operable as long as the chamber pressure remains above 70 psia and the propellant tank ullage pressures are greater than 160 psia. The maximum pressure differential between the fuel and oxidizer tank ullage pressures is 20 psi to guarantee a smooth engine start and the capability of maintaining the oxidizer-to-fuel mixture ratio in the range of 1.4 to 1.8. A summary of propellant tank pressure limits is presented in Table 4.5-2. A summary of results for exceeding these limits is presented in Table 3.5-1.

4.5.1.6 Propellant Temperature Limits. The propellant temperature limits are as follows:

- a) Bulk propellant
- | | |
|-------------------|--------------|
| Noncritical burns | 40° to 110°F |
| Critical burns | 30° to 110°F |
- b) Propellant feed line
- | | |
|-------------------|--------------|
| Noncritical burns | 40° to 110°F |
| Critical burns | 25° to 110°F |
- c) Propellant utilization valve
- | | |
|-------------------|--------------|
| Noncritical burns | 40° to 110°F |
| Critical burns | 20° to 110°F |
- d) The temperature of the fuel must be within 60°F of the temperature of the oxidizer.
- e) The propellant temperature limits of the engine bipropellant valve are 40° to 160°F.

For additional SPS temperature limits, see the SPS propulsion limitations in Table 3.5-1.

4.5.1.7 Propellant Tank Pressure-Temperature Limits.† Figure 4.5-7* identifies the propellant tank limits in terms of operating temperatures and pressures.

4.5.2 Propellant Feed System

4.5.2.1 Fuel and Oxidizer Flow Rates*. Steady-state propellant flow rates for the propellant utilization valve in the nominal position (normal primary) for fuel and oxidizer, respectively, are 24.9 and 39.6 lbm/sec for SPS engine single-bore operation and 25.7 and 40.9 lbm/sec for engine dual-bore operation.

†NASA Data Source

*The data shown are typical values only. Specific data for CSM 111 will be furnished as these data become available.

4.5.2.2 Propellant Flow Resistance.* The system propellant flow resistance from the sump tanks (including the retention reservoir) to the engine interface for the propellant utilization valve in the nominal position is:

$$\begin{aligned}\text{Oxidizer} &= 116 \text{ lbf-sec}^2/\text{lbm-ft}^5 \\ \text{Fuel} &= 51 \text{ lbf-sec}^2/\text{lbm-ft}^5\end{aligned}$$

The engine flow resistance from the engine interface to the combustion chamber is:

	<u>Engine Operation</u>	
	<u>Single Bore</u>	<u>Dual Bore</u>
Oxidizer	528 lbf-sec ² /lbm-ft ⁵	461 lbf-sec ² /lbm-ft ⁵
Fuel	983 lbf-sec ² /lbm-ft ⁵	873 lbf-sec ² /lbm-ft ⁵

4.5.2.3 Propellant Pressure Drop Flow Rate Data

4.5.2.3.1 Ullage-to-Interface Pressure Drop. Figure 4.5-8 presents propellant pressure drop from tank ullage to the engine interface (from SP0003P to SP0931P for the oxidizer and from SP0006P to SP0930P for the fuel). Propellant flow rate is dependent on propellant head, therefore the data are plotted for two propellant load cases, zero percent and 55 percent (corresponding to an empty and full tank, respectively).

4.5.2.3.2 Interface-to-Chamber Pressure Drop. Propellant flow rate as a function of pressure drop from the engine interface to the SPS engine chamber (from SP0931P to SP0661P for the oxidizer and from SP0930P to SP0661P for the fuel) is presented in Figure 4.5-9.

4.5.2.4 Propellant Utilization and Gaging System (PUGS). The propellant utilization gaging system (PUGS) consists of two independent systems. The primary system uses a continuous capacitance probe. The auxiliary system uses eight discrete point sensors in each tank with an electronic integrator to interpolate between readings (see Table 4.5-3). The PUGS, by means of GSE, will be used for propellant loading only and will be deactivated for flight.

4.5.2.5 Propellant Pressure Limits at the Engine Interface. Propellant pressure limits at the engine interface during dual-bore firings are presented in Figure 4.5-10 as a safe-operation envelope. The limits for safe engine operation in a contingency situation are maximum and minimum chamber pressure (P_c) of 110 and 70 psia, respectively, and a mixture ratio range from 1.4 to 1.8. Any interface pressure condition inside the envelope will result in safe engine operation. During nonfiring periods, the interface pressure limits are equivalent to the ullage pressure limits given in Paragraph 4.5.1.5.

*The data shown are typical values only. Specific data for CSM 111 will be furnished as these data become available.

4.5.2.6 Blowdown Capability. It is possible that a contingency may arise in which the helium supply pressure to the propellant tanks is lost. In this situation, it is possible to ignite the engine (or continue a firing) by using the existing trapped ullage gas pressure in a blowdown mode of operation. During blowdown, system pressure will decay and engine performance will be degraded. The system is normally operable as long as chamber pressure remains at more than 70 psia.

4.5.3 Helium Pressurization System

4.5.3.1 Helium Pressurization System Performance Parameters. See Table 4.5-4.

4.5.3.2 Helium Pressure and Temperature Limits. See Figure 4.5-11.

4.5.3.3 Helium Loading Window. See Figure 4.5-11.

4.5.3.4 Pressure Loss Budget. The helium pressurization system loss budget is shown in Table 4.5-5.

4.5.4 Nitrogen Pressurization System

4.5.4.1 Nitrogen Tank Capacity and Trapped Quantities. Nominal nitrogen storage tank capacity and trapped quantities for the engine pneumatic actuation system nitrogen tanks are shown in Table 4.5-6. The weight of nitrogen is based on a nominal tank volume of 120 cubic inches, a nitrogen temperature of 70°F, and tank pressures of 2500 psig and 350 psia for initial and final conditions, respectively.

4.5.4.2 Nitrogen Pressure System Characteristics. The nitrogen pressure system characteristics are shown in Table 4.5-6.

4.5.4.3 Nitrogen Tank Pressure Loading Limits. The nominal loading pressure for each tank is 2500 ±50 psig at a temperature of 70°F. Loading pressures for nitrogen temperatures ranging from 30° to 140°F are shown in Figure 4.5-12. The nitrogen pressure-temperature relationships are based on the loaded nitrogen weight shown in Table 4.5-6.

4.5.4.4 Nitrogen Tank Temperature Loading Limits. The nominal nitrogen tank loading temperature is 70°F. The upper and lower temperature limits are 140° and 30°F and are based on engine ball valve temperature limitations. The pressure-temperature relationship for a nominal nitrogen tank loaded weight is shown in Figure 4.5-12.

4.5.5 SPS Engine Performance

4.5.5.1 SPS Engine Design Characteristics. The SPS engine design characteristics are shown in Table 4.5-7.

4.5.5.2 SPS Engine Performance Characteristics.† TBS

†NASA Data Source

4.5.5.3 Minimum Impulse. The minimum impulse bit is defined as the total time integral of the thrust resulting from a given G&C thrust-on signal duration (the time between FS₁ and FS₂). It should be noted that the time between FS₁ and FS₂ is the G&C electrical signal duration only and that the impulse for the minimum impulse bit is accumulated for considerable time after FS₂ (approximately 2 seconds). The minimum impulse bit is required by specification to be equal to, or less than, 5000 pound-seconds, with a run-to-run tolerance for a specific engine of ± 600 pound-seconds.

The SPS is capable of accepting a shutdown signal at any time after the start signal. However, the minimum recommended G&C, FS₁-to-FS₂ fire switch duration, is 0.35 second for a noncritical burn (see Paragraph 3.5.8). Figure 4.5-13 presents typical impulse bit curves for single- and dual-bore operation as a function of G&C thrust-on signal duration.

4.5.5.4 Start and Shutdown Thrust Transients. Typical Block II SPS engine start and shutdown thrust transients for single- and dual-bore operation are presented in Figure 4.5-14. The curves are plotted as a function of elapsed time for the corresponding G&C start and/or shutdown signal. Rated thrust is based on nominal engine inlet conditions.

The start and shutdown thrust transient limits for Block II engines are given in Table 4.5-8. Specific transient data will be provided as available.

4.5.5.5 Minimum Chamber Pressure. The SPS engine thrust chamber lower pressure limit for noncritical burns is 70 psia. The system is normally operable as long as the chamber pressure remains at more than 70 psia and tank pressure remains above 160 psia. A noncritical SPS burn may be initiated if the propellant tank inlet pressures are greater than 160 psia. A critical SPS burn may be initiated, however, if fuel and oxidizer inlet pressures are greater than 115 psia. This lower limit was established at WSTF and, if exceeded, will cause the chamber pressure to decrease to a value that will result in rough combustion of the engine.

Ground tests at WSTF also show that if the delta pressure between the fuel and oxidizer tank pressures exceeds 20 psi, mixture ratio limits will be exceeded and rough combustion may result. Noncritical SPS burns will be inhibited or terminated if the delta pressure is equal to or greater than 20 psi. A critical burn will not be terminated if the delta pressure is equal to or greater than 20 psi.

4.5.5.6 Chamber Pressure Overshoot Limit. The chamber pressure overshoot limit is 130 percent of nominal chamber pressure.

4.5.5.7 Time Between Starts. There is no maximum limit time between starts. The minimum limit time between starts and number of consecutive starts are presented in paragraphs 3.5.8 and 4.5.1.4.2, respectively.

4.5.5.8 Blowdown Performance. The SPS performance characteristics during ullage blowdown operation can be estimated by using Figures 4.5-15 and 4.5-16. Figure 4.5-17 provides an estimate of engine chamber pressure as a function of ullage pressure. The following list of conditions should be considered before applying the data:

- a) The initial blowdown occurs with both the fuel and oxidizer ullage pressures at approximately the same value and with equal percentages of propellant remaining.
- b) The propellant and ullage temperatures are constant at 70°F.
- c) The propellant utilization valve is placed in and remains in the NORMAL position.
- d) Engine single-bore operation is utilized for the first 3.5 seconds and dual-bore operation is utilized for the remainder of the burn.
- e) The SPS engine dual-bore specific impulse and thrust at nominal interface conditions are 312.5 seconds and 20,400 lbf, respectively.
- f) The CSM weight excluding SPS propellant is constant at 24,078 pounds. (Note that 900 pounds PSM propellant is included.)
- g) Propellant limited cases are based on nominal usable values (i.e., trapped propellant both inside and outside the tank is considered unusable. Mixture ratio, gaging, and loading uncertainty allowances are not subtracted out).
- h) Delta velocity from the RCS is not included.
- i) The delta velocity and burn time capability are limited by propellant depletion or by a minimum chamber pressure of 70 psia.

4.5.6 SPS Thermal Control System (TCS). The function of the SPS TCS is to maintain SPS engine component temperatures in a range which will ensure the safe operation of the engine. The heater system is composed of two redundant circuits (A and B), each containing six heaters. Heater wattages are listed in the MEEL. (Refer to Section 4.1.)

4.5.6.1 Attitude Constraints. No mission attitude constraints are anticipated for the currently designed system. The SPS heaters will be manually cycled to maintain the feedline temperature between 45° and 75°F and the engine valve temperature above 45°F. The temperature limits for noncritical and critical SPS burns are defined in Table 3.5-1.

4.5.6.2 TCS Operation. The TCS heaters are to be operated by the astronauts using the engine fuel feedline temperature sensor, SP0048T, displayed in the CM as the primary control sensor. The System A heaters are to be activated when the control temperature falls below 45°F and deactivated when the temperature rises to 75°F. In the event of failure of the primary control sensor, the engine oxidizer feedline temperature sensor, SP0049T, also displayed in the CM will be used as a backup control sensor. If the engine valve temperature falls below 45°F as indicated by the engine valve body temperature sensor, SP0045T (TLM only), the TCS heaters will be activated upon ground control request.

4.5.6.3 Propellant Temperature. Bulk temperature limits versus local temperature limits for SPS propellant were established with the knowledge that the propellant will normally be colder than average near the propellant line mounting brackets and will normally be warmer than average near the heaters when they are energized. However, because of mixing and high propellant flow rates during engine operation, the engine is sensitive to the average (bulk) propellant temperature only. The local temperature limits are established to assure propellant temperature safely above the freezing points (12°F for oxidizer and 19°F for fuel) and safely below the propellant boiling points (above 160°F). The bulk limits were established to maintain the average propellant temperature limits within the design range used by the engine manufacturer and demonstrated in the engine qualification test program (40°F minimum, 110°F maximum). (Refer to Table 3.5-1.)

4.5.7 Miscellaneous

4.5.7.1 Gimbal Motor and Clutch Temperature Characteristics

- a) Figure 4.5-18. Clutch heating rate with the gimbal motors energized and quiescent currents applied
- b) Figure 4.5-19. Clutch heating rate during an SPS engine firing
- c) Figure 4.5-20. Cooldown rate of the clutch with the gimbal motors not operating and thrust vector control off

4.5.7.2 CSM Angular Acceleration by SPS Hardover. Figure 4.5-21 presents the maximum possible spacecraft angular acceleration at the beginning of an SPS burn resulting from a worst-case engine hardover plus 3° thrust angle tolerance and actuator limits, described as a function of vehicle weight.

Table 4.5-1. SPS Propellant System Data
(See Paragraph 4.5.1.3)

	Oxidizer (N ₂ O ₄)	Fuel (A ₅₀)	Total
Total propellant system capacity (maximum capacity at 175 psia and 70°F) (ft ³)	163.6	163.6	327.2
Number of tanks	1	1	2
Maximum propellant (loaded to top of standpipe at 25 psia and 70°F) (lb)	13,860.9	8,670.6	22,531.5
Residuals (lb)			
Retention reservoir	97.5	61.4	158.9
Vapor at 80°F	41.1	3.4	44.5
Feedlines	44.7	29.5	74.2
Engine	<u>47.4</u>	<u>29.6</u>	<u>77.0</u>
Total	230.7	123.9	354.6
Usable (maximum) (lb)*			
Maximum propellant load	13,860.9	8,670.6	22,531.5
Residual (unusable)	<u>230.7</u>	<u>123.9</u>	<u>354.6</u>
Total	13,630.2	8,546.7	22,176.9
Allowances (lb)			
Restart allowance (lb/burn)	8.85	5.53	14.38
Mixture ratio allowance		See Figure 4.5-3	
Loading uncertainty		See Figure 4.5-4	
Required to cover upper screens (lb)	1033.0	645.0	1678.0**
Required to cover lower screens (lb)	561.0	351.0	912.0***

*For data on actual propellant load, see Volume II of the ASTP Operational Data Book.

**Total does not include 45 lb of vapor and 101 lb for dispersion. Therefore, the total would be 1824 lb.

***Total does not include 45 lb of vapor and 101 lb for dispersion. Therefore, the total would be 1058 lb.

Table 4.5-2. Propellant Tank Ullage Pressure Limits
(See Paragraph 4.5.1.5)

<u>Parameter</u>	<u>Value</u>
Minimum Ullage Pressure - Noncritical Burn	160 psia
Minimum Ullage Pressure - Critical Burn	115 psia
Maximum Fuel and Oxidizer Tank Pressure Differential	20 psi
Pressure Regulator Assembly Maximum Lockup Pressure	205 psig
Minimum Relief Valve Burst Disk Burst Pressure	213 psig
Maximum Relief Valve Burst Disk Burst Pressure	225 psig
Minimum Relief Valve Relief Pressure	212 psig
Maximum Relief Valve Relief Pressure	225 psig
Minimum Relief Valve Reseat Pressure	208 psig

Table 4.5-3. SPS Point Sensor Locations (176.60 psia and 70°F)
(See Paragraph 4.5.2.4)

<u>Sensor Number</u>	<u>Height (in.)</u>	<u>Maximum Gage Reading (percent)</u>	<u>Gageable Weight (lb)</u>	
			<u>Oxidizer Tank</u>	<u>Fuel Tank</u>
8	131.60	52.0	12,688.08	7,936.64
9	116.54	45.5	11,102.07	6,944.56
10	101.72	39.0	9,516.06	5,952.48
11	86.89	32.5	7,930.05	4,960.40
12	72.07	26.0	6,344.04	3,968.32
13	57.25	19.5	4,758.03	2,976.24
14	41.34	13.0	3,172.02	1,984.16
15	25.36	6.5	1,586.01	992.08